Graphite Characterisation Stage 2 – Inactive and Active Graphite Analysis and Graphite Inventory Modelling

Customer: Nuclear Decommissioning Authority

Issue 1
March 2010

Title	Graphite Characterisation Stage 2 – Inactive and Active Graphite Analysis and Graphite Inventory Modelling		
UKAEA Reference	TSG (10) 0658		
Issue	Issue 1		
Date	31/3/10		
Customer	NDA		
Customer Reference	DRP Lot 3		
Marking	None		
Copyright	This document and its attachments have been prepared by UKAEA in connection with a contract to supply goods and/or services and are for the sole use of the named customer. The contents must not be disclosed to third parties other than in accordance with the terms of the contract.		
Prepared by	UKAEA Ltd The Manor Court Harwell Oxfordshire OX11 0RN		
	Name	***Signature***	***Date***
Author	Tony Lansdell		31/3/10
Author	Mike Newland		31/3/10
Reviewed by	Colette Hunt		31/3/10
Approved by	Colette Hunt		31/3/10

DOCUMENT REVISION RECORD

Issue Number	Reason	Author	Date
Issue 1 draft	Issued for client comment	Tony Lansdell	31/3/10

DOCUMENT DISTRIBUTION

Organisation	Name	Hard Copy	Electronic Copy
NDA	Lisa Hughes		y
	Darrell Morris		y

EXECUTIVE SUMMARY

This report describes the initial findings of the 'active' phase of the Stage 2 assessment work on graphite characterisation, prepared by UKAEA Ltd under the NDAs' Direct Research Portfolio (DRP). This report also concludes the inactive phase of the Stage 2 assessment. It is expected that the completion of the active analysis will be reported in a later issue of this report. The overall objective of this work is to assist the NDA in its assessment of management options for UK reactor graphite wastes.

The main conclusions are;

- Inactive graphite samples retrieved from the Downton archive for representative reactors have been analysed for a wide range of precursor concentrations as specified in the stage 1 work;
    - For many precursors there was a good degree of agreement between results, however in some cases there were significant variance between reactors.;
    - This was especially true for chlorine and lithium precursors, and NPL are currently reassessing chlorine precursors due to a suspected contamination issue with the samples;
- Development and optimisation of activation models has been used to predict inventories for key nuclides and compare them with RWI data;
- Generally, the model gave a good level of agreement to the RWI, especially for key radionuclides such as tritium, carbon-14 and cobalt-60;
    - Where significant differences have been found between inventories they are thought to be associated with differences or omissions in precursor concentrations used in the calculations;
- Evidence of scalability of results across the Magnox fleet is present;
    - Radionuclide inventories predicted by MCNP and FISPACT for each reactor are very similar when considering the same set of elemental precursors;
    - Inactive graphite analysis by NPL suggested that several elemental precursors, such as cobalt and nitrogen, are very similar across five different reactor sites;
- Limited active graphite samples have been available to date for analysis. Comparison between physical active analysis and modelled analysis demonstrate a high degree of agreement;
    - Further active analysis is required for justification purposes.

CONTENTS

Executive Summary **4**

1 Introduction **11**
1.1 Background: UK Reactor Graphite Wastes 11

2 Summary of previous work and Progress towards Programme Objectives **13**

3 Inactive Graphite Analysis **15**
3.1 Graphite Sampling and retrieval 15
3.2 NPL Inactive graphite analysis 16

4 Active Graphite Assessment **22**
4.1 Comparative Modelling 23

5 Modelling **25**
5.1 Introduction 25
5.2 Assumptions 25
5.3 Limitations of the Model 27
5.4 Results – FISPACT analysis 30
5.5 Results – Heavy and transuranic nuclides 32
5.6 Results – Observations and comments 35

6 Comparison with 2007 RWI **43**
6.1 Assumptions and clarifications 43
6.2 Sizewell A – Reactor 1 43
6.3 Wylfa – Reactor 1 45
6.4 Discussion of Results 46

7 Active Graphite and comparison with model predictiuons **48**
7.1 NPL Active Analysis 49
7.2 Comparison to modelling work 49
7.3 Discussion of the results 51

8 Summary and Further Work **52**
8.1 Summary 52
8.2 Further work 53

9 References **54**

Appendix 1: Graphite Samples Retrieved **55**

Appendix 2 – Inactive Graphite Analysis by NPL **58**

Appendix 3 – Inactive Graphite Comparison **59**

Appendix 4 – NPL Limits of Detection **60**

Appendix 5 – Comparison of Elemental Precursors (PGA) **61**

Appendix 6 – Comparison of Elemental Precursors (PGB) **70**

Appendix 7 – Requested and received samples from NNL **78**

Appendix 8 – New Neutron energy spectra **80**

Appendix 9 – Sizewell A Reactor 1 Radionuclide inventory by position radially and axially in the core and reflector regions **82**

Appendix 10 – Wylfa Reactor 1 Radionuclide inventory by position radially and axially in the core and reflector regions **103**

Appendix 11 – Pathway Analysis **134**

Appendix 12 – Uranium Irradiation 161

Appendix 13 – Thorium Irradiation..... 164

Appendix 14 – Derivation of pointwise values of flux in a three-dimensional system (Bessel's function)..... 167

Appendix 15 – Testing the model..... 170

Appendix 16 – NPL Active Graphite Analysis 174

Appendix 17 – Comparison to FISPACT modelling..... 175

FIGURES

Figure 1: Lithium PGA graphite elemental precursors for inactive graphite 17
Figure 2: Nitrogen PGA graphite elemental precursors for inactive graphite 18
Figure 3: Nitrogen PGB graphite elemental precursors for inactive graphite 18
Figure 4: Chlorine PGA graphite elemental precursors for inactive graphite 19
Figure 5: Chlorine PGB graphite elemental precursors for inactive graphite 20
Figure 6: Cobalt PGA graphite elemental precursors for inactive graphite 21
Figure 7: Cobalt PGB graphite elemental precursors for inactive graphite 21
Figure 8: Photograph displaying active sample and associated sample code 22
Figure 9: Active comparison model 23
Figure 10: Active comparison model detailing the detectors. 24
Figure 11: Reactor core for Sizewell A showing fuel channels on a vertical cut away and the points sampled using MCNP highlighted in blue 26
Figure 17: Comparison between the average spectrum used to calculate the inventory, and the spectrum in the graphite facing the fuel channel 29
Figure 12: Lithium precursors from NPL analysis 36
Figure 13: A comparison of relative euoropium-152 magnitude to the inverse square of relative flux in Sizewell A 38
Figure 14: A comparison of neutron energy spectra in the centre of the core in Sizewell A and Wylfa 41
Figure 15: A comparison of neutron energy spectra in the outermost radial reflector in Sizewell A and Wylfa 42
Figure 16: A comparison of four normalised neutron energy spectra located at four points radially from the core centre (in metres) for Wylfa 42
Figure 18: A comparison of PGA lithium concentration across five Magnox reactors with error bars ..... **Error! Bookmark not defined.**
Figure 19: Comparison between NPL (averaged with errors), John Jowett and Magnox RWI precursor information 59
Figure 20: Comparison between reactors for PGA graphite for Barium 62
Figure 21: Comparison between reactors for PGA graphite for Boron 62
Figure 22: Comparison between reactors for PGA graphite for Calcium 63
Figure 23: Comparison between reactors for PGA graphite for Chlorine 63
Figure 24: Comparison between reactors for PGA graphite for Cobalt 64
Figure 25: Comparison between reactors for PGA graphite for Copper 64
Figure 26: Comparison between reactors for PGA graphite for Iron 65
Figure 27: Comparison between reactors for PGA graphite for Lithium 65
Figure 28: Comparison between reactors for PGA graphite for Magnesium 66
Figure 29: Comparison between reactors for PGA graphite for Molybdenum 66
Figure 30: Comparison between reactors for PGA graphite for Nickel 67
Figure 31: Comparison between reactors for PGA graphite for Nitrogen 67
Figure 32: Comparison between reactors for PGA graphite for Potassium 68
Figure 33: Comparison between reactors for PGA graphite for Sodium 68
Figure 34: Comparison between reactors for PGA graphite for Strontium 69
Figure 35: Comparison between reactors for PGA graphite for Zinc 69
Figure 36: Comparison between reactors for PGB graphite for Barium 70
Figure 37: Comparison between reactors for PGB graphite for Boron 70
Figure 38: Comparison between reactors for PGB graphite for Calcium 71
Figure 39: Comparison between reactors for PGB graphite for Chlorine 71
Figure 40: Comparison between reactors for PGB graphite for Cobalt 72
Figure 41: Comparison between reactors for PGB graphite for Copper 72
Figure 42: Comparison between reactors for PGB graphite for Iron 73
Figure 43: Comparison between reactors for PGB graphite for Magnesium 73
Figure 44: Comparison between reactors for PGB graphite for Molybdenum 74
Figure 45: Comparison between reactors for PGB graphite for Nickel 74

Figure 46: Comparison between reactors for PGB graphite for Nitrogen 75
Figure 47: Comparison between reactors for PGB graphite for Potassium 75
Figure 48: Comparison between reactors for PGB graphite for Sodium..... 76
Figure 49: Comparison between reactors for PGB graphite for Strontium 76
Figure 50: Comparison between reactors for PGB graphite for Zinc 77
Figure 51: Normalised energy spectra for fuel channel and control rod channels for samples located at the top or base of a reactor 80
Figure 52: Comparison between fuel and control rod channel neutron energy spectra taken from active comparison modelling and the neutron energy spectrum used in the main model 81
Figure 53: Radionuclide trends for Radial nuclides in the Sizewell A reactor (1/2) 84
Figure 54: Radionuclide trends for Radial nuclides in the Sizewell A reactor (2/2) 85
Figure 55: Radionuclide trends for Axial nuclides in the Sizewell A reactor (1/2)..... 87
Figure 56: Radionuclide trends for Axial nuclides in the Sizewell A reactor (2/2)..... 88
Figure 57: Radionuclide trends for Radial nuclides in the Sizewell A reactor (1/2) 90
Figure 58: Radionuclide trends for Radial nuclides in the Sizewell A reactor (2/2) 91
Figure 59: Radionuclide trends for Axial nuclides in the Sizewell A reactor (1/2)..... 93
Figure 60: Radionuclide trends for Axial nuclides in the Sizewell A reactor (2/2)..... 94
Figure 61: Radionuclide trends for Radial nuclides in the Sizewell A reactor (1/2) 96
Figure 62: Radionuclide trends for Radial nuclides in the Sizewell A reactor (2/2) 98
Figure 63: Radionuclide trends for Axial nuclides in the Sizewell A reactor (1/2)..... 100
Figure 64: Radionuclide trends for Axial nuclides in the Sizewell A reactor (2/2)..... 102
Figure 65: Radionuclide trends for Radial nuclides in the Wylfa reactor (1/2)..... 105
Figure 66: Radionuclide trends for Radial nuclides in the Wylfa reactor (2/2)..... 106
Figure 67: Radionuclide trends for Axial nuclides in the Wylfa reactor (1/2) 108
Figure 68: Radionuclide trends for Axial nuclides in the Wylfa reactor (2/2) 109
Figure 69: Radionuclide trends for Radial nuclides in the Wylfa reactor (1/2)..... 111
Figure 70: Radionuclide trends for Radial nuclides in the Wylfa reactor (2/2)..... 112
Figure 71: Radionuclide trends for Axial nuclides in the Wylfa reactor (1/2) 114
Figure 72: Radionuclide trends for Axial nuclides in the Wylfa reactor (2/2) 115
Figure 73: Radionuclide trends for Radial nuclides in the Wylfa reactor (1/2)..... 117
Figure 74: Radionuclide trends for Radial nuclides in the Wylfa reactor (2/2)..... 118
Figure 75: Radionuclide trends for Axial nuclides in the Wylfa reactor (1/2) 120
Figure 76: Radionuclide trends for Axial nuclides in the Wylfa reactor (2/2) 121
Figure 77: Graphical trends of 7 key heavy nuclides for radial variation in Sizewell A 124
Figure 78: Graphical trends of 7 key heavy nuclides for axial variation in Sizewell A..... 127
Figure 79: Graphical trends of 7 key heavy nuclides for radial variation in Sizewell A 130
Figure 80: Graphical trends of 7 key heavy nuclides for axial variation in Sizewell A..... 133
Figure 81: NPL Active analysis of 4 graphite samples from Sizewell A 174

TABLES

Table 11: Limitations and the way they were addressed in the MCNP modelling 28
Table 12: Limitations and the way they were addressed in the FISPACT modelling..... 30
Table 1: Average inventory of Sizewell A reactor 1 as modelled in FISPACT assuming a density of 1.74 te/m^3, values decayed from 2016 to 2106 using MicroShield V7.02 31
Table 2: Average inventory of Wylfa reactor 1 as modelled in FISPACT assuming a density of 1.74 te/m^3, values decayed from 2019 to 2109 using MicroShield V7.02..... 32
Table 3: A comparison between the activities of key transuranic radionuclides within Sizewell A and Wylfa decayed to 10 years after reactor shutdown 33
Table 4: A comparison between the activities of key transuranic radionuclides within Sizewell A and Wylfa decayed to 100 years after reactor shutdown 33
Table 5: Parent nuclides, half-lives and decay methods for key transuranic radionuclides, data from RadSum (ORNL) 34
Table 6: Percentage contribution from Uranium and Thorium to daughter transuranic nuclide, based on Wylfa data 35
Table 7: Tritium content of Sizewell A and Wylfa based on John Jowett elemental precursors 35
Table 8: A summary of the pathway analysis investigation showing the parent nuclides that lead rise to a selection of radionuclide products (results based on 10 years of decay after reactor shutdown)..... 40
Table 9: Pathway analysis investigating tritium regeneration for the core region of Sizewell A and Wylfa..... 40
Table 10: Pathway analysis investigating tritium regeneration for the reflector region of Sizewell A and Wylfa 40
Table 13: Comparison of key radionuclides between the 2007 RWI and FISPACT calculations based on NPL and Jowett precursor information for Sizewell A 44
Table 14: Comparison of key radionuclides between the 2007 RWI and FISPACT calculations based on NPL and John Jowett precursor information for Wylfa A 45
Table 15: Cobalt-60 activity comparison..... 49
Table 16: Caesium activity comparison 50
Table 17: Barium activity comparison 50
Table 18: Europium activity comparison 50
Table 19 Unirradiated graphite samples retrieved from Magnox's archive, Downton..... 56
Table 20 Samples from Pallet 53 (crate NNL03), Box 198 supplied to NPL for analysis..... 56
Table 21: Precursor concentrations for inactive graphite samples analysed by NPL and retrieved from Downton National Archive, units are in ng/g (ppb) 58
Table 22: This table details the requested and achieved limits of detection, those where LoDs were achieved are marked as N/A 60
Table 23: Radial Activity in Bq/kg for Jowett Precursors in the Sizewell A Reactor 83
Table 24: Axial Activity in Bq/kg for Jowett Precursors in the Sizewell A Reactor..... 86
Table 25: Radial Activity in Bq/kg for NPL Maximum Precursors in the Sizewell A Reactor 89
Table 26: Axial Activity in Bq/kg for NPL maximum Precursors in the Sizewell A Reactor... 92
Table 27: Radial Activity in Bq/kg for NPL Average Precursors in the Sizewell A Reactor... 95
Table 28: Axial Activity in Bq/kg for NPL Average Precursors in the Sizewell A Reactor..... 99
Table 29: Radial Activity in Bq/kg for Jowett Precursors in the Wylfa Reactor 104
Table 30: Axial Activity in Bq/kg for Jowett Precursors in the Wylfa Reactor..... 107
Table 31: Radial Activity in Bq/kg for NPL Maximum Precursors in the Wylfa Reactor..... 110
Table 32: Axial Activity in Bq/kg for NPL maximum Precursors in the Wylfa Reactor 113
Table 33: Radial Activity in Bq/kg for NPL Average Precursors in the Wylfa Reactor 116
Table 34: Axial Activity in Bq/kg for NPL Average Precursors in the Wylfa Reactor..... 119
Table 35: Heavy nuclide concentrations as a function of radial position, activates stated for 2016 in units of Bq/kg 123
Table 36: Heavy nuclide concentrations as a function of axial position, activates stated for 2016 in units of Bq/kg 126

Table 37: Heavy nuclide concentrations as a function of radial position, activates stated for 2016 in units of Bq/kg 129
Table 38: Heavy nuclide concentrations as a function of axial position, activates stated for 2016 in units of Bq/kg 132
Table 39: A comparison of the 18 radionuclides of interest 161
Table 40: The 20 most abundant nuclides by activity 162
Table 41: The 20 most abundant nuclides by dose rate 163
Table 42: The activity of transuranic elements 163
Table 43: A comparison of the 18 radionuclides of interest 164
Table 44: The 20 most abundant nuclides by activity 165
Table 45: The 20 most abundant nuclides by dose rate 166
Table 46: The activity of transuranic elements 166
Table 47: Comparison between Active Sampling and FISPACT modelling for 1215/2 utilising John Jowett Precursors 175
Table 48: Comparison between Active Sampling and FISPACT modelling for 1215/10 utilising John Jowett Precursors 175
Table 49: Comparison between Active Sampling and FISPACT modelling for 1215/2 utilising NPL Precursors 176
Table 50: Comparison between Active Sampling and FISPACT modelling for 1215/10 utilising NPL Precursors 176
Table 51: Comparison between Active Sampling and FISPACT modelling for 1215/2 utilising NPL Average Precursors 177
Table 52: Comparison between Active Sampling and FISPACT modelling for 1215/10 utilising NPL Average Precursors 177

1 INTRODUCTION

This report describes the findings of Stage 2 of a programme of work to improve the radiological characterisation of irradiated Magnox graphite for potential treatment and ultimate disposal purposes. This work was undertaken by UKAEA Ltd under the NDA's Direct Research Portfolio (DRP). The overall objective of project is to assist the NDA in its assessment of management options for UK reactor graphite wastes.

Stage 1 work [1] identified a forward programme to help improve the accuracy of the radionuclide inventory of graphite for high mobility, long lived nuclides. Stage 1 utilised the US Data Quality Objectives (DQO) methodology to direct and focus future work to be conducted in Stage 2 [2] in order maximise benefits and ensure programme objectives were achieved.

Stage 2 involves the development of a reliable activation model of a Magnox reactor that could be used to predict the activity of core graphite at various positions to the required level of accuracy, and validation of this model by analysis of a relevant subset of samples from active graphite sample archives.

Elements of the experimental and modelling programme defined in Stage 1 have been implemented and this report describes its findings. The provision of active samples from archive facilities is delayed for a variety of reasons. It is anticipated therefore that this report will be released as a higher version in the future and include the complete set of active sample results.

This work forms the main part of the 'inactive' phase of Stage 2 and includes initial results from the 'active' phase of the programme. The 'inactive' phase involved recovery of unirradiated graphite samples from the archive and their subsequent laboratory analysis for elements that are precursors to key radionuclides when graphite is irradiated; followed by modelling of their activation in reactor. The 'active' phase involved recovery and analysis of irradiated samples chosen from the archive and modelling of their irradiation history and activation.

1.1 Background: UK Reactor Graphite Wastes

There are over 99,000 tonnes (79,000 m^3) of graphite in the UK arising from operational and reactor decommissioning activities. This accounts for 33% of the total volume of all wastes destined for disposal in the Geological Disposal Facility (GDF). This volume therefore accounts for a significant contribution to the GDF footprint, with approximately half of the waste deriving from the UK Magnox reactor fleet.

However, at least 20% of the graphite inventory destined for the GDF is classified as Low Level Waste (LLW) but is not suitable for disposal at the Low Level Waste Repository (LLWR). There is therefore the potential for a significant reduction in the size of the GDF if an alternative management option for graphite could be utilised.

The current NDA position on graphite management is stated in its 2006 strategy document [3] "We will explore the management/treatment option for graphite waste, taking account of worldwide developments and best practice. Finding an innovative solution to graphite wastes would inform a business case for accelerated decommissioning at Magnox reactor sites".

The are various management/treatment options in varying stages of development that may enable alternative disposal routes, the reduction of activity in the waste to levels that would

enable disposal outside the GDF, or reduction in volumes that would allow a reduction in the GDF footprint.

A key requirement in the assessment of suitable management/treatment options is a comprehensive understanding of the radionuclide inventory of the graphite waste. Data published in the 2007 UK Radioactive Waste Inventory [2] for Magnox reactor graphite declares significant uncertainties in the concentrations of key radionuclides.

2 SUMMARY OF PREVIOUS WORK AND PROGRESS TOWARDS PROGRAMME OBJECTIVES

A previous interim report [4] described the initial programme to analyse the concentration of key impurities in graphite and development of neutron flux and graphite activation modelling of two Magnox cores. That work used preliminary impurities for a portion of the major graphite precursors (obtained by analysis work carried out by NPL) identified in the Stage 1 report [1] to calculate predicted radionuclide inventories at various points within two Magnox reactors (Sizewell A and Wylfa).

The interim report [4] concluded;

- Inactive graphite samples for representative reactors have been recovered from Downton archive;
- Analysis has been conducted for the full range of precursor concentrations as specified in Stage 1 work;
- Development and optimisation of activation models has been used to predict inventories for key nuclides and compare them with RWI data. Where differences have been found between inventories they are associated with differences in precursor concentrations used in the calculations and that found by laboratory analysis;
- Agreement was found between RWI data and model predictions for Carbon-14, based on activation of measured precursor concentrations in unirradiated graphite and not taking account of other process that can influence inventories e.g. effect of CO2 coolant;

For a limited number of precursors, the limits of detection achieved using the chosen analytical methods were not sufficient to enable meaningful calculations for certain nuclides. For these precursors an alternative analysis method was pursued (Appendix 2a – Analytical methods used for each elemental analysis). It should be pointed out that for most precursors positive analytical results were achieved and that only a few elements were below detection limits. The detection limit requirements as specified in stage 1 were also particularly challenging for some elements, particularly when taking into account the nature of the sample matrix in which they were held. The completion of the analysis of the identified precursors allowed full inventories to be calculated for each reactor (Appendix 2b – Inactive Graphite Analysis by NPL).

The objectives for this Stage 2 report is to describe progress and completed including:

- Report full analysis of inactive graphite samples from both modelled reactors and other stations;
- Further modelling to include high fidelity calculations inside the reflector regions of the reactors and inclusion of reactor support structure;
- Full reactor activation calculations using the complete set of graphite elemental precursors measured by NPL;
- Comparison of the modelled radionuclide inventory with the UK 2007 RWI;
- Preliminary comparison to available active graphite sample results;

- Investigate the scalability of results between reactors by comparing calculated activities and radionuclides trends along with specific reactor data.

It is intended that the information within this document and that in a subsequent report, detailing the final results of analysis of irradiated graphite, will be used to verify model predictions and help to test and improve confidence in the radionuclide inventory of Magnox graphite reported in the UK 2007 RWI [2] to support NDA's assessment of graphite management/treatment options including final disposal.

3 INACTIVE GRAPHITE ANALYSIS

The accuracy and confidence of the predicted radionuclide inventory of the graphite is significantly dependent on the accuracy of data on elemental impurity concentrations. Impurities are precursors to most of the nuclides generated in graphite during its irradiation in the reactor core. Therefore, during Stage 1 the list of archived inactive graphite [1] was interrogated and a range of PGA and PGB samples were recommended for retrieval and analysis for key impurities. This section discusses the inactive samples retrieved (based on Stage 1 recommendations) and the results of their analysis.

3.1 Graphite Sampling and retrieval

The Stage 1 report identified and recommended the retrieval of a number of unirradiated graphite samples from the national archive at Downton [5]. However, due to a number of samples not being present at their catalogued location, a number of additional equivalent samples were retrieved in their place. Additionally, it was found that upon inspection the original list of samples for retrieval contained more than sufficient material for analysis of graphite for certain grades of graphite for some reactors. Therefore, in order to preserve as many potentially important samples at the archive, some samples identified in the Stage 1 report were not retrieved.

Figure 1: Inactive graphite samples from the Downton archive – not all the samples shown were removed

Appendix 1: Graphite contains details on the unirradiated graphite material, including the substituted samples that were retrieved from the Downton archive for analysis. The table includes the details provided in the NNL report of the material within the archive [5], however, it is worth noting that more information written directly onto boxes is still legible, for example, graphite heat information.

The samples recovered from the archive include PGA and PGB graphite samples which were manufactured at the same time, and from the same material, as used in the Wylfa, Oldbury, Sizewell A, Hinkley Point and Trawsfynydd Magnox reactors (see Appendix 1: Graphite for details).

Table 19 in Appendix 2b – Inactive Graphite Analysis by NPL also includes details of those samples 'swapped in' to replace samples that could not be located.

3.2 NPL Inactive graphite analysis

Analysis of unirradiated graphite samples was undertaken by the National Physical Laboratory (NPL – Teddington).

In total, NPL analysed 28 different elemental precursors outlined in the Stage 1 report [1]. The findings of this analysis can be found in Appendix 2b – Inactive Graphite Analysis by NPL. A comparison of these elemental precursors has been made against those used in the calculation of the existing 2007 RWI and those for a typical PGA graphite waste stream provided by John Jowett (NDA RWMD).

Detailed graphical comparative work between PGA and PGB graphite for all reactors can be found in Appendix 5 – Comparison of Elemental Precursors (PGA)and Appendix 6 – Comparison of Elemental Precursors (PGB). Analysis of four key elemental precursors of short and long term radiological concern have been highlighted from these Appendices for discussion below;

- Lithium;
    - Key precursor to Tritium;
- Nitrogen;
    - Key precursor (alongside Carbon-13) to Carbon-14;
- Chlorine;
    - Key precursor to Chlorine-36;
- Cobalt;
    - Key precursor to Cobalt-60.

The results of these investigations are reported in Sections 3.2.1 to 3.2.4.

It should be noted that there were a number of sets analysed for PGA, but less for PGB reflecting the relative quantity of graphite type to be managed.

3.2.1 Key elemental precursor – Lithium

Lithium is a key elemental precursor for tritium [6]. Tritium is of interest due to its high mobility and potential for absorption by the biosphere. This is offset in the long term by its relatively short half-life of 12.35 years. Activation to tritium from lithium-6 occurs by way of a neutron-alpha (n,α) reaction.

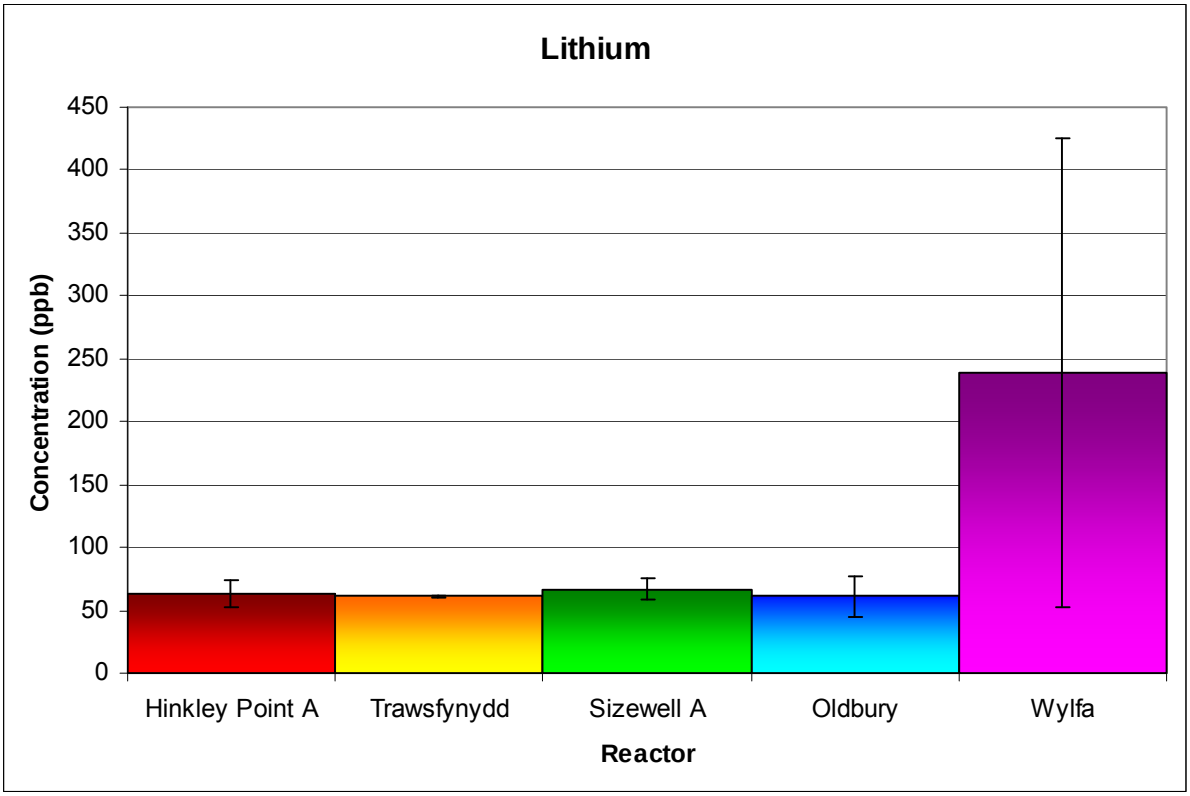

Figure 2: Lithium PGA graphite elemental precursors for inactive graphite

It should be noted that the limit of detection was not achieved by NPL for the PGA graphite samples for lithium, with the exception of Wylfa. Here two samples suggested very high lithium concentrations. PGB graphite did not achieve the LoD for lithium during analysis. The LoD achieved by NPL during the inactive analysis for lithium was 70 ppb, a level which was considered to be unlikely to improve by alternative available techniques or by change to sample preparation methods.

3.2.2 Key elemental precursor - Nitrogen

Nitrogen is the key elemental precursor to carbon-14, alongside carbon-13 [7]. Carbon-14 is of interest due to its potential for absorption into the biosphere and its long half life of 5,730 years. Nitrogen-13 undergoes a neutron-proton (n,p) reaction to form carbon-14.

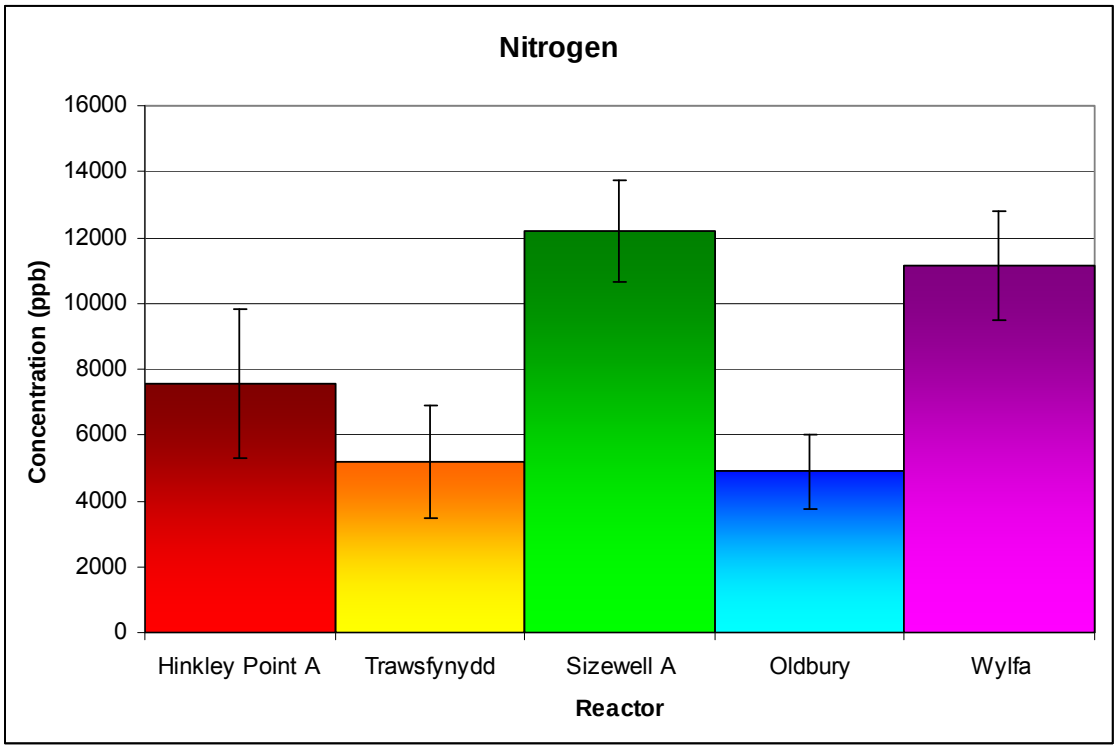

Figure 3: Nitrogen PGA graphite elemental precursors for inactive graphite

Figure 3 suggests that nitrogen concentration is quite uniform (within a factor of 3) across the fleet, when error bars are accounted for. This suggests a certain degree of scalability for results concerning carbon-14 activity – as similar precursor concentrations between two similar reactors may allow for a direct comparison.

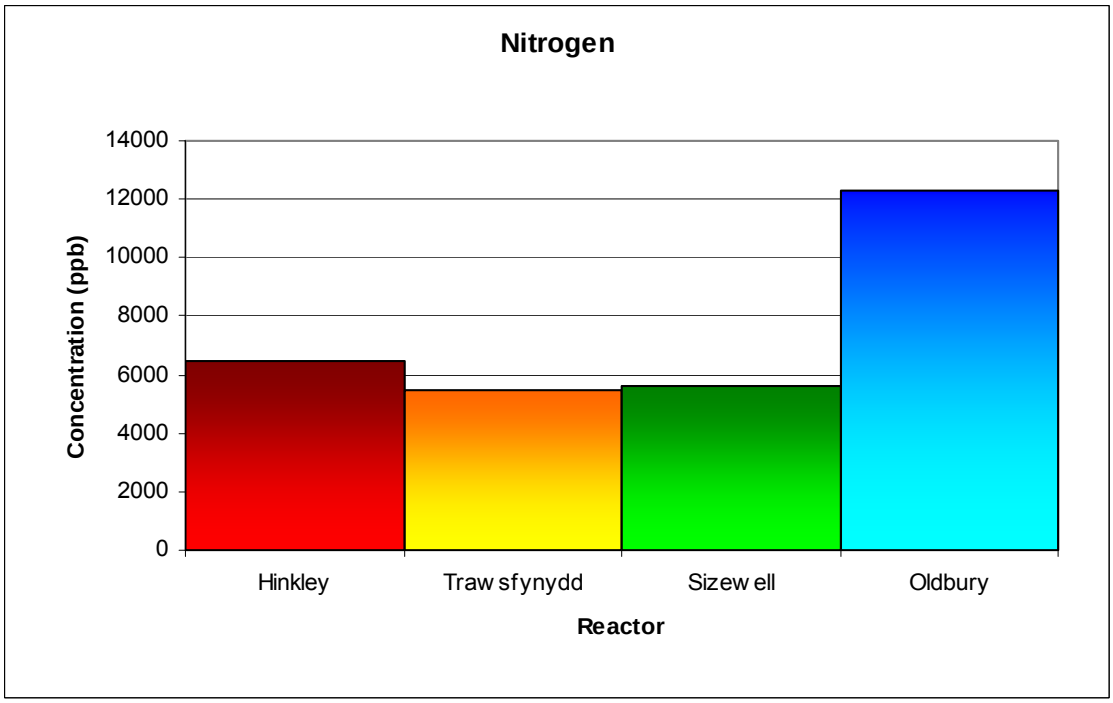

Figure 4: Nitrogen PGB graphite elemental precursors for inactive graphite

Figure 4 displays a similar range of nitrogen content to Figure 3, this potentially backs up any scalability of results between reactors. It was also observed that the difference between Sizewell A PGA and PGB is quite high, being roughly half the concentration in the PGB graphite

3.2.3 Key elemental precursor – Chlorine

Chlorine is the key elemental precursor to chlorine-36. Chlorine-36 is of interest due to its potential for absorption into the biosphere and its long half life of 301,000 years. Chlorine-35 undergoes a neutron-gamma (n,g) reaction to form chlorine-36.

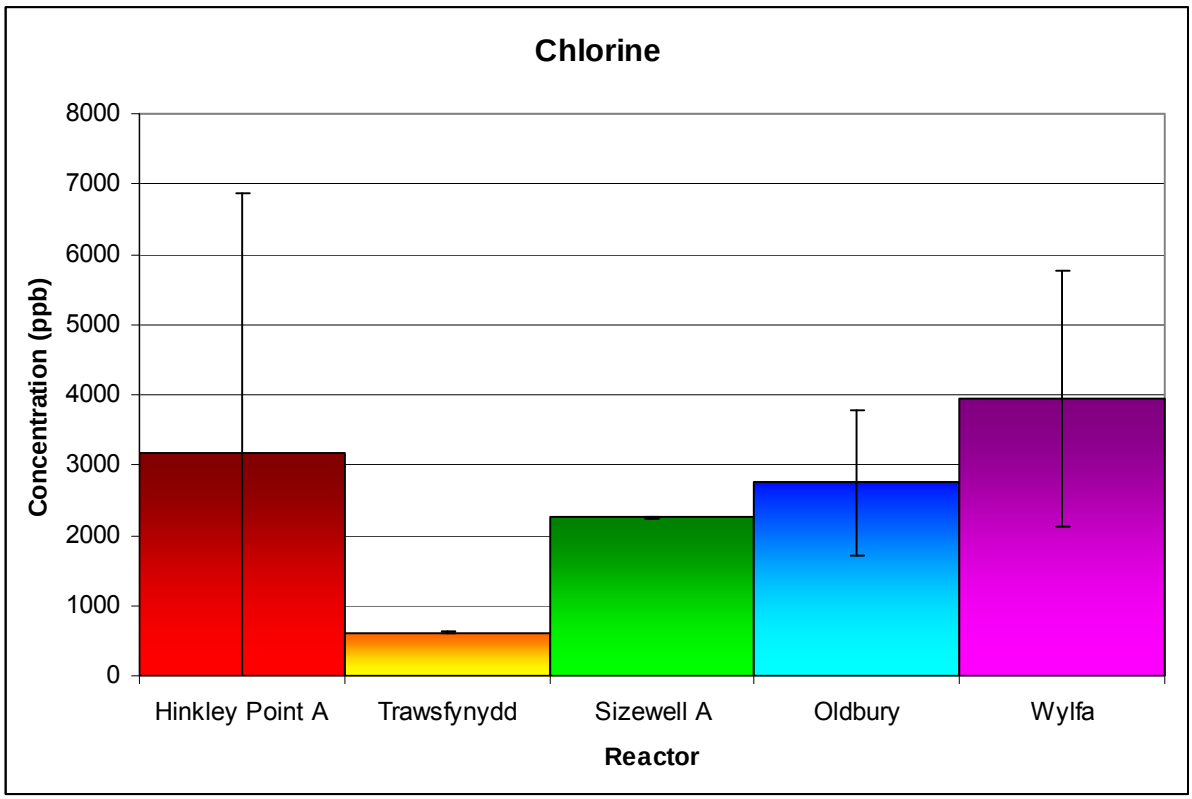

Figure 5: Chlorine PGA graphite elemental precursors for inactive graphite

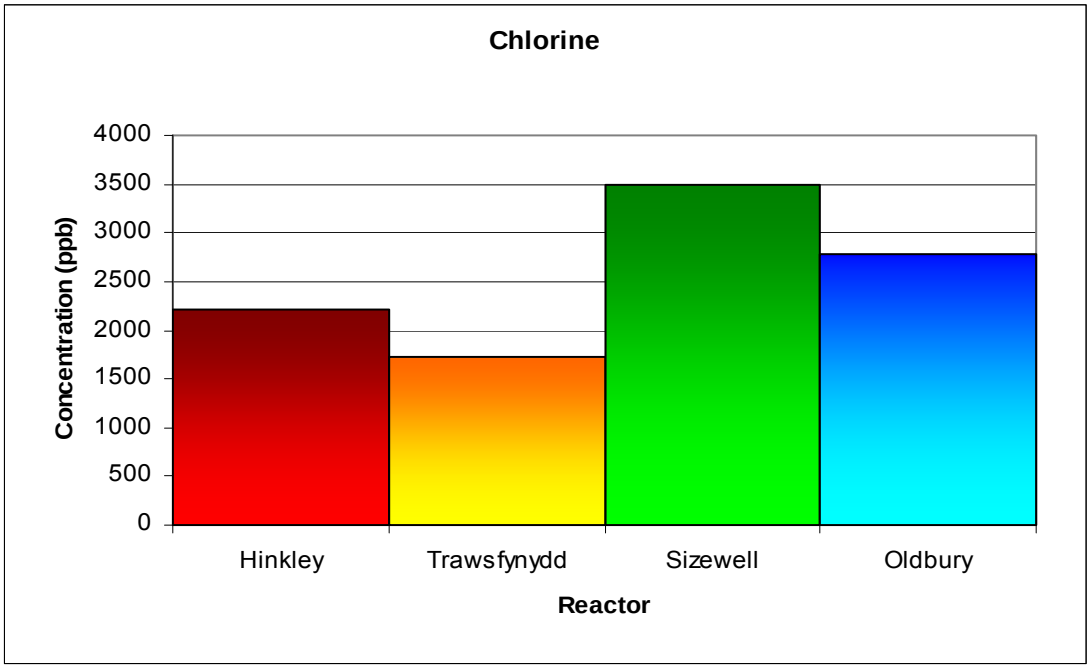

Figure 6: Chlorine PGB graphite elemental precursors for inactive graphite

Figure 5 and Figure 6 suggest a variable concentration of chlorine within graphite, even within the same reactor. This can be seen by the large error bars on Hinkley Point A, Wylfa and Oldbury. This may be due to chlorine contamination of the graphite This may be due to chlorine contamination of the graphite sample during its preparation and storage in the archive or during preparation for analysis.

3.2.4 Key elemental precursor – Cobalt

Cobalt is the key elemental precursor to cobalt-60. As a strong gamma emitter with a relatively short half life of 5.271 years, cobalt-60 is of interest for dose rate management during accelerated decommissioning, Cobalt-59 undergoes a neutron-gamma (n,g) reaction to form cobalt-60.

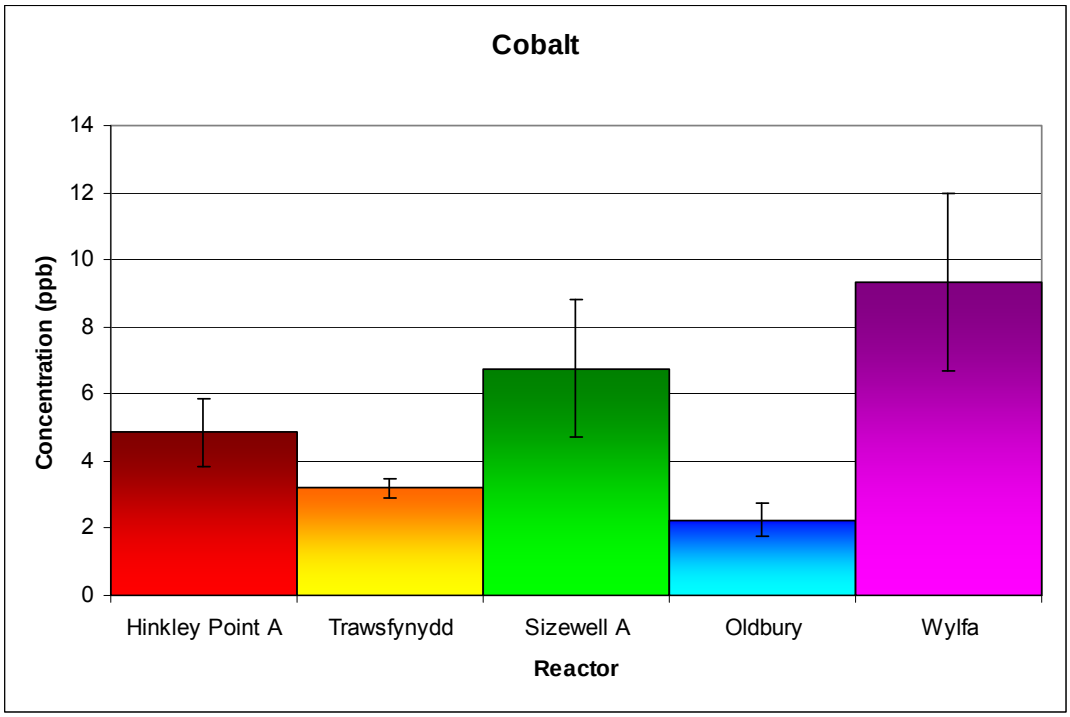

Figure 7: Cobalt PGA graphite elemental precursors for inactive graphite

Figure 7 shows the cobalt contamination for PGA graphite. When error bars are considered, there is a large factor of agreement between the results. In a similar vain to nitrogen, this suggests a certain degree of scalability.

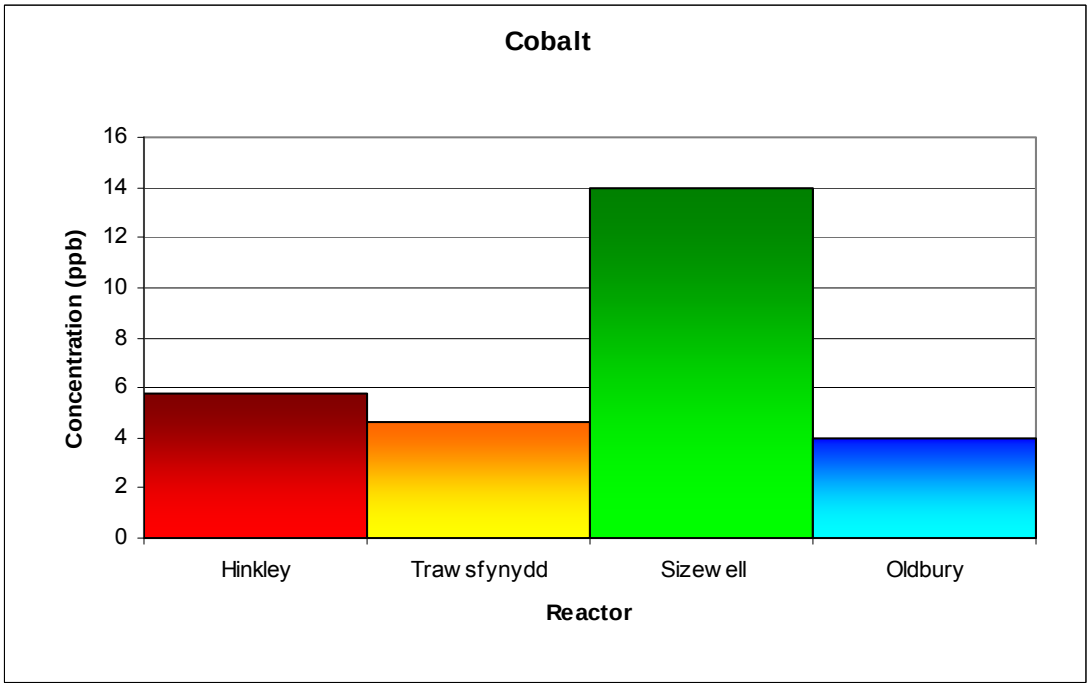

Figure 8: Cobalt PGB graphite elemental precursors for inactive graphite

Figure 8 (PGB graphite) shows a similar range of cobalt concentration to Figure 7 (PGA graphite).

4 ACTIVE GRAPHITE ASSESSMENT

NPL is also undertaking active graphite measurements on retrieved graphite samples from the irradiated graphite archives at Berkeley and Sellafield (managed by NNL). This involves various radiological tests in order to quantify the concentration of various key radionuclides within graphite removed from the core at a known location and date. The samples for analysis were identified in Stage 1 of this project, along with the analysis protocol.

The samples consisted of trepanned pieces of graphite taken from locations along fuel and control rod channels within the core. Samples were taken from a 2 cm deep bore into the channel wall, and cut into three segments, known as “slices” which are labelled as 1-3, where ‘1’ is at the channel surface. Because of their location (generally near the surface of a fuel channel) a more detailed model must be run to compare predicted inventories as calculated by FISPACT to the samples analysed by NPL. This is because the samples may have a different neutron/activation environment to ‘average’ graphite away from fuel channel surfaces (ignoring contamination issues, see later).

Because of delays with the recovery of samples from the archives, only a very limited number of active samples have been received at NPL. An example of a sample is shown below (Figure 9). Initial results from the analysis of the available samples are given in Appendix 16 – NPL Active Graphite Analysis and are discussed later.

Figure 9: Photograph displaying active sample and associated NPL assigned sample code

4.1 Comparative Modelling

To make a direct comparison with the fuel active samples, additional modelling was required to investigating neutron energy spectra at specific sampling points within the core. To do this, a model was created that represented a snapshot of the core (Figure 10).

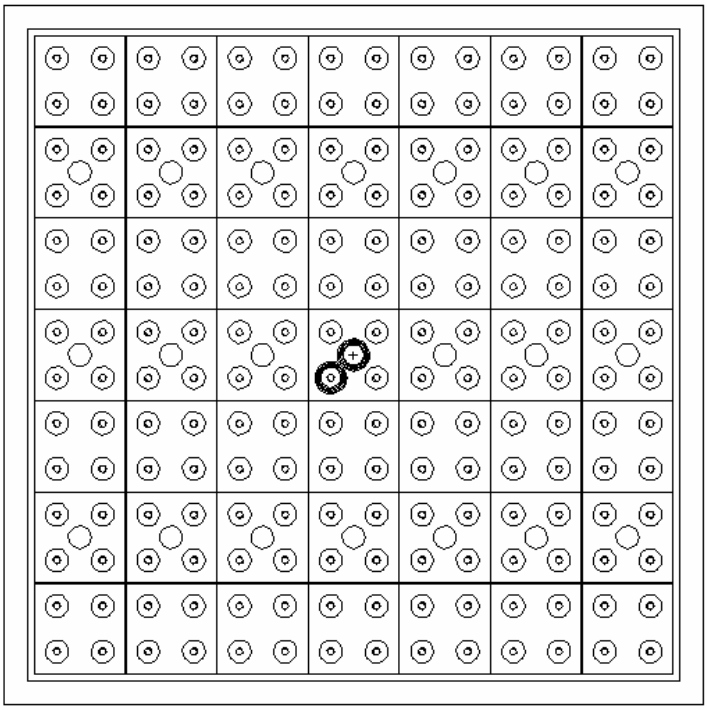

Figure 10: Active comparison model

Figure 10 shows a small section of the core, measuring 2.8 x 2.8 x 4 m – this related to 3.5 x 3.5 chargepans by 3 fuel rods in height. In this model, the same assumptions relating to material were made as were made for the main model, and it is also subject to the same limitations.

To mimic the samples trepanned from the core for active analysis, several detectors were used in the centre of the model. These consisted of 3 cylindrical detectors measuring 0.6 cm in thickness. This is to mimic the effective thickness of each sample, where it is assumed 0.1cm will be lost during each cut of a slice from a trepanned core. These detectors were positioned within the graphite, inline with halfway up the fuel rod.

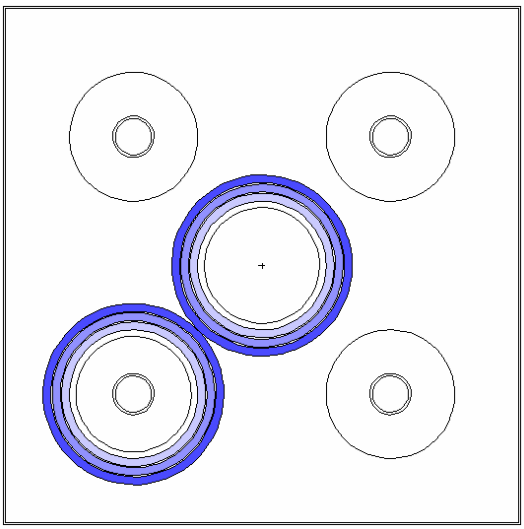

Figure 11: Active comparison model detailing the detectors.

Figure 11 details the detectors (shaded in blue) to mimic the trepanned samples. Two sets of detectors were used, one on the control rod channel, and one on a fuel rod channel.

In total, two new models were run to simulated samples removed from the centre and the top/bottom of the core. These returned new neutron energy spectra for these locations (Appendix 8 – New Neutron energy spectra). Flux calculations from previous modelling work were then used with the new energy spectra for neutron activation. It is assumed MCNP will account for any streaming effects of neutrons within a fuel channel, and this effect will not impact the local flux seen by a sample.

5 MODELLING

5.1 Introduction

Inventory modelling was carried out on two Magnox reactors; Sizewell A R1 (SZA) and Wylfa R1. These represented the two types of reactor used in the commercial Magnox fleet; those with concrete pressure vessels, and those with steel. These two were chosen as Wylfa is still operational and is the largest Magnox reactor built; whilst Sizewell A is representative of a large proportion of the Magnox fleet. These two reactors have a similar core layout, and so enabled an investigation into how the radionuclide inventory from different reactors designs and power outputs are comparable. Most importantly, these reactors also had the best coverage in terms of available appropriate active samples to help verify code treatments. Descriptions and details of the code models calculations are given in a previous report. [4].

5.2 Assumptions

Several assumptions were made within various treatments within the overall model. These were made to fill gaps in available knowledge or to simplify the model in order to enable it to run efficiently but still maintain the required level of accuracy in its predictions. While the model could be improved in certain areas these are judged to have insufficient impact to be warranted. Likewise, the model could be made more efficient in its structure however the structure reflects the model's development as more information became available on the reactor cores and their operational regimes.

The assumptions made can be broadly split into two categories; those made whilst modelling the reactors in MCNP and FISPACT and those made afterwards whilst analysing the data.

5.2.1 Neutron Modelling Assumptions

The following assumptions were made to assist in the design and implementation of model;

1. No density loss within the reactor graphite occurred during the reactor cores operational life;
    a. Graphite density for both PGA and PGB was 1.74 te/m^3;
    b. A separate study has been implemented to investigate this phenomenon;
2. No fuel shuffling or fuel manipulation was used to create a "flat" flux region; and an Average fuel content was used throughout core;
3. No Magnox cladding elements were present[1];
4. The reactors were encased in "silicon killed mild steel" supports[2] measuring 8.5cm on the bottom, 10cm on the sides and 4.5cm on the top of the reactor;
5. The coolant gas was taken as pure CO_2, with a density of 0.054 g/cc[3], coolant gas was static in the system (e.g. no flow);
6. The core graphite was taken as being a homogenous carbon medium, with no gaps, cracks or voids other than the fuel rod/control rod channels;
7. Control rods (black and grey) were inserted 5% on average through the reactors lifetime;

[1] Due to the low thickness and neutron capture cross sectional area, moderation and capture effects were assumed to be negligible for the Magnox cladding elements. Appendix 15 – Testing the model expands on this assumption

[2] In reality, these have holes on the top and base, and are ring supports on the side of the reactors, but given there reflective properties, it was a conservative assumption to model them all as a solid structure

[3] Equivalent to CO_2 gas at 360°C and 20 atmospheres of pressure

8. Modelling of the reactor temperature in MCNP and FISPACT occurred at default values of standard temperature and pressure (STP).

Modelling used a spatial resolution of one chargepan radially (~80 cm) and 1 meter axially. However, in the extreme regions (the edges of the core axially and radially), this resolution increased to 25 cm intervals. This provided a final investigated array of the reactor definable by a 13x13 grid.

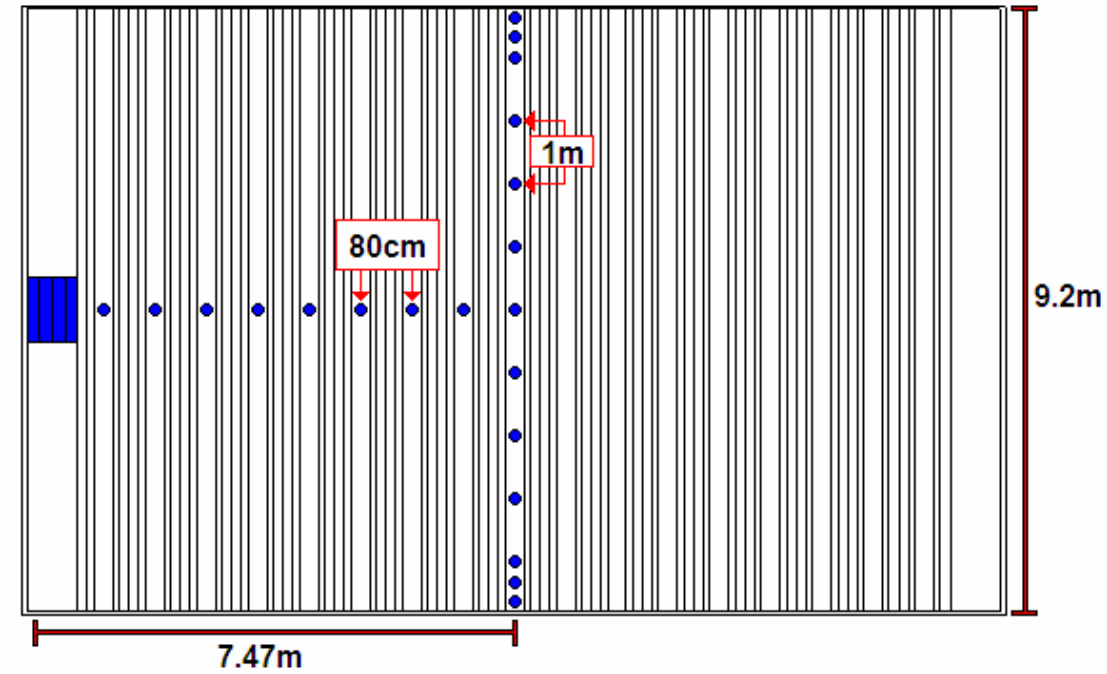

Figure 12: Reactor core for Sizewell A showing fuel channels on a vertical cut away and the points sampled using MCNP highlighted in blue

Figure 12 shows the spatial distribution of points sampled within the core to make up a 13x13 array of points to be analysed within Sizewell A. Wylfa uses a 15x15 array at the same dimensions due to its larger size.

5.2.2 Activation Analysis Assumptions and clarifications

The following assumptions were made to assist in the analysis of the modelling work and the subsequent reporting of the information;

1. No volatilisation of radionuclides due to temperature/chemistry;
2. No loss or gain of radionuclides/precursors into or from the reactor coolant;
3. Data presented is an <u>averaged</u> value across the whole core (unless otherwise stated), and individual points will have an activity that may be higher or lower than the one stated;
    a. All data is given in units of Bq/m^3 unless otherwise stated;
4. All data is given 100 years after reactor shutdown, unless otherwise stated;
    a. 31st December 2106 for Sizewell;
    b. 31st December 2109 for Wylfa;
5. No decay heat present in the core;
    a. All thermal power within the core is due to fission of uranium -235;
    b. All (non neutrino) fission energy (202.5 MeV) is deposited in the core;
    c. Each fission of uranium-235 results in 2.426 neutrons being emitted;

6. All graphite is the same grade and there are no uncertainties in the precursor information;
    a. Reactor graphite is PGA or PGB;
7. Reactor thermal power histories are correct to those supplied for each reactor;
8. Flux follows a radial symmetry around the core;

Due to there being no viable information on actual reactor fluxes, a first principles estimation was required. These calculations used relative fluence, as calculated by MCNP, and turned them into flux. This was done by taking a few known parameters to make a 'first principles' assumption on flux. It was assumed that all energy in the core was due to direct fission of uranium-235, and each fission released 202.5 MeV of energy that was absorbed into the core. This could be converted into MWh/fission, and given a known thermal power history, converted into fissions/MWh. It is known that each fission of uranium-235 emits 2.426 neutrons on average, so given a known number of fissions per MWh, the number of neutrons in the core can be calculated. Conversion into neutrons/MWh into neutrons/s can then be made, and by multiplication with MCNPs' relative fluence value (n/cm^2/neutron) a value for flux can be predicted at a particular location within the core.

These calculations used the previously stated assumptions on thermal power histories for each reactor and the fission energy of uranium-235.

5.3 Limitations of the Model

The methodology used to model generation and evolution of the radioactive inventory of core graphite is split into 2 parts. The first part uses MCNP to predict the neutron field in which the graphite is exposed; the second part uses FISPACT to calculate the resulting neutron activation and generation of radionuclides within the graphite matrix. There is naturally a compromise in the development of the model between maximising accuracy and resolution and what is needed and practical. For example a highly complex MCNP model would require significant run time to yield results and could become unmanageable. However in this project the situation is helped by the relatively simple repeated structure of the Magnox core and the data requirements of the programme. These requirements are to provide inventories of sufficient accuracy and precision to help decisions about future graphite management options. Thus the models have been developed to meet this objective.

Calculations using MCNP and FISPACT within this report are subject to several limiting factors. These are either factors that are too complex to be modelled accurately, or involve the use of information that was not available. These limitations and assumptions have been recognised and are listed below, with brief discussions about how they were addressed and the likely effects on the inventory where appropriate.

5.3.1 MCNP Calculations

Identified limitations that may have an affect on the MCNP modelling predictions and subsequent activation calculations include;

1. Use of a 'static' system model involving:
    a. No change in fuel burn-up with time
    b. Fixed control rod positions while reactor is operating
    c. Fixed graphite bulk properties, these are assumed to be constant and no effects of aging is included
    d. No growth of neutron poisons in reactor materials
    e. No changes in reactor operating conditions from the base conditions.

2. Prediction of an average neutron energy spectrum for each location in the core graphite
3. Modelling of neutron spectrum at long reactor core axis
4. Calculation output is a relative neutron fluence
5. MCNP cannot model different types of chemical bond that may alter neutron transport (carbon bonded to carbon in graphite may have different properties to carbon bonded to oxygen in CO_2)
6. Any geometrical irregularities not known cannot be modelled

Limitation	UKAEA Response
No fuel burn-up	Average U-235 content used for the fuel
Cannot vary control rod position	Average control rod position taken [8]
Model cannot age graphite properties during the run	To be addressed alongside comprehensive active results[4]
Model cannot account for reactor poisoning	To be addressed alongside comprehensive active results
Events, such as burst cartridges, cannot be accounted for	To be addressed alongside comprehensive active results
Energy Spectrum	For direct comparison to active sample locations, more detailed models were made.
Models only part of the whole reactor	Bessel's function used to predict flux and activity at other points[5]
Calculation gives fluence, not flux	First principles approach to convert thermal power to fissions per second for U-235
Chemical bonding (e.g. of graphite)	All materials modelled as a homogenous mass and assume no effect on neutron transport based on the nature of chemical bond

Table 1: Limitations and the way they were addressed in the MCNP modelling

The MCNP work was, when detailed data was not available, designed to be conservative. For example, when concerned with the energy spectrum, a larger area will be irradiated by a spectrum that is more shifted towards the thermal energy range. This generally predicts higher activation rates for key radionuclides, such as carbon-14, chlorine-36 and cobalt-60.

[4] This will be addressed directly in the active stage when actual samples can be compared to the modelled samples for activity. From this an estimate of the graphite age can be made
[5] Please see Appendix 14 – Derivation of pointwise values of flux in a three-dimensional system (Bessel's function)

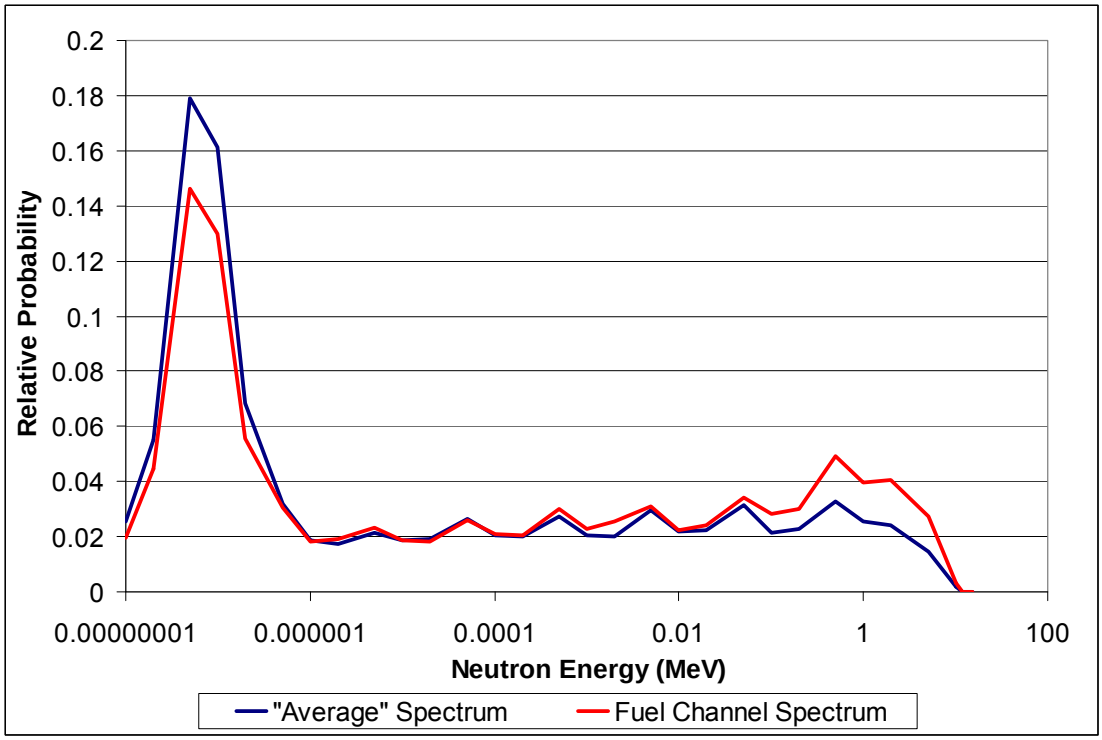

Figure 13: Comparison between the average spectrum used to calculate the inventory, and the spectrum in the graphite facing the fuel channel

Figure 13 shows a comparison between the spectrum used to calculate the inventory at a certain region of the Sizewell A reactor, and the spectrum from that same region, but in a 0.6 cm thick slice of graphite facing the fuel channel (a location where trepanned active samples are taken). This shows that the average spectrum has a much higher thermal spectrum. As a 'rule of thumb', thermal neutrons contribute to activation more than fast by having a higher interaction probability. These two regions are assumed to experience the same flux at any one particular time.

5.3.2 FISPACT Activation Calculations

The following limitations where identified that may have an affect on the FISPACT modelling;

1. Volatilisation/migration of any radionuclides or their precursors is not addressed;
2. Deposition of precursors or radionuclides is not addressed e.g. from reactor coolant or from failed fuel;
3. EAF cross sectional libraries have a degree of uncertainty;
4. Assumes homogenous distribution of atoms.

Limitation	UKAEA response
Volatilisation of radionuclides	To be addressed alongside comprehensive active results
deposition of precursors/activity	To be addressed alongside comprehensive active results
Physical geometry	It is unlikely that there would be any

Limitation	UKAEA response
	affect on activation by physical geometry
EAF cross sectional library errors	Uncertainty analysis will be carried out alongside active sampling
Assumes homogenous distribution of precursors	It is unlikely that there would be any affect on activation by distribution of elemental precursors

Table 2: Limitations and the way they were addressed in the FISPACT modelling

The difficulty in calculating the radionuclide inventory of some isotopes is highlighted by Bruynooghe and Bièth's [10] study of irradiated graphite from the French Bugey 1 reactor. Their calculations greatly overestimated the tritium content and had difficulty reproducing carbon-14 and chlorine-36 distributions across the reactor core. The overestimation of tritium was considered likely due to the calculations not accounting for leakage; whilst the discrepancies in other calculations was considered due to the sensitivity of the activation pathway to the calculated flux, unexpected distribution of impurities, accuracy of original precursor concentrations, degassing and no rational to account for fuel element failure.

This exemplifies the 'real world' effects, not incorporated into the modelling approach, that need to be assessed separately from the model.

5.4 Results – FISPACT analysis

FISPACT calculations provide the radionuclide inventory for key nuclides at different positions radially and axially within the core. Concentrations of different radionuclides were then analysed to predict radionuclide concentrations within the entire core. Extrapolation across the core was achieved using "Bessel's Function", a mathematical algorithm to predict the value at a point based on known values at other points within a cylinder. Appendix 14 – Derivation of pointwise values of flux in a three-dimensional system (Bessel's function) details the theory behind the use of "Bessel's function" in this case. Bessel's Function can typically be implemented for predicting reactor flux [9], however, because activation is directly linked to the flux, the same technique can be applied.

Appendix 9 – Sizewell A Reactor 1 Radionuclide inventory by position radially and axially in the core and reflector regions and Appendix 10 – Wylfa Reactor 1 Radionuclide inventory by position radially and axially in the core and reflector regions contains detailed information on Sizewell and Wylfa inventory data trends. Comments on these trends, as well as those contained within this section are covered in Section 5.6.

Data is presented from calculations using three sets of precursor concentrations for the graphite; Jowett precursors (generic precursor concentrations supplied by RWMD for graphite activation calculations); and NPL measured concentrations (average and maximum values obtained as part of this project).

5.4.1 Sizewell A

Table 3 describes the data obtained by running FISPACT models using a flux calculated from MCNP results [4] for Sizewell A reactor 1. This data presents the average activity over the core for a graphite density of 1.74 te/m^3 (the density of unirradiated PGA graphite).

Nuclide	Jowett Precursors (Bq/m^3)	NPL Precursors (Bq/m^3)	NPL (Average) precursors (Bq/m^3)
H3	5.03E+09	4.92E+09	4.51E+09
C14	3.10E+11	2.05E+11	1.76E+11
Cl36	4.16E+08	2.02E+09	1.54E+09
Na22	N/A	N/A	N/A
Co60	2.07E+05	1.13E+05	7.52E+04
Kr85	7.47E+07	1.01E+05	1.01E+05
Nb94	4.18E+08	6.14E+01	6.57E+02
Ag108m	2.84E+06	N/A	N/A
Sn121m	3.09E+05	6.60E+04	6.59E+04
I129	1.50E+04	2.77E+03	2.77E+03
Cs134	5.16E-04	8.07E-02	8.07E-02
Ba133	3.09E+06	2.04E+06	1.14E+06
Cs137	5.97E+07	8.23E+07	8.20E+07
Pm145	1.78E+06	1.17E+06	1.17E+06
Eu152	2.22E+03	2.36E+04	2.36E+04
Eu154	1.05E+06	4.42E+06	4.42E+06
Eu155	2.22E+03	5.07E+03	5.07E+03
Ho166m	1.75E+07	5.04E+03	5.26E+03

Table 3: Average inventory of Sizewell A reactor 1 as modelled in FISPACT assuming a density of 1.74 te/m^3, values decayed from 2016 to 2106 using MicroShield V7.02

The data in Table 3 shows good agreement between certain key radionuclides, especially Tritium, carbon-14 and Cobalt-60. There are, however, a few key radionuclides particularly chlorine-36 that show a relatively large disagreement. In these cases, the difference in predictions is primarily because of a large difference between the elemental precursors used (see Appendix 2b – Inactive Graphite Analysis by NPL). For chlorine-36, there was a suspected contamination issue, and NPL are currently re-investigating the inactive graphite to improve the chlorine results. In some cases, the Jowett elemental precursors contained precursors not analysed for in the NPL data – this is because these precursors were thought to have no significant impact on the inventory for management/treatment purposes.

A full, detailed inventory for Sizewell A reactor 1 can be found in Appendix 9 – Sizewell A Reactor 1 Radionuclide inventory by position radially and axially in the core and reflector regions.

5.4.2 Wylfa

Table 4 lists the data obtained from FISPACT models using a flux calculated from MCNP results for Wylfa reactor 1. This data presents the average activity over the core for a graphite density of 1.74 te/m^3 (the density of unirradiated PGA graphite).

Nuclide	Jowett Precursors (Bq/m^3)	NPL Precursors (Bq/m^3)	NPL (Average) precursors (Bq/m^3)
H3	5.03E+09	2.99E+10	1.65E+10

Nuclide	Jowett Precursors (Bq/m^3)	NPL Precursors (Bq/m^3)	NPL (Average) precursors (Bq/m^3)
C14	3.13E+11	2.06E+11	1.91E+11
Cl36	3.99E+08	3.11E+09	2.18E+09
Na22	N/A	N/A	N/A
Co60	2.45E+05	1.52E+05	1.10E+05
Kr85	9.46E+07	1.18E+05	1.18E+05
Nb94	4.19E+08	1.15E+02	8.73E+01
Ag108m	1.36E+07	6.71E-03	9.81E-03
Sn121m	3.21E+05	6.99E+04	7.04E+04
I129	1.62E+04	2.63E+03	2.64E+03
Cs134	5.17E-06	2.54E-04	2.54E-04
Ba133	3.50E+06	1.80E+06	8.12E+05
Cs137	6.41E+07	9.60E+07	9.70E+07
Pm145	1.77E+06	1.17E+06	1.17E+06
Eu152	2.19E+04	1.97E+04	1.97E+04
Eu154	4.68E+06	5.77E+06	5.75E+06
Eu155	7.22E+03	6.49E+03	6.48E+03
Ho166m	1.43E+07	6.73E+03	6.89E+03

Table 4: Average inventory of Wylfa reactor 1 as modelled in FISPACT assuming a density of 1.74 te/m^3, values decayed from 2019 to 2109 using MicroShield V7.02

The data in Table 4 shows good agreement between certain key radionuclides, in a similar vain as Table 3. However, unlike the results for Sizewell A, there is a large discrepancy for tritium. This is caused by a large difference in precursor information for lithium between Jowett and NPL precursor information.

5.5 Results – Heavy and transuranic nuclides

Approximately 50 'transuranic' radionuclides were identified as part of this investigation in varying quantities. Doing detailed analysis and regression for all the radionuclides would be a time consuming exercise, as a result, several key radionuclides were identified as being of key concern to waste management and disposal.

These results have only been reported for NPL data as Uranium and Thorium were removed[6] in the Jowett precursor information. This was done as originally it was thought that the trace amounts of uranium and thorium would not have a significant impact on the inventory.

All activity data is averaged across the core and reported in Bq/m3, assuming a graphite density of 1,740 kg/m^3.

Nuclide	Sizewell A Activity (Bq/m^3)	Wylfa Activity (Bq/m^3)

[6] John Jowett precursor information contains 82 elemental precursors, however, for the purposes of this investigation, Uranium and Thorium were not included as they were previously regarded as having little impact on the waste inventory based on the RWI

Nuclide	Sizewell A Activity (Bq/m^3)	Wylfa Activity (Bq/m^3)
U235	1.67E+00	1.57E+00
U238	2.39E+02	2.56E+02
Pu239	4.44E+05	4.74E+05
Pu240	9.71E+05	9.75E+05
Pu241	1.03E+08	1.12E+08
Am241	3.13E+06	3.32E+06
Cm244	1.10E+08	1.28E+08

Table 5: A comparison between the activities of key transuranic radionuclides within Sizewell A and Wylfa decayed to 10 years after reactor shutdown

Nuclide	Sizewell A Activity (Bq/m^3)	Wylfa Activity (Bq/m^3)
U235	1.68E+00	1.59E+00
U238	2.39E+02	2.56E+02
Pu239	4.44E+05	4.75E+05
Pu240	1.44E+06	1.45E+06
Pu241	1.35E+06	1.46E+06
Am241	5.77E+06	6.12E+06
Cm244	3.45E+06	4.00E+06

Table 6: A comparison between the activities of key transuranic radionuclides within Sizewell A and Wylfa decayed to 100 years after reactor shutdown

The data in Table 5 and Table 6 suggest that there is an ingrowth of a few of these key nuclides, namely uranium-235, plutonium-239, plutonium-240 and americium-241. However it should be noted that only plutnoium-240 and americium-241 experience significant ingrowth. This effect is explained by investigating the pathways to each key nuclide.

Daughter		Parent		Decay Method
Nuclide	**Half-life (years)**	**Nuclide**	**Half-life (years)**	**Mode**
U-235	*7.03E+8*	Pa-235	24.5 minutes	Beta
		Pu-239	2.41E+4	Alpha
U-238	*4.47E+9*	Pa-238	2.3 minutes	Beta
		Pu-242	3.76E+5	Alpha
Pu-239	*2.41E+4*	Np-239	2.5 days	Beta

Daughter		Parent		Decay Method
Nuclide	**Half-life (years)**	**Nuclide**	**Half-life (years)**	**Mode**
		Cm-243	28.5	Alpha
Pu-240	*6,537*	Np-240	65 minutes	Beta
		Cm-244	18.11	Alpha
Pu-241	*14.4*	Np-241	13.9 minutes	Beta
		Cm-245	8,500	Alpha
Am-241	*432.2*	Pu-241	14.4	Beta
		Bk-245	4.94 days	Alpha
Cm-244	*18.11*	Am-244	10.1 hours	Beta
		Cf-248	333.5 days	Alpha

Table 7: Parent nuclides, half-lives and decay methods for key transuranic radionuclides, data from RadSum (ORNL)

Table 7 shows potential decay methods for various parent nuclides to daughters. It can be seen in Table 5 and Table 6 that over 90 years curium-244 decays by two orders of magnitude. This is because it undergoes 5 half-lives. Because its parents are very short lived (~1 year at maximum) it will not be regenerated by further decay. These short parent half-lives also explain why there is an initially very high concentration of curium-244. Nuclides which experience significant ingrowth, such as americium-241 do so because they have a relatively long half life compared to its parents,

It was found through separate FISPACT results specialising in single nuclide irradiation (Appendix 12 – Uranium Irradiation and Appendix 13 – Thorium Irradiation) that the results presented in Table 5 and Table 6 were scalable to initial Uranium and Thorium concentrations[7].

Nuclide	Contribution from Uranium	Contribution from Thorium
U235	0.34%	99.66%
U238	99.99%	0.01%
Pu239	99.22%	0.78%
Pu240	99.56%	0.44%
Pu241	99.33%	0.67%
Am241	99.33%	0.67%

[7] NPL precursor information did not reach the limit of detection figure for Uranium and Thorium. For Uranium this was more significant as the LoD achieved by NPL was 500 ng/g (0.5 ppm) whilst it was required to be 1 ppb. In this case, the Jowett figure for Uranium was placed in its stead in order to not be overly pessimistic.

Nuclide	Contribution from Uranium	Contribution from Thorium
Cm244	99.83%	0.17%

Table 8: Percentage contribution from Uranium and Thorium to daughter transuranic nuclide, based on Wylfa data

Table 8 breaks down where certain key transuranic radionuclides are generated, based on FISPACT irradiation.

5.6 Results – Observations and comments

5.6.1 Radionuclide data trends

The interpretation of final FISPACT predicted inventories is helped by the pathway analysis to important nuclides (given in Appendix 9 – Sizewell A Reactor 1 Radionuclide inventory by position radially and axially in the core and reflector regions and Appendix 10 – Wylfa Reactor 1 Radionuclide inventory by position radially and axially in the core and reflector regions). The process of generating nuclides can be complex involving various activation routes to nuclides, sometimes involving different precursor elements or intermediates. Precursors can also be burnt-out by activation (and also formed) depending on their concentration, the neutron flux and time. Short lived nuclides can decay and some nuclides can themselves be activated to generate other nuclides which may in their turn be precursors to other nuclides. FISPACT can also fission appropriate radionuclides to provide fission product radionuclides.

In the following sections some observations are made for some important nuclides based on FISPACT activation data (Appendix 9 – Sizewell A Reactor 1 Radionuclide inventory by position radially and axially in the core and reflector regions and Appendix 10 – Wylfa Reactor 1 Radionuclide inventory by position radially and axially in the core and reflector regions) . Units of Bq/kg are assumed, unless otherwise stated.

Generally, the FISPACT data demonstrates close agreement between the two reactor inventories for all key isotopes, suggesting that extrapolation of the model to predict other reactor inventory may be feasible. Additionally, comparison between the two reactors modelled shows a very high degree of similarity in predicted activities by FISPACT (when utilising the same precursor data), as can be seen in Table 9, suggesting a scalability of the model across different reactors. The eight radionuclides discussed in this section have been highlighted as the key 8 for short, medium and long term decommissioning and disposal.

5.6.1.1 Tritium

Direct comparison of the modelled tritium content of Sizewell A and Wylfa is shown in table 9 using Jowett precursors.

Nuclide	Sizewell A (Bq/m^3)	Wylfa (Bq/m^3)
H3	5.03E+09	5.03E+09

Table 9: Tritium content of Sizewell A and Wylfa based on John Jowett elemental precursors

This close agreement indicates that, as modelled, the tritium content is not sensitive to overall neutron flux over the lifetime of the two reactors. To confirm this, pathway analysis was carried out (Section 5.6.2).

However the NPL laboratory results from the analysis of inactive graphite samples (Appendix 2b – Inactive Graphite Analysis by NPL) indicate lithium concentrations that are much higher in Wylfa the other reactors analysed (Figure 2) and it is therefore not appropriate, in the case of tritium, to assume the same precursor inventory for Wylfa. Modelling using NPL data for lithium precursor concentrations indicate higher Tritium levels for Wylfa compared to Sizewell.

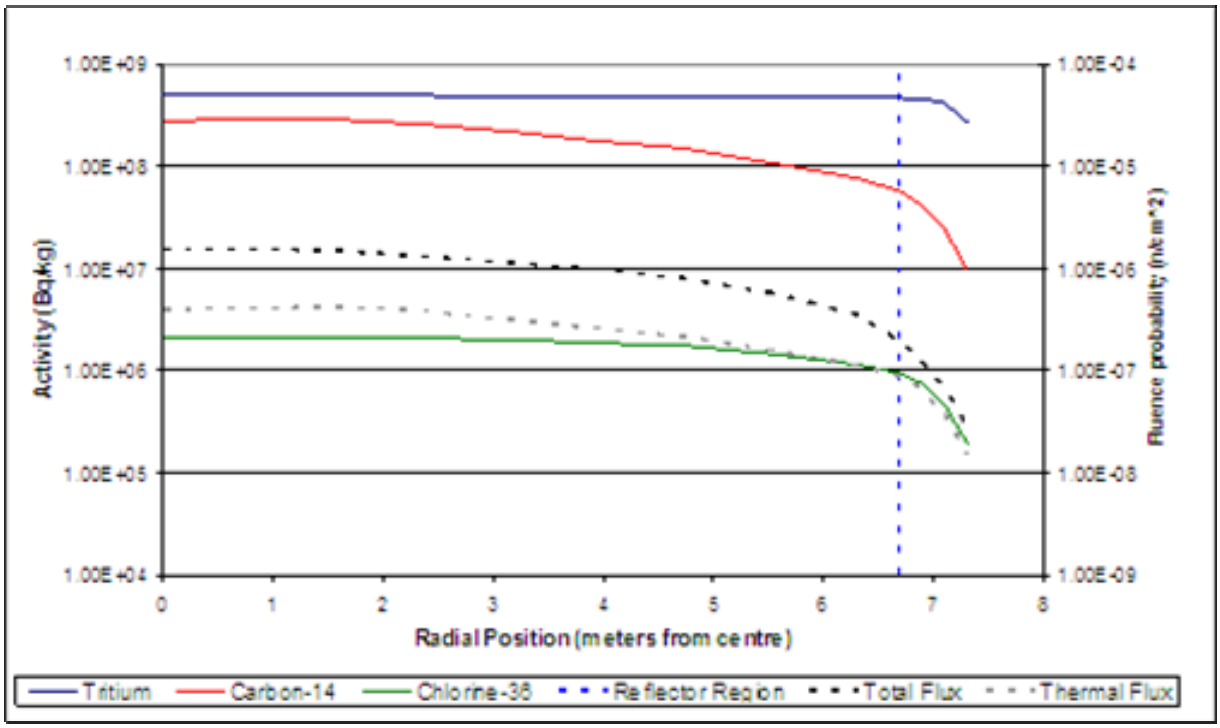

Figure 14: Activity trends for tritium, carbon-14 and chlorine-36 compared to alteration in relative fluence of thermal and total flux

The predicted tritium inventory is relatively independent of flux, staying relatively constant throughout the fuelled region. It is only in the outer edges of the reflector region that there is a sharp drop in tritium content. This suggests that at places with lower total neutron dose the lithium precursor to tritium not completely exhausted, and that where there is complete burn out of lithium-6, the tritium concentration is maintained by re-activation of the helium-3 decay product of tritium.

5.6.1.2 Carbon-14

The modelled carbon-14 concentration shows a similar behaviour to tritium in that the Sizewell and Wylfa activities using the Jowett elemental precursors are very similar, supporting a case for extrapolation of the model across the fleet of Magnox reactors.

Also, the provided Jowett nitrogen precursor inventory is in agreement with the laboratory results for the inactive graphite samples analysed under this project. This results in the calculated carbon-14 activities being similar, regardless of which precursor sets are used– ranging from the lowest concentration of $1.76e^{11}$ Bq/m^3 to the highest of $3.13e^{11}$ Bq/m^3.

Carbon-14 appears to follow thermal flux very closely; as a result, activities in the reflector region are much lower than in the core.

Carbon-14 can be generated from either nitrogen-14 or carbon-13 with the dominate path dependent on their relative proportions. As the carbon-13 concentration is a naturally abundant isotope in carbon, this precursor will provide a lower limit of carbon-14 generation,

below which inventories will not drop irrespective of the nitrogen precursor concentration., however, nitrogen-13 is a more favourable precursor to carbon-14, having a higher neutron capture cross sectional area.

5.6.1.3 Chlorine-36

Chlorine-36 follows the same trend as carbon-14 and tritium of having similar activities in both reactors when comparing the equivalent calculations with Jowett precursors.

A comparison between Jowett and NPL precursors calculations indicates, as expected, a higher chlorine-36 activity associated with higher NPL precursor concentrations. This higher precursor concentration is thought to arise from a contamination issue in the samples, and NPL are currently re-investigating chlorine precursor concentrations of inactive graphite. The ratio of the final activities to the elemental precursors for chlorine for each model suggests that chlorine-36 is present entirely as an activation product from elemental chlorine – chlorine-35, as also demonstrated in pathway analysis in Appendix 11 – Pathway Analysis.

Chlorine-36 follows the same trend as carbon-14 in that as the thermal flux decreases, as does its activity; however, the relationship is not quite as linear.

5.6.1.4 Cobalt-60

Cobalt-60 concentrations follow a similar trend as seen for chlorine-36, dropping loosely with flux. This suggests that there is a faster burn-up in the centre of the reactor.

Because of its short half-life, cobalt-60 activity drops by approximately two orders of magnitude of activity every 30 years.

5.6.1.5 Caesium-137

Through pathway analysis (Appendix 11 – Pathway Analysis) it is observed that caesium-137 comes from two different sources. Utilising the Jowett precursors yields caesium-137 from direct activation of naturally occurring xenon-136 (9% of elemental xenon), which was not analysed for by NPL during the inactive testing. However, in the NPL precursor FISPACT models, caesium-137 primarily came from uranium and thorium fission, which was not included in models run using the Jowett precursors. As a result, caesium-137 activity will be approximately twice that reported in Table 3 and Table 4.

However, it was found that caesium radionuclides were burnt out in the reactor (Appendix 16 – NPL Active Graphite Analysis), and as a result, further inactive testing would not yield better predicted data by FISPACT analysis.

Analysing the trend of caesium-137, it follows a similar trend to carbon-14 which is closely linked to the thermal flux. As a result, caesium-137 activities are much lower in the reflector region.

5.6.1.6 Europium

Europium activities are on average higher in Wylfa than for Sizewell A. This is explainable by analysing the activity trends with flux. Europium activities increase dramatically depending on flux – lower fluxes tend to increase europium activities dramatically.

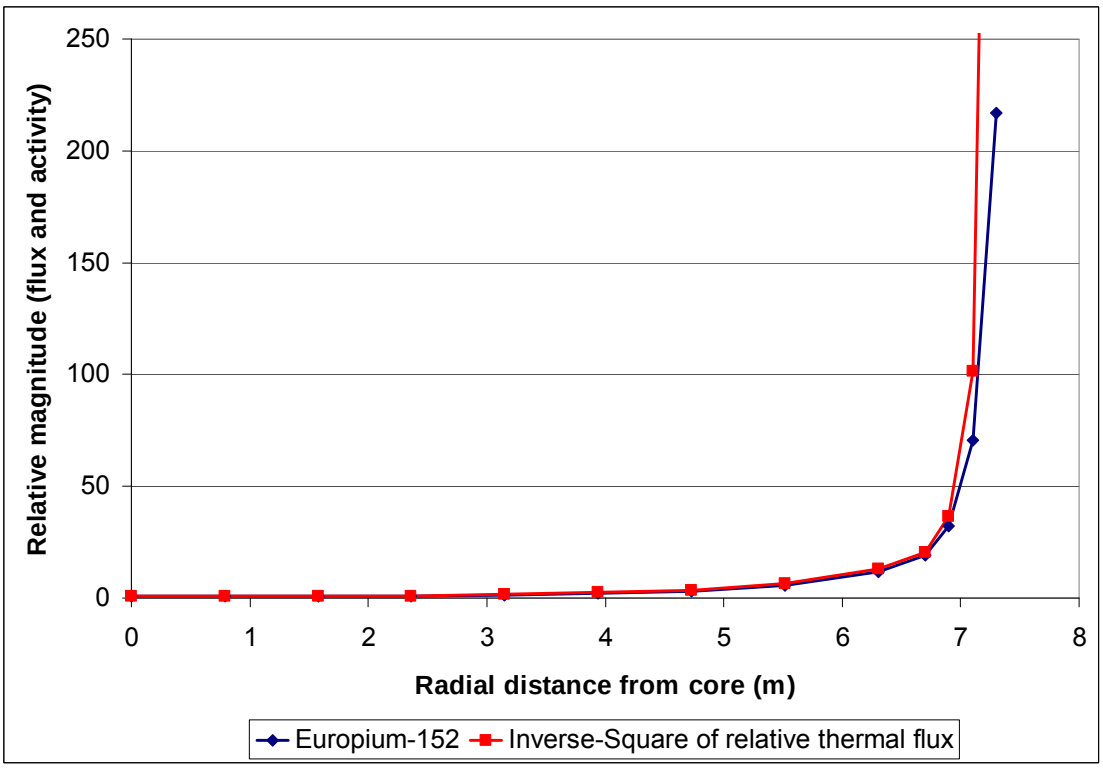

Figure 15: A comparison of relative euoropium-152 magnitude to the inverse square of relative flux in Sizewell A

Figure 15 demonstrates a comparison between europium-152 activity and the inverse square of flux radially in the Sizewell A core. This shows a good degree of comparison up to the very outer edge of the reactor core.

Because europium activities are so dependant on flux, the larger unfuelled reflector region in Wylfa results in a higher europium activity by up to an order of magnitude.

5.6.1.7 Summary

Analysis of the key radionuclides reveals that there is good scalability of across the two reactors. This suggests that estimates of other reactors inventories could potentially be made to a sufficient sensitivity to support graphite management/treat and disposal option assessments, based on their elemental precursors. To underpin this conclusion additional active sample analysis for the two reactors modelled is required.

UKAEA has also been asked to complete laboratory inventory analysis (inactive and active) for Hunterston A core graphite. This data will allow the preposition that the model can provide a simple extrapolation method to determine other Magnox core inventories can be tested.

5.6.2 Pathway Analysis

Pathway analysis is a sensitivity study that is carried out in FISPACT. It allows daughter nuclides to be linked with parent nuclides and activation/decay chains identified. These pathways identify how much of a particular radionuclide product is made up from a particular parent, and hence, how sensitive the output is to changes in precursor information.

Pathway analysis was carried out for eight key radionuclides, as these are the ones expected to have the most significant impact on any long or short term decommissioning options.

The Jowett precursor information was analysed for Sizewell A and Wylfa in the centre of the core and the very outer edge of the reflector region. This allowed for a direct comparison of how activation in both reactors occurred, and similarities and differences to be drawn up and observed. The Jowett precursor data set was used in this example as it had the same elemental composition for both reactors.

Full pathway analysis, showing complete decay and activation chains, for the reflector and core region radially for both reactors using all precursor data sets can be found in Appendix 11 – Pathway Analysis.

Radionuclide	Parent nuclide	Wylfa		Sizewell	
		Centre	Reflector	Centre	Reflector
H-3	*Li-6*	92.5%	~100%	93.5%	~100%
	C-12	4.5%		4%	
	H-1	1%		1%	
C-14	*N-14*	70%	72%	70%	72%
	C-13	29.5%	28%	30%	28%
	O-17	0.1%	0.1%	0.1%	<0.1%
Cl-36	*Cl-35*	95%	99.5%	95.5%	~100%
	S-34	4%	0.5%	3.5%	<0.1%
Cobalt-60	*Co-59*	69%	~100%	71%	~100%
	Ni-58	16.5%	<0.1%	13.5%	<0.1%
	Fe-56	4.5%		3.5%	
	Fe-57	2.5%		2.5%	
	Fe-58	7%	0.1%	6.5%	<0.1%
Cs-137	*Xe-136*	98.5%	~100%	99%	~100%
	Cs-133	0.5%		0.5%	
Eu-152	*Nd-148*	24.5%	0.5%	24.5%	0.5%
	Nd-150	14.5%	34%	14.5%	1%
	Sm-147	22%		22%	
	Sm-148	16.5%	0.5%	16.5%	<0.5%
	Sm-149	2%	64%	3%	62.5%
	Sm-150	2%	34%	2.5%	33.5%
	Eu-151				2.5%
Eu-154	*Nd-150*	13.5%		13.5%	
	Sm-147	20%		18.5%	
	Sm-148	15.5%		15%	
	Sm-149	4%	4%	~6.5%	2%
	Sm-150	4%	1%	~5.5%	0.5%
	Sm-152		48.5%		43%
	Eu-151		~21%		~22%
	Eu-153		27.5%		32%
Eu-155	*Nd-150*	8.5%		8.5%	
	Sm-148	10%		9.5%	

Radionuclide	Parent nuclide	Wylfa		Sizewell	
		Centre	Reflector	Centre	Reflector
	Sm-149	2.5%	1.5%	4%	3%
	Sm-150	2.5%	1%	3.5%	0.5%
	Sm-152		42%		36.5%
	Sm-154	36%	9%	36%	11%
	Eu-151		19%		~18%
	Eu-153		26.5%		30%

Table 10: A summary of the pathway analysis investigation showing the parent nuclides that lead rise to a selection of radionuclide products (results based on 10 years of decay after reactor shutdown)

Table 10 shows the parent nuclides, and their relative contributions, that give rise to eight specific daughter nuclides; tritium, carbon-14, chlorine-36, cobalt-60, caesium-137, europium-152, 154 and 155. These nuclides are of significant radiological importance in the short, medium and long terms. This data suggests a very high degree of comparison between the two reactors in each specific zone, whilst there is a much bigger difference within each reactor in the core and reflector region. This would suggest that there is a certain amount of scalability between reactors with a similar chargepan layout, but different thermal histories and precursor information.

It was found that the presence of tritium was primarily due to a regenerative route. Here, tritium is formed through activation of lithium-6, and then undergoes radioactive decay itself to form helium-3. This decay product is then itself reactivated, as can be seen in Table 11 and Table 12.

Radionuclide	Parent Nuclide	Pathway	Contribution to final activity (Sizewell A)	Contribution to final activity (Wylfa)
H-3	Li-6	Li6(n,a)H3(b-)He3(n,p)H3	83.5%	80.5%
	C-12	C12(n,a)Be9(n,a)He6(b-) Li6(n,a)H3(b-)He3(n,p)H3	2%	2.5%

Table 11: Pathway analysis investigating tritium regeneration for the core region of Sizewell A and Wylfa

Radionuclide	Parent Nuclide	Pathway	Contribution (Sizewell A)	Contribution (Wylfa)
H-3	Li-6	Li6(n,a)H3(b-)He3(n,p)H3	60.5%	62%

Table 12: Pathway analysis investigating tritium regeneration for the reflector region of Sizewell A and Wylfa

This data shows that this regenerating route accounts for roughly 85% of tritium radionuclides in the core, and roughly 65% in the reflector, assuming no helium is released from the graphite [10]. The data in Table 11 is consistent with literature, which suggests a figure of 85% of all tritium found in reactor graphite is formed through regeneration [6].

5.6.3 Neutron energy spectra

A neutron energy spectrum is the relative probability of a neutron existing at a particular energy. This is calculated using Monte Carlo techniques to show general energy trends at different locations within the core. MCNP will typically calculate this to be relative to the entire region of interest (e.g. normalised to the probability of the neutron existing at any location at any energy within the reactor). However, by normalising these figures to themselves (e.g. the sum of the area under the curve is equal to one) it is possible to make direct comparisons between different locations and reactors, independently of a reactors actual power history.

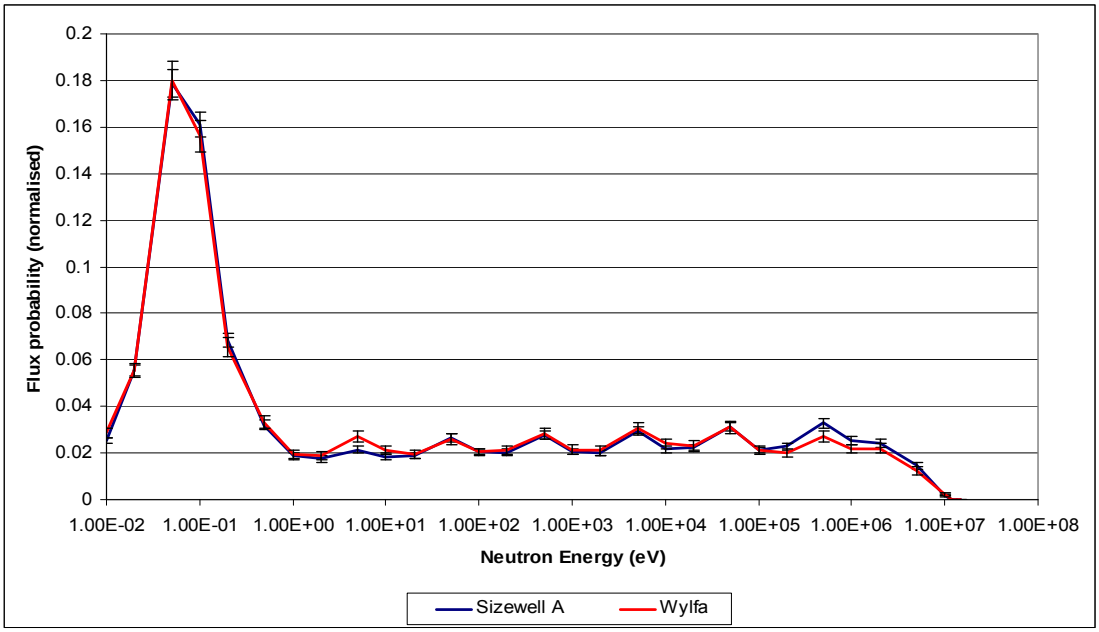

Figure 16: A comparison of neutron energy spectra in the centre of the core in Sizewell A and Wylfa

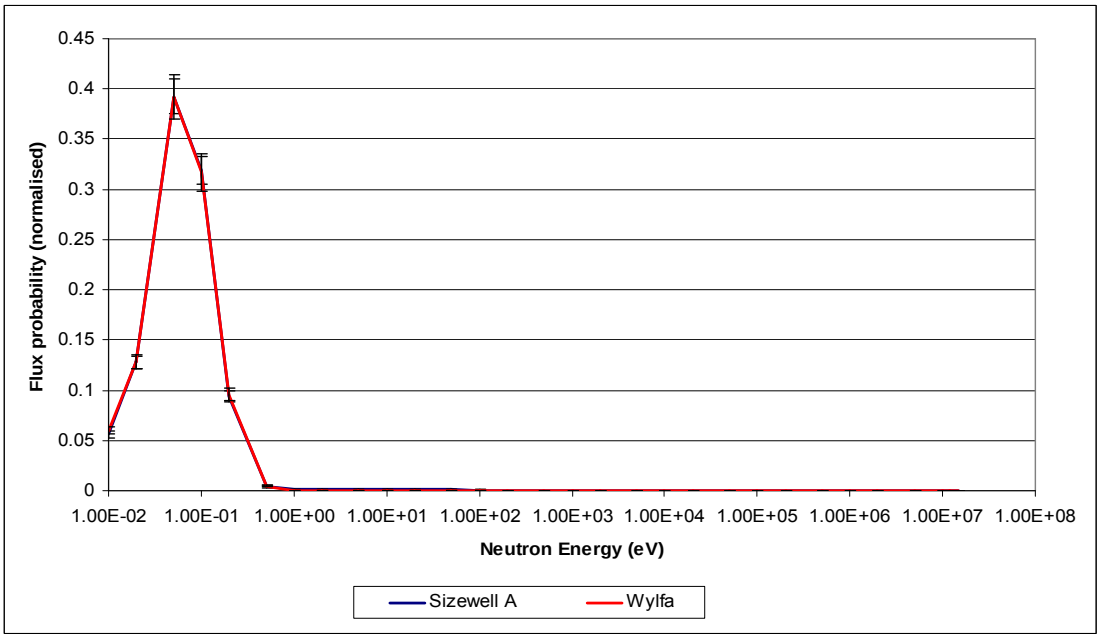

Figure 17: A comparison of neutron energy spectra in the outermost radial reflector in Sizewell A and Wylfa

Figure 16 and Figure 17 show a comparison of the two neutron energy spectra for the core and reflector regions in Sizewell A and Wylfa. It can be seen that they follow a very close comparison. This suggests that similar reactors will experience similar neutron irradiation for a given power. This is of particular interest as Sizewell A had half the volume and ran at a lower thermal power and achieved a remarkably similar spectrum at these points.

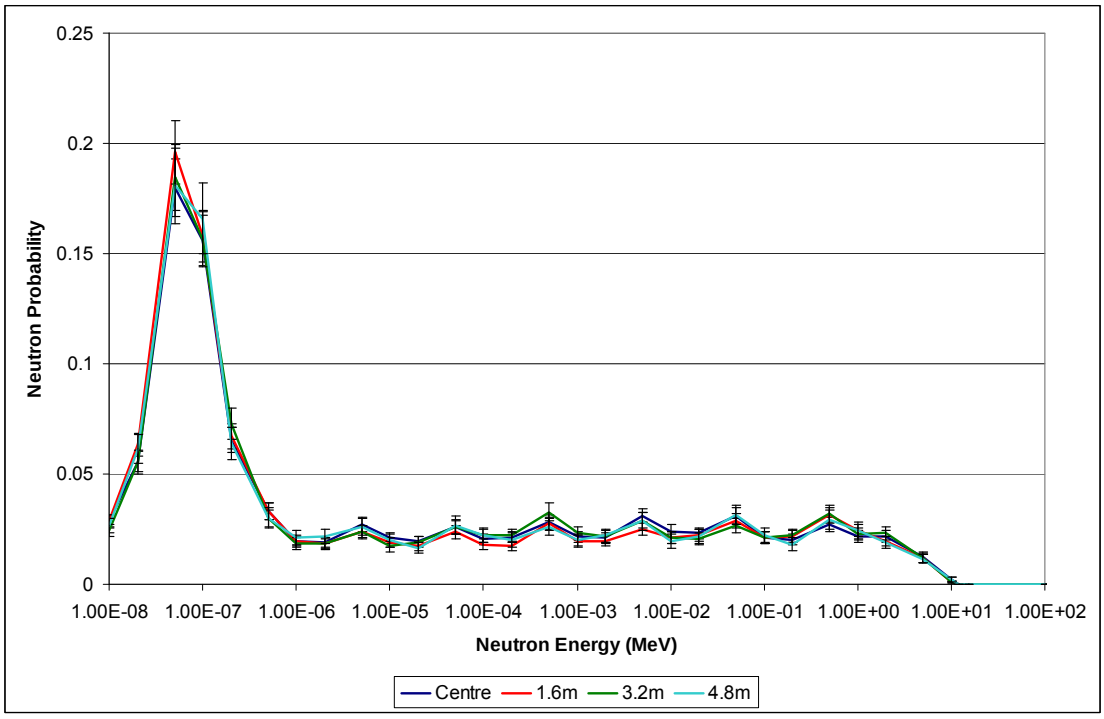

Figure 18: A comparison of four normalised neutron energy spectra located at four points radially from the core centre (in metres) for Wylfa

Figure 18 shows four neutron energy spectra within Wylfa. These are located at different points radially, at the centre and 1.6, 3.2 and 4.8m from the centre. These show a good level of comparison. There is a slight disagreement at 1.6m in the thermal-epithermal region; however, this is within the computational error margin (5%) for the MCNP calculation.

This implies that throughout the fuelled region of the core, neutron energy spectra are relatively comparable. Comparing Figure 18 with Figure 17, however, shows that in the reflector region, much of the fast flux (>1eV) drops off. This is because there is no new fuel generating fast neutrons. The increase in thermal and epithermal neutrons would increase activation if not for the decreased flux in these regions.

When each reactor is exposed to the same thermal loading factor, the neutron flux is very similar (within 10%) at comparable locations (such as the very centre of the core). This is likely due to the two reactors having a similar power density across the graphite, due to them having similar designs and fuel rod spacing.

6 COMPARISON WITH 2007 RWI

The 2007 RWI describes the stocks of radioactive waste held in the UK at 1 April 2007. It also predicts wastes that could arise from the operation and decommissioning of current facilities and gives information on materials that could be classified as waste in the future. The 2007 Inventory contains details of over one thousand individual wastes that have been reported by organisations responsible for their management.

Of these individual waste streams, 9H311 and 9F312 describe graphite waste for Wylfa reactor 1 and Sizewell A reactor 1. These were caculated by Magnox Electric using a Lotus 123 spreadsheet [11]. This used basic activation rates and pathways to predict an activity based off a given set of elemental precursors. The 2007 RWI reports a graphite density of 1,250 kg/m^3, and reports activities in units of TBq/m^3.

This section compares the RWI07 to the inventory derived during this report which has used laboratory analysed inactive graphite precursor data and detailed MCNP and FISPACT modelling. Where possible, the assumptions and units have been carried through. It should be highlighted that the comparisons made are, therefore, between the results of inventory predictions from two models which use broadly similar methods and assumptions, and not with actual measurements of activity in graphite.

6.1 Assumptions and clarifications

Several assumptions were made when using FISPACT calculations – these are detailed in Section 5.2.2 previously;

6.2 Sizewell A – Reactor 1

Table 13 (below) lists some key nuclides from the 2007 RWI for Sizewell A and compares it to those calculated as a result of this report. Overall, three sets of data have been compared to the RWI; Calculations based on Jowett Precursors, and the maximum and average precursors found by inactive graphite analysis by NPL (Section 3.2).

Nuclide	RWI	Jowett (Bq/m^3)	NPL Max (Bq/m^3)	NPL Average (Bq/m^3)
H3	1.00E+09	3.61E+09	3.53E+09	3.24E+09
C14	1.00E+11	2.23E+11	1.47E+11	1.27E+11
Cl36	3.00E+08	2.99E+08	1.45E+09	1.11E+09
Na22[8]	N/A	0.00E+00	0.00E+00	0.00E+00
Co60	3.00E+04	1.49E+05	8.09E+04	5.40E+04
Kr85	N/A	5.37E+07	7.26E+04	7.25E+04
Nb94*	8.00E+05	3.00E+08	4.41E+01	4.72E+02
Ag108m*	2.00E+06	2.04E+06	0.00E+00	0.00E+00
Sn121m	2.00E+08	2.22E+05	4.74E+04	4.74E+04
I129	N/A	1.08E+04	1.99E+03	1.99E+03
Cs134	N/A	3.70E-04	5.80E-02	5.80E-02
Ba133	2.00E+05	2.22E+06	1.47E+06	8.19E+05
Cs137	N/A	4.29E+07	5.91E+07	5.89E+07

[8] Rows greyed out were not quantified in the 2007 RWI

Nuclide	RWI	Jowett (Bq/m^3)	NPL Max (Bq/m^3)	NPL Average (Bq/m^3)
Pm145	8.00E+04	1.28E+06	8.43E+05	8.43E+05
Eu152	6.00E+03	1.60E+03	1.70E+04	1.70E+04
Eu154	1.00E+05	7.51E+05	3.17E+06	3.17E+06
Eu155	N/A	1.60E+03	3.64E+03	3.65E+03
Ho166m	3.00E+06	1.26E+07	3.62E+03	3.78E+03

Table 13: Comparison of key radionuclides between the 2007 RWI and FISPACT calculations based on NPL and Jowett precursor information for Sizewell A

Analysis of Table 13 was carried out to compare trends between the RWI and FISPACT calculations carried out utilising the Jowett and NPL (maximum and average) precursors. Several observations and comments were made from the information in Table 13;

- UKAEA calculations predicts generally higher activities;
    - Potentially due to FISPACT using more activation chains, and included more precursors than the existing RWI calculations considered;
- Neither UKAEA calculations or RWI07 calculations accounted for any leeching or volatilisation of nuclides;
    - This has been outlined in Section 5.3 as a limitation of the model;
    - The Lotus spreadsheets used to calculate the existing RWI are not thought to account for this,;
- Up to a factor of three difference in H-3 activity is predicted;
    - It is unknown if RWI07 accounted for regeneration of tritium which accounts for ~80-85% of activity at end of life (Appendix 11 – Pathway Analysis);
        - Li6(n,a)H3(b-)He3(n,p)H3;
        - Less in the reflector region (~65%);
        - This regeneration route is in agreement with published material [6];
- General agreement in carbon-14 activity predictions;
    - FISPACT calculations utilising the NPL gave very close agreement to the existing RWI07;
- Up to a factor of five difference in chlorine-36 activity measurements;
    - The inactive graphite provided for analysis is suspected to have been contaminated with chlorine given higher chlorine precursors compared to Jowett levels;
- Up to a factor of five difference in cobalt-60 activity measurements;

- Activity calculations based on analysis fo the inactive graphite samples by NPL give better agreement to the RWI than that based on equivalent Jowett calculations.

6.3 Wylfa – Reactor 1

Table 14 (below) compares the existing RWI07 to the analysis carried out using FISPACT on the three sets of elemental precursors for Wylfa. A comparison of elemental precursors can be found in Appendix 3 – Inactive Graphite Comparison.

Nuclide	RWI	Jowett (Bq/m^3)	NPL Max (Bq/m^3)	NPL Average (Bq/m^3)
H3	2.00E+09	3.61E+09	2.15E+10	1.19E+10
C14	7.00E+10	2.25E+11	1.48E+11	1.37E+11
Cl36	2.00E+08	2.87E+08	2.23E+09	1.57E+09
Na22	N/A	0.00E+00	0.00E+00	0.00E+00
Co60	3.00E+04	1.76E+05	1.10E+05	7.88E+04
Kr85	N/A	6.79E+07	8.45E+04	8.50E+04
Nb94	2.00E+05	3.01E+08	8.24E+01	6.27E+01
Ag108m	2.00E+06	9.79E+06	4.82E-03	7.04E-03
Sn121m	1.00E+08	2.30E+05	5.02E+04	5.05E+04
I129	N/A	1.17E+04	1.89E+03	1.90E+03
Cs134	N/A	3.72E-06	1.82E-04	1.82E-04
Ba133	1.00E+05	2.51E+06	1.29E+06	5.83E+05
Cs137	N/A	4.61E+07	6.90E+07	6.97E+07
Pm145	7.00E+04	1.27E+06	8.42E+05	8.42E+05
Eu152	2.00E+05	1.58E+04	1.41E+04	1.41E+04
Eu154	3.00E+05	3.36E+06	4.14E+06	4.13E+06
Eu155	N/A	5.19E+03	4.66E+03	4.65E+03
Ho166m	2.00E+06	1.03E+07	4.83E+03	4.95E+03

Table 14: Comparison of key radionuclides between the 2007 RWI and FISPACT calculations based on NPL and John Jowett precursor information for Wylfa

Observations and comments;

- FISPACT predicts generally higher activities than 2007 RWI;
- Up to a factor of ten difference in tritium activity predictions;
  - Utilising NPL precursors, especially the maximum recorded value, tritium levels are higher, this is due to higher lithium concentration (Figure 2); and possibly the inclusion of the pathway to tritium from helium-3.
  - Utilising Jowett precursor information, there is only a minor difference between the FISPACT calculated and RWI07 figure for tritium;
- Up to a factor of three difference in carbon-14 activity predictions;

    - It is unknown why the values reported in the 2007 RWI for carbon-14 activity for Wylfa 2007 RWI is slightly less than those reported for Sizewell A;

    - The analysis of the inactive graphite by NPL found that Nitrogen (the primary precursor, along with carbon-13 for carbon-14 activation) was very similar for all samples analysed in all reactors for all grades (PGA and PGB) and shows inventories higher than that reported in the RWI07;

- Up to a factor of ten difference in chlorine-36 activity measurements;

    - Again, due to the higher chlorine-36 levels reported in NPL measurements which may reflect sample contamination

- Up to a factor of five difference in cobalt-60 activity measurements;

    - As seen previously in the Sizewell data, cobalt-60 activity is less in the calculations based on inactive graphite precursors measured for this project by NPL than from the Jowett precursors and is more consistent with that reported in RWI07;

        - This is because the inactive graphite measurements recorded lower elemental cobalt concentration (Section 3.2).

6.4 Discussion of Results

The results provided in the above section allow comparison of model predictions of radioactive inventory. The RWI07 data is calculated using a predicted flux history and a generic list of precursor concentrations.

The UKAEA provided data are derived from a MCNP/FISPACT model developed as part of this work, combined with a generic list of precursors (Jowett) or reactor specific precursors measured by this project. A comparison of the John Jowett and reactor specific precursors can be found in Appendix 3 – Inactive Graphite Comparison.

Therefore differences in the inventory predictions between the RWI07 and this project originate from either the code treatment of important processes (flux and activation etc) within the model, or differences in input data (precursor concentrations, flux levels, operating history) used by the model. Neither of the models take into account other processes that could alter radioactive inventories such as the impact of coolant flow or volatilisation of radionuclides.

Analysis of data from Sections 6.2 and 6.3 reveals several common trends between the data. These relate to how the FISPACT calculations (utilising both Jowett and NPL analysed precursor information) compare to the existing RWI07;

- Generally, this project has returned slightly higher activities that reported in the RWI07;

    - This is likely due to differences in precursor information and FISPACT considering more activation routes and pathways;

- Generally, however, there is good agreement to the 2007 RWI on key nuclides when considering all sets of precursor data;

- Especially carbon-14, tritium and cobalt-60;

- Chlorine-36 results have been affected by contamination of samples during chlorine precursor testing, NPL are currently re-investigating chlorine precursors in inactive graphite;

- However, with the exception of carbon-14, there are noted variations in the results based on the three sets of precursors –Jowett, NPL (maximum) and NPL (average) although these are unlikely to influence significantly considerations of graphite management, treatment or disposal options.

7 ACTIVE GRAPHITE AND COMPARISON WITH MODEL PREDICTIUONS

NPL has undertaken analysis of the available active samples retrieved from Berkeley Centre store for the Sizewell A reactor. Further analysis is to be conducted on additional samples from Sizewell A and Wylfa and Hunterston A in future work.

Due to sample recovery delays, only limited active graphite sample analysis has been performed at the writing of this report. The samples analysed (from Sizewell A) were extracted from a graphite core located in fuel channel 1215, graphite block 2 and 10, with slices 1 and 3 from each. These will be referred to as;

- 1215/10/1;
- 1215/10/3;
- 1215/2/1;
- 1215/2/3.

It should be noted that the above nomenclature does not reflect which sample was nearest to the fuel channel in a core. This information was not available and as a result, when concerning NPL active analysis, slices are given the "A" or "B" suffix in place of the slice numbers "1" or "3". It is also worthy of note that the two slices from a graphite core were held in contact with each other in a plastic bag and therefore surface contamination is a possibility.

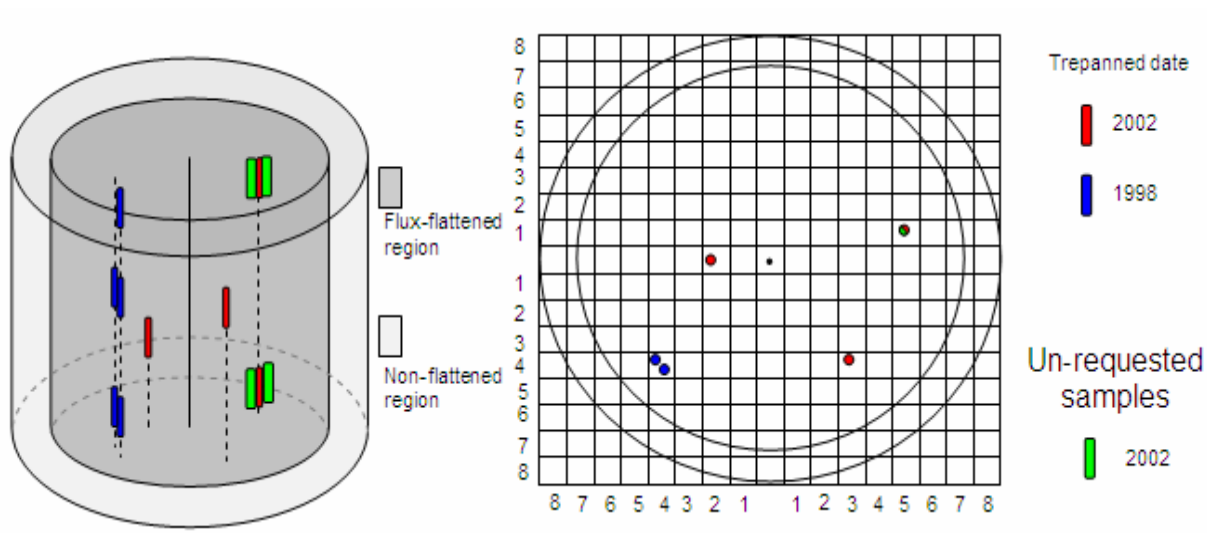

Figure 19: Location of samples analysed

Figure 19 shows the location (marked in green) of the samples analysed by NPL inside the Sizewell A core.

7.1 NPL Active Analysis

Appendix 16 – NPL Active Graphite Analysis provides the data obtained from laboratory analysis.

Since the analysis methods are destructive, the samples provided from the higher regions of the core were used to measure concentrations of transuranic elements on the basis that any elements introduced from burst cartridges may be transported by the coolant gas. The lower region samples are to be analysed for lighter radionuclides. However, all samples will subject to gamma spectroscopy.

7.2 Comparison to modelling work

The following section compares inventories predicted by the UKAEA FISPACT modelling using measured inactive graphite precursor data as described in Section 5 with the results of active sample analysis. Detailed comparison information can be found in Appendix 17 – Comparison to FISPACT modelling.

Many results were below the limit of detection, which were very low, typically a few tens of Bq/g or lower. Therefore, only those results above the Limit of Detection are discussed in the following sections, with the exception of Caesium.

Error analysis on the MCNP and FISPACT calculations has not been undertaken yet, but will be part of future work.

7.2.1 Cobalt 60

Co60	Calculated Activity (FISPACT)				NPL Analysis	
	Average (Bq/g)		Max (Bq/g)		A	B
Nuclide	1	3	1	3	Bq/g	Bq/g
1215/10: Co60	9209	9388	14020	14290	9570 ± 790	13800 ± 1200
1215/2: Co60	9047	9225	13770	14040	23100 ± 1900	12200 ± 1100
Range	9047 - 14290 Bq/g				8780 - 15000 Bq/g	

Table 15: Cobalt-60 activity comparison for Sizewell A for all active samples

Table 15 shows a comparison between the calculated activities of cobalt-60 for Sizewell A samples. The active sample laboratory analysis results agree with UKAEA's model predictions using measured inactive graphite precursor quantities.

7.2.2 Caesium 134/137

Cs134/137	Calculated Activity (FISPACT)				NPL Analysis	
	Average (Bq/g)		Max (Bq/g)		A	B
Nuclide	1	3	1	3	Bq/g	Bq/g
1215/10: Cs134	1001000	1004000	1001000	1004000	27 ± 3	27 ± 5
1215/2: Cs134	992700	995600	992700	995600	62 ± 6	65 ± 7
1215/10: Cs137	303.8	309.2	303.8	309.2	25 ± 4	24 ± 4
1215/2: Cs137	295.8	301	295.8	301	41 ± 6	47 ± 6
Range: Cs134	992700 - 1004000 Bq/g				22 - 72 Bq/g	
Range: Cs137	295.8 - 309.2 Bq/g				20 - 53 Bq/g	

Table 16: Caesium activity comparison

Table 16 describes the comparison between predicted and measured activity. Here, unlike in the case of cobalt-60, there is a large difference. This difference can be explained by the inaccurate levels of precursors used in the model for caesium-134 and caesium-137, as well as the volatilisation of caesium nuclides. NPL are currently repeating inactive graphite analysis on various precursor concentrations, including caesium. These have been revised down based on additional inactive analysis for relevant elements (caesium and uranium).

7.2.3 Barium 133

Ba-133	Calculated Activity (FISPACT)				NPL Analysis	
	Average (Bq/g)		Max (Bq/g)		A	B
Nuclide	1	3	1	3	Bq/g	Bq/g
1215/10: Ba133	267.5	273	478.7	488.6	313 ± 24	306 ± 24
1215/2: Ba133	261.8	267.2	468.5	478.2	732 ± 54	874 ± 64
Range	261.8 - 488.6 Bq/g				282 - 938 Bq/g	

Table 17: Barium activity comparison

Table 17 compares barium-133 activities for samples analysed computationally using FISPACT and physically by NPL and shows good agreement for one core. Samples 1215/2/A and B report twice the activity of samples 1215/10/A and B. This could mean that there is a localised region of higher precursor concentration.

7.2.4 Europium 154/155

Eu 154/155	Calculated Activity (FISPACT)				NPL Analysis	
	Average (Bq/g)		Max (Bq/g)		A	B
Nuclide	1	3	1	3	Bq/g	Bq/g
1215/10: Eu154	1677	1618	1677	1618	923 ± 65	918 ± 66
1215/2: Eu154	1744	1683	1744	1683	558 ± 41	624 ± 45
1215/10: Eu155	903.6	883.3	903.6	883.3	458 ± 46	447 ± 45
1215/2: Eu155	934	913.4	934	913.4	273 ± 29	301 ± 31
Range: Eu154	1618 - 1744 Bq/g				517 - 988 Bq/g	
Range: Eu155	903.6 - 934 Bq/g				244 - 504 Bq/g	

Table 18: Europium activity comparison

Table 18 shows the predicted activity for europium nuclides (calculated using FISPACT) compared to measured activities by NPL. Here, there are three evident points of interest;

- Europium inactive radionuclide precursors were below the Limit of Detection, as can be seen by the maximum and average activities being the same; and therefore an upper bound for the precursor is provided by inactive graphite analysis;

- Calculated and measured activities are similar, roughly to a factor of 2 which may reflect the upper bounding limit used for precursor concentrations;

- Europium 154 has an activity that is roughly twice that of europium-155; this effect is seen in both the modelled and measured results.

Interestingly, there is a higher activity at the top of the reactor (1215/10) than at the bottom (1215/2). For europium, this suggests that there is a lower flux at the top than the bottom (europium radionuclides tend to get burnt out in high fluxes, see Appendix 9 – Sizewell A Reactor 1 Radionuclide inventory by position radially and axially in the core and reflector regions). This could be because of control rods lowering flux. This would be consistent with results seen in Section 7.2.3 where barium activities are lower than they are at the bottom.

7.3 Discussion of the results

At this stage it is difficult to draw many conclusions from the active analysis results as only a limited number of samples have been analysed and a number of important nuclides are still to be measured.

Analysis and comparison of the results generally show a good agreement with those modelled. In the case of cobalt-60, UKAEA's model results based on measured inactive precursor data is in close agreement with the inventory measured in the active graphite sample. This provides confidence that UKAEA's model accuracy for predicting radionuclide inventory.

The active results also indicate that certain nuclides e.g. niobium and silver, (not measured in the inactive graphite samples for this project) are not present in significant activities, which would suggest that precursor concentrations for these nuclides are lower than indicated in the Jowett data set, and therefore may not be significant.

8 SUMMARY AND FURTHER WORK

8.1 Summary

The objectives of this report were to;

- Report full laboratory analysis data of inactive graphite samples from both modelled reactors and other Magnox stations;
- Further modelling to include high fidelity calculations inside the reflector regions and inclusion of reactor support structure;
- Full reactor activation calculations using the complete set of measured graphite elemental precursors;
- Comparison of the modelled radionuclide inventory with the UK 2007 RWI;
- Preliminary comparison to available active graphite sample results;
- Investigate the scalability of results between reactors by comparing calculated activities and radionuclides trends along with specific reactor data.

Inactive analysis was carried out on graphite samples from five reactors; Wylfa, Oldbury, Sizewell A, Trawsfynydd and Hinkley Point A. It concluded that for many precursors there was a good degree of agreement between results, however in some cases there were significant variance between reactors. This was especially true for chlorine and lithium precursors. NPL are currently reassessing chlorine precursors due a suspected contamination issue with the samples.

Modelling was carried out on the Sizewell A and Wylfa reactors and yielded full trends of radionuclide inventories. However, several limiting factors were highlighted concerning the shape of the flux profile in the reactor which may have an effect on the overall inventory. It was observed that activities between the two reactors were comparable in some cases, especially when precursor information was similar.

Results from the modelling were analysed and compared against the existing 2007 RWI. This revealed that key radionuclides showed good agreement between the modelled inventory and the reported inventory. The model generally predicted marginally higher activities. It was concluded that this is because FISPACT accounts for more pathways and precursors than the existing RWI.

It was concluded that reactor inventories could potentially be quite scalable. Results between Sizewell A and Wylfa were similar, given similar precursors; this was evident when comparing results between the two reactors when Jowett and measured graphite precursors were used. This is likely because both reactors had a similar lifetime loading factor of ~75% thermal power and similar chargepan design. Assuming other reactors have a similar chargepan design/fuel spacing (power density), there would likely be a good degree of scalability.

8.2 Further work

UKAEA with NPL is expecting to analyse more active graphite samples from Wylfa and Sizewell A reactors for validation of model predictions. The timescale for this is dominated by the timescale to access the samples. These results will be issued in a further report, along comments on the uncertainty in the computational analysis and graphite density loss, and any potential effects of burst fuel cartridges on the activity of graphite.

In addition UKAEA has been asked to incorporate Hunterston A graphite sleeve and core, inactive and active samples into its laboratory campaign. This data will allow UKAEA to test its preposition that detailed modelling can be used for simple extrapolation to provide sufficiently accurate inventory information across the Magnox fleet to support graphite management, treatment and disposal considerations.

Further inactive graphite assessments are being made by NPL for key precursors requiring further attention to improve model accuracy. For example, in the case of chlorine, there was a suspected contamination issue, so further active analysis is being carried out to improve the fidelity of these results. These will be used to scale the FISPACT calculated activities by considering activation pathways.

9 REFERENCES

1 Parry, S. and Cox, J. (June 2009) Graphite Characterisation (Stage 1- Define Characterisation Programme). UKAEA/TSG(09)0532.

2 The 2007 UK Radioactive Waste Inventory, NDA-RWMD, NDA/RWMD/004, March 2008.

3 NDA Final Strategy, April 2006 (www.nda.gov.uk)

4 Parry, S and Lansdell, A Graphite Characterisation Interim Report (Stage 2 – Inactive Analysis and Inventory Modelling), UKAEA/TSG(09)0607, December 2009

5 Implementation of Archive Group Recommendations – Securing the Magnox Materials Archive: Task 3 Inactive Graphite, Metcalfe, M.P., NNL (09) 10006, Issue 1, February 2009.

6 Production, Location and Retention of Tritium in Irradiated Graphite, SA/RJCB/RD03510001/R02, Issue 2, Marsden BJ, July 2002

7 Production, Location and Retention of Carbon-14 in Irradiated Graphite, SA/RJCB/RD03510001/R01, Issue 2, Marsden BJ, July 2002

8 Private Communication with Denis Buckley, Magnox South, 3rd August 2009

9 Nuclear Reactor Engineering: Reactor Systems Engineering, Fourth Edition, Volume 2, S. Glasstone, A. Sesonske, 1994

10 Bruynooghe, C., Bièth, M., Grappling with Graphite, Nuclear Engineering International, February 2009.

11 A Review of the Magnox Reactor Activation Inventories, Hancock, R, 2004

APPENDIX 1: GRAPHITE SAMPLES RETRIEVED

NNL Magnox Graphite Pallet #	NNL crate #	Description	Station	Grade	No. of samples removed from archive	Further detail follows in Table:	Removed form store	Comment
23	Box 102	Compressive strength & unrestrained growth spares	Wylfa R1	PGA & PGB	74 & 12	3	YES	Heat no 7934 and 8954 Unrestrained growth samples were not found. No replacement taken.
23	Box 97	Vented Chem pots	Wylfa R1	PGA	33	N/A	YES	Only 31 (of original 33 off) samples present in Box 97
23	Box 95	Enclosed Chem pots	Wylfa R1	PGA	36	N/A	YES	
53	Box 160 Box 161	Controls	Sizewell R1	PGA	~90 ~90	4 5	YES YES	
56	Box 253	Controls	Sizewell R1	PGB	154	6	YES	
53 (crate NNL03)	Box 198	Controls (for Channel 8, set 587)	Oldbury R1	PGA	98 (12 bags x single sample; 43 bags x double sample)	7	YES	Swapped in for Box 184 185 186; Box 198 HELD by UKAEA*
53 (crate NNL03)	Box 444	Controls (for Channel 8, set 583)	Oldbury R1	PGA	97 (13 bags x single sample; 42 bags x double sample)	8	YES	Swapped in for Box 184 185 186
53	‘Box‘ 3 ‘Box‘ 5 ‘Box’ 6	Chem samples (Parallel)	Oldbury R1	PGB (Heat 472 472 444)	16 14 16	9	YES YES YES	Small Cardboard boxes of samples rather then ‘ice-cream’ tubs
56	Box 429 Box 432 Box 433	Stored energy Long Long	Traws R1	PGB PGA PGA	28 (number unchecked) 75 “ 60 “	10 11 12	YES YES YES	

NNL Magnox Graphite Pallet #	NNL crate #	Description	Station	Grade	No. of samples removed from archive		Further detail follows in Table:	Removed form store	Comment
57	Box 273	Comp.	Hinkley Point A	PGA	~130	“	13	YES	
	Box 274	Comp		PGA	~190	“	14	YES	
	Box 275	Oxi.		PGA	~70	“	15	YES	
		Oxi		PGA	~70	“	16	YES	
57	Box 276 Box 296	Stored energy	Hinkley Point A	PGB	38	“	17	YES	

Table 19 Unirradiated graphite samples retrieved from Magnox’s archive, Downton

* Pallet 53 (crate NNL03), Box 198 – These graphite samples are for use in both this Graphite Characterisation study and the Graphite Behaviour study by UKAEA Ltd for the NDA. Therefore, these samples have been subdivided. The samples listed in Table 20 have been supplied to NPL for analysis, the remaining samples have been retained by UKAEA Ltd at Manor Court, for future supply to The University of Manchester for inclusion in the Graphite Behaviour study.

Table 20 Samples from Pallet 53 (crate NNL03), Box 198 supplied to NPL for analysis

Sample Serial No.	Samples per package	Sample Serial No.	Samples per package	Sample Serial No.	Samples per package
8702C	2	8721C	2	8743C	2
8706C	2	8729C	2	8744C	2
8712C	2	8730C	2	8745C	2
8715C	2	8731C	2	8753C	2
8720C	2	8742C	2	8754C	2

Total mass of material (including plastic bags) = 168 g. Approximate total mass of graphite = 150 g

APPENDIX 2A – ANALYTICAL METHODS USED FOR EACH ELEMENTAL ANALYSIS

Element	Analysis method
Chlorine	Ion Chromatography
Nitrogen	Combustion and chemiluminescence
Barium	ICP-MS
Beryllium	ICP-MS
Boron	ICP-OES with pre-concentration
Caesium	ICP-OES with pre-concentration
Calcium	ICP-OES
Cerium	ICP-OES
Cobalt	ICP-MS
Copper	ICP-MS
Europium	ICP-MS
Gadolinium	ICP-MS
Iron	ICP-OES
Lithium	ICP-OES
Magnesium	ICP-OES
Molybdenum	ICP-MS
Neodymium	ICP-MS
Nickel	ICP-MS
Potassium	ICP-OES with pre-concentration
Rubidium	ICP-MS with pre-concentration
Samarium	ICP-MS
Selenium	ICP-MS
Sodium	ICP-OES with pre-concentration
Strontium	ICP-OES with pre-concentration
Tellurium	ICP-MS
Thorium	ICP-MS
Uranium	ICP-MS
Zinc	ICP-MS

APPENDIX 2B – INACTIVE GRAPHITE ANALYSIS BY NPL

Analyses of inactive graphite (unvalidated as of 11-Dec-09)			Pallet 57 Hinkley 1 Oxidation Channel 1-5 Grade A	Pallet 57 Box 276 Hinkley1 Oxidation Channel 6-0 Grade A	Pallet 57 Box 296 Hinkley 2 All Channels Grade B	Box 274 Hinkley 1 Compressive Channel 6-0 Grade A	Pallet 57 Box 273 Hinkley 1 Compressive Channel 1-5 Grade A	Pallet 56 Box 429 Trawsfynydd K All channels Grade B	Pallet 56 Box 432 Trawsfynydd K Channel 5 Grade A	Pallet 56 Box 433 Trawsfynydd K Channel 6-0 Grade B	Pallet 53 NNL01 Box161x Sizewell 1 grade A Channel 8 Set 388	Pallet 53 NNL01 Box160 Sizewell 1 Grade A Channel 8 Set 387	Pallet 56 Box 253 Sizewell 1 Grade A All channels	Pallet 53 NNL04 Oldbury 1 Box 4, 5, 6	Pallet 53 NNL03 Box 444 Oldbury 1 Grade A Channel 8 Set 583	Oldbury Box 198 PGA	Pallet 23 Box 102 Wylfa	Wylfa 1 Box 97	Wylfa 1 Box 95
Sample	**Units**	**Detection limit**	**Hinkley Point A Station**					**Trawsfynydd**			**Sizewell A Station**			**Oldbury**			**Wylfa**		
Chlorine	ng/g	10	8680	1810	2220	961	1290	1730	633	607	2260	2240	3490	2780	2010	3480	5620	1990	4220
Nitrogen	ng/g	100	7800	10600	6500	5300	6600	5500	6400	4000	13300	11100	5600	12300	5700	4100	13000	9900	10500
Barium	ng/g	10	157	115	348	47	63	219	22	52	95	1120	1790	317	218	100	1390	163	319
Beryllium	ng/g	0.1	<0.1	<0.1	<0.1	<0.1	<0.093	<0.1	<0.1	<0.1	<0.1	<0.1	<0.1	<0.11	<0.1	<0.1	<0.1	<0.1	<0.1
Boron	ng/g	1	116	116	71	72	66	81	63	62	147	113	71	117	74	<10	120	123	63
Caesium	ng/g	1	<10000	<10000	<9900	11200	9300	<10000	12300	<10000	<10400	<10000	<9900	<11000	<10000	<10000	<9900	<10000	<10000
Calcium	ng/g	100	29600	28500	28100	38900	32900	19200	29000	22800	28500	29800	49000	40500	14800	15300	32000	24700	25000
Cerium	ng/g	100	<100	<100	<99	<100	<93	<100	<100	<100	<100	<100	<99	<110	<100	<100	<99	<100	<100
Cobalt	ng/g	0.1	5.3	4.5	5.8	6.0	3.6	4.6	3.4	3.0	8.2	5.3	14.0	4.0	1.9	3	9.3	6.7	12.0
Copper	ng/g	1	76	53	45	72	56	196	84	57	101	170	156	93	60	49	295	38	69
Europium	ng/g	0.01	<10	<10	<10	<10	<9.3	<10	<10	<10	<10	<10	<10	<11	<10	<10	<10	<10	<10
Gadolinium	ng/g	0.01	10	<10	<10	10	<9.3	<10	<10	<10	<10	10	11	<11	<10	<10	11	<10	12
Iron	ng/g	100	1360	1360	1590	1730	1870	1400	1640	1330	1670	1930	2190	2330	819	830	4460	2650	4010
Lithium	ng/g	0.1	73	<52	<60	71	56	<60	62	<61	73	61	<70	<53	<73	<50	60	224	432
Magnesium	ng/g	1	84	73	179	61	1510	160	103	82	94	213	40	169	73	<10	317	194	226
Molybdenum	ng/g	1	77	67	43	69	93	46	67	52	73	112	43	62	39	33	119	112	134
Neodymium	ng/g	1	<31	<31	<30	<30	<28	<30	<31	<31	<31	<30	<30	<32	<31	<30	<30	<31	<31
Nickel	ng/g	10	668	889	696	1010	606	618	349	205	699	599	1190	550	101	56	962	1220	3090
Potassium	ng/g	10	292	230	199	162	700	289	113	102	209	274	308	243	<10	<10	357	224	124
Rubidium	ng/g	100	<0.1	<0.1	<0.1	<0.1	<0.09	<0.1	<0.1	<0.1	<0.1	<0.1	<0.1	<0.11	<0.1	<0.1	<0.1	<0.1	<0.1
Samarium	ng/g	0.1	31	<31	<30	<30	<28	<30	<31	<31	31	<30	<30	<32	<31	<30	<30	<31	<31
Selenium	ng/g	10	<0.52	<0.52	<0.5	<0.51	<0.47	<0.5	<0.51	<0.51	1.4	<0.51	<0.5	<0.53	<0.52	<0.5	<0.5	<0.51	<0.51
Sodium	ng/g	10	1040	732	597	508	466	1200	308	307	<10	914	795	847	<10	<10	595	611	103
Strontium	ng/g	10	157	84	159	91	93	120	41	61	104	295	358	550	176	140	337	183	226
Tellurium	ng/g	10	<210	<210	<200	<200	<190	<200	<210	<200	<210	<200	<200	<210	<210	<200	<200	<200	<210
Thorium	ng/g	10	<10	<10	<10	<10	<9	<10	<10	<10	<10	<10	<10	<11	<10	<10	<10	<10	<10
Uranium	ng/g	10	<520	<520	<500	<510	<470	<500	<510	<510	<520	<510	<500	<530	<520	<500	<500	<510	<510
Zinc	ng/g	1	56	49	38	30	28	27	48	36	59	129	62	74	39	20	215	55	100

Table 21: Precursor concentrations for inactive graphite samples analysed by NPL and retrieved from Downton National Archive, units are in ng/g (ppb)

Table 21 details the inactive graphite analysed carried out by NPL on the samples retrieved from the Downton National Archive (Appendix 1: Graphite). It can be seen that many of the results have the prefix '<'. This means that the element came in under the achieved LoD. Discussion on LoD's can be found in Appendix 4 – NPL Limits of Detection.

A comparative study based on the analysis carried out into precursor concentrations can be found in Appendix 5 – Comparison of Elemental Precursors (PGA) and **Appendix 6 – Comparison of** Elemental Precursors (PGB)

.

APPENDIX 3 – INACTIVE GRAPHITE COMPARISON

			Sizewell A		Wylfa	
Element	**Jowett (normalised)**	**Magnox Values**	**NPL Average**	**Uncertainty**	**NPL Average**	**Uncertainty**
Chlorine	100.00%	114.45%	381.02%	26.88%	564.14%	46.43%
Nitrogen	100.00%	100.00%	40.00%	39.66%	44.53%	14.77%
Barium	100.00%	22.22%	37.10%	85.23%	23.11%	107.04%
Beryllium	100.00%	N/A	0.37%	LoD	0.37%	LoD
Boron	100.00%	N/A	73.56%	34.50%	68.00%	33.15%
Caesium	100.00%	0.14%	7142.86%	LoD	7142.86%	LoD
Calcium	100.00%	50.11%	81.47%	32.09%	62.03%	15.17%
Cerium	100.00%	0.00%	5.00%	LoD	5.00%	LoD
Cobalt	100.00%	65.20%	36.67%	48.33%	37.33%	28.39%
Copper	100.00%	N/A	44.48%	25.63%	41.88%	104.69%
Europium	100.00%	0.41%	2.13%	LoD	2.13%	LoD
Gadolinium	100.00%	N/A	178.27%	5.59%	195.25%	LoD
Iron	100.00%	400.40%	19.32%	13.47%	37.10%	25.42%
Lithium	100.00%	202.98%	90.66%	9.18%	322.96%	78.11%
Magnesium	100.00%	N/A	55.08%	76.52%	116.98%	25.98%
Molybdenum	100.00%	N/A	33.04%	45.52%	52.90%	9.24%
Neodymium	100.00%	N/A	20.00%	LoD	20.67%	LoD
Nickel	100.00%	58.82%	48.78%	38.14%	103.37%	66.08%
Potassium	100.00%	N/A	8.40%	19.08%	7.48%	49.74%
Rubidium	100.00%	N/A	0.00%	LoD	0.00%	LoD
Samarium	100.00%	24.99%	66.10%	LoD	66.10%	LoD
Selenium	100.00%	0.00%	0.10%	LoD	0.04%	LoD
Sodium	100.00%	N/A	65.73%	85.72%	33.56%	66.18%
Strontium	100.00%	N/A	42.13%	52.42%	41.51%	31.96%
Tellurium	100.00%	N/A	105.00%	LoD	100.00%	LoD
Thorium	100.00%	N/A	34.48%	LoD	34.48%	LoD
Uranium*	**100.00%**	**N/A**	**100.00%**	**LoD**	**100.00%**	**LoD**
Zinc	100.00%	N/A	49.02%	47.49%	72.55%	66.90%

Figure 20: Comparison between NPL (averaged with errors), John Jowett and Magnox RWI precursor information

APPENDIX 4 – NPL LIMITS OF DETECTION

Note; where the achieved LoD is "N/A", the element was in a sufficient quantity to surpass the LoD, so it is unknown what the actual LoD achieved was.

	Requested LoD	Achieved LoD
Chlorine	10	N/A
Nitrogen	100	N/A
Barium	10	N/A
Beryllium	**0.1**	**0.1**
Boron	1	N/A
Caesium	**1**	**10,000**
Calcium	100	N/A
Cerium	**100**	**100**
Cobalt	0.1	N/A
Copper	1	N/A
Europium	**0.01**	**10**
Gadolinium	**0.01**	**10**
Iron	100	N/A
Lithium	**0.1**	**N/A (70)**
Magnesium	1	N/A
Molybdenum	1	N/A
Neodymium	**1**	**31**
Nickel	10	N/A
Potassium	10	N/A
Rubidium	**100**	**0.1**
Samarium	**0.1**	**30**
Selenium	**10**	**1**
Sodium	10	N/A
Strontium	10	N/A
Tellurium	**10**	**210**
Thorium	**10**	**10**
Uranium	**10**	**500**
Zinc	1	N/A

Table 22: This table details the requested and achieved limits of detection, those where LoDs were achieved are marked as N/A

APPENDIX 5 – COMPARISON OF ELEMENTAL PRECURSORS (PGA)

The following elements did not reach there LoD, and hence have not presented graphically;

- Beryllium
- Caesium
- Cerium
- Europium
- Gadolinium
- Lithium[9]
- Neodymium
- Rubidium
- Samarium
- Selenium
- Tellurium
- Thorium
- Uranium

[9] Lithium achieved LoD for Wylfa, however there is evidence of contamination here due to a large increase in Lithium concentration for a few results, as a result, PGA Lithium data will be presented, but not PGB, which did not reach LoD

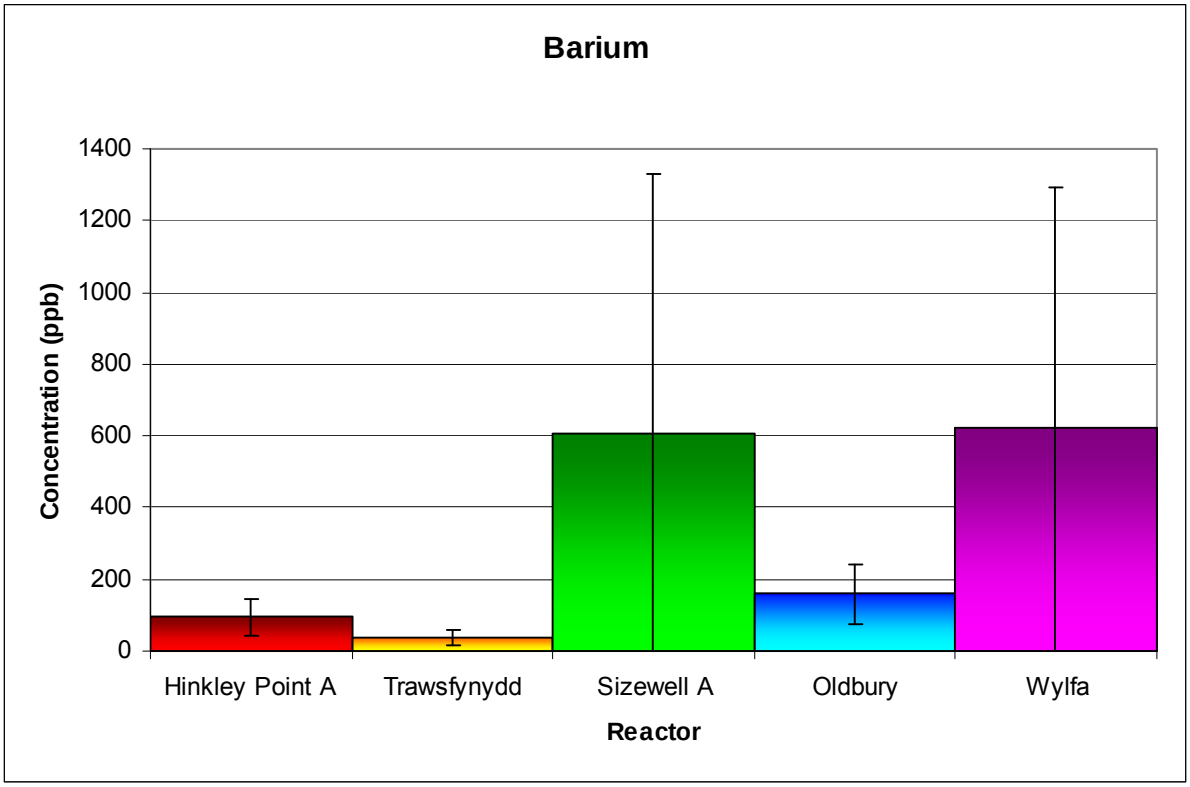

Figure 21: Comparison between reactors for PGA graphite for Barium

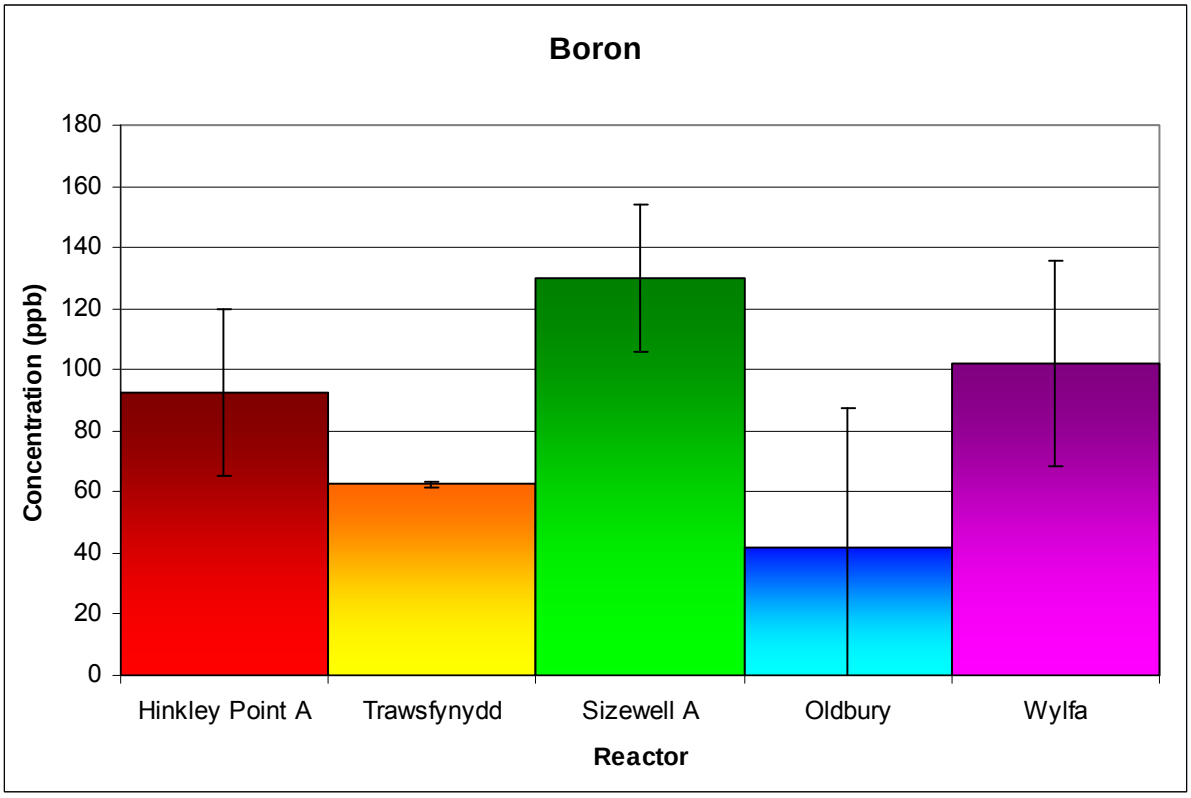

Figure 22: Comparison between reactors for PGA graphite for Boron

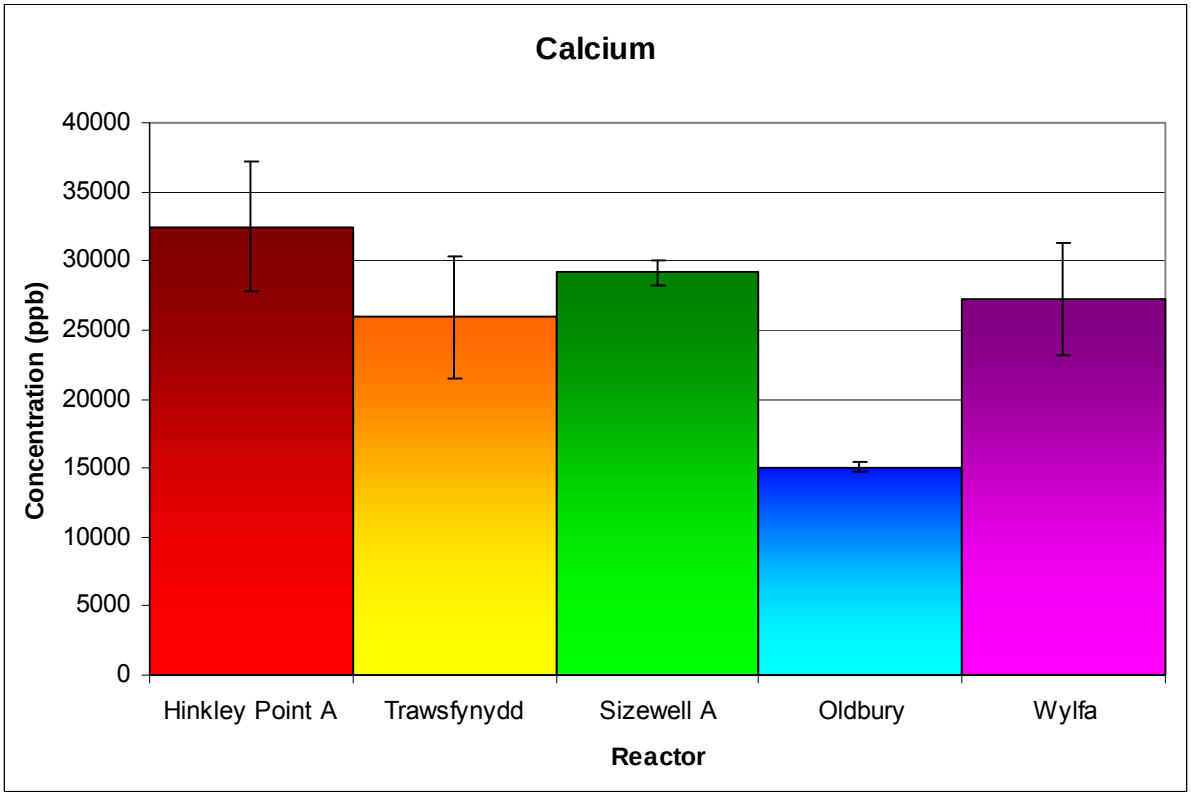

Figure 23: Comparison between reactors for PGA graphite for Calcium

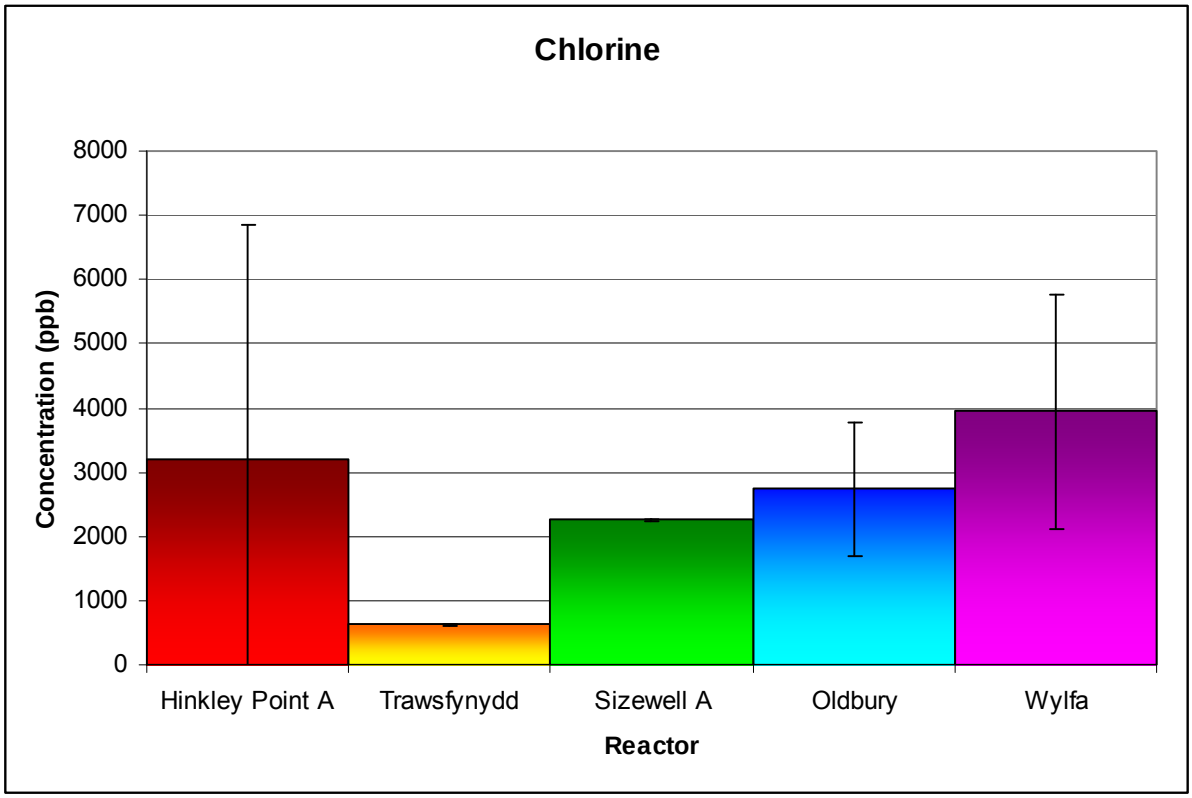

Figure 24: Comparison between reactors for PGA graphite for Chlorine

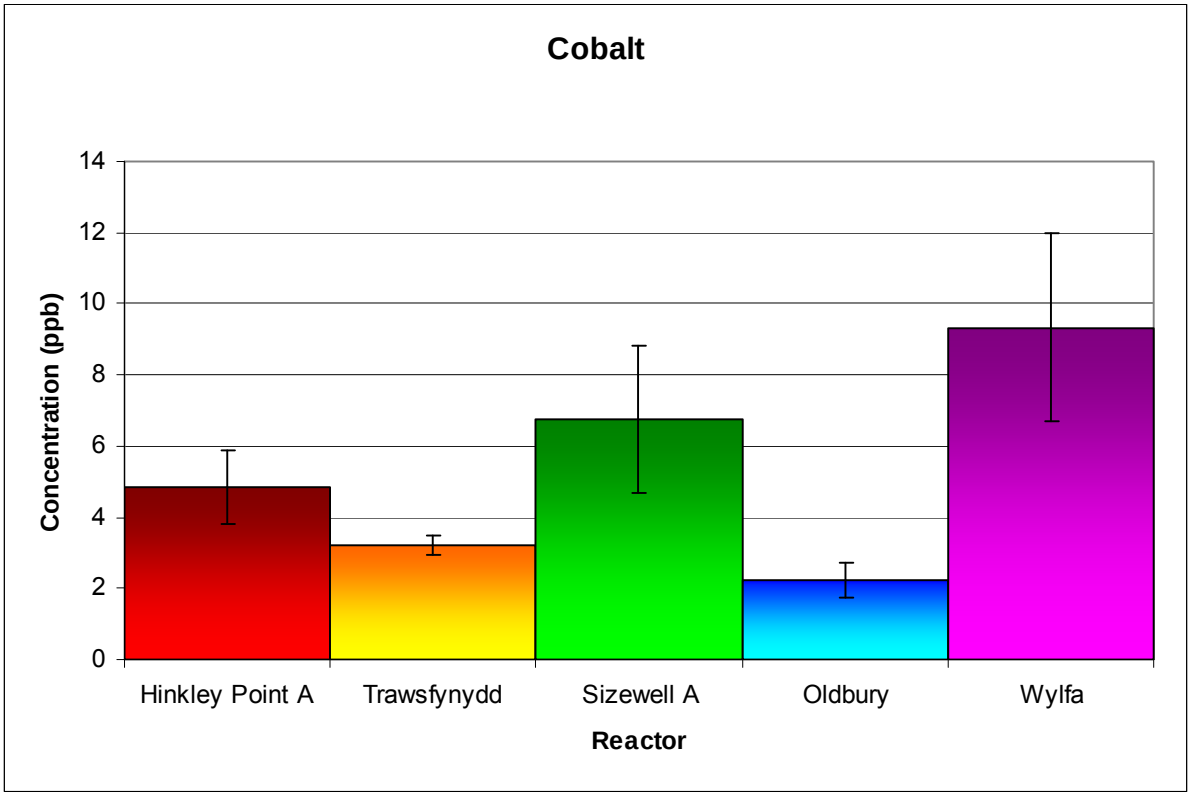

Figure 25: Comparison between reactors for PGA graphite for Cobalt

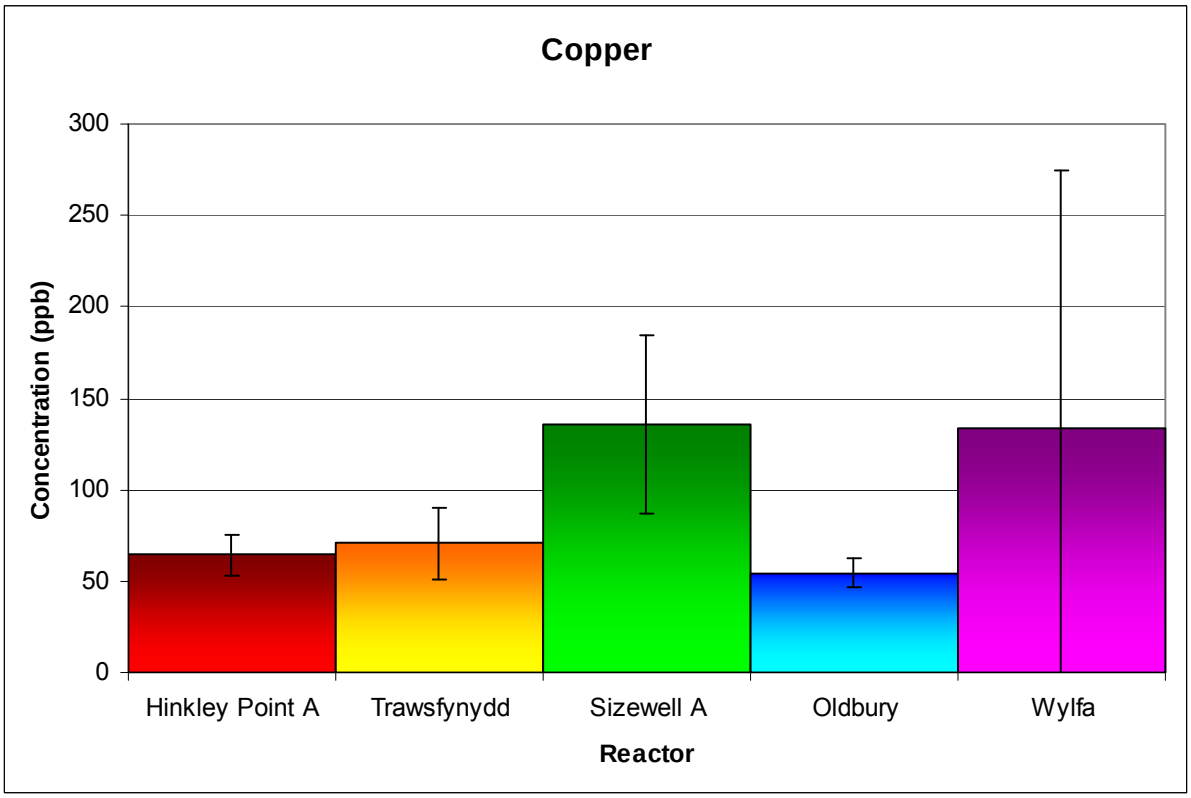

Figure 26: Comparison between reactors for PGA graphite for Copper

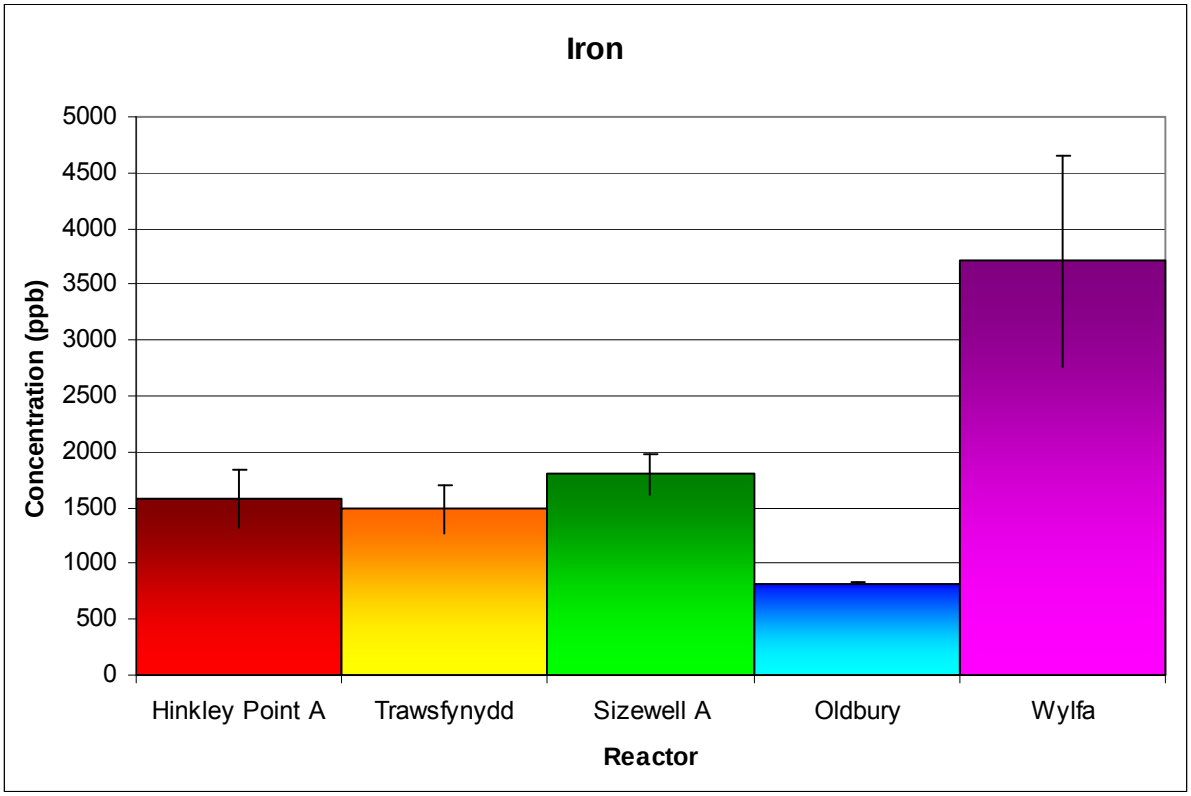

Figure 27: Comparison between reactors for PGA graphite for Iron

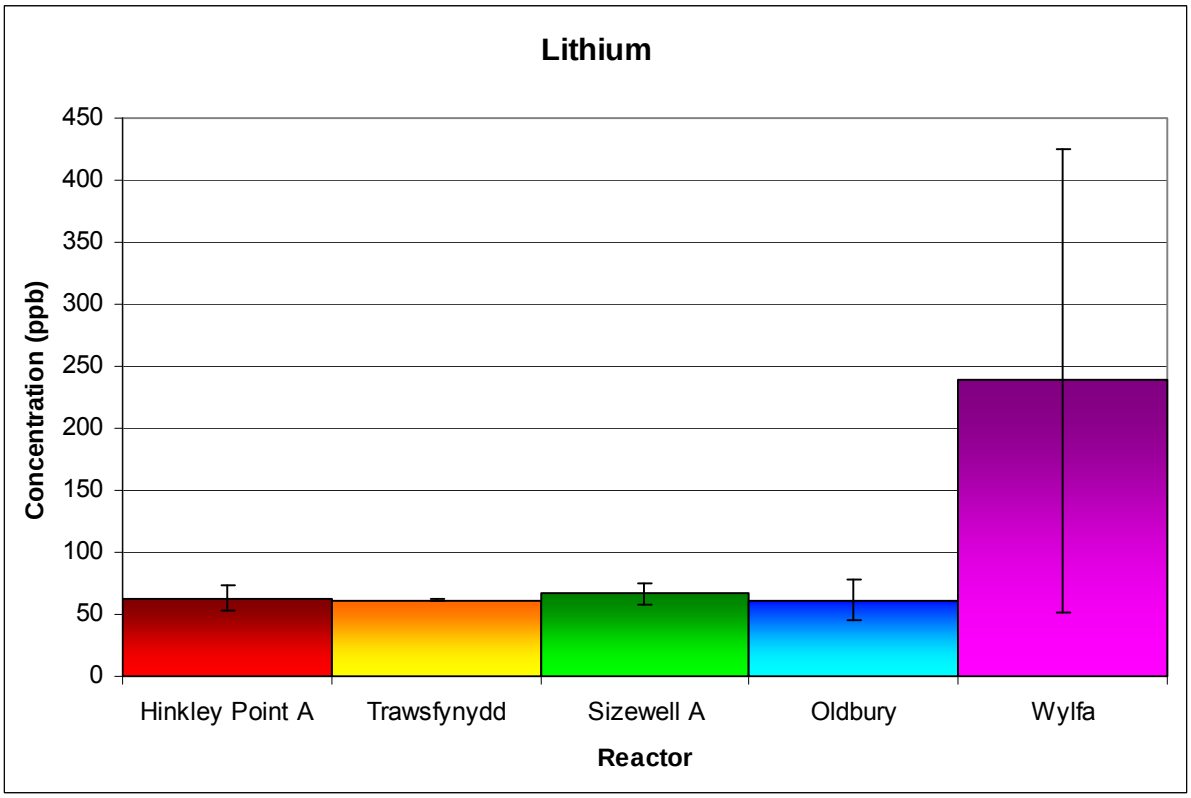

Figure 28: Comparison between reactors for PGA graphite for Lithium

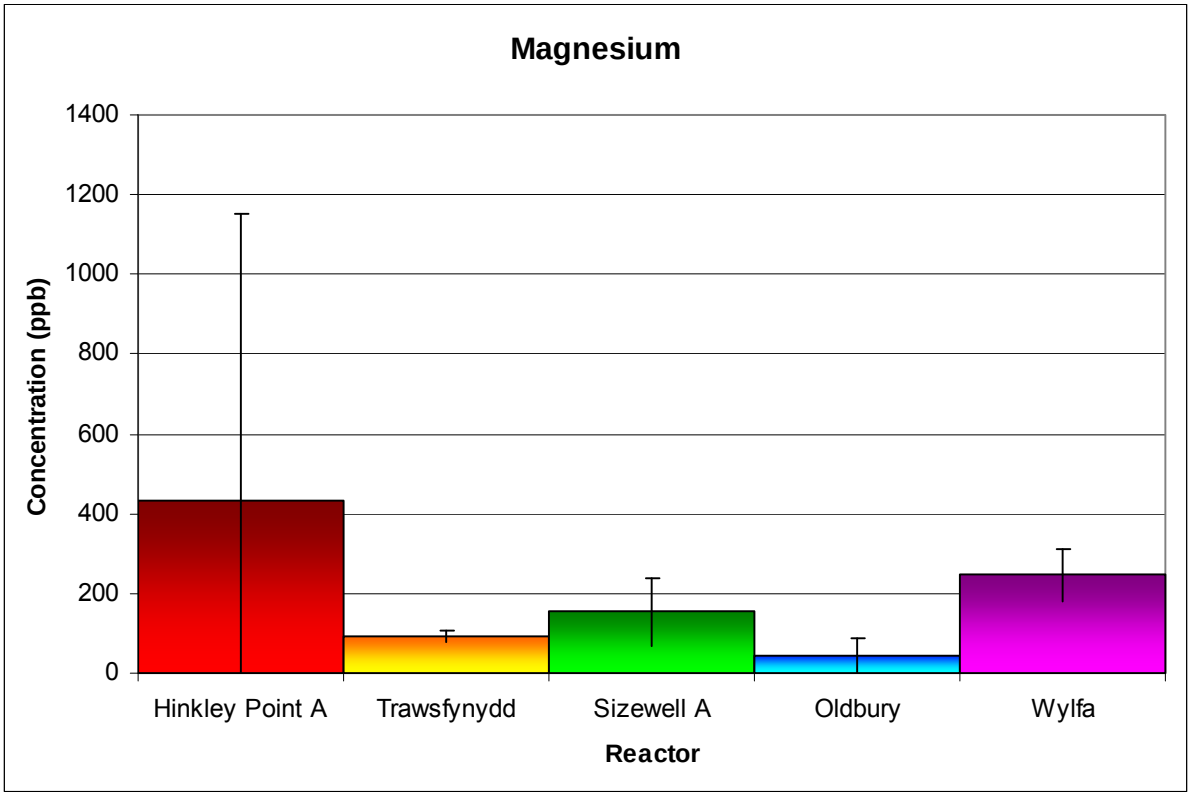

Figure 29: Comparison between reactors for PGA graphite for Magnesium

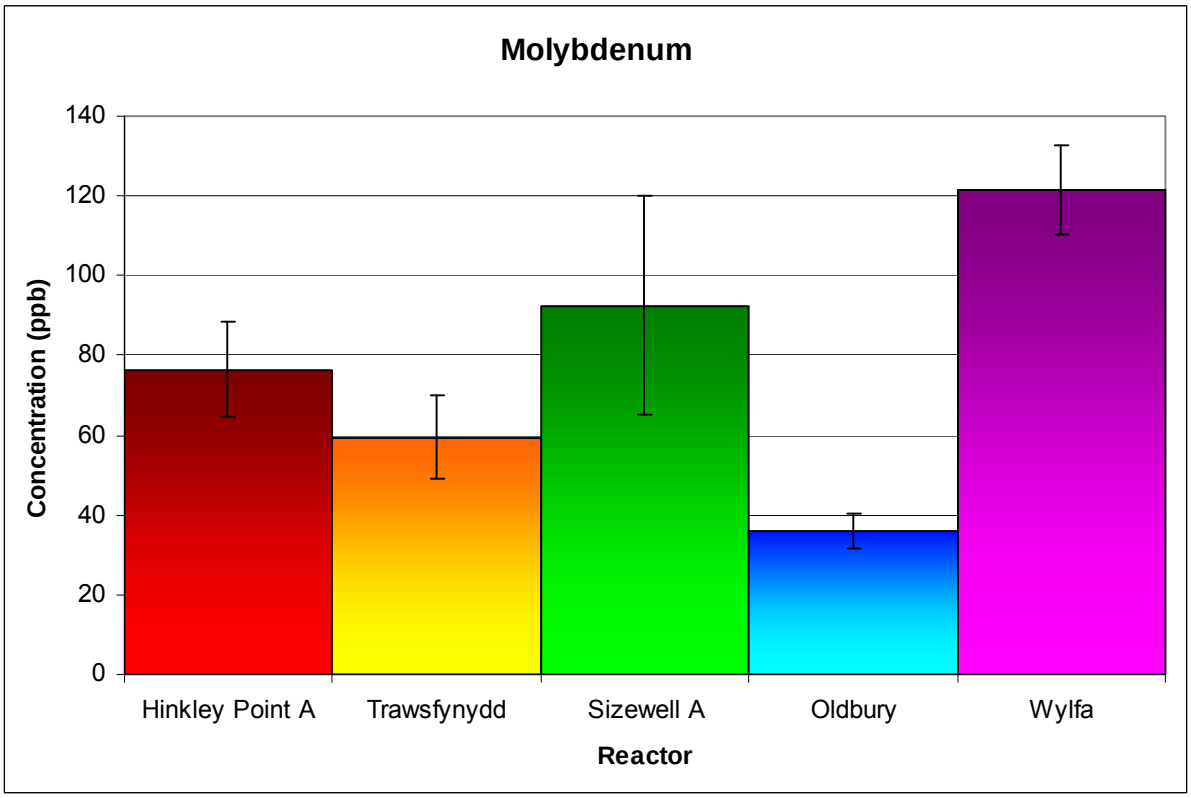

Figure 30: Comparison between reactors for PGA graphite for Molybdenum

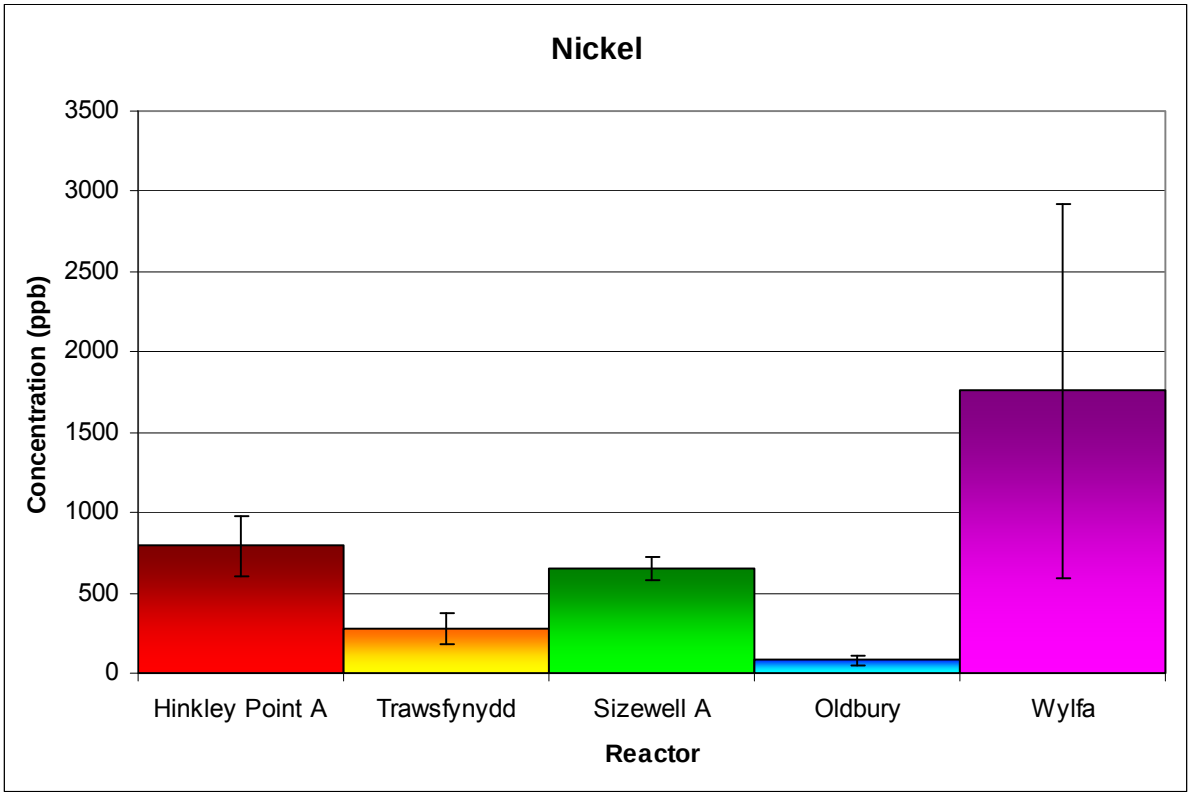

Figure 31: Comparison between reactors for PGA graphite for Nickel

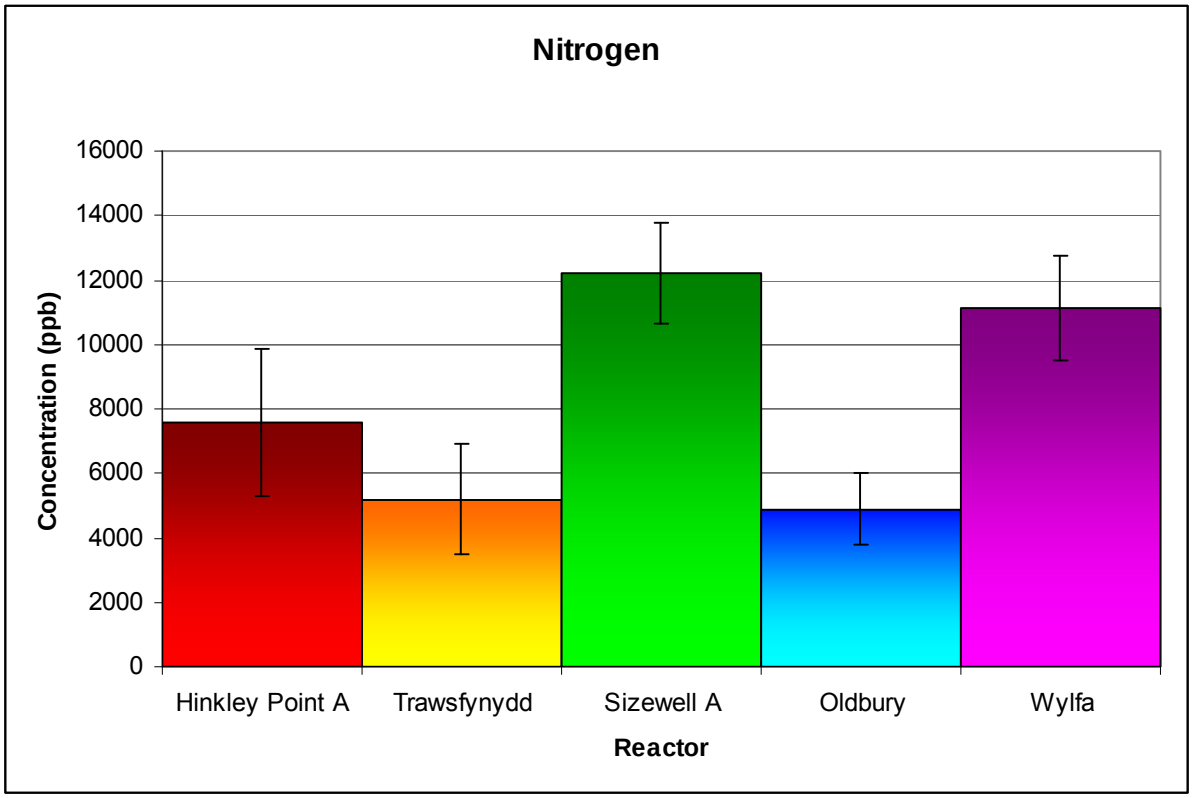

Figure 32: Comparison between reactors for PGA graphite for Nitrogen

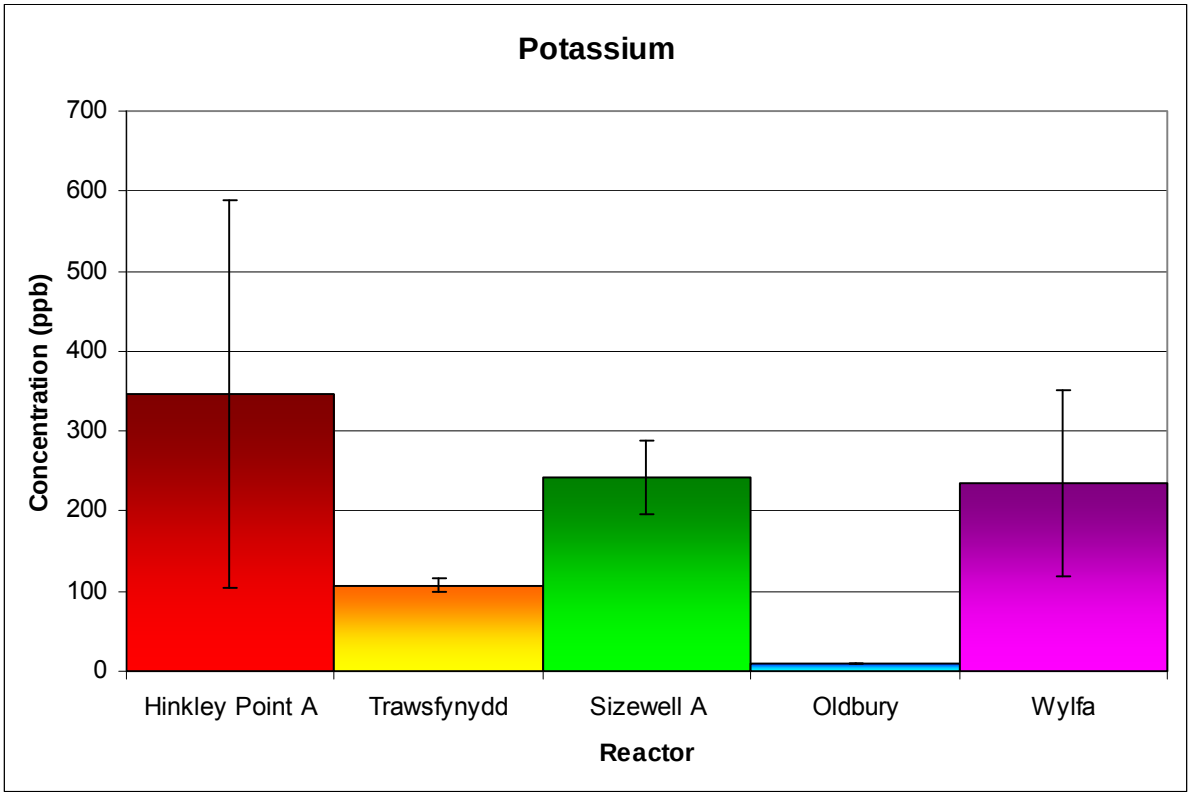

Figure 33: Comparison between reactors for PGA graphite for Potassium

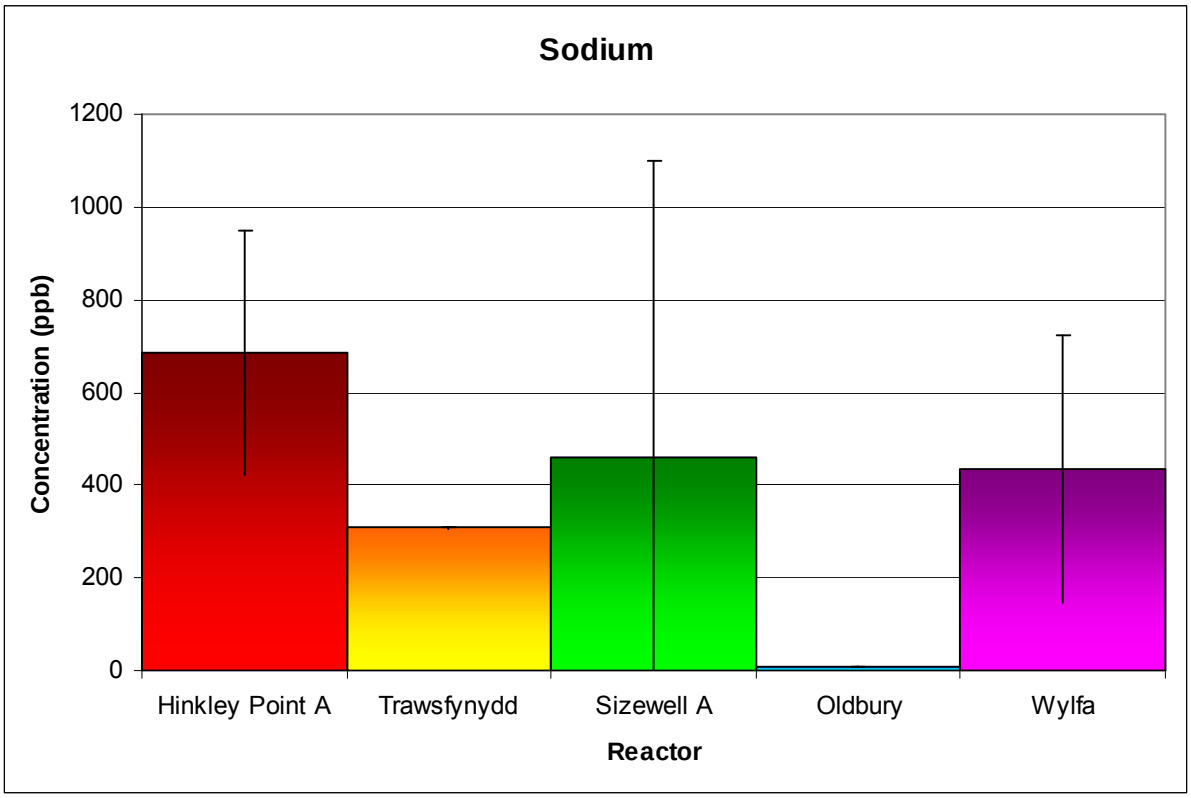

Figure 34: Comparison between reactors for PGA graphite for Sodium

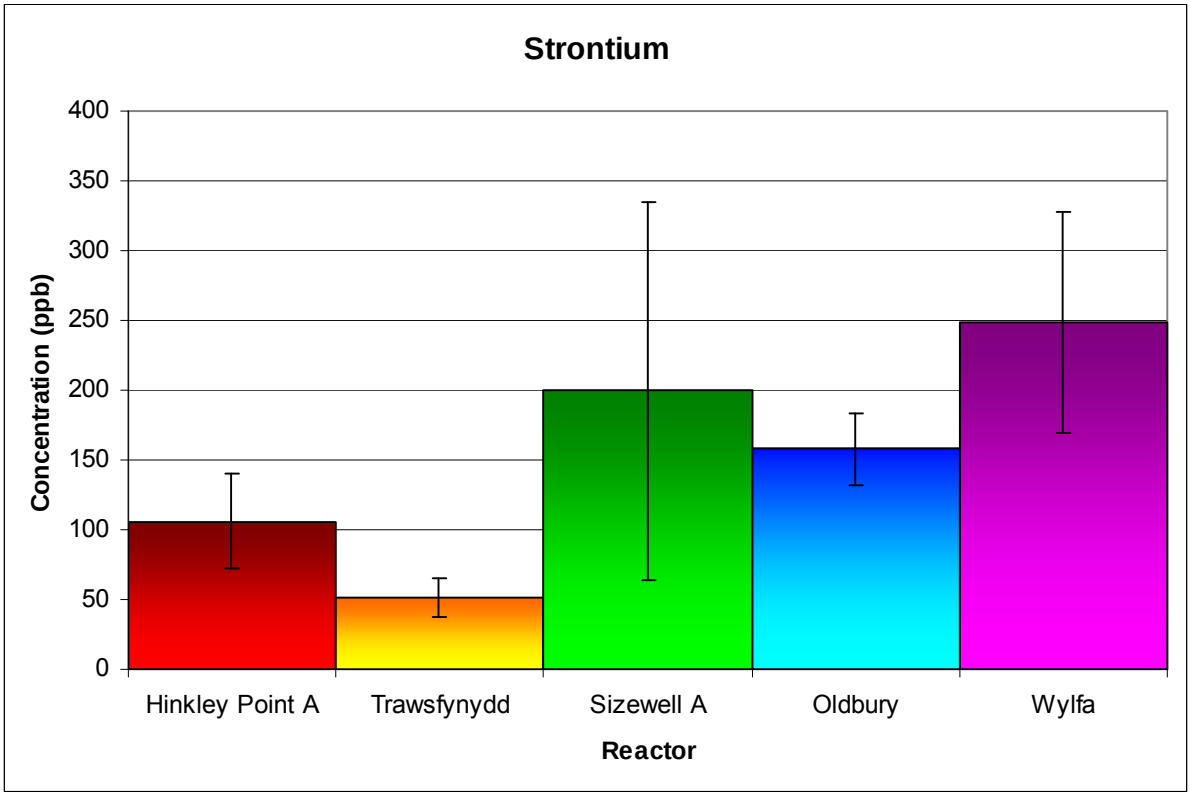

Figure 35: Comparison between reactors for PGA graphite for Strontium

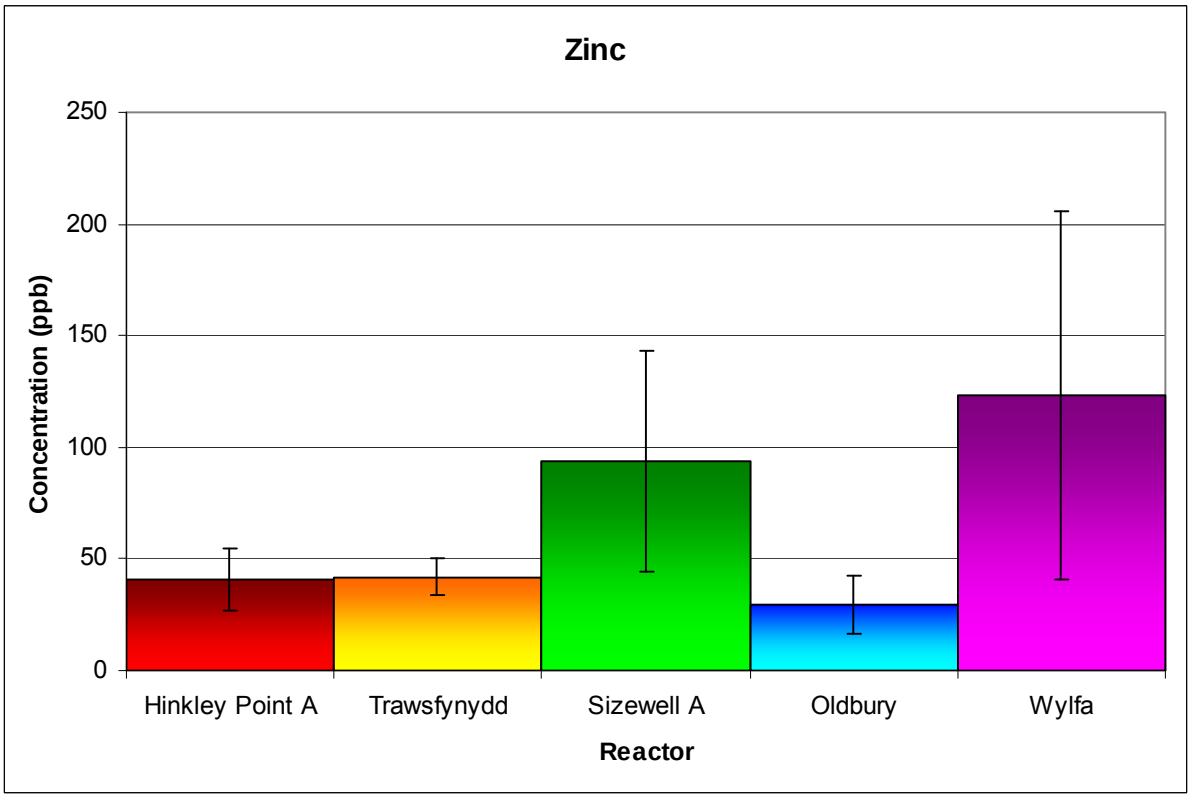

Figure 36: Comparison between reactors for PGA graphite for Zinc

APPENDIX 6 – COMPARISON OF ELEMENTAL PRECURSORS (PGB)

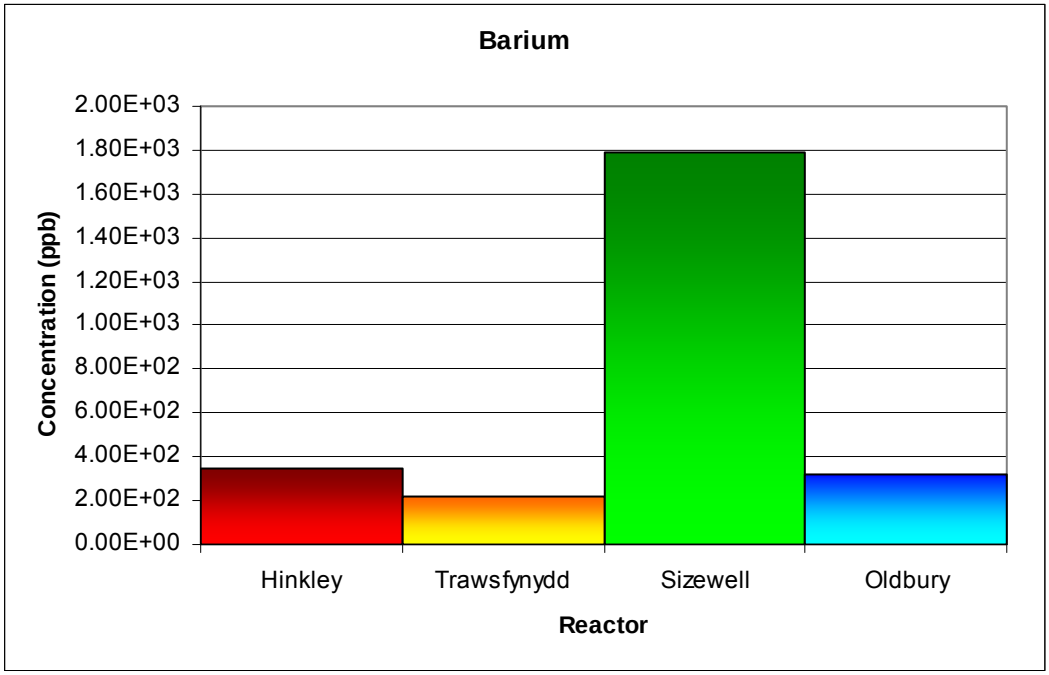

Figure 37: Comparison between reactors for PGB graphite for Barium

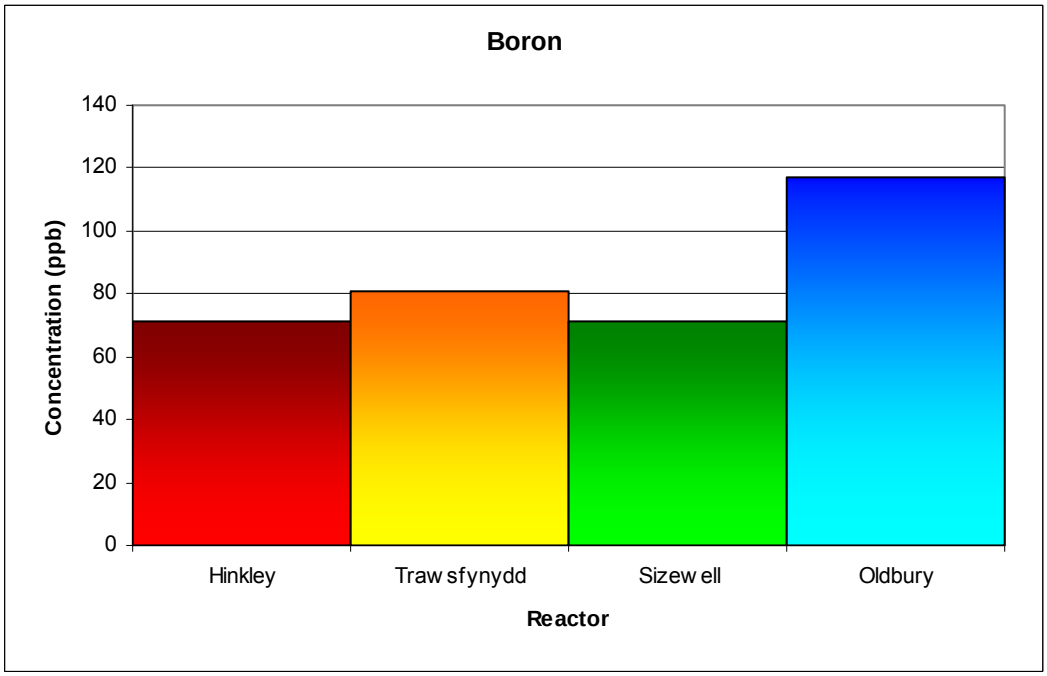

Figure 38: Comparison between reactors for PGB graphite for Boron

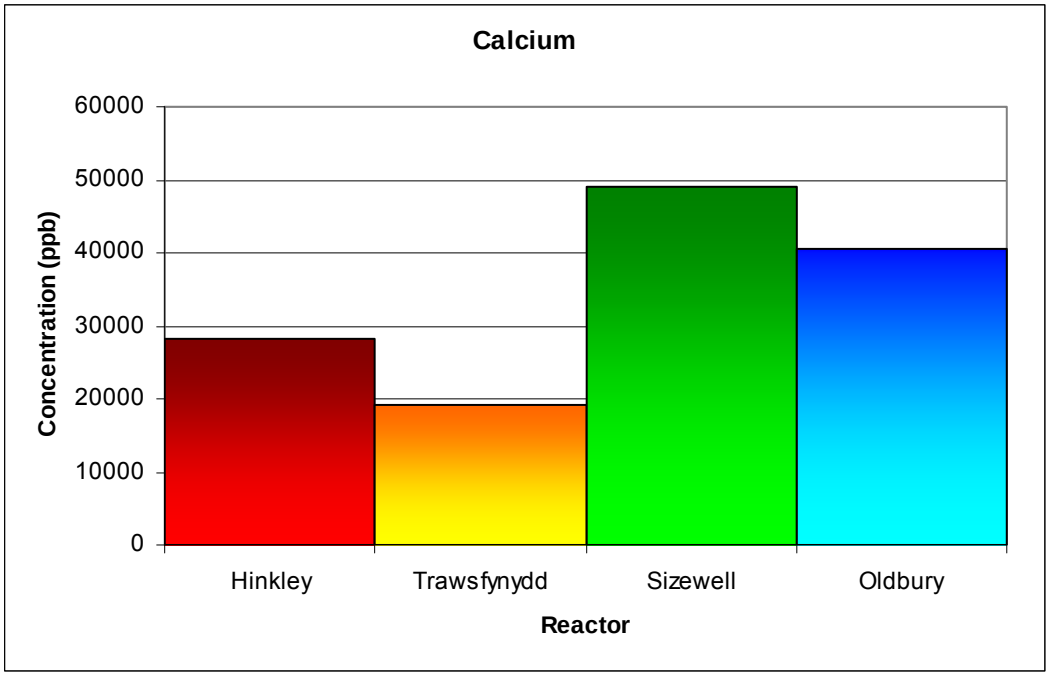

Figure 39: Comparison between reactors for PGB graphite for Calcium

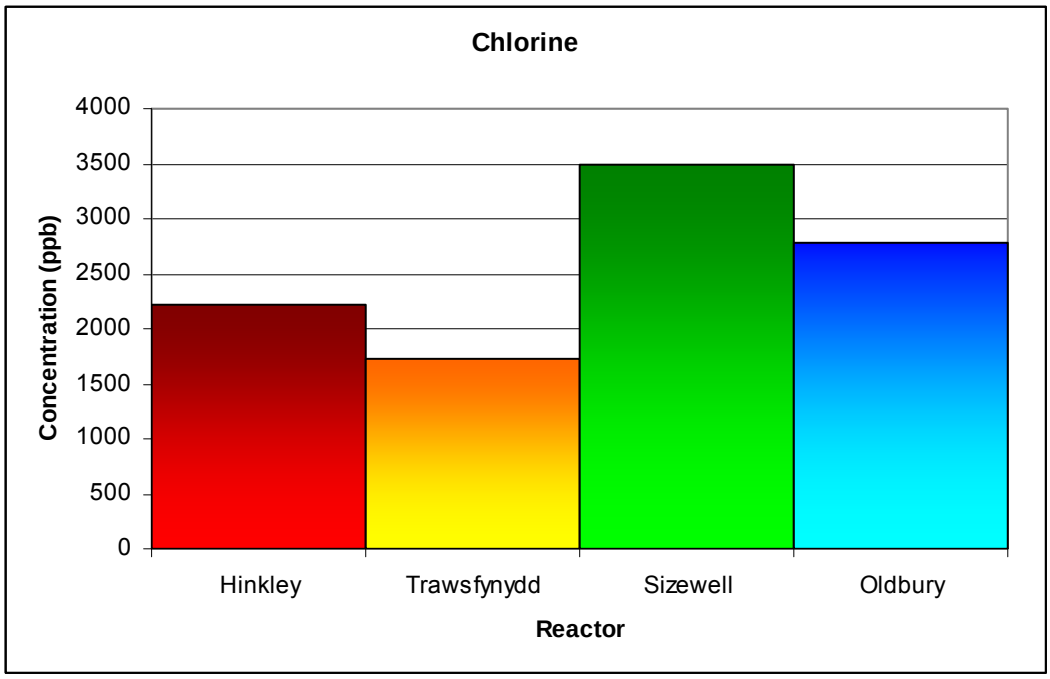

Figure 40: Comparison between reactors for PGB graphite for Chlorine

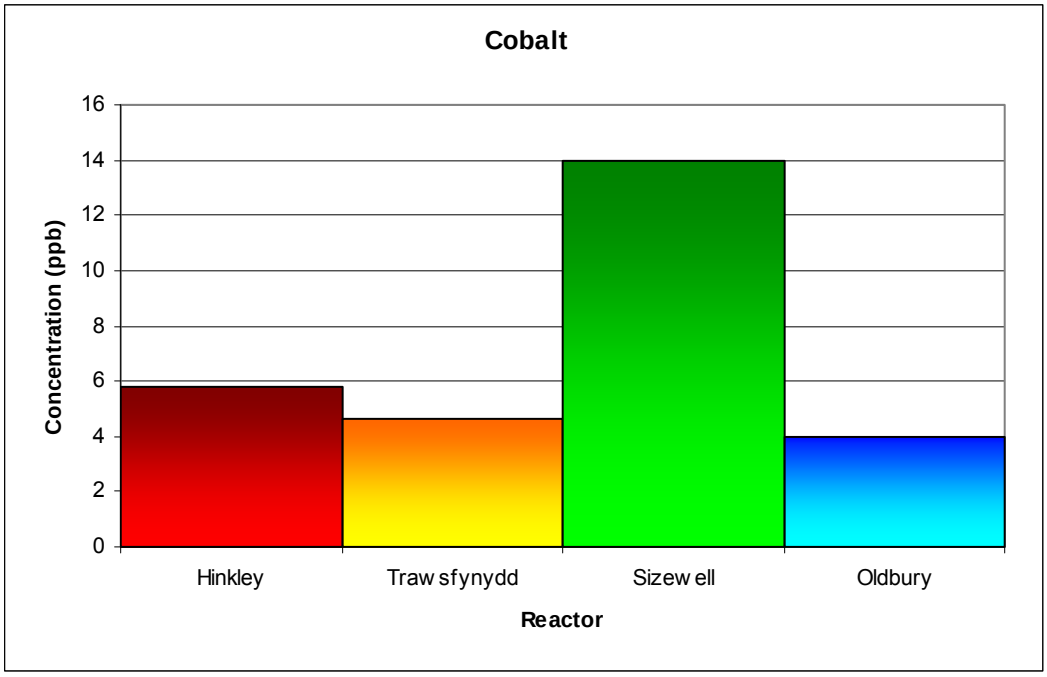

Figure 41: Comparison between reactors for PGB graphite for Cobalt

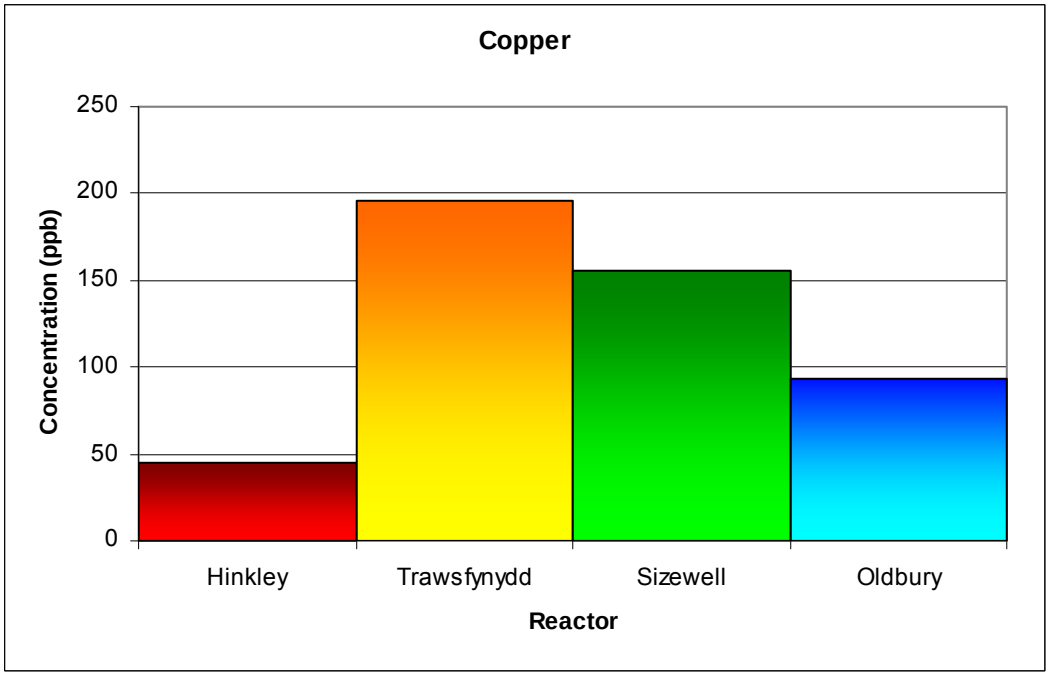

Figure 42: Comparison between reactors for PGB graphite for Copper

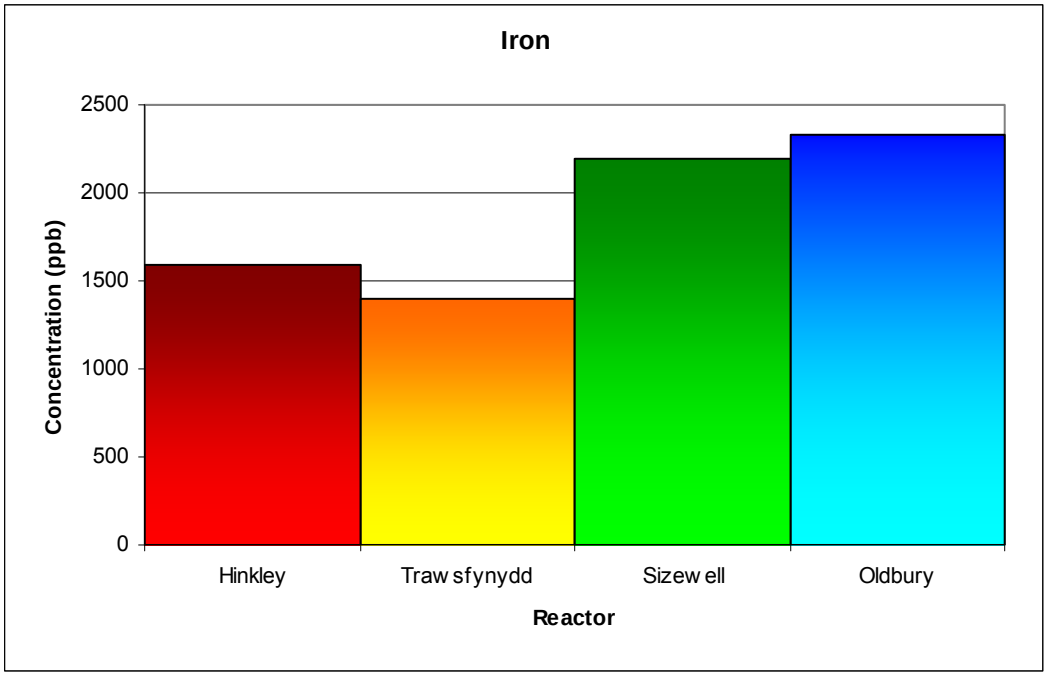

Figure 43: Comparison between reactors for PGB graphite for Iron

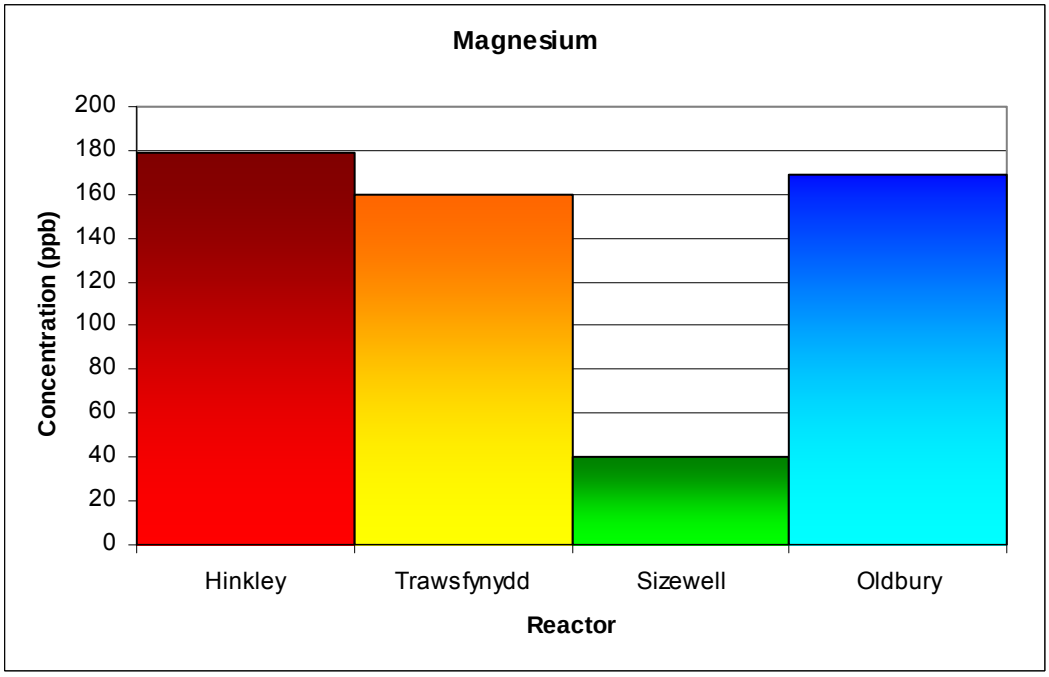

Figure 44: Comparison between reactors for PGB graphite for Magnesium

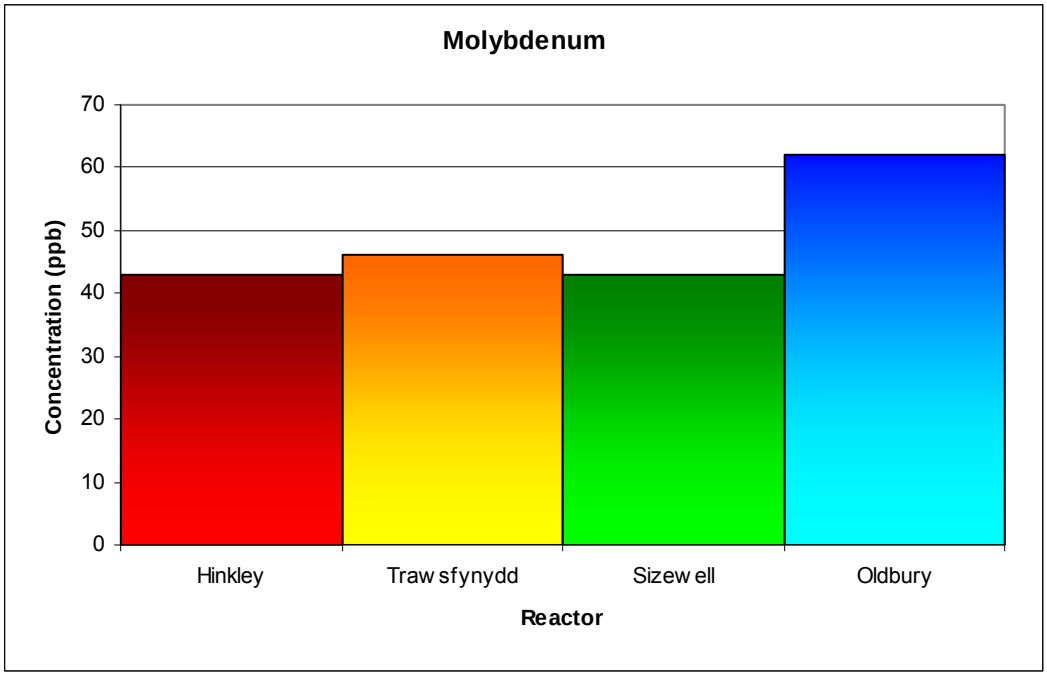

Figure 45: Comparison between reactors for PGB graphite for Molybdenum

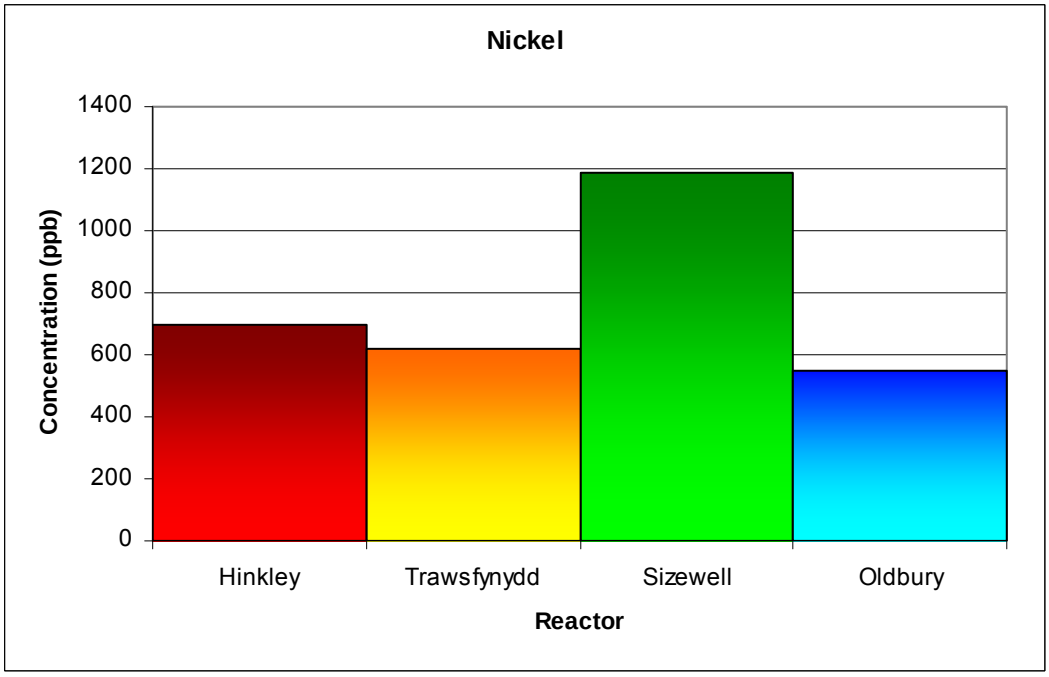

Figure 46: Comparison between reactors for PGB graphite for Nickel

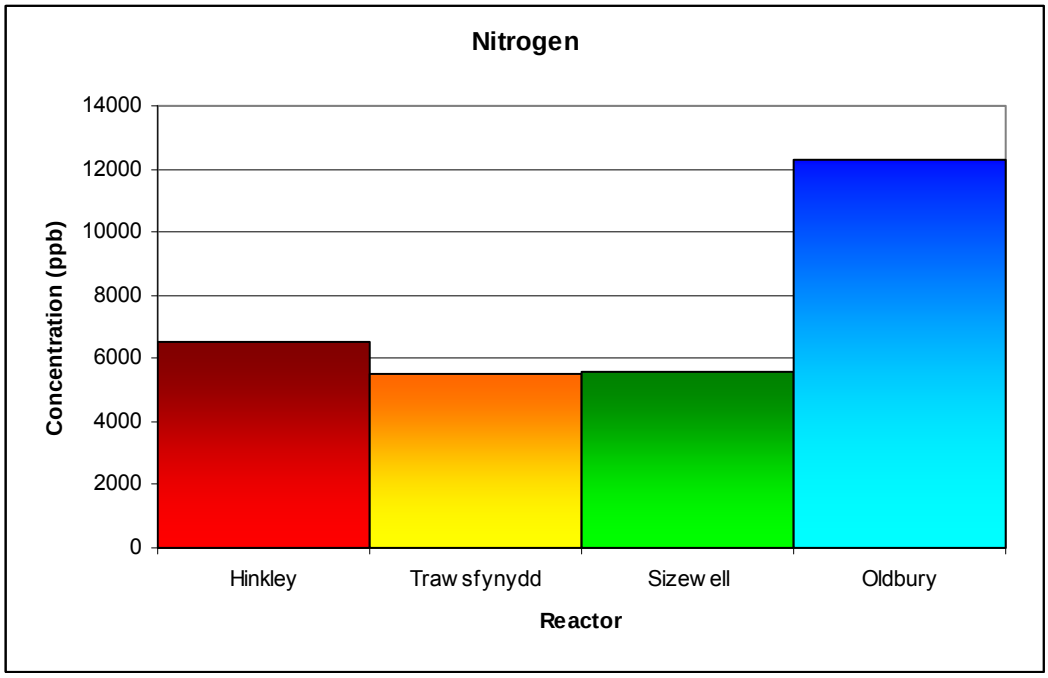

Figure 47: Comparison between reactors for PGB graphite for Nitrogen

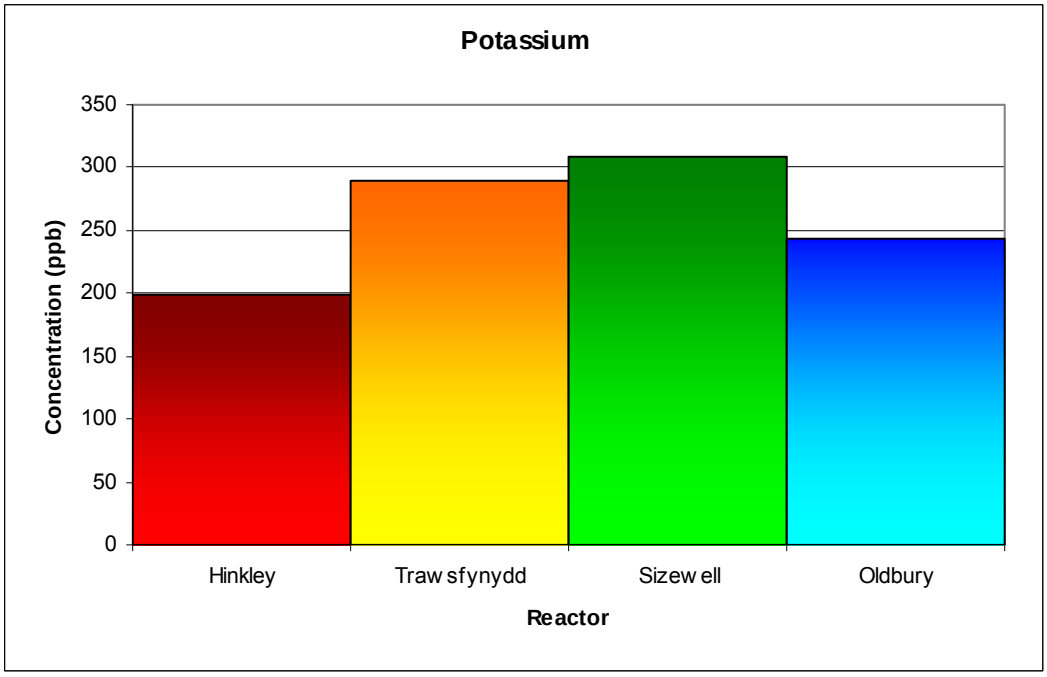

Figure 48: Comparison between reactors for PGB graphite for Potassium

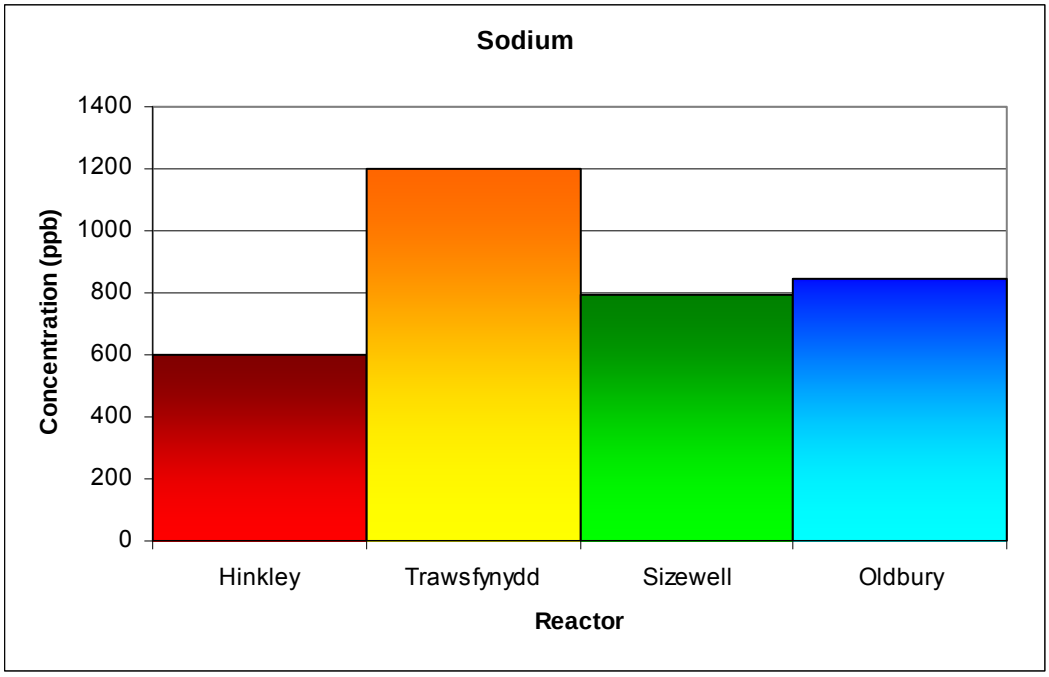

Figure 49: Comparison between reactors for PGB graphite for Sodium

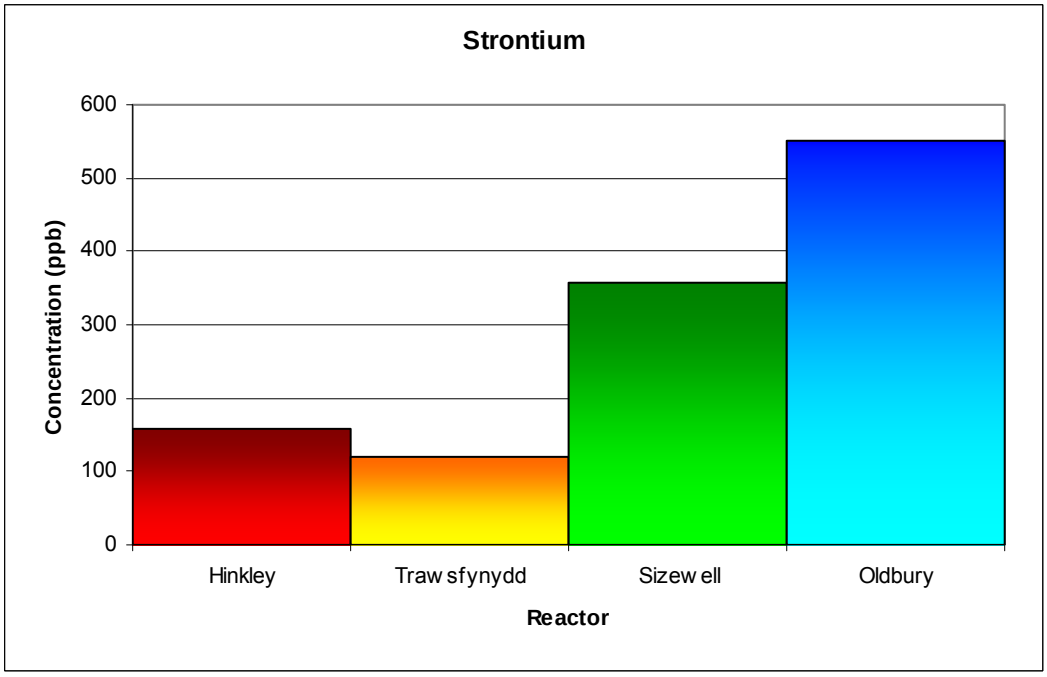

Figure 50: Comparison between reactors for PGB graphite for Strontium

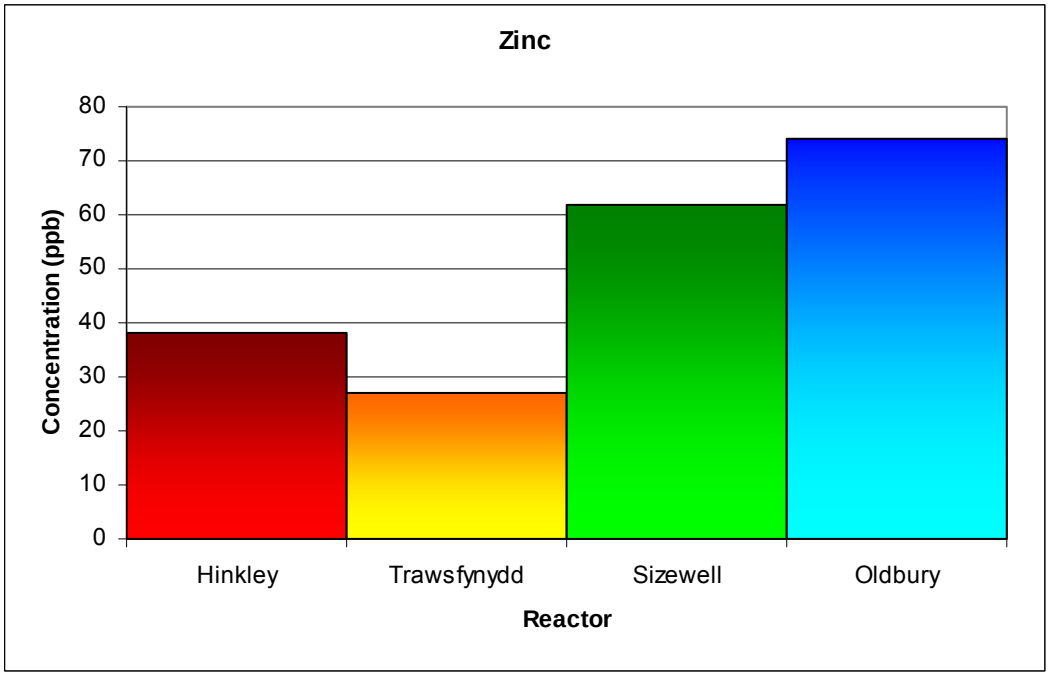

Figure 51: Comparison between reactors for PGB graphite for Zinc

APPENDIX 7 – REQUESTED AND RECEIVED SAMPLES FROM NNL

Sizewell A Reactor 1 – Active Samples for Analysis

Analysis	Current sample location	Trepanned date (Month/year)	Sample ID	Core number	Comments and any other info	Where are they now
Samples requested from Berkeley						
Pyro	Berkeley	Jun-02	1215/10	2	Fuel channel slice 2	Berkeley unable to locate
Pyro	Berkeley	Jun-02		10	Fuel channel slice 2	Berkeley unable to locate
Pyro	Berkeley	Jun-02	1443C	7	Interstitial channel slice 1	Berkeley unable to locate
Pyro + I2	Berkeley	Jun-98	1644/10	4	Fuel channel slices 1 and 2	Berkeley unable to locate
Alpha	Berkeley	Jun-98		14	Fuel channel slices 1 and 2	Berkeley unable to locate
Pyro	Berkeley	Jun-98	1644C	4	Interstitial channel slices 1 and 2	Berkeley unable to locate
Alpha	Berkeley	Jun-98		14	Interstitial channel slices 1 and 2	Berkeley unable to locate
Pyro	Berkeley	Jun-98		18	Interstitial channel slices 1 and 2	Berkeley unable to locate
Pyro	Berkeley	Jun-02	1702/C	5	Interstitial channel slice 1	Berkeley unable to locate
Un-requested samples supplied by Berkeley (Magnox) to NPL						
Pyro x 2	NPL	Jun-02	1215/10	2	Fuel channel slices 1 and 3	NPL
Alpha x 2	NPL	Jun-02	1215/10	10	Fuel channel slices 1 and 3	NPL

Wylfa Reactor 1 – Active Samples for Analysis

Analysis	Current sample location	Trepanned date (Month/year)	Sample ID	Core number	Comments and any other info	Where are they now
Samples requested from Berkeley						
Pyro	Berkeley	May-03	1224CR	12	Interstitial channel slice 1	Berkeley unable to locate
Alpha	Berkeley	May-03	1224CR	17	Interstitial channel slice 1	Berkeley unable to locate
Pyro	Berkeley	May-03	1224CR	21	Interstitial channel slice 3	Berkeley unable to locate
Pyro x 3	Berkeley	May-97	1608/03	9	Outside flattened zone. Fuel channel slices 1-3 available	Berkeley unable to locate
	Berkeley	May-97	1608/03	13	Outside flattened zone. Fuel channel slices 1-3 available	Berkeley unable to locate
Pyro x 3	Berkeley	May-97	1608/03	18	Outside flattened zone. Fuel channel slices 1-3 available	Berkeley unable to locate
Un-requested samples supplied by Berkeley (Magnox) to NPL						
Unusable	NPL	May-03	1224/CR	12	Interstitial Slices 2 and 3	NPL
Unusable	NPL	May-03	1224/CR	17	Interstitial Slices 2 and 3	NPL
Unusable	NPL	May-03	1224/CR	21	Interstitial Slice 2	NPL

Pyro = Pyrolysis followed by LSC analysis for H3, C14, Cl36; Pyro+ I2 = Pyrolysis followed by LSC analysis for H3, C14, Cl36 plus I129; Alpha = Dissolution followed by alpha spectroscopy. Yellow boxes indicates samples that have not been subject to previous testing.

APPENDIX 8 – NEW NEUTRON ENERGY SPECTRA

	Fuel			Control		
Energy	**202**	**204**	**206**	**212**	**214**	**216**
1.00E-08	2.09E-02	2.17E-02	2.25E-02	2.28E-02	2.24E-02	2.23E-02
2.00E-08	4.43E-02	4.54E-02	4.55E-02	4.81E-02	4.86E-02	4.78E-02
5.00E-08	1.49E-01	1.52E-01	1.52E-01	1.57E-01	1.57E-01	1.56E-01
1.00E-07	1.32E-01	1.35E-01	1.36E-01	1.37E-01	1.39E-01	1.39E-01
2.00E-07	5.88E-02	5.96E-02	5.93E-02	6.09E-02	6.00E-02	6.07E-02
5.00E-07	3.01E-02	2.94E-02	2.94E-02	3.13E-02	3.01E-02	2.99E-02
1.00E-06	1.92E-02	2.01E-02	1.87E-02	1.94E-02	1.93E-02	1.92E-02
2.00E-06	1.98E-02	1.91E-02	1.82E-02	1.91E-02	1.93E-02	2.00E-02
5.00E-06	2.46E-02	2.52E-02	2.54E-02	2.49E-02	2.61E-02	2.57E-02
1.00E-05	1.88E-02	1.86E-02	1.84E-02	1.92E-02	1.96E-02	2.01E-02
2.00E-05	1.97E-02	2.00E-02	1.98E-02	1.99E-02	2.05E-02	2.00E-02
5.00E-05	2.70E-02	2.74E-02	2.79E-02	2.72E-02	2.69E-02	2.73E-02
1.00E-04	2.00E-02	2.08E-02	2.07E-02	2.16E-02	2.10E-02	2.21E-02
2.00E-04	2.16E-02	2.16E-02	2.16E-02	2.10E-02	2.16E-02	2.22E-02
5.00E-04	3.12E-02	3.11E-02	3.18E-02	2.92E-02	2.95E-02	2.93E-02
1.00E-03	2.26E-02	2.31E-02	2.33E-02	2.24E-02	2.33E-02	2.22E-02
2.00E-03	2.43E-02	2.34E-02	2.39E-02	2.43E-02	2.44E-02	2.40E-02
5.00E-03	3.19E-02	3.17E-02	3.13E-02	2.97E-02	3.10E-02	3.20E-02
1.00E-02	2.45E-02	2.49E-02	2.50E-02	2.32E-02	2.34E-02	2.38E-02
2.00E-02	2.50E-02	2.59E-02	2.53E-02	2.39E-02	2.40E-02	2.47E-02
5.00E-02	3.42E-02	3.36E-02	3.32E-02	3.53E-02	3.37E-02	3.50E-02
1.00E-01	2.84E-02	2.87E-02	2.97E-02	2.78E-02	2.79E-02	2.77E-02
2.00E-01	3.01E-02	2.92E-02	2.95E-02	3.05E-02	3.01E-02	2.93E-02
5.00E-01	4.45E-02	4.16E-02	4.17E-02	4.19E-02	4.02E-02	3.86E-02
1.00E+00	3.54E-02	3.37E-02	3.38E-02	3.30E-02	3.23E-02	3.16E-02
2.00E+00	3.52E-02	3.32E-02	3.21E-02	2.97E-02	2.86E-02	2.94E-02
5.00E+00	2.45E-02	2.17E-02	2.14E-02	1.81E-02	1.79E-02	1.79E-02
1.00E+01	2.41E-03	2.16E-03	2.17E-03	1.70E-03	1.93E-03	1.94E-03
1.20E+01	2.24E-05	1.51E-05	1.42E-05	6.60E-05	3.77E-05	2.84E-05
1.50E+01	2.31E-05	1.55E-05	1.46E-05	0.00E+00	0.00E+00	6.31E-06
1.00E+02	0.00E+00	0.00E+00	0.00E+00	0.00E+00	0.00E+00	1.25E-05

Figure 52: Normalised energy spectra for fuel channel and control rod channels for samples located at the top or base of a reactor

Here, “202”, “204” and “206” represent slices “1”, “2” and “3” respectively.

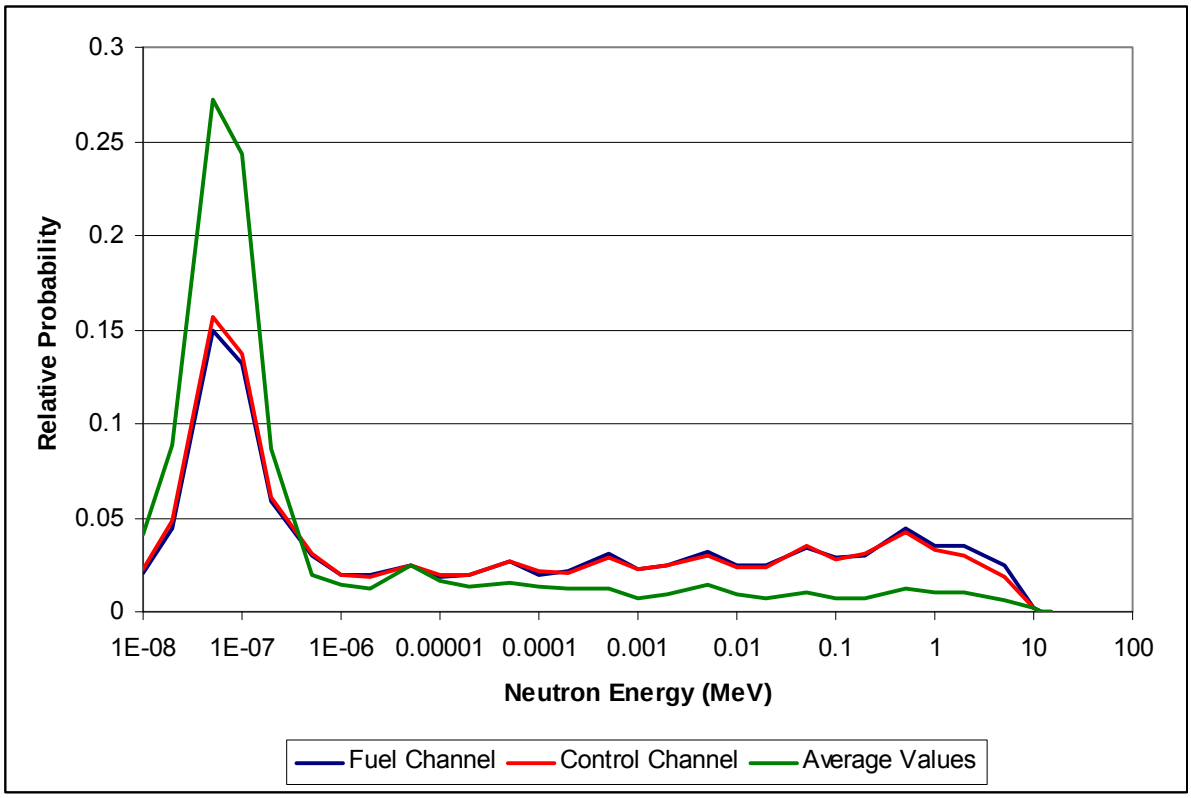

Figure 53: Comparison between fuel and control rod channel neutron energy spectra taken from active comparison modelling and the neutron energy spectrum used in the main model

Figure 53 compares energy spectra from the fuel and control rod channels from calculations using the active model. This is then compared against the spectrum used for a similar location on the main model, labeled the “average” spectrum. It can be seen that the fuel and control rod channel spectra consist of a much harder fast neutron region (>1 eV), whilst the average region consists of more thermal and epithermal neutrons (<1 eV).

APPENDIX 9 – SIZEWELL A REACTOR 1 RADIONUCLIDE INVENTORY BY POSITION RADIALLY AND AXIALLY IN THE CORE AND REFLECTOR REGIONS

Data is presented in the following, tabular format:

	Region the data refers to (e.g. reflector, or 'core')			
Nuclides of Interest	**Position in meters either radially or Axially from the centre of the core**			
Nuclide	Nuclide activity in Bq/kg	**…**	**…**	**…**
Flux Values assuming a loading factor of 750 MWh(th)	Flux values in n/s/cm^2	**…**	**…**	**…**

Note: All activities listed here are correct for ten years of decay post reactor shutdown (2106)

Jowett Precursor Information

Radial Data

Nuclides	0	0.7878	1.5756	2.3634	3.1512	3.939	4.7268	5.5146	6.3024	6.7	6.9	7.1	7.3
H3	5.24E+08	5.15E+08	5.16E+08	5.09E+08	5.00E+08	4.96E+08	4.93E+08	4.86E+08	4.78E+08	4.71E+08	4.61E+08	4.27E+08	2.79E+08
C14	4.19E+08	4.32E+08	4.35E+08	3.92E+08	3.26E+08	2.69E+08	2.27E+08	1.66E+08	1.15E+08	8.57E+07	6.34E+07	3.78E+07	1.46E+07
Cl36	4.34E+05	4.35E+05	4.35E+05	4.30E+05	4.13E+05	3.86E+05	3.59E+05	3.01E+05	2.36E+05	1.90E+05	1.49E+05	9.46E+04	3.87E+04
Na22	N/A	N/A	N/A	N/A	N/A	N/A	N/A	N/A	N/A	N/A	N/A	N/A	N/A
Co60	3.06E+07	3.09E+07	3.10E+07	2.98E+07	2.78E+07	2.58E+07	2.38E+07	2.01E+07	1.57E+07	1.25E+07	9.65E+06	6.13E+06	2.53E+06
Kr85	6.12E+07	5.81E+07	5.43E+07	4.26E+07	3.48E+07	2.81E+07	2.03E+07	1.25E+07	6.15E+06	2.42E+06	1.20E+06	5.99E+05	2.14E+05
Nb94	5.36E+05	5.37E+05	5.20E+05	4.84E+05	4.44E+05	4.10E+05	3.50E+05	2.67E+05	1.76E+05	1.14E+05	7.91E+04	4.68E+04	1.83E+04
Ag108m	5.14E+03	4.95E+03	4.86E+03	6.07E+03	7.19E+03	9.00E+03	9.83E+03	1.07E+04	1.08E+04	1.05E+04	8.91E+03	5.97E+03	2.55E+03
Sn121m	1.29E+03	1.26E+03	1.24E+03	1.15E+03	1.05E+03	9.43E+02	7.99E+02	6.03E+02	3.88E+02	2.32E+02	1.59E+02	9.34E+01	3.64E+01
I129	3.18E+01	3.09E+01	2.96E+01	2.50E+01	2.11E+01	1.73E+01	1.30E+01	7.92E+00	3.62E+00	1.56E+00	8.57E-01	4.20E-01	1.38E-01
Cs134	3.68E+06	3.66E+06	3.48E+06	4.00E+06	4.63E+06	5.24E+06	5.50E+06	5.59E+06	4.87E+06	3.53E+06	2.54E+06	1.58E+06	6.54E+05
Ba133	1.42E+06	1.44E+06	1.43E+06	1.35E+06	1.22E+06	1.09E+06	9.55E+05	7.42E+05	5.18E+05	3.70E+05	2.68E+05	1.61E+05	6.33E+04
Cs137	6.36E+05	6.57E+05	6.60E+05	5.93E+05	4.91E+05	4.03E+05	3.40E+05	2.47E+05	1.71E+05	1.29E+05	9.53E+04	5.68E+04	2.20E+04
Pm145	6.31E+04	6.48E+04	6.37E+04	6.30E+04	5.91E+04	5.56E+04	5.15E+04	4.27E+04	3.39E+04	2.77E+04	21520	1.35E+04	5.44E+03
Eu152	1.37E+01	1.28E+01	1.24E+01	1.33E+01	1.91E+01	2.86E+01	3.91E+01	7.63E+01	1.60E+02	2.65E+02	4.43E+02	9.69E+02	2.97E+03
Eu154	2.41E+05	2.30E+05	2.25E+05	2.48E+05	3.04E+05	4.22E+05	5.53E+05	9.74E+05	1.84E+06	2.55E+06	2.78E+06	2.58E+06	1.53E+06
Eu155	1.70E+05	1.65E+05	1.64E+05	1.76E+05	2.07E+05	2.61E+05	3.20E+05	5.05E+05	8.30E+05	1.19E+06	1.25E+06	1.02E+06	4.18E+05
Ho166m	1.33E+04	1.27E+04	1.30E+04	1.44E+04	1.55E+04	1.41E+04	1.22E+04	8.25E+03	3.73E+03	2.79E+03	2.97E+03	3.40E+03	3.84E+03
Total Flux	1.53E-06	1.52E-06	1.5E-06	1.31E-06	1.15E-06	9.73E-07	7.96E-07	5.74E-07	3.51E-07	1.9E-07	1.22E-07	6.95E-08	2.66E-08
Thermal	3.98E-07	4.13E-07	4.21E-07	3.83E-07	3.12E-07	2.56E-07	2.14E-07	1.58E-07	1.11E-07	8.78E-08	6.6E-08	3.96E-08	1.53E-08
Epithermal	4.3E-07	4.48E-07	4.38E-07	3.55E-07	3.16E-07	2.67E-07	2.27E-07	1.54E-07	1.02E-07	6.99E-08	4.94E-08	2.9E-08	1.11E-08
Fast Flux	7.06E-07	6.62E-07	6.44E-07	5.71E-07	5.24E-07	4.5E-07	3.55E-07	2.62E-07	1.38E-07	3.21E-08	6.54E-09	9.69E-10	1.48E-10

Table 23: Radial Activity in Bq/kg for Jowett Precursors in the Sizewell A Reactor

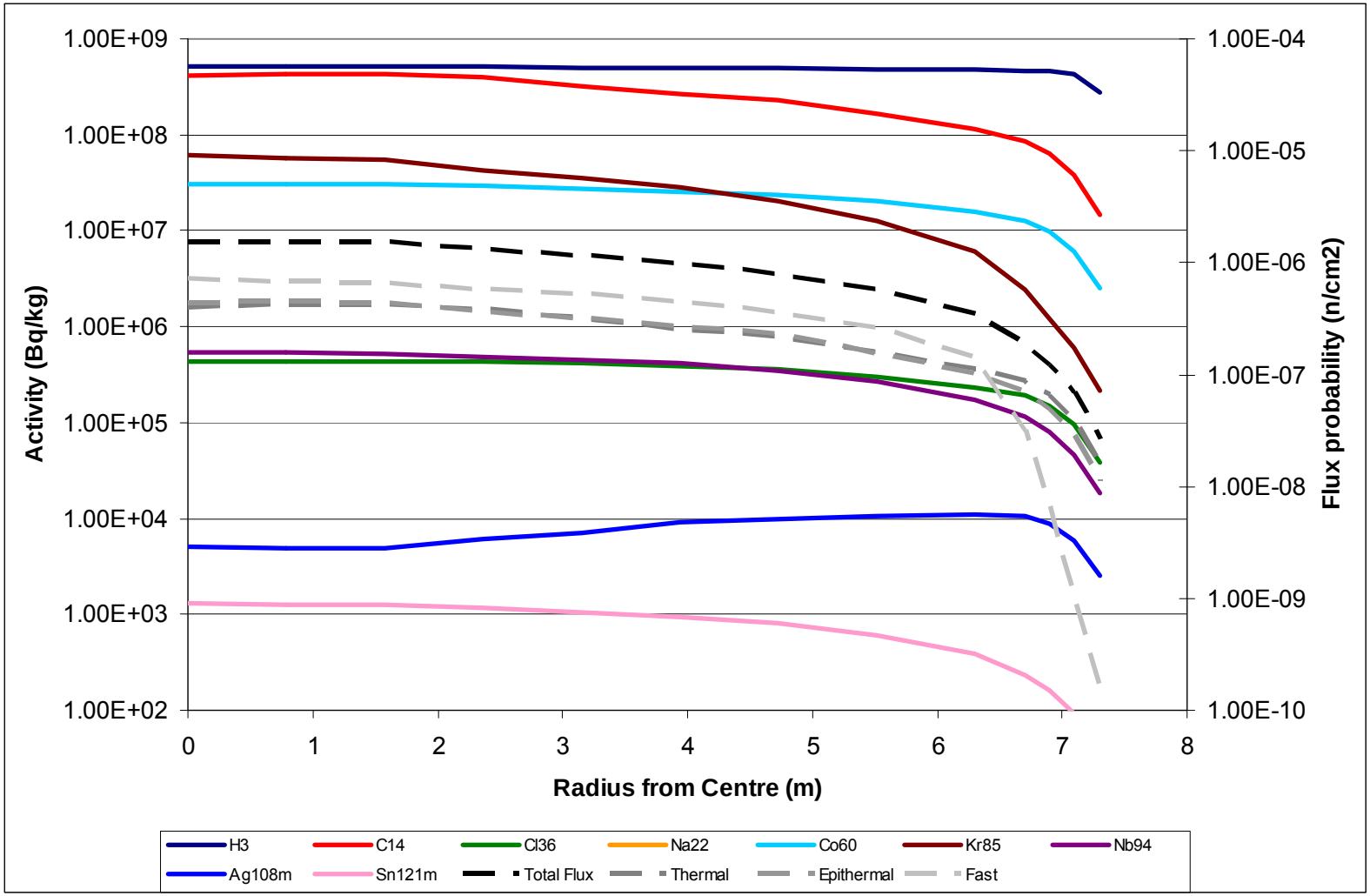

Figure 54: Radionuclide trends for Radial nuclides in the Sizewell A reactor (1/2)

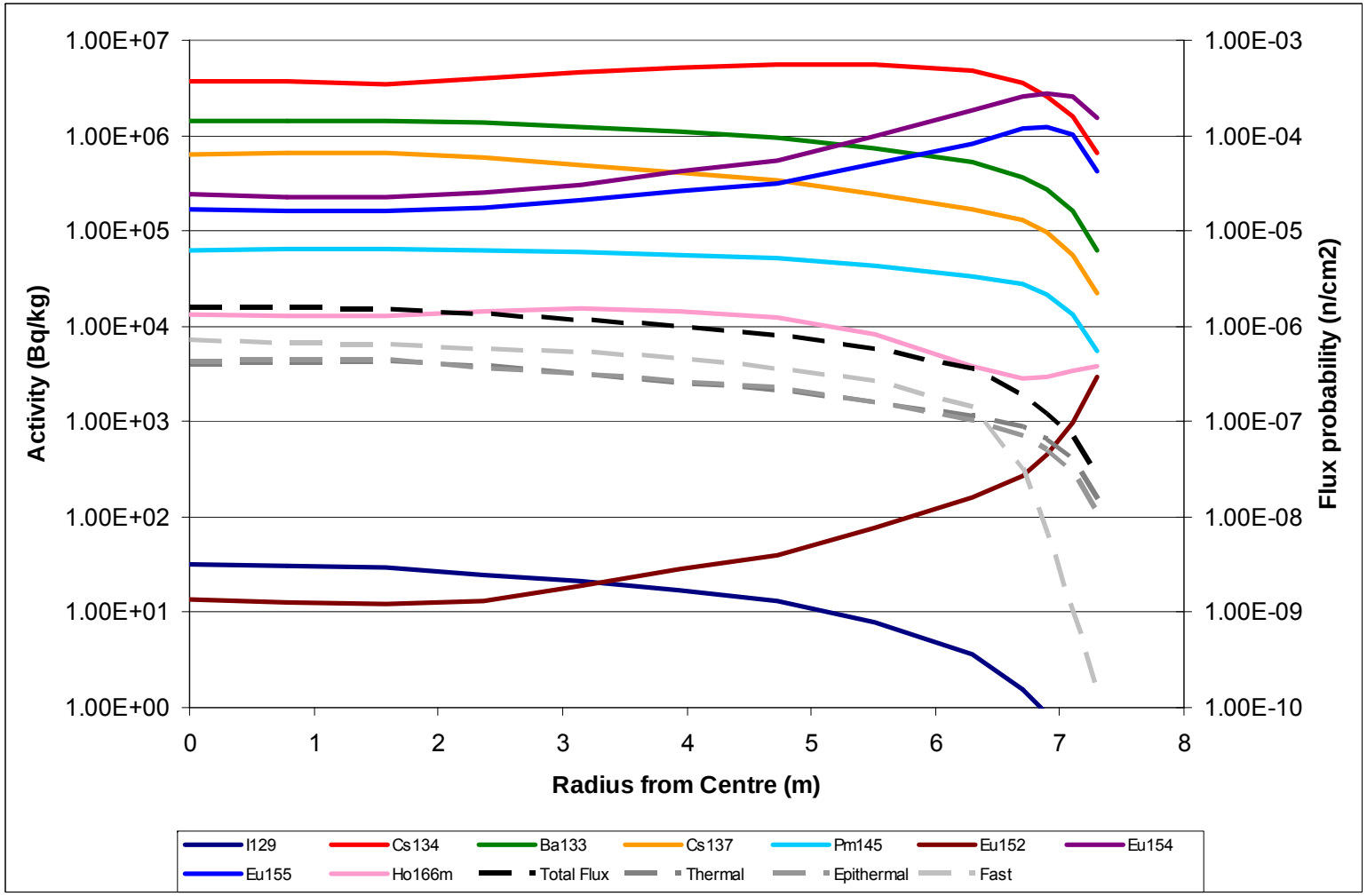

Figure 55: Radionuclide trends for Radial nuclides in the Sizewell A reactor (2/2)

Axial Data

Nuclides	-4.5	-4.25	-4	-3	-2	-1	0	1	2	3	4	4.25	4.5
H3	4.26E+08	4.69E+08	4.76E+08	4.93E+08	5.03E+08	5.08E+08	5.12E+08	5.14E+08	5.11E+08	4.93E+08	4.79E+08	4.67E+08	4.21E+08
C14	3.76E+07	8.04E+07	1.01E+08	2.45E+08	3.91E+08	4.19E+08	4.52E+08	4.14E+08	3.30E+08	2.34E+08	1.15E+08	7.54E+07	3.55E+07
Cl36	9.35E+04	1.80E+05	2.15E+05	3.73E+05	4.30E+05	4.34E+05	4.36E+05	4.33E+05	4.14E+05	364350	2.38E+05	1.72E+05	8.93E+04
Na22	N/A	N/A	N/A	N/A	N/A	N/A	N/A	N/A	N/A	N/A	N/A	N/A	N/A
Co60	6.18E+06	1.20E+07	1.46E+07	2.46E+07	2.98E+07	3.05E+07	3.15E+07	3.04E+07	2.80E+07	23999000	1.56E+07	1.11E+07	5.80E+06
Kr85	9.44E+05	2.98E+06	5.46E+06	1.73E+07	4.09E+07	5.00E+07	6.42E+07	5.30E+07	4.01E+07	1.68E+07	3.60E+06	1.67E+06	5.96E+05
Nb94	5.08E+04	1.17E+05	1.60E+05	3.40E+05	4.83E+05	5.13E+05	5.54E+05	5.20E+05	4.57E+05	3.30E+05	1.53E+05	9.55E+04	4.42E+04
Ag108m	5.97E+03	9.71E+03	1.02E+04	1.03E+04	6.18E+03	5.27E+03	4.51E+03	5.14E+03	6.73E+03	9.79E+03	1.15E+04	9.92E+03	5.66E+03
Sn121m	1.04E+02	2.41E+02	3.44E+02	7.60E+02	1.10E+03	1.21E+03	1.32E+03	1.24E+03	1.08E+03	7.48E+02	3.19E+02	1.92E+02	8.86E+01
I129	4.86E-01	1.69E+00	2.95E+00	1.20E+01	2.47E+01	2.84E+01	3.22E+01	2.89E+01	2.44E+01	1.17E+01	2.58E+00	1.12E+00	3.99E-01
Cs134	1.68E+06	3.91E+06	4.59E+06	5.42E+06	4.10E+06	3.77E+06	3.35E+06	3.76E+06	4.46E+06	5.47E+06	4.65E+06	3.02E+06	1.59E+06
Ba133	1.67E+05	3.64E+05	4.73E+05	9.80E+05	1.35E+06	1.41E+06	1.47E+06	1.40E+06	1.24E+06	9.45E+05	4.93E+05	3.18E+05	1.52E+05
Cs137	5.62E+04	1.21E+05	1.51E+05	3.68E+05	5.94E+05	6.35E+05	6.88E+05	6.27E+05	4.96E+05	350560	1.73E+05	1.13E+05	5.33E+04
Pm145	1.34E+04	2.60E+04	3.10E+04	5.41E+04	6.36E+04	6.42E+04	6.48E+04	6.37E+04	5.74E+04	5.26E+04	3.44E+04	2.50E+04	1.27E+04
Eu152	1.04E+03	3.19E+02	2.16E+02	3.11E+01	1.35E+01	1.27E+01	1.18E+01	1.36E+01	1.94E+01	3.47E+01	1.54E+02	3.43E+02	1.05E+03
Eu154	2.63E+06	2.65E+06	2.10E+06	4.93E+05	2.48E+05	2.31E+05	2.29E+05	2.36E+05	3.03E+05	5.27E+05	1.85E+06	2.64E+06	2.69E+06
Eu155	1.03E+06	1.16E+06	9.46E+05	3.11E+05	1.78E+05	1.68E+05	1.62E+05	1.65E+05	2.06E+05	3.08E+05	9.11E+05	1.20E+06	1.01E+06
Ho166m	3.39E+03	2.82E+03	3.26E+03	1.24E+04	1.42E+04	1.34E+04	1.21E+04	1.29E+04	1.61E+04	1.18E+04	3.29E+03	2.65E+03	3.53E+03
Total Flux	8.18E-08	2.06E-07	3.18E-07	7.63E-07	1.24E-06	1.42E-06	1.58E-06	1.48E-06	1.2E-06	7.54E-07	2.82E-07	1.56E-07	6.56E-08
Thermal	3.65E-08	8.16E-08	9.84E-08	2.39E-07	3.88E-07	3.99E-07	4.42E-07	3.91E-07	3.12E-07	2.23E-07	1.13E-07	7.59E-08	3.72E-08
Epithermal	3.35E-08	7.15E-08	9.66E-08	2.27E-07	3.62E-07	4.16E-07	4.41E-07	4.33E-07	3.22E-07	2.27E-07	1.03E-07	6.74E-08	2.61E-08
Fast Flux	1.17E-08	5.3E-08	1.23E-07	2.96E-07	4.95E-07	6.02E-07	6.97E-07	6.54E-07	5.68E-07	3.04E-07	6.59E-08	1.26E-08	2.19E-09

Table 24: Axial Activity in Bq/kg for Jowett Precursors in the Sizewell A Reactor

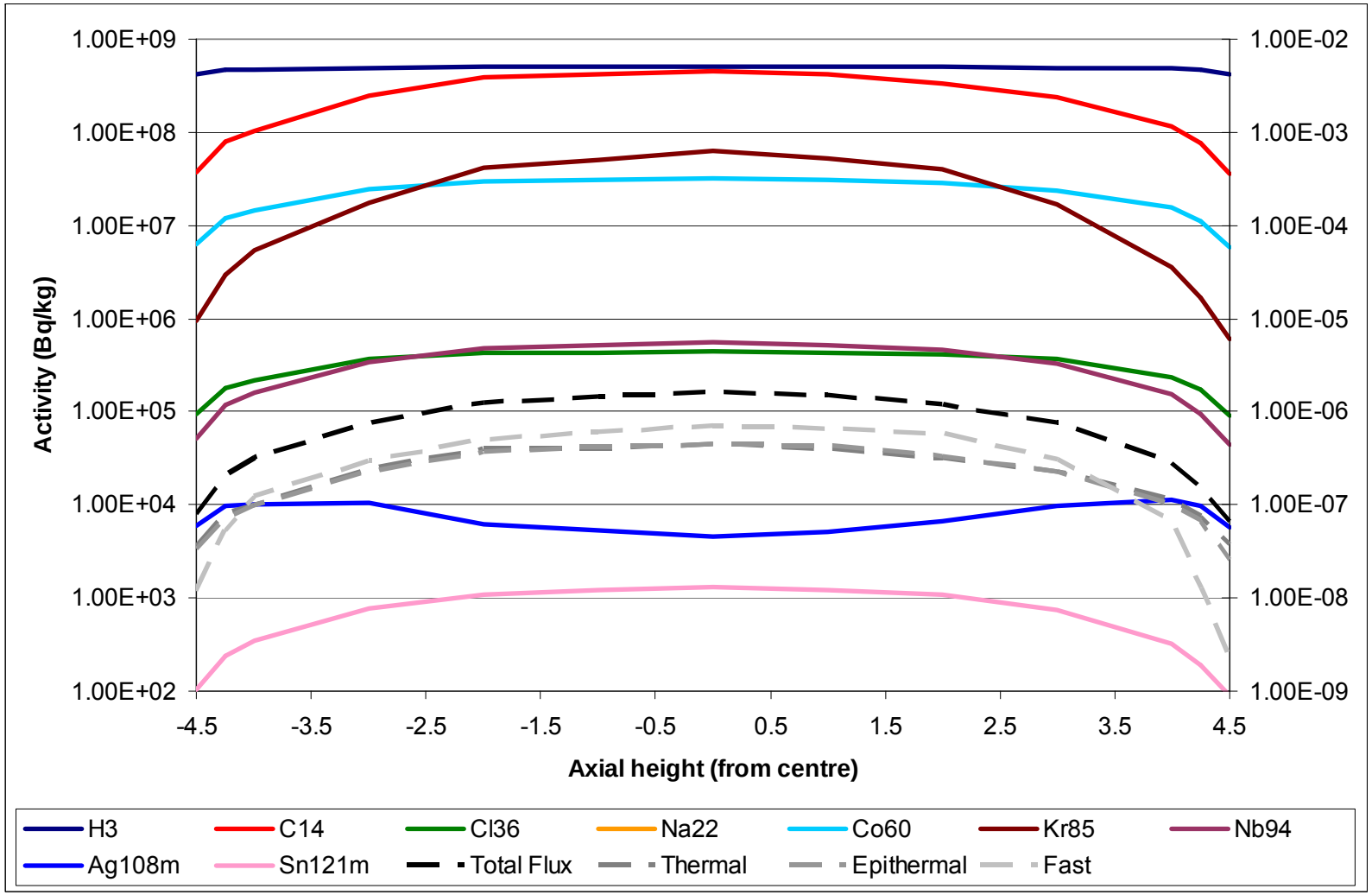

Figure 56: Radionuclide trends for Axial nuclides in the Sizewell A reactor (1/2)

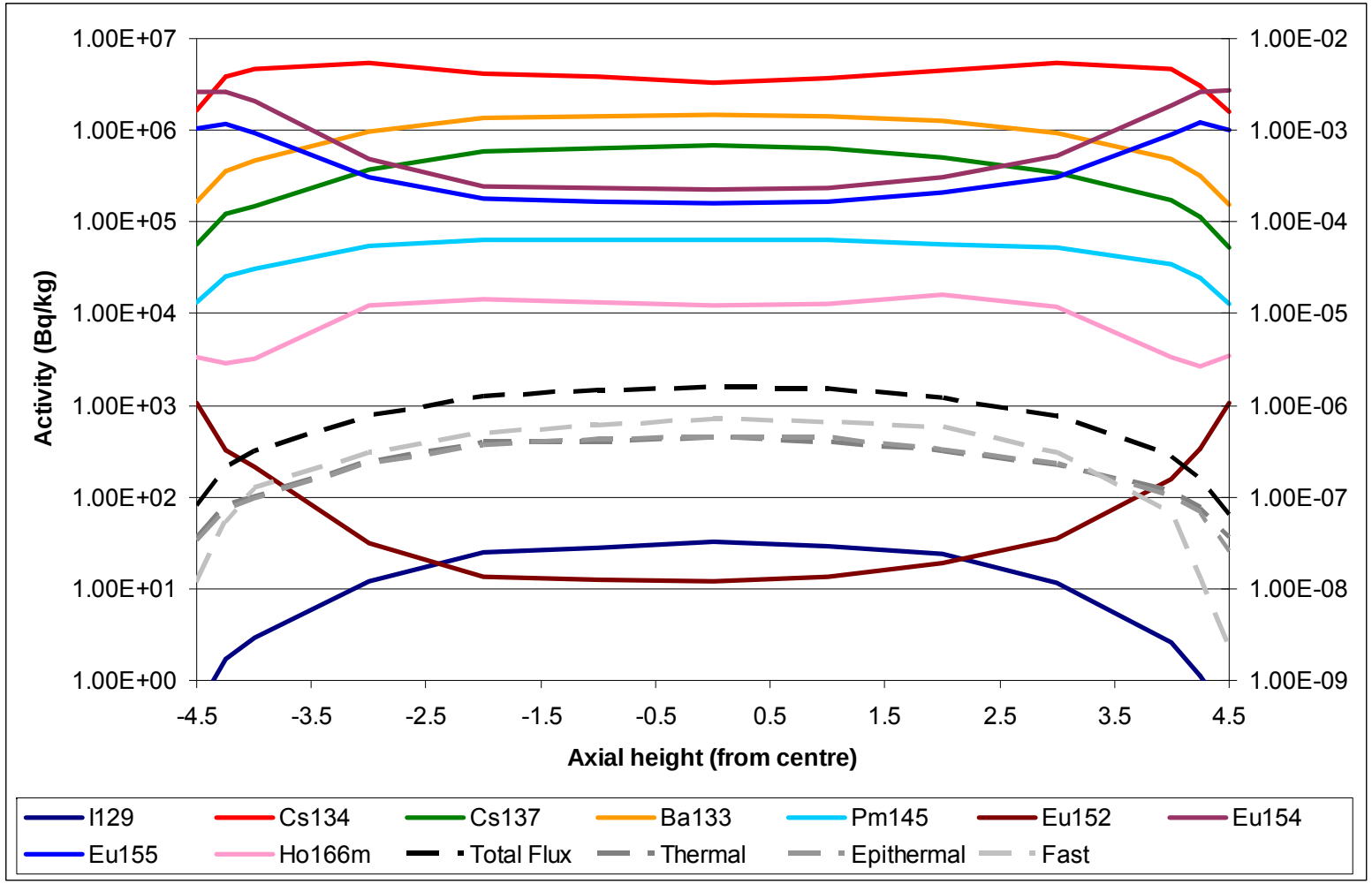

Figure 57: Radionuclide trends for Axial nuclides in the Sizewell A reactor (2/2)

NPL (Maximum) Precursor Information

Radial Data

Nuclides	0	0.7878	1.5756	2.3634	3.1512	3.939	4.7268	5.5146	6.3024	6.7	6.9	7.1	7.3
H3	5.07E+08	4.98E+08	4.99E+08	4.94E+08	4.88E+08	4.86E+08	4.84E+08	4.78E+08	4.72E+08	4.65E+08	4.55E+08	4.22E+08	2.76E+08
C14	2.81E+08	2.90E+08	2.91E+08	2.63E+08	2.18E+08	1.80E+08	1.52E+08	1.11E+08	7.62E+07	5.68E+07	4.19E+07	2.50E+07	9.67E+06
Cl36	2.09E+06	2.09E+06	2.09E+06	2.07E+06	2.01E+06	1.89E+06	1.76E+06	1.48E+06	1.17E+06	9.45E+05	7.40E+05	4.71E+05	1.93E+05
Na22	N/A	N/A	N/A	N/A	N/A	N/A	N/A	N/A	N/A	N/A	N/A	N/A	N/A
Co60	1.65E+07	1.66E+07	1.66E+07	1.62E+07	1.53E+07	1.42E+07	1.32E+07	1.12E+07	8.73E+06	6.95E+06	5.38E+06	3.43E+06	1.41E+06
Kr85	4.55E+04	4.50E+04	4.51E+04	4.20E+04	3.84E+04	3.39E+04	2.94E+04	2.33E+04	1.47E+04	8.18E+03	4.94E+03	2.53E+03	7.47E+02
Nb94	1.64E-01	1.43E-01	1.41E-01	1.12E-01	8.90E-02	7.98E-02	6.27E-02	3.85E-02	1.88E-02	5.48E-03	1.82E-03	4.40E-04	2.18E-05
Ag108m	N/A	N/A	N/A	N/A	N/A	N/A	N/A	N/A	N/A	N/A	N/A	N/A	N/A
Sn121m	2.90E+02	2.80E+02	2.85E+02	2.69E+02	2.53E+02	2.25E+02	2.00E+02	1.64E+02	1.00E+02	4.18E+01	1.92E+01	8.31E+00	2.25E+00
I129	3.38E+00	3.31E+00	3.27E+00	3.09E+00	2.95E+00	2.73E+00	2.42E+00	1.91E+00	1.29E+00	8.12E-01	5.63E-01	3.36E-01	1.32E-01
Cs134	2.35E+08	2.34E+08	2.21E+08	2.61E+08	3.11E+08	3.60E+08	3.81E+08	3.93E+08	3.45E+08	2.51E+08	1.81E+08	1.12E+08	4.67E+07
Ba133	9.43E+05	9.52E+05	9.50E+05	8.94E+05	8.09E+05	7.25E+05	6.33E+05	4.92E+05	3.43E+05	2.46E+05	1.78E+05	1.07E+05	4.20E+04
Cs137	1.10E+06	1.08E+06	1.08E+06	9.32E+05	7.85E+05	6.39E+05	5.24E+05	3.98E+05	2.34E+05	1.09E+05	5.73E+04	2.77E+04	8.76E+03
Pm145	4.17E+04	4.28E+04	4.21E+04	4.16E+04	3.90E+04	3.68E+04	3.41E+04	2.83E+04	2.24E+04	1.83E+04	1.42E+04	8.91E+03	3.60E+03
Eu152	6.12E+00	5.70E+00	5.48E+00	6.11E+00	9.24E+00	1.47E+01	2.13E+01	4.49E+01	9.93E+01	1.69E+02	2.86E+02	6.31E+02	2.04E+03
Eu154	1.15E+05	1.09E+05	1.06E+05	1.23E+05	1.62E+05	2.41E+05	3.34E+05	6.35E+05	1.32E+06	2.00E+06	2.43E+06	2.74E+06	2.24E+06
Eu155	1.08E+05	1.05E+05	1.05E+05	1.12E+05	1.33E+05	1.68E+05	2.09E+05	3.39E+05	5.96E+05	9.31E+05	1.09E+06	1.08E+06	5.90E+05
Ho166m	1.81E+01	1.69E+01	1.76E+01	1.37E+01	1.06E+01	6.72E+00	4.45E+00	2.13E+00	5.70E-01	1.33E-01	3.55E-02	4.36E-03	0
Total Flux	1.53E-06	1.52E-06	1.5E-06	1.31E-06	1.15E-06	9.73E-07	7.96E-07	5.74E-07	3.51E-07	1.9E-07	1.22E-07	6.95E-08	2.66E-08
Thermal	3.98E-07	4.13E-07	4.21E-07	3.83E-07	3.12E-07	2.56E-07	2.14E-07	1.58E-07	1.11E-07	8.78E-08	6.6E-08	3.96E-08	1.53E-08
Epithermal	4.3E-07	4.48E-07	4.38E-07	3.55E-07	3.16E-07	2.67E-07	2.27E-07	1.54E-07	1.02E-07	6.99E-08	4.94E-08	2.9E-08	1.11E-08
Fast Flux	7.06E-07	6.62E-07	6.44E-07	5.71E-07	5.24E-07	4.5E-07	3.55E-07	2.62E-07	1.38E-07	3.21E-08	6.54E-09	9.69E-10	1.48E-10

Table 25: Radial Activity in Bq/kg for NPL Maximum Precursors in the Sizewell A Reactor

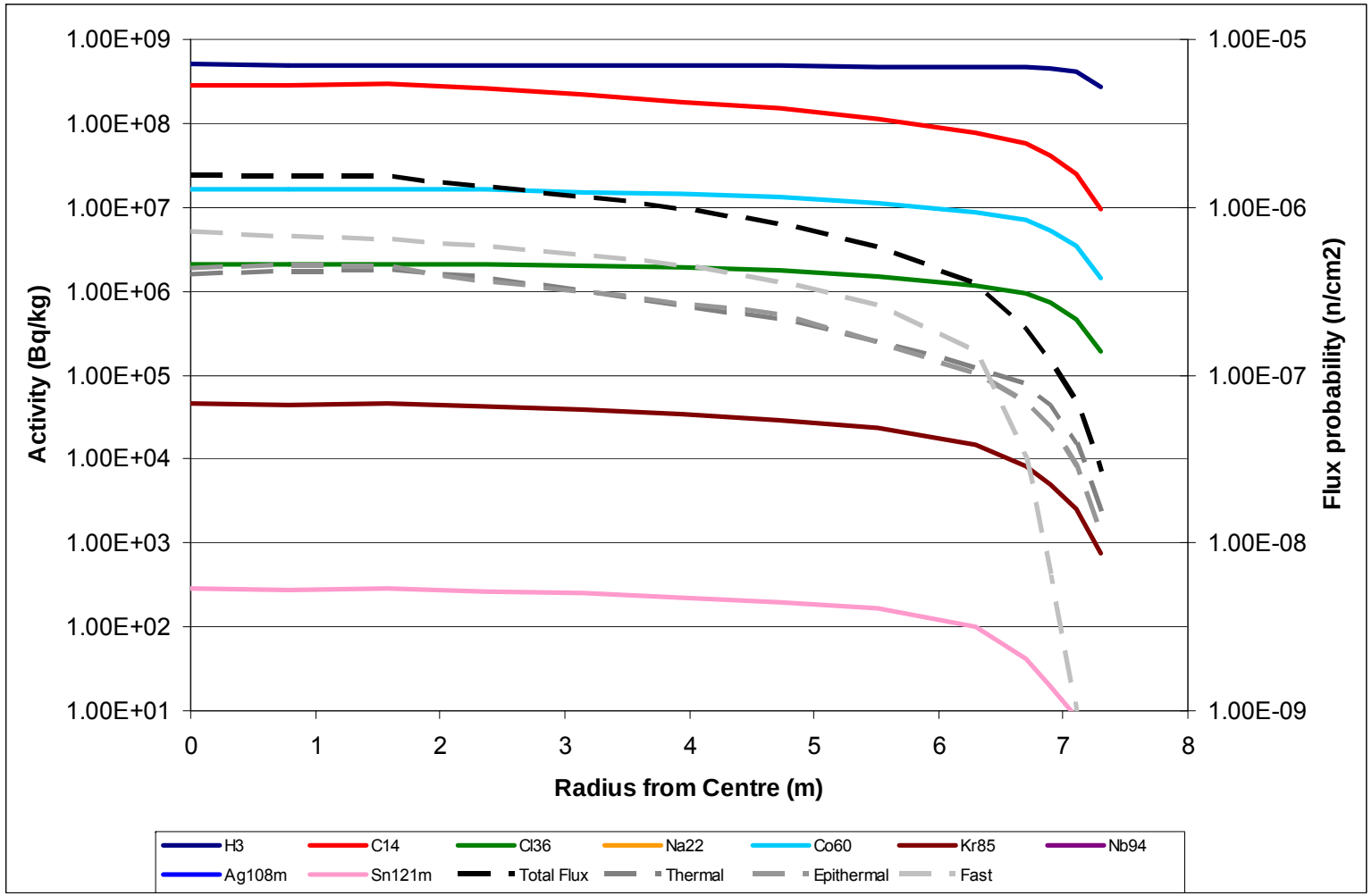

Figure 58: Radionuclide trends for Radial nuclides in the Sizewell A reactor (1/2)

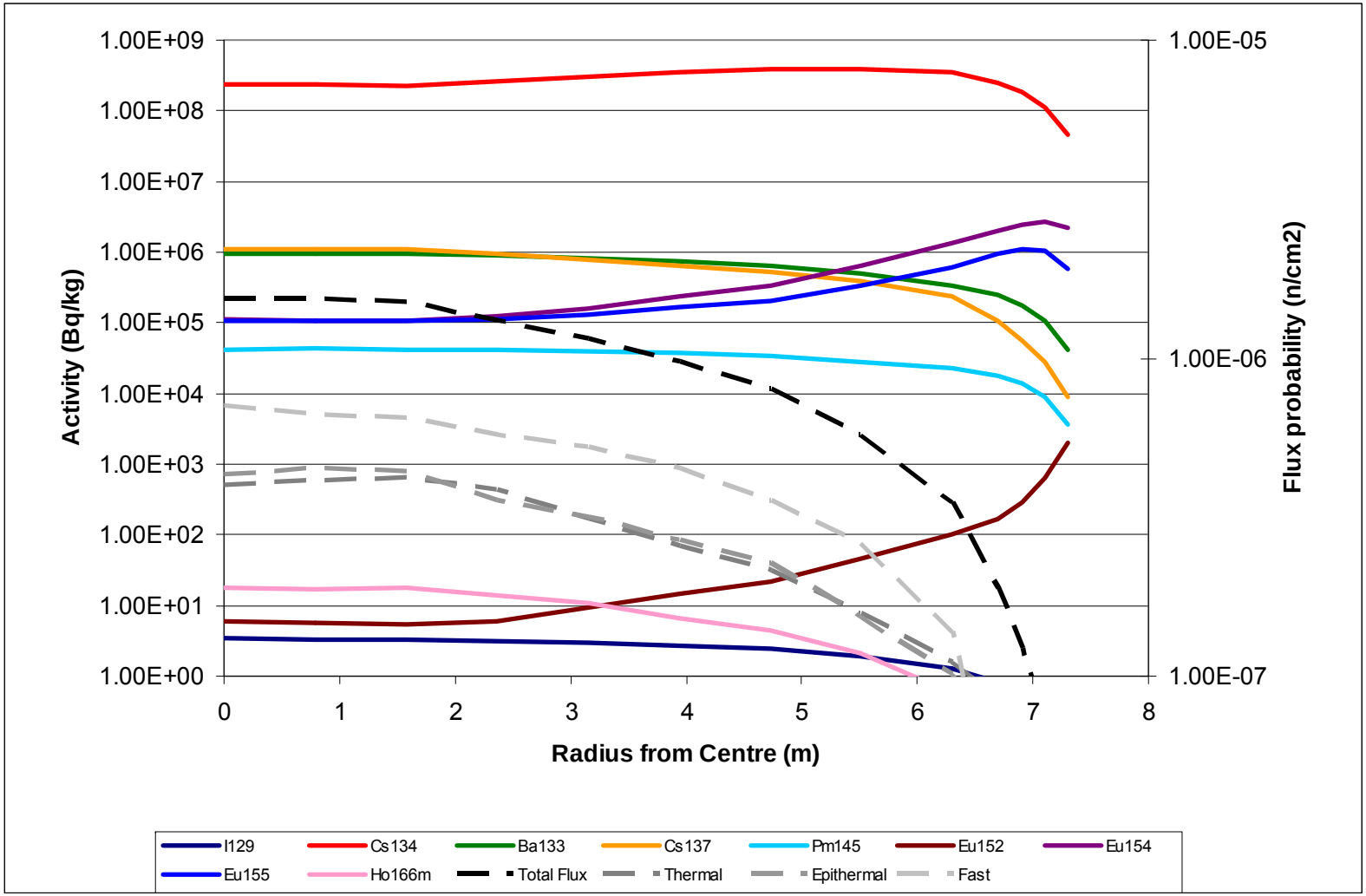

Figure 59: Radionuclide trends for Radial nuclides in the Sizewell A reactor (2/2)

Axial Data

Nuclides	-4.5	-4.25	-4	-3	-2	-1	0	1	2	3	4	4.25	4.5
H3	4.21E+08	4.63E+08	4.69E+08	4.84E+08	4.89E+08	4.92E+08	5.07E+08	4.98E+08	4.98E+08	4.84E+08	4.72E+08	4.61E+08	4.16E+08
C14	2.49E+07	5.32E+07	6.74E+07	1.63E+08	2.61E+08	2.80E+08	2.81E+08	2.77E+08	2.21E+08	1.56E+08	7.61E+07	4.99E+07	2.35E+07
Cl36	4.66E+05	8.96E+05	1.06E+06	1.82E+06	2.08E+06	2.09E+06	2.09E+06	2.08E+06	2.01E+06	1.79E+06	1.18E+06	8.53E+05	4.45E+05
Na22	N/A	N/A	N/A	N/A	N/A	N/A	N/A	N/A	N/A	N/A	N/A	N/A	N/A
Co60	3.45E+06	6.72E+06	8.11E+06	1.36E+07	1.61E+07	1.65E+07	1.65E+07	1.64E+07	1.54E+07	1.33E+07	8.71E+06	6.20E+06	3.24E+06
Kr85	2.93E+03	9.12E+03	1.30E+04	2.90E+04	4.17E+04	4.37E+04	4.55E+04	4.39E+04	4.10E+04	2.85E+04	1.25E+04	6.14E+03	2.50E+03
Nb94	5.70E-03	5.69E-03	1.67E-02	5.63E-02	9.44E-02	1.18E-01	1.64E-01	1.37E-01	1.26E-01	5.51E-02	1.61E-02	2.52E-03	1.89E-03
Ag108m	N/A	N/A	N/A	N/A	N/A	N/A	N/A	N/A	N/A	N/A	N/A	N/A	N/A
Sn121m	1.29E+01	5.58E+01	8.60E+01	1.90E+02	2.60E+02	2.74E+02	2.90E+02	2.79E+02	2.78E+02	1.91E+02	7.70E+01	2.61E+01	9.63E+00
I129	3.69E-01	8.43E-01	1.16E+00	2.30E+00	3.03E+00	3.21E+00	3.38E+00	3.27E+00	3.05E+00	2.28E+00	1.08E+00	6.78E-01	3.21E-01
Cs134	1.20E+08	2.78E+08	3.26E+08	3.75E+08	2.69E+08	2.43E+08	2.35E+08	2.42E+08	2.98E+08	3.80E+08	3.29E+08	2.15E+08	1.13E+08
Ba133	1.11E+05	2.41E+05	3.14E+05	6.50E+05	8.93E+05	9.32E+05	9.43E+05	9.30E+05	8.24E+05	6.26E+05	3.27E+05	2.11E+05	1.01E+05
Cs137	3.51E+04	1.36E+05	2.03E+05	5.09E+05	9.16E+05	1.01E+06	1.10E+06	1.02E+06	8.74E+05	5.02E+05	1.87E+05	7.48E+04	2.91E+04
Pm145	8.85E+03	1.72E+04	2.05E+04	3.58E+04	4.20E+04	4.24E+04	4.17E+04	4.21E+04	3.80E+04	3.47E+04	2.27E+04	1.65E+04	8.38E+03
Eu152	6.79E+02	2.03E+02	1.35E+02	1.67E+01	6.17E+00	5.67E+00	6.12E+00	6.12E+00	9.29E+00	1.90E+01	9.67E+01	2.20E+02	6.82E+02
Eu154	2.76E+06	2.08E+06	1.54E+06	2.96E+05	1.23E+05	1.11E+05	1.15E+05	1.14E+05	1.58E+05	3.19E+05	1.34E+06	2.17E+06	2.88E+06
Eu155	1.08E+06	9.13E+05	6.96E+05	2.01E+05	1.13E+05	1.07E+05	1.08E+05	1.06E+05	1.32E+05	2.01E+05	6.59E+05	9.87E+05	1.08E+06
Ho166m	5.61E-03	1.58E-01	4.17E-01	4.41E+00	1.30E+00	1.60E+01	1.81E+01	1.55E+01	1.33E+01	4.09E+00	4.05E-01	6.68E-02	3.65E-03
Total Flux	8.18E-08	2.06E-07	3.18E-07	7.63E-07	1.24E-06	1.42E-06	1.58E-06	1.48E-06	1.2E-06	7.54E-07	2.82E-07	1.56E-07	6.56E-08
Thermal	3.65E-08	8.16E-08	9.84E-08	2.39E-07	3.88E-07	3.99E-07	4.42E-07	3.91E-07	3.12E-07	2.23E-07	1.13E-07	7.59E-08	3.72E-08
Epithermal	3.35E-08	7.15E-08	9.66E-08	2.27E-07	3.62E-07	4.16E-07	4.41E-07	4.33E-07	3.22E-07	2.27E-07	1.03E-07	6.74E-08	2.61E-08
Fast Flux	1.17E-08	5.3E-08	1.23E-07	2.96E-07	4.95E-07	6.02E-07	6.97E-07	6.54E-07	5.68E-07	3.04E-07	6.59E-08	1.26E-08	2.19E-09

Table 26: Axial Activity in Bq/kg for NPL maximum Precursors in the Sizewell A Reactor

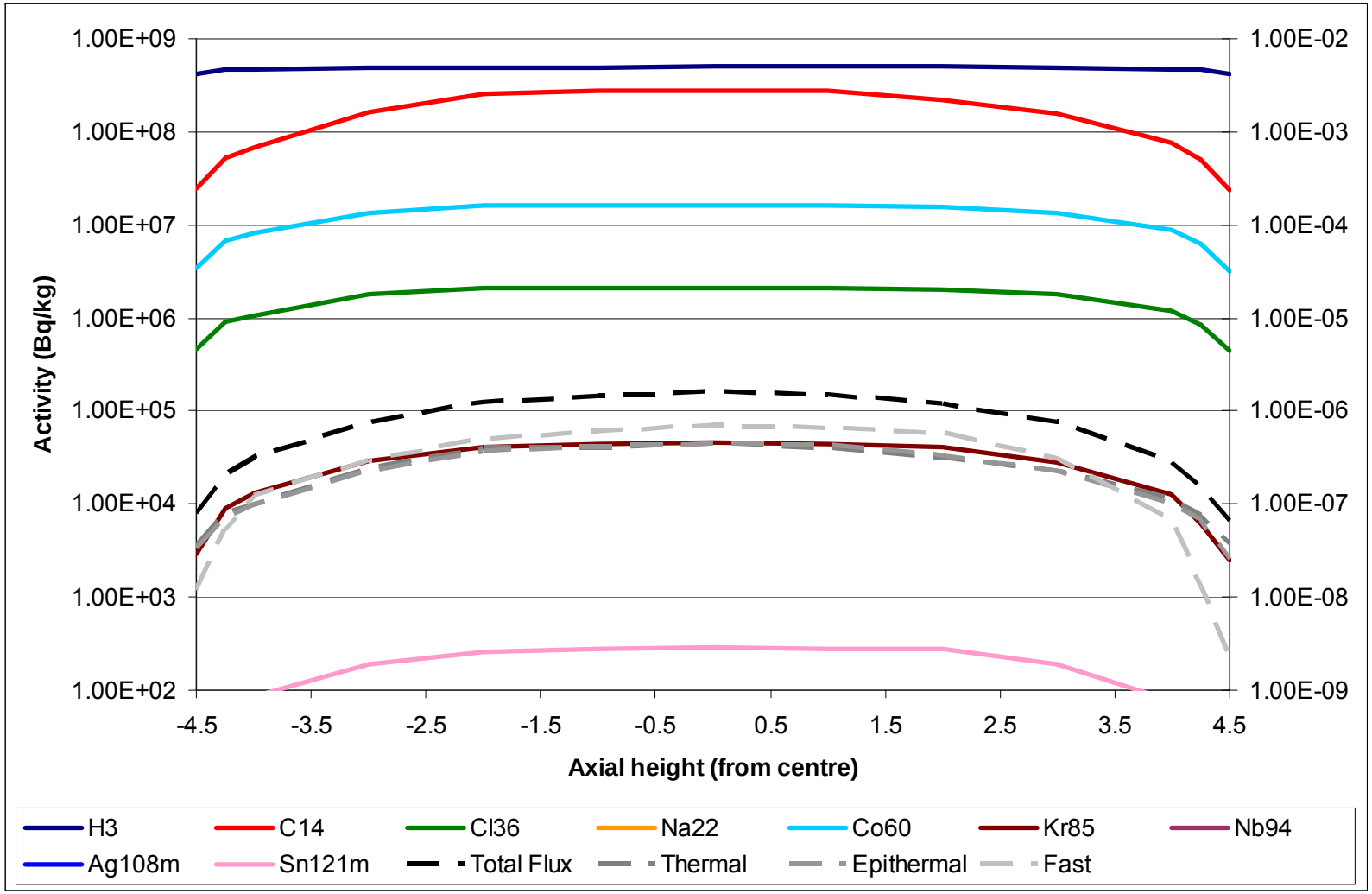

Figure 60: Radionuclide trends for Axial nuclides in the Sizewell A reactor (1/2)

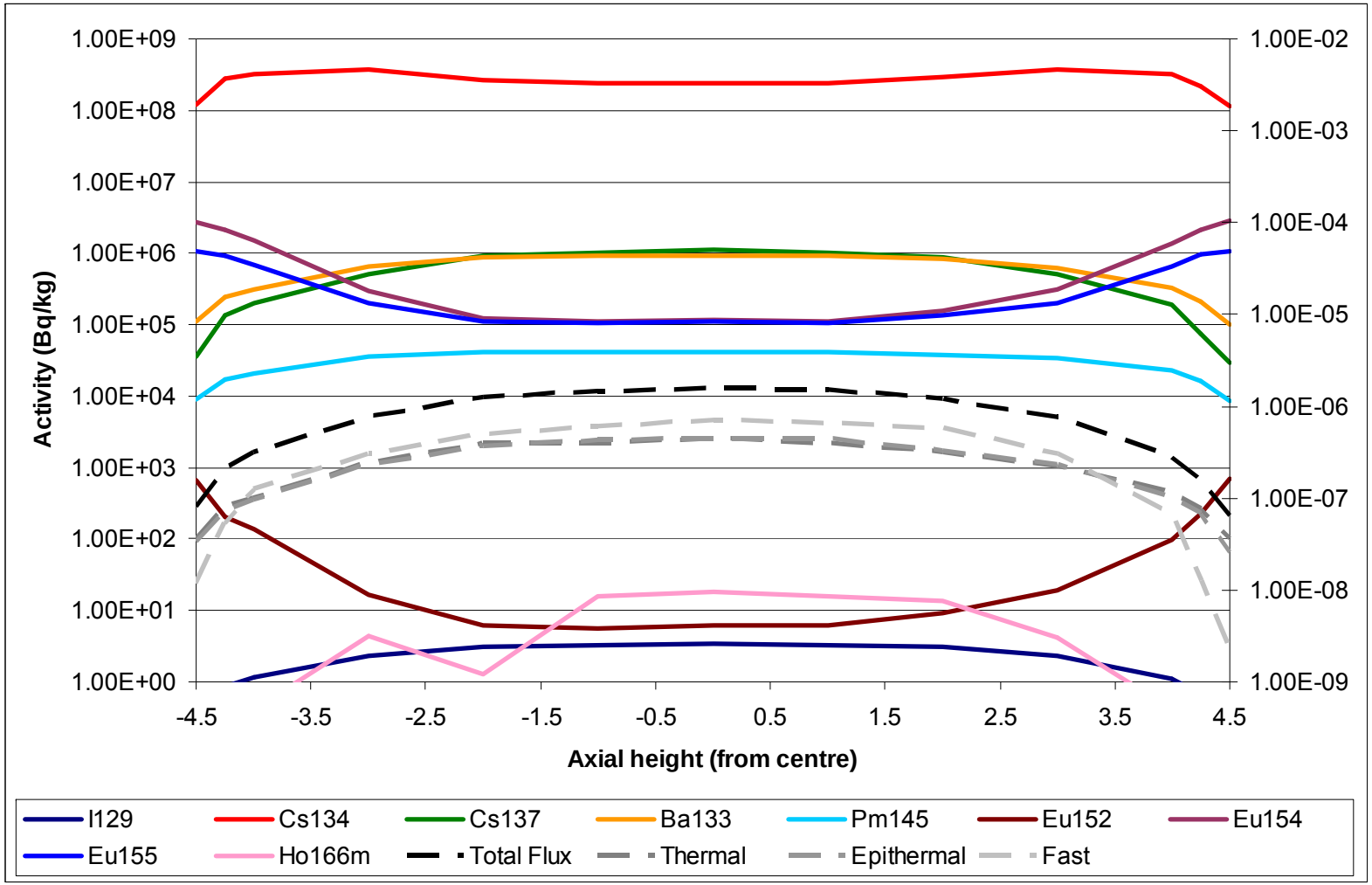

Figure 61: Radionuclide trends for Axial nuclides in the Sizewell A reactor (2/2)

NPL (Average) Precursor Information

Radial Data

Nuclides	0	0.7878	1.5756	2.3634	3.1512	3.939	4.7268	5.5146	6.3024	6.7	6.9	7.1	7.3
H3	4.66E+08	4.58E+08	4.58E+08	4.54E+08	4.48E+08	4.46E+08	4.44E+08	4.39E+08	4.33E+08	4.27E+08	4.18E+08	3.87E+08	2.53E+08
C14	2.42E+08	2.39E+08	2.51E+08	2.26E+08	1.88E+08	1.55E+08	1.31E+08	9.52E+07	6.55E+07	4.87E+07	3.59E+07	2.14E+07	8.28E+06
Cl36	1.59E+06	1.59E+06	1.59E+06	1.58E+06	1.53E+06	1.44E+06	1.34E+06	1.13E+06	8.89E+05	7.20E+05	5.64E+05	3.59E+05	1.47E+05
Na22	N/A	N/A	N/A	N/A	N/A	N/A	N/A	N/A	N/A	N/A	N/A	N/A	N/A
Co60	1.11E+07	1.11E+07	1.13E+07	1.09E+07	1.02E+07	9.47E+06	8.73E+06	7.37E+06	5.74E+06	4.56E+06	3.53E+06	2.25E+06	9.25E+05
Kr85	4.55E+04	4.39E+04	4.51E+04	4.20E+04	3.84E+04	3.39E+04	2.94E+04	2.33E+04	1.47E+04	8.18E+03	4.94E+03	2.53E+03	7.47E+02
Nb94	1.13E-01	9.45E-02	9.73E-02	7.78E-02	6.20E-02	5.56E-02	4.38E-02	2.71E-02	1.34E-02	4.08E-03	1.43E-03	3.87E-04	2.18E-05
Ag108m	N/A	N/A	N/A	N/A	N/A	N/A	N/A	N/A	N/A	N/A	N/A	N/A	N/A
Sn121m	2.90E+02	2.79E+02	2.85E+02	2.69E+02	2.53E+02	2.25E+02	2.00E+02	1.64E+02	1.00E+02	4.18E+01	1.92E+01	8.31E+00	2.25E+00
I129	3.38E+00	3.27E+00	3.27E+00	3.09E+00	2.95E+00	2.73E+00	2.42E+00	1.91E+00	1.29E+00	8.12E-01	5.63E-01	3.36E-01	1.32E-01
Cs134	2.35E+08	2.42E+08	2.21E+08	2.61E+08	3.11E+08	3.60E+08	3.81E+08	3.93E+08	3.45E+08	2.51E+08	1.81E+08	1.12E+08	4.67E+07
Ba133	5.27E+05	5.20E+05	5.31E+05	5.00E+05	4.52E+05	4.05E+05	3.54E+05	2.75E+05	1.92E+05	1.37E+05	9.94E+04	5.97E+04	2.35E+04
Cs137	1.10E+06	1.02E+06	1.08E+06	9.32E+05	7.85E+05	6.39E+05	5.24E+05	3.98E+05	2.34E+05	1.09E+05	5.73E+04	2.77E+04	8.76E+03
Pm145	4.17E+04	4.21E+04	4.21E+04	4.16E+04	3.90E+04	3.68E+04	3.41E+04	2.83E+04	2.24E+04	1.83E+04	1.42E+04	8.91E+03	3.60E+03
Eu152	6.12E+00	6.12E+00	5.48E+00	6.11E+00	9.24E+00	1.47E+01	2.13E+01	4.49E+01	9.93E+01	1.69E+02	2.86E+02	6.31E+02	2.04E+03
Eu154	1.15E+05	1.14E+05	1.06E+05	1.23E+05	1.62E+05	2.41E+05	3.34E+05	6.35E+05	1.32E+06	2.00E+06	2.43E+06	2.74E+06	2.24E+06
Eu155	1.08E+05	1.06E+05	1.05E+05	1.12E+05	1.33E+05	1.68E+05	2.09E+05	3.39E+05	5.96E+05	9.31E+05	1.09E+06	1.08E+06	5.90E+05
Ho166m	1.75E+01	1.50E+01	1.71E+01	1.32E+01	1.02E+01	6.45E+00	4.26E+00	2.03E+00	5.45E-01	1.27E-01	3.39E-02	4.16E-03	0
Total Flux	1.53E-06	1.52E-06	1.5E-06	1.31E-06	1.15E-06	9.73E-07	7.96E-07	5.74E-07	3.51E-07	1.9E-07	1.22E-07	6.95E-08	2.66E-08
Thermal	3.98E-07	4.13E-07	4.21E-07	3.83E-07	3.12E-07	2.56E-07	2.14E-07	1.58E-07	1.11E-07	8.78E-08	6.6E-08	3.96E-08	1.53E-08
Epithermal	4.3E-07	4.48E-07	4.38E-07	3.55E-07	3.16E-07	2.67E-07	2.27E-07	1.54E-07	1.02E-07	6.99E-08	4.94E-08	2.9E-08	1.11E-08
Fast Flux	7.06E-07	6.62E-07	6.44E-07	5.71E-07	5.24E-07	4.5E-07	3.55E-07	2.62E-07	1.38E-07	3.21E-08	6.54E-09	9.69E-10	1.48E-10

Table 27: Radial Activity in Bq/kg for NPL Average Precursors in the Sizewell A Reactor

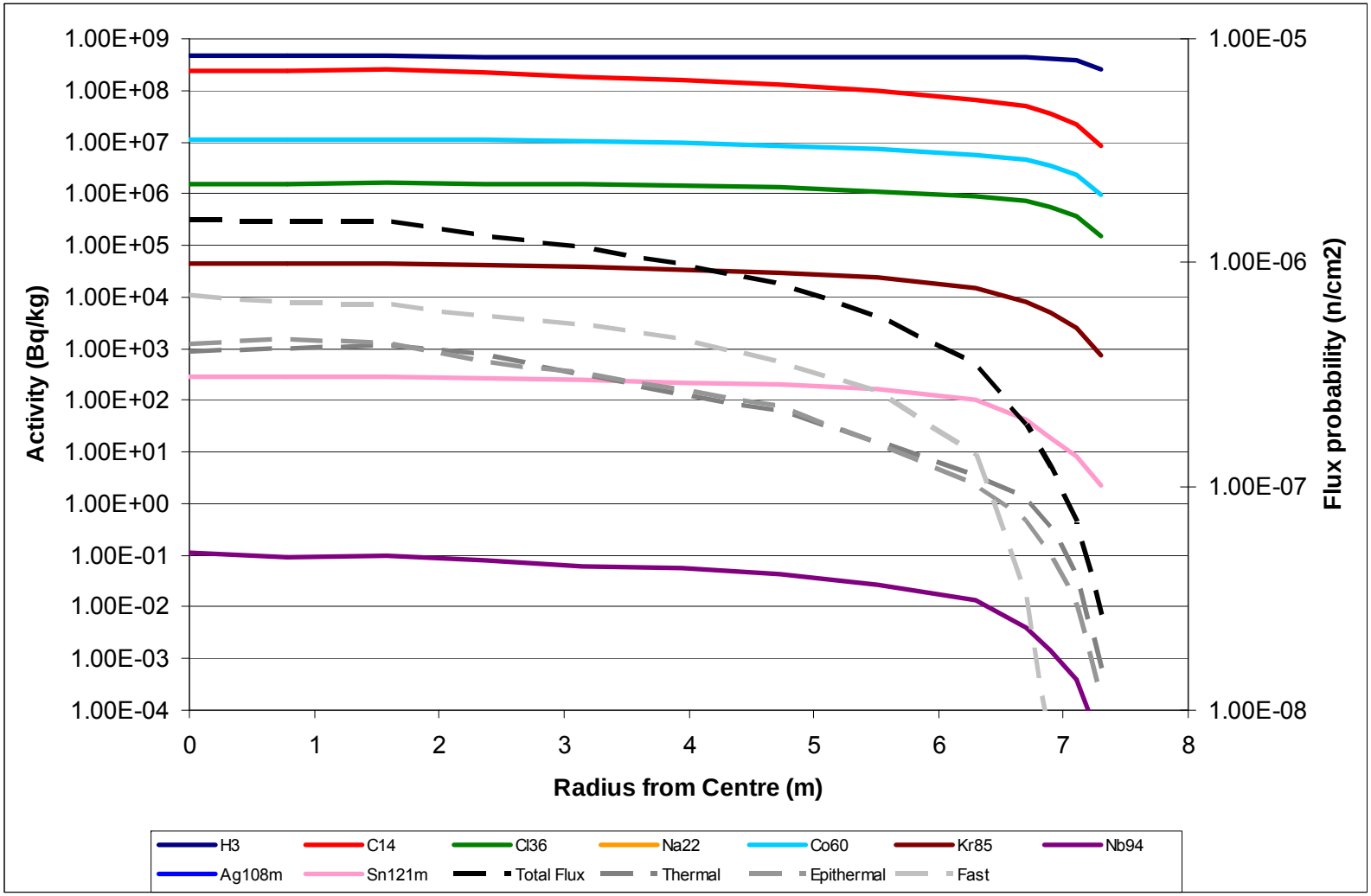

Figure 62: Radionuclide trends for Radial nuclides in the Sizewell A reactor (1/2)

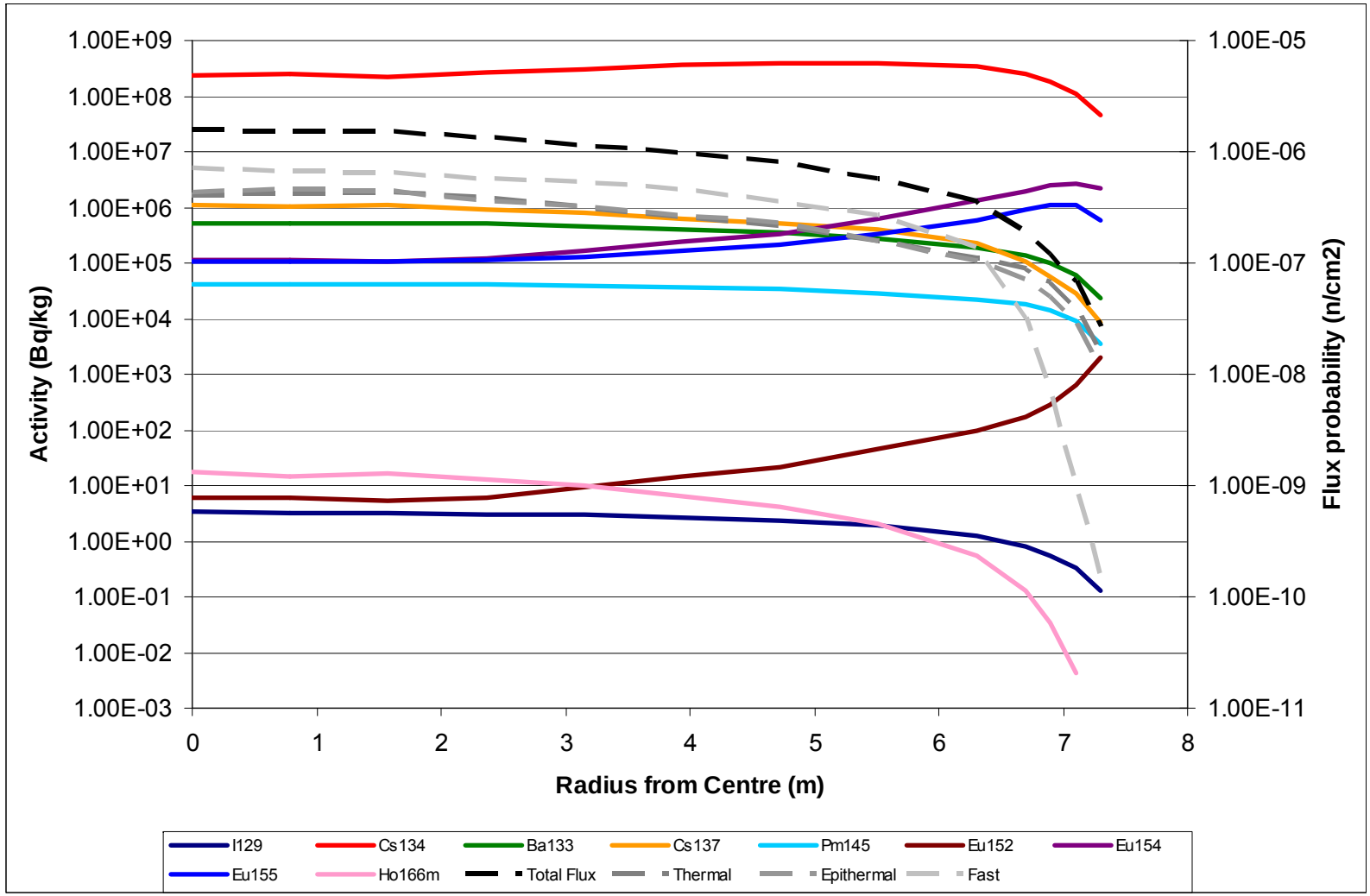
1.00E+09
1.00E+08
1.00E+07
1.00E+06
1.00E+05
1.00E+04
1.00E+03
1.00E+02
1.00E+01
1.00E+00
1.00E-01
1.00E-02
1.00E-03
Activity (Bq/kg)
1.00E-05
1.00E-06
1.00E-07
1.00E-08
1.00E-09
1.00E-10
1.00E-11
Flux probability (n/cm2)
0
1
2
3
4
5
6
7
8
Radius from Centre (m)
I129
Cs134
Ba133
Cs137
Pm145
Eu152
Eu154
Eu155
Ho166m
Total Flux
Thermal
Epithermal
Fast

Figure 63: Radionuclide trends for Radial nuclides in the Sizewell A reactor (2/2)

Axial Data

Nuclides	-4.5	-4.25	-4	-3	-2	-1	0	1	2	3	4	4.25	4.5
H3	3.86E+08	4.25E+08	4.31E+08	4.44E+08	4.49E+08	4.52E+08	4.66E+08	4.58E+08	4.58E+08	4.44E+08	4.33E+08	4.23E+08	3.81E+08
C14	2.13E+07	4.56E+07	5.79E+07	1.41E+08	2.25E+08	2.42E+08	2.42E+08	2.39E+08	1.90E+08	1.34E+08	6.53E+07	4.27E+07	2.01E+07
Cl36	3.55E+05	6.83E+05	8.11E+05	1.39E+06	1.58E+06	1.59E+06	1.59E+06	1.59E+06	1.53E+06	1.36E+06	8.96E+05	6.50E+05	3.39E+05
Na22	N/A	N/A	N/A	N/A	N/A	N/A	N/A	N/A	N/A	N/A	N/A	N/A	N/A
Co60	2.26E+06	4.41E+06	5.33E+06	9.01E+06	1.09E+07	1.11E+07	1.11E+07	1.11E+07	1.03E+07	8798000	5.73E+06	4.07E+06	2.12E+06
Kr85	2.93E+03	9.12E+03	1.30E+04	2.90E+04	4.17E+04	4.37E+04	4.55E+04	4.39E+04	4.10E+04	2.85E+04	1.25E+04	6.14E+03	2.50E+03
Nb94	3.99E-03	4.26E-03	1.19E-02	3.94E-02	6.58E-02	8.17E-02	1.13E-01	9.45E-02	8.72E-02	3.86E-02	1.15E-02	1.97E-03	1.38E-03
Ag108m	N/A	N/A	N/A	N/A	N/A	N/A	N/A	N/A	N/A	N/A	N/A	N/A	N/A
Sn121m	1.29E+01	5.58E+01	8.60E+01	1.90E+02	2.60E+02	2.74E+02	2.90E+02	2.79E+02	2.78E+02	1.91E+02	7.70E+01	2.61E+01	9.63E+00
I129	3.69E-01	8.43E-01	1.16E+00	2.30E+00	3.03E+00	3.21E+00	3.38E+00	3.27E+00	3.05E+00	2.28E+00	1.08E+00	6.78E-01	3.21E-01
Cs134	1.20E+08	2.78E+08	3.26E+08	3.75E+08	2.69E+08	2.43E+08	2.35E+08	2.42E+08	2.98E+08	3.80E+08	3.29E+08	2.15E+08	1.13E+08
Ba133	6.18E+04	1.35E+05	1.75E+05	3.63E+05	4.99E+05	5.21E+05	5.27E+05	5.20E+05	4.61E+05	3.50E+05	1.83E+05	1.18E+05	5.63E+04
Cs137	3.51E+04	1.36E+05	2.03E+05	5.09E+05	9.16E+05	1.01E+06	1.10E+06	1.02E+06	8.74E+05	501700	1.87E+05	7.48E+04	2.91E+04
Pm145	8.85E+03	1.72E+04	2.05E+04	3.58E+04	4.20E+04	4.24E+04	4.17E+04	4.21E+04	3.80E+04	3.47E+04	2.27E+04	1.65E+04	8.38E+03
Eu152	6.79E+02	2.03E+02	1.35E+02	1.67E+01	6.17E+00	5.67E+00	6.12E+00	6.12E+00	9.29E+00	1.90E+01	9.67E+01	2.20E+02	6.82E+02
Eu154	2.76E+06	2.08E+06	1.54E+06	2.96E+05	1.23E+05	1.11E+05	1.15E+05	1.14E+05	1.58E+05	3.19E+05	1.34E+06	2.17E+06	2.88E+06
Eu155	1.08E+06	9.13E+05	6.96E+05	2.01E+05	1.13E+05	1.07E+05	1.08E+05	1.06E+05	1.32E+05	2.01E+05	6.59E+05	9.87E+05	1.08E+06
Ho166m	5.35E-03	1.51E-01	3.98E-01	4.22E+00	1.25E+01	1.25E+01	1.75E+01	1.50E+01	1.28E+01	3.92E+00	3.87E-01	6.38E-02	3.47E-03
Total Flux	8.18E-08	2.06E-07	3.18E-07	7.63E-07	1.24E-06	1.42E-06	1.58E-06	1.48E-06	1.2E-06	7.54E-07	2.82E-07	1.56E-07	6.56E-08
Thermal	3.65E-08	8.16E-08	9.84E-08	2.39E-07	3.88E-07	3.99E-07	4.42E-07	3.91E-07	3.12E-07	2.23E-07	1.13E-07	7.59E-08	3.72E-08
Epithermal	3.35E-08	7.15E-08	9.66E-08	2.27E-07	3.62E-07	4.16E-07	4.41E-07	4.33E-07	3.22E-07	2.27E-07	1.03E-07	6.74E-08	2.61E-08
Fast Flux	1.17E-08	5.3E-08	1.23E-07	2.96E-07	4.95E-07	6.02E-07	6.97E-07	6.54E-07	5.68E-07	3.04E-07	6.59E-08	1.26E-08	2.19E-09

Table 28: Axial Activity in Bq/kg for NPL Average Precursors in the Sizewell A Reactor

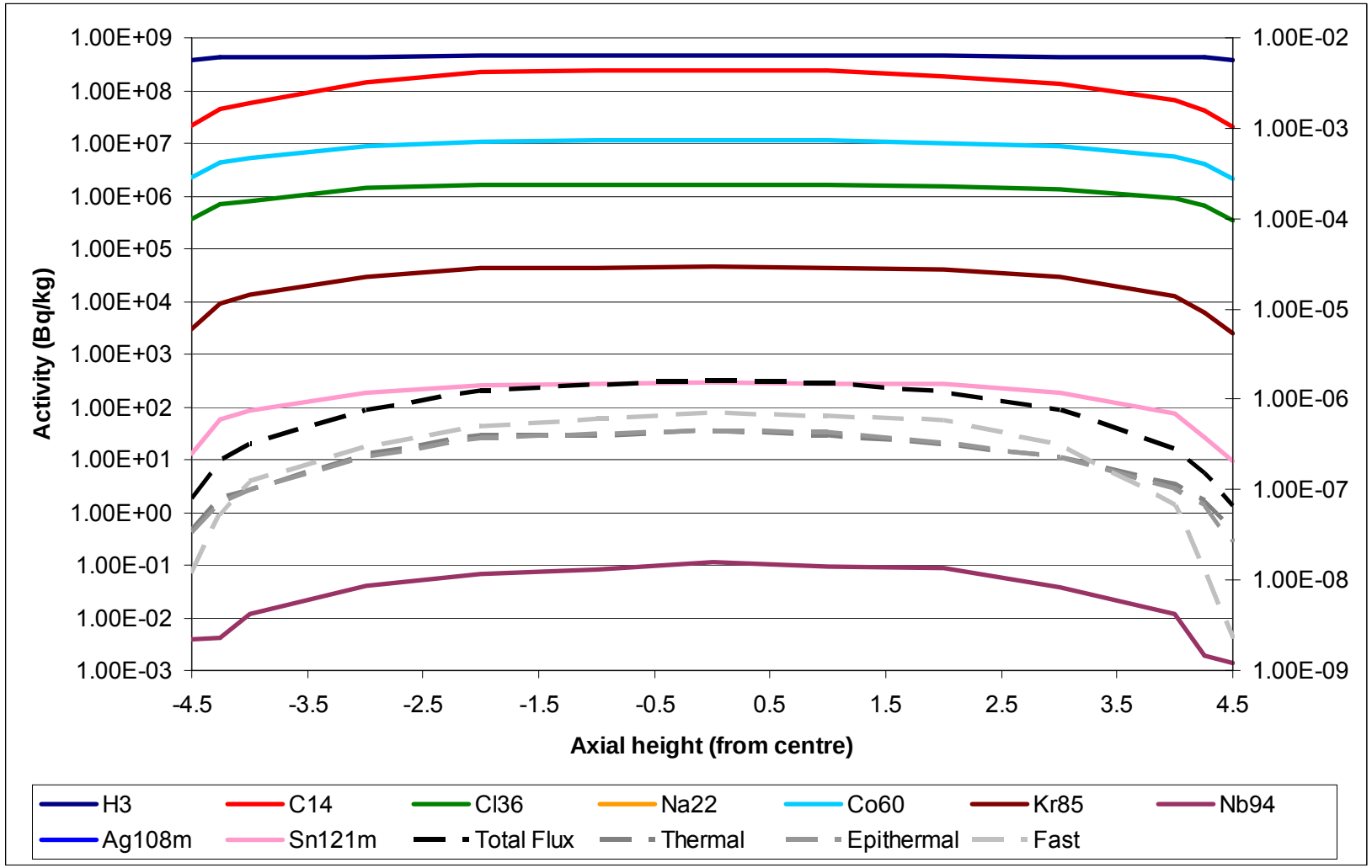

Figure 64: Radionuclide trends for Axial nuclides in the Sizewell A reactor (1/2)

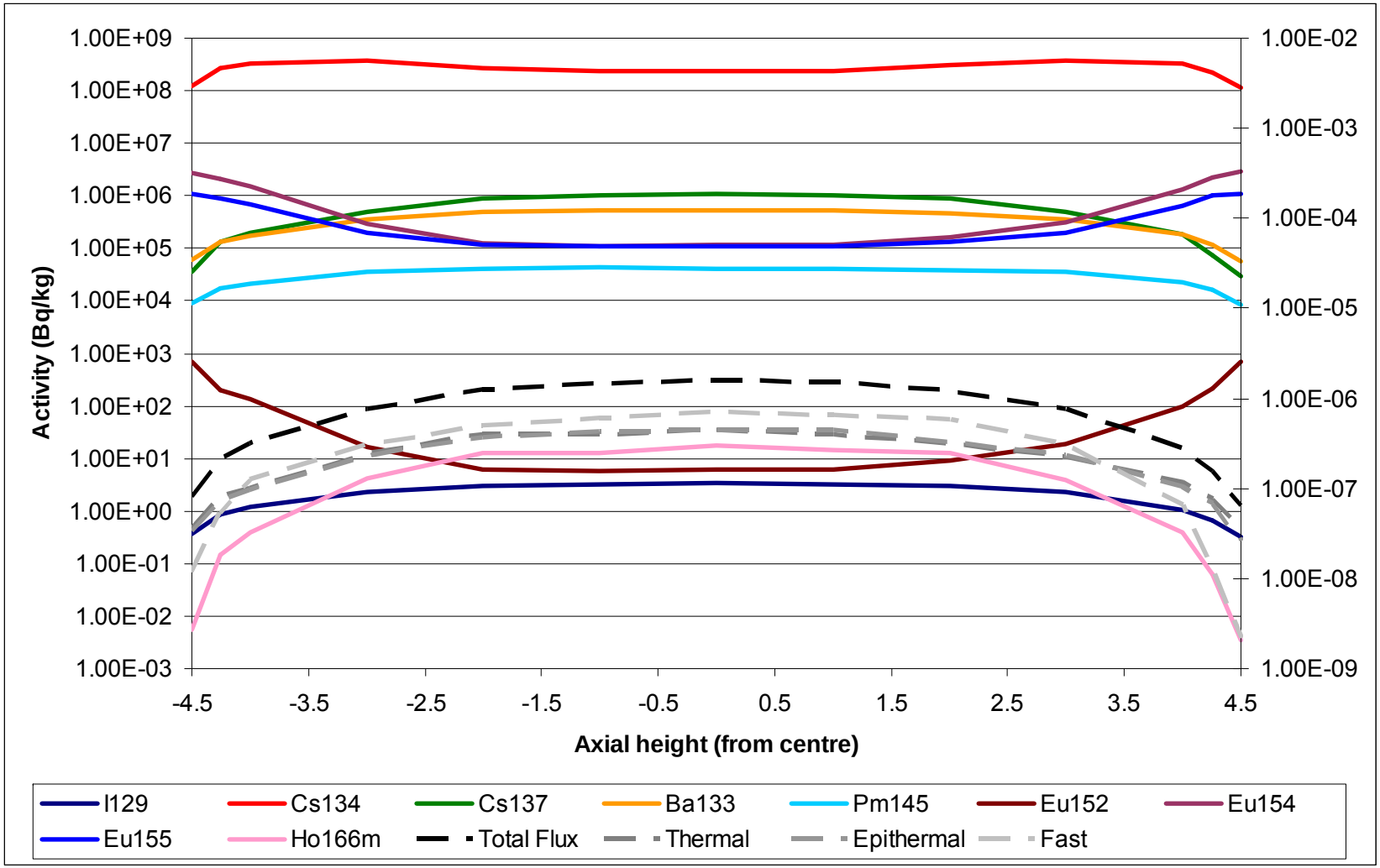
1.00E+09
1.00E+08
1.00E+07
1.00E+06
1.00E+05
1.00E+04
1.00E+03
1.00E+02
1.00E+01
1.00E+00
1.00E-01
1.00E-02
1.00E-03
1.00E-02
1.00E-03
1.00E-04
1.00E-05
1.00E-06
1.00E-07
1.00E-08
1.00E-09
Activity (Bq/kg)
-4.5
-3.5
-2.5
-1.5
-0.5
0.5
1.5
2.5
3.5
4.5
Axial height (from centre)
I129
Cs134
Cs137
Ba133
Pm145
Eu152
Eu154
Eu155
Ho166m
Total Flux
Thermal
Epithermal
Fast

Figure 65: Radionuclide trends for Axial nuclides in the Sizewell A reactor (2/2)

APPENDIX 10 – WYLFA REACTOR 1 RADIONUCLIDE INVENTORY BY POSITION RADIALLY AND AXIALLY IN THE CORE AND REFLECTOR REGIONS

Data is presented in the following, tabular format:

	Region the data refers to (e.g. reflector, or 'core')			
Nuclides of Interest	**Position in meters either radially or Axially from the centre of the core**			
Nuclide	Nuclide activity in Bq/kg	**…**	**…**	**…**
Flux Values assuming a loading factor of 75% (1200 MWh(th))	Flux values in n/s/cm^2	**…**	**…**	**…**

Note: All activities listed here are correct for ten years of decay post reactor shutdown (2109)

Jowett Precursor Information

Radial Data

	Core Region											Reflector Region			
Nuclides	0.00	0.78	1.57	2.35	3.14	3.92	4.71	5.49	6.28	7.06	7.85	8.25	8.55	8.85	9.15
H3	5.3E+08	5.2E+08	5.2E+08	5.2E+08	5.1E+08	5.0E+08	5.1E+08	5.0E+08	4.9E+08	4.9E+08	4.8E+08	4.8E+08	4.7E+08	4.4E+08	3.5E+08
C14	4.7E+08	4.6E+08	4.9E+08	4.2E+08	4.0E+08	3.4E+08	3.1E+08	2.4E+08	2.0E+08	1.4E+08	9.4E+07	1.0E+08	7.4E+07	4.2E+07	2.0E+07
Cl36	4.4E+05	4.4E+05	4.4E+05	4.3E+05	4.3E+05	4.2E+05	4.1E+05	3.7E+05	3.3E+05	2.7E+05	2.0E+05	2.2E+05	1.7E+05	1.0E+05	5.2E+04
Na22	N/A	N/A	N/A	N/A	N/A	N/A	N/A	N/A	N/A	N/A	N/A	N/A	N/A	N/A	N/A
Co60	3.9E+07	3.9E+07	3.9E+07	3.7E+07	3.7E+07	3.4E+07	3.3E+07	2.9E+07	2.7E+07	2.2E+07	1.6E+07	1.7E+07	1.3E+07	8.0E+06	4.0E+06
Kr85	8.8E+07	8.5E+07	7.9E+07	6.5E+07	6.7E+07	4.1E+07	3.5E+07	2.4E+07	1.5E+07	1.2E+07	6.0E+06	3.1E+06	1.4E+06	7.4E+05	3.4E+05
Nb94	5.8E+05	5.7E+05	5.7E+05	5.3E+05	5.3E+05	4.5E+05	4.3E+05	3.5E+05	3.0E+05	2.4E+05	1.5E+05	1.3E+05	9.0E+04	5.2E+04	2.5E+04
Ag108m	3.9E+03	4.2E+03	4.2E+03	4.6E+03	5.4E+03	6.2E+03	7.3E+03	8.9E+03	9.8E+03	1.1E+04	1.0E+04	1.2E+04	1.0E+04	6.6E+03	3.4E+03
Sn121m	1.4E+03	1.4E+03	1.4E+03	1.3E+03	1.3E+03	1.1E+03	1.0E+03	8.4E+02	6.9E+02	5.5E+02	3.4E+02	2.7E+02	1.9E+02	1.1E+02	5.1E+01
I129	3.7E+01	3.6E+01	3.5E+01	3.1E+01	3.1E+01	2.4E+01	2.0E+01	1.4E+01	9.3E+00	6.3E+00	2.7E+00	1.9E+00	1.0E+00	4.7E-01	1.9E-01
Cs134	3.4E+06	3.7E+06	3.6E+06	4.0E+06	4.5E+06	5.0E+06	5.6E+06	6.3E+06	6.6E+06	6.2E+06	5.2E+06	4.5E+06	3.3E+06	2.0E+06	1.0E+06
Ba133	1.7E+06	1.7E+06	1.7E+06	1.6E+06	1.6E+06	1.4E+06	1.3E+06	1.1E+06	9.6E+05	7.4E+05	4.9E+05	4.8E+05	3.5E+05	2.0E+05	9.7E+04
Cs137	7.6E+05	7.5E+05	7.9E+05	6.8E+05	6.4E+05	5.4E+05	4.9E+05	3.8E+05	3.1E+05	2.2E+05	1.5E+05	1.6E+05	1.2E+05	6.7E+04	3.2E+04
Pm145	6.5E+04	6.5E+04	6.7E+04	6.4E+04	6.4E+04	6.0E+04	6.0E+04	5.3E+04	5.1E+04	4.2E+04	3.2E+04	3.4E+04	2.7E+04	1.6E+04	8.0E+03
Eu152	9.5E+00	1.0E+01	8.6E+00	1.1E+01	1.2E+01	1.4E+01	1.7E+01	2.8E+01	4.3E+01	9.1E+01	2.1E+02	1.6E+02	2.8E+02	7.0E+02	1.8E+03
Eu154	2.3E+05	2.4E+05	2.2E+05	2.3E+05	2.6E+05	2.9E+05	3.4E+05	4.8E+05	7.4E+05	1.4E+06	2.4E+06	2.3E+06	2.7E+06	2.8E+06	2.0E+06
Eu155	1.6E+05	1.7E+05	1.6E+05	1.7E+05	1.8E+05	2.0E+05	2.2E+05	2.9E+05	3.8E+05	6.9E+05	1.1E+06	1.1E+06	1.3E+06	1.2E+06	6.7E+05
Ho166m	1.1E+04	1.2E+04	1.1E+04	1.3E+04	1.4E+04	1.5E+04	1.4E+04	1.4E+04	9.2E+03	5.4E+03	3.0E+03	2.8E+03	2.8E+03	3.4E+03	3.8E+03
Total Flux	8.0E+13	7.9E+13	7.8E+13	7.3E+13	6.8E+13	5.5E+13	5.1E+13	4.0E+13	3.2E+13	2.3E+13	1.4E+13	1.0E+13	6.4E+12	3.6E+12	1.7E+12
Thermal	2.1E+13	2.1E+13	2.3E+13	1.8E+13	1.8E+13	1.5E+13	1.4E+13	1.0E+13	8.4E+12	6.4E+12	4.3E+12	4.8E+12	3.6E+12	2.1E+12	9.7E+11
Epithermal	2.2E+13	2.2E+13	2.2E+13	2.1E+13	1.9E+13	1.5E+13	1.4E+13	1.1E+13	9.3E+12	6.2E+12	4.1E+12	3.8E+12	2.6E+12	1.5E+12	6.9E+11
Fast Flux	3.7E+13	3.6E+13	3.4E+13	3.3E+13	3.1E+13	2.5E+13	2.3E+13	1.8E+13	1.4E+13	1.1E+13	5.5E+12	1.5E+12	1.8E+11	1.5E+10	4.5E+09

Table 29: Radial Activity in Bq/kg for Jowett Precursors in the Wylfa Reactor

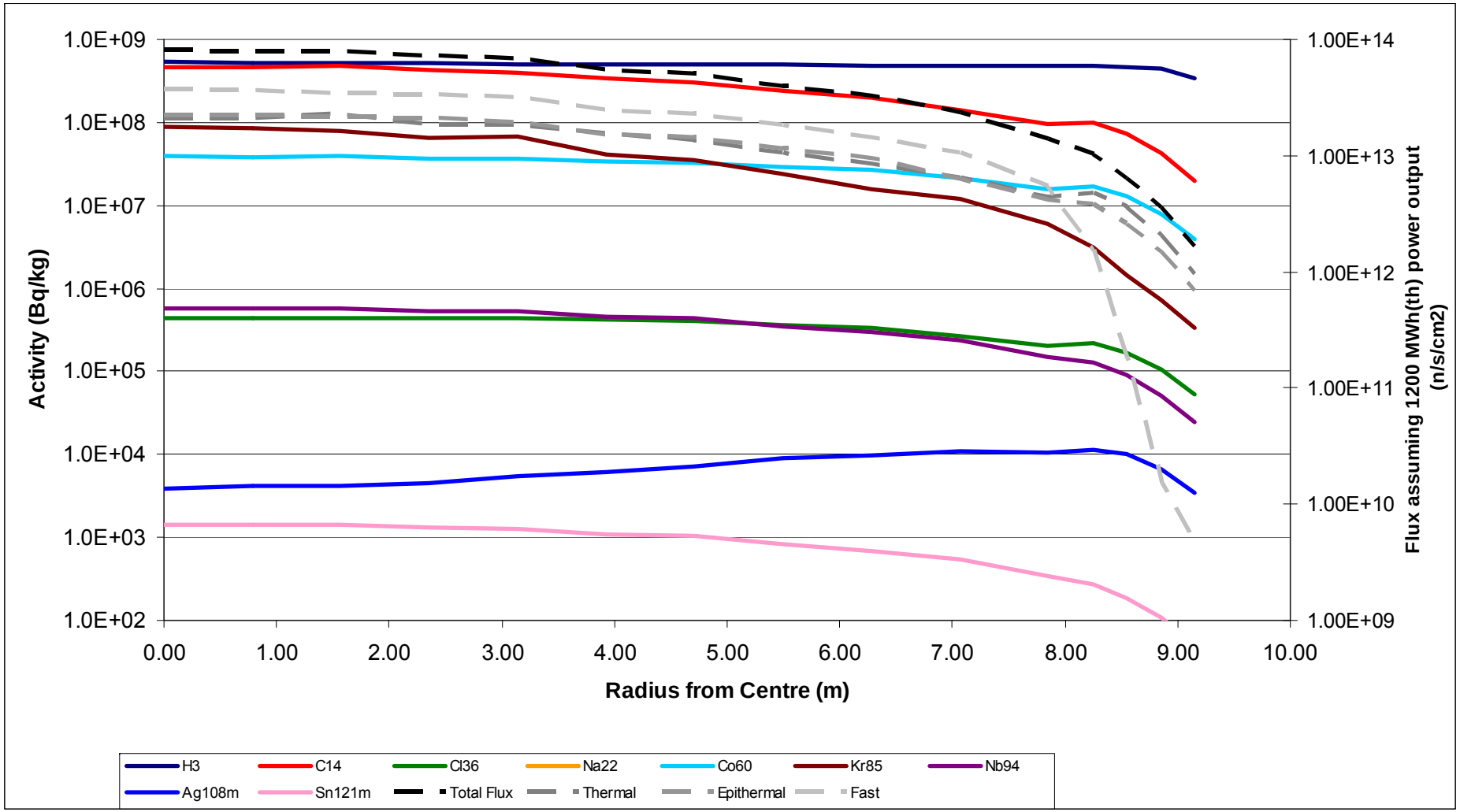

Figure 66: Radionuclide trends for Radial nuclides in the Wylfa reactor (1/2)

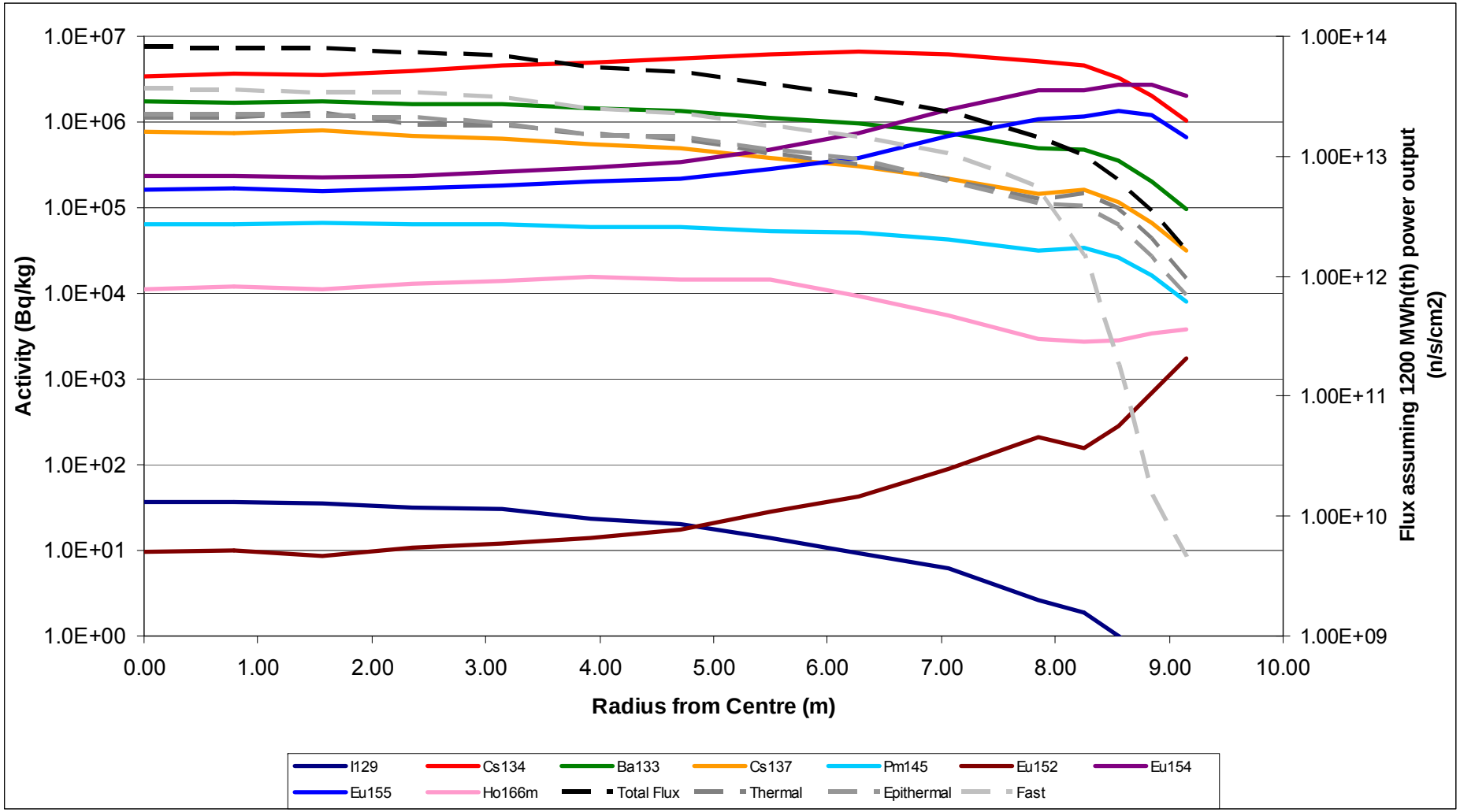

Figure 67: Radionuclide trends for Radial nuclides in the Wylfa reactor (2/2)

Axial Data

	Bottom of the Reactor			Core Region									Top of the Reactor		
Nuclides	-5.00	-4.75	-4.50	-4.00	-3.00	-2.00	-1.00	0.00	1.00	2.00	3.00	4.00	4.50	4.75	5.00
H3	4.6E+08	4.8E+08	4.8E+08	4.9E+08	5.0E+08	5.1E+08	5.3E+08	5.3E+08	5.1E+08	5.1E+08	5.0E+08	4.9E+08	4.8E+08	4.7E+08	4.4E+08
C14	6.1E+07	9.7E+07	9.2E+07	1.8E+08	3.1E+08	3.9E+08	5.3E+08	4.7E+08	5.6E+08	4.2E+08	3.2E+08	1.7E+08	8.8E+07	6.5E+07	4.1E+07
Cl36	1.4E+05	2.1E+05	2.0E+05	3.1E+05	4.0E+05	4.3E+05	4.4E+05	4.4E+05	4.3E+05	4.3E+05	4.1E+05	3.0E+05	1.9E+05	1.5E+05	1.0E+05
Na22	N/A	N/A	N/A	N/A	N/A	N/A	N/A	N/A	N/A	N/A	N/A	N/A	N/A	N/A	N/A
Co60	1.1E+07	1.6E+07	1.6E+07	2.6E+07	3.3E+07	3.6E+07	4.1E+07	3.9E+07	4.2E+07	3.7E+07	3.4E+07	2.4E+07	1.6E+07	1.2E+07	8.0E+06
Kr85	1.5E+06	3.9E+06	5.6E+06	1.6E+07	4.0E+07	5.4E+07	8.8E+07	8.8E+07	7.8E+07	6.3E+07	3.3E+07	1.6E+07	4.9E+06	2.5E+06	1.3E+06
Nb94	7.9E+04	1.3E+05	1.5E+05	2.9E+05	4.5E+05	5.0E+05	5.7E+05	5.8E+05	5.9E+05	5.3E+05	4.3E+05	2.8E+05	1.4E+05	9.5E+04	5.6E+04
Ag108m	8.3E+03	1.1E+04	1.0E+04	1.1E+04	7.5E+03	5.2E+03	3.3E+03	3.9E+03	4.0E+03	5.2E+03	7.0E+03	1.1E+04	9.8E+03	8.5E+03	6.3E+03
Sn121m	1.7E+02	2.9E+02	3.4E+02	6.7E+02	1.1E+03	1.2E+03	1.4E+03	1.4E+03	1.4E+03	1.3E+03	1.0E+03	6.4E+02	3.1E+02	2.1E+02	1.2E+02
I129	8.8E-01	2.2E+00	2.7E+00	8.8E+00	2.2E+01	2.9E+01	3.8E+01	3.7E+01	3.4E+01	3.0E+01	1.9E+01	8.2E+00	2.6E+00	1.2E+00	6.2E-01
Cs134	3.3E+06	5.1E+06	5.3E+06	6.6E+06	5.6E+06	4.3E+06	3.0E+06	3.4E+06	3.5E+06	4.2E+06	5.4E+06	6.5E+06	5.3E+06	4.1E+06	2.9E+06
Ba133	3.0E+05	4.8E+05	5.0E+05	9.2E+05	1.4E+06	1.6E+06	1.8E+06	1.7E+06	1.8E+06	1.6E+06	1.4E+06	8.7E+05	4.8E+05	3.4E+05	2.1E+05
Cs137	9.7E+04	1.5E+05	1.4E+05	2.8E+05	4.9E+05	6.3E+05	8.5E+05	7.6E+05	9.2E+05	6.8E+05	5.1E+05	2.6E+05	1.4E+05	1.0E+05	6.5E+04
Pm145	2.2E+04	3.2E+04	3.1E+04	4.8E+04	6.0E+04	6.3E+04	6.5E+04	6.5E+04	7.3E+04	6.6E+04	6.2E+04	4.6E+04	3.0E+04	2.4E+04	1.6E+04
Eu152	4.6E+02	1.8E+02	2.2E+02	5.5E+01	1.8E+01	1.2E+01	7.9E+00	9.5E+00	6.6E+00	1.0E+01	1.5E+01	6.1E+01	2.4E+02	3.8E+02	7.9E+02
Eu154	2.9E+06	2.3E+06	2.4E+06	9.0E+05	3.4E+05	2.5E+05	2.2E+05	2.3E+05	2.0E+05	2.4E+05	3.1E+05	1.0E+06	2.5E+06	3.2E+06	3.5E+06
Eu155	1.3E+06	1.1E+06	1.1E+06	4.9E+05	2.2E+05	1.7E+05	1.6E+05	1.6E+05	1.5E+05	1.7E+05	2.0E+05	5.2E+05	1.2E+06	1.5E+06	1.4E+06
Ho166m	2.7E+03	3.2E+03	3.3E+03	8.6E+03	1.5E+04	1.4E+04	9.7E+03	1.1E+04	1.0E+04	1.3E+04	1.5E+04	7.4E+03	3.4E+03	3.3E+03	3.7E+03
Total Flux	6.6E+12	1.1E+13	1.4E+13	2.9E+13	5.2E+13	6.6E+13	8.4E+13	8.0E+13	7.7E+13	6.9E+13	5.2E+13	2.8E+13	1.4E+13	7.9E+12	4.4E+12
Thermal	2.9E+12	4.7E+12	4.1E+12	7.6E+12	1.4E+13	1.8E+13	2.4E+13	2.1E+13	2.6E+13	1.9E+13	1.4E+13	7.5E+12	4.0E+12	3.2E+12	1.9E+12
Epithermal	2.7E+12	3.9E+12	4.1E+12	8.5E+12	1.4E+13	1.9E+13	2.3E+13	2.2E+13	2.6E+13	2.0E+13	1.5E+13	7.3E+12	3.7E+12	2.4E+12	1.6E+12
Fast Flux	9.2E+11	2.8E+12	6.0E+12	1.3E+13	2.4E+13	2.9E+13	3.6E+13	3.7E+13	2.5E+13	3.1E+13	2.3E+13	1.3E+13	5.9E+12	2.3E+12	8.9E+11

Table 30: Axial Activity in Bq/kg for Jowett Precursors in the Wylfa Reactor

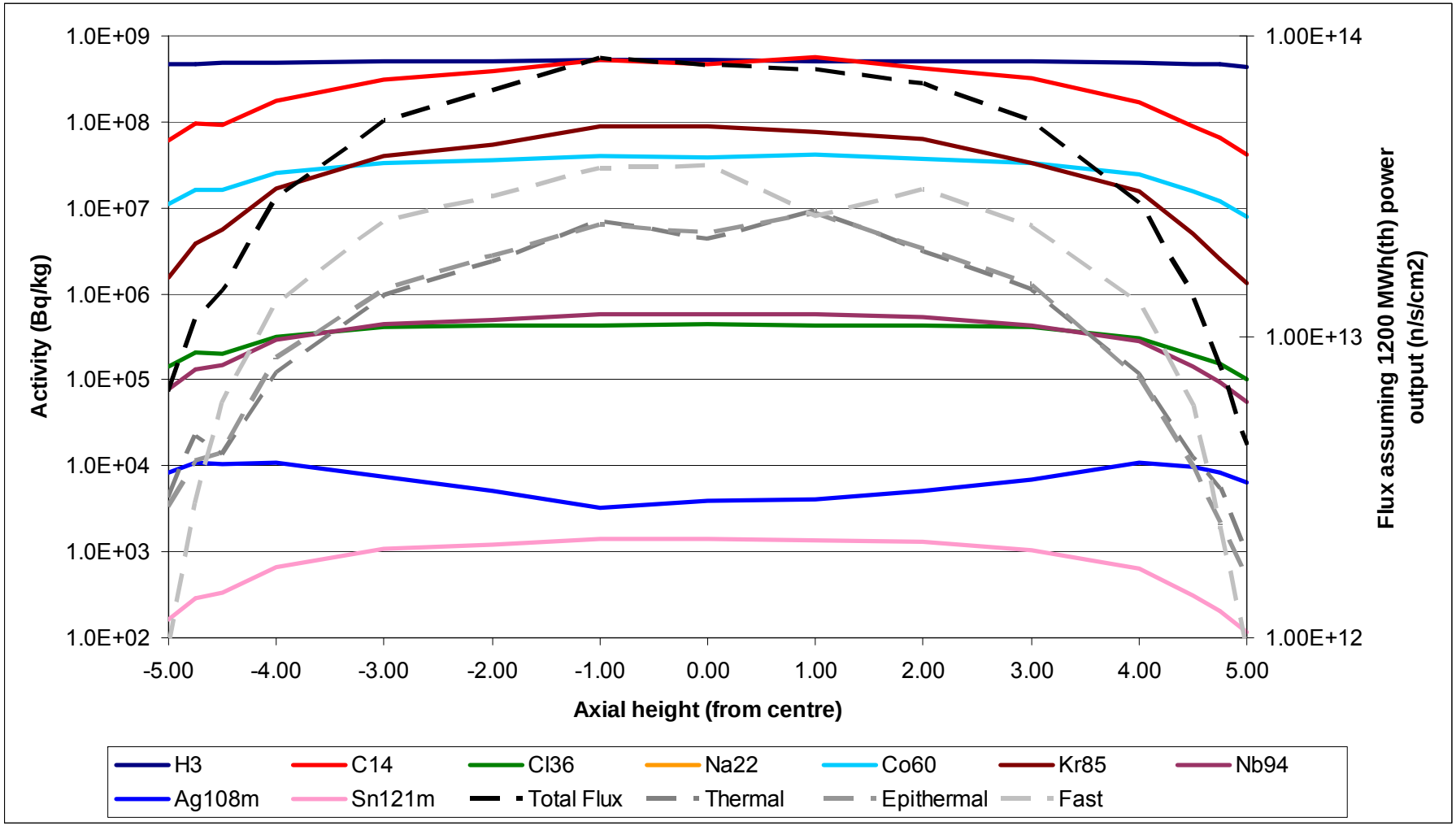

Figure 68: Radionuclide trends for Axial nuclides in the Wylfa reactor (1/2)

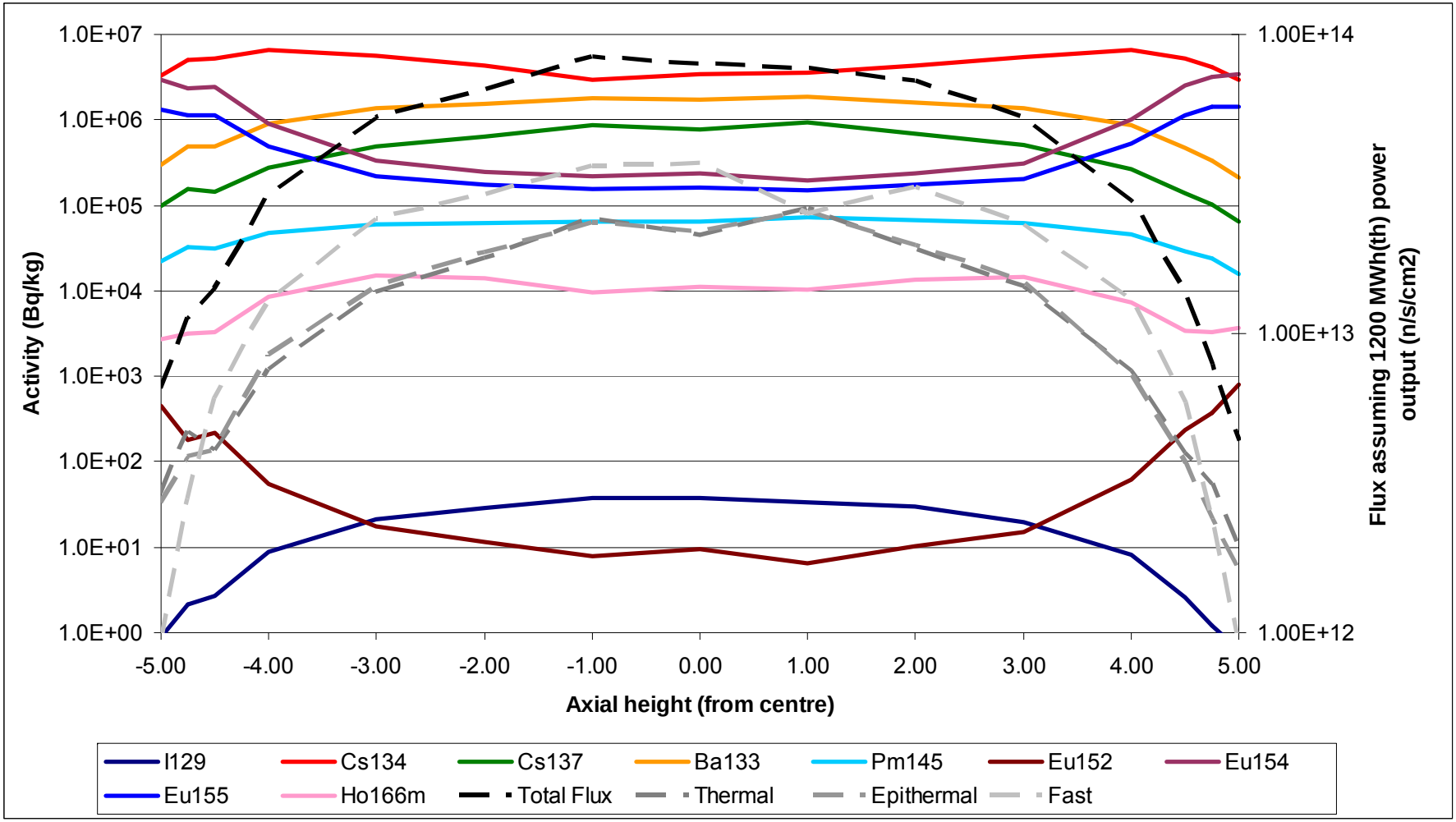

Figure 69: Radionuclide trends for Axial nuclides in the Wylfa reactor (2/2)

NPL (Maximum) Precursor Information

Radial Data

	Core Region											Reflector Region			
Nuclides	0.00	0.78	1.57	2.35	3.14	3.92	4.71	5.49	6.28	7.06	7.85	8.25	8.55	8.85	9.15
H3	2.9E+09	2.9E+09	2.9E+09	2.9E+09	2.9E+09	2.9E+09	2.9E+09	2.9E+09	2.8E+09	2.8E+09	2.8E+09	2.8E+09	2.8E+09	2.6E+09	2.0E+09
C14	3.1E+08	3.1E+08	3.2E+08	2.8E+08	2.6E+08	2.2E+08	2.0E+08	1.6E+08	1.3E+08	9.2E+07	6.2E+07	6.6E+07	4.8E+07	2.8E+07	1.3E+07
Cl36	3.4E+06	3.4E+06	3.4E+06	3.4E+06	3.3E+06	3.3E+06	3.2E+06	2.9E+06	2.6E+06	2.1E+06	1.6E+06	1.7E+06	1.3E+06	8.4E+05	4.2E+05
Na22	N/A	N/A	N/A	N/A	N/A	N/A	N/A	N/A	N/A	N/A	N/A	N/A	N/A	N/A	N/A
Co60	2.8E+07	2.7E+07	2.8E+07	2.5E+07	2.4E+07	2.2E+07	2.0E+07	1.7E+07	1.4E+07	1.1E+07	7.8E+06	8.3E+06	6.3E+06	3.9E+06	1.9E+06
Kr85	5.6E+04	5.5E+04	5.4E+04	5.2E+04	5.1E+04	4.7E+04	4.3E+04	3.7E+04	2.9E+04	2.2E+04	1.3E+04	1.1E+04	6.3E+03	3.2E+03	1.3E+03
Nb94	2.2E-01	1.7E-01	1.7E-01	1.8E-01	1.4E-01	9.6E-02	1.2E-01	8.3E-02	4.9E-02	3.7E-02	1.5E-02	6.0E-03	1.6E-03	5.7E-04	1.6E-04
Ag108m	6.1E-04	N/A	N/A	5.7E-04	N/A	N/A	N/A	N/A	N/A	N/A	N/A	N/A	N/A	N/A	N/A
Sn121m	3.2E+02	3.1E+02	3.0E+02	3.1E+02	2.9E+02	2.9E+02	2.6E+02	2.4E+02	1.8E+02	1.4E+02	8.0E+01	4.9E+01	2.1E+01	9.4E+00	3.4E+00
I129	3.4E+00	3.4E+00	3.3E+00	3.2E+00	3.3E+00	2.8E+00	2.7E+00	2.4E+00	2.0E+00	1.6E+00	1.1E+00	8.8E-01	6.0E-01	3.5E-01	1.7E-01
Cs134	2.1E+08	2.3E+08	2.2E+08	2.5E+08	2.9E+08	3.3E+08	3.8E+08	4.3E+08	4.6E+08	4.4E+08	3.7E+08	3.2E+08	2.3E+08	1.4E+08	7.3E+07
Ba133	8.9E+05	8.8E+05	9.0E+05	8.4E+05	8.2E+05	7.3E+05	6.9E+05	5.8E+05	4.9E+05	3.8E+05	2.5E+05	2.5E+05	1.8E+05	1.0E+05	5.0E+04
Cs137	1.4E+06	1.4E+06	1.3E+06	1.2E+06	1.1E+06	9.6E+05	8.1E+05	6.4E+05	4.7E+05	3.3E+05	1.9E+05	1.3E+05	6.6E+04	3.2E+04	1.3E+04
Pm145	4.3E+04	4.3E+04	4.5E+04	4.2E+04	4.2E+04	4.0E+04	4.0E+04	3.5E+04	3.3E+04	2.8E+04	2.1E+04	2.2E+04	1.8E+04	1.1E+04	5.3E+03
Eu152	4.1E+00	4.4E+00	3.7E+00	4.9E+00	5.5E+00	6.8E+00	8.5E+00	1.5E+01	2.4E+01	5.5E+01	1.3E+02	1.0E+02	1.8E+02	4.5E+02	1.2E+03
Eu154	1.1E+05	1.1E+05	1.0E+05	1.1E+05	1.2E+05	1.5E+05	1.8E+05	2.9E+05	4.7E+05	9.5E+05	1.8E+06	1.7E+06	2.3E+06	2.8E+06	2.7E+06
Eu155	1.1E+05	1.1E+05	1.0E+05	1.1E+05	1.2E+05	1.3E+05	1.4E+05	1.9E+05	2.5E+05	4.7E+05	8.2E+05	8.6E+05	1.1E+06	1.2E+06	8.9E+05
Ho166m	2.4E+01	2.4E+01	2.1E+01	2.0E+01	1.8E+01	1.4E+01	9.4E+00	6.5E+00	2.9E+00	1.3E+00	3.3E-01	2.2E-01	5.9E-02	7.3E-03	N/A
Total Flux	8.0E+13	7.9E+13	7.8E+13	7.3E+13	6.8E+13	5.5E+13	5.1E+13	4.0E+13	3.2E+13	2.3E+13	1.4E+13	1.0E+13	6.4E+12	3.6E+12	1.7E+12
Thermal	2.1E+13	2.1E+13	2.3E+13	1.8E+13	1.8E+13	1.5E+13	1.4E+13	1.0E+13	8.4E+12	6.4E+12	4.3E+12	4.8E+12	3.6E+12	2.1E+12	9.7E+11
Epithermal	2.2E+13	2.2E+13	2.2E+13	2.1E+13	1.9E+13	1.5E+13	1.4E+13	1.1E+13	9.3E+12	6.2E+12	4.1E+12	3.8E+12	2.6E+12	1.5E+12	6.9E+11
Fast Flux	3.7E+13	3.6E+13	3.4E+13	3.3E+13	3.1E+13	2.5E+13	2.3E+13	1.8E+13	1.4E+13	1.1E+13	5.5E+12	1.5E+12	1.8E+11	1.5E+10	4.5E+09

Table 31: Radial Activity in Bq/kg for NPL Maximum Precursors in the Wylfa Reactor

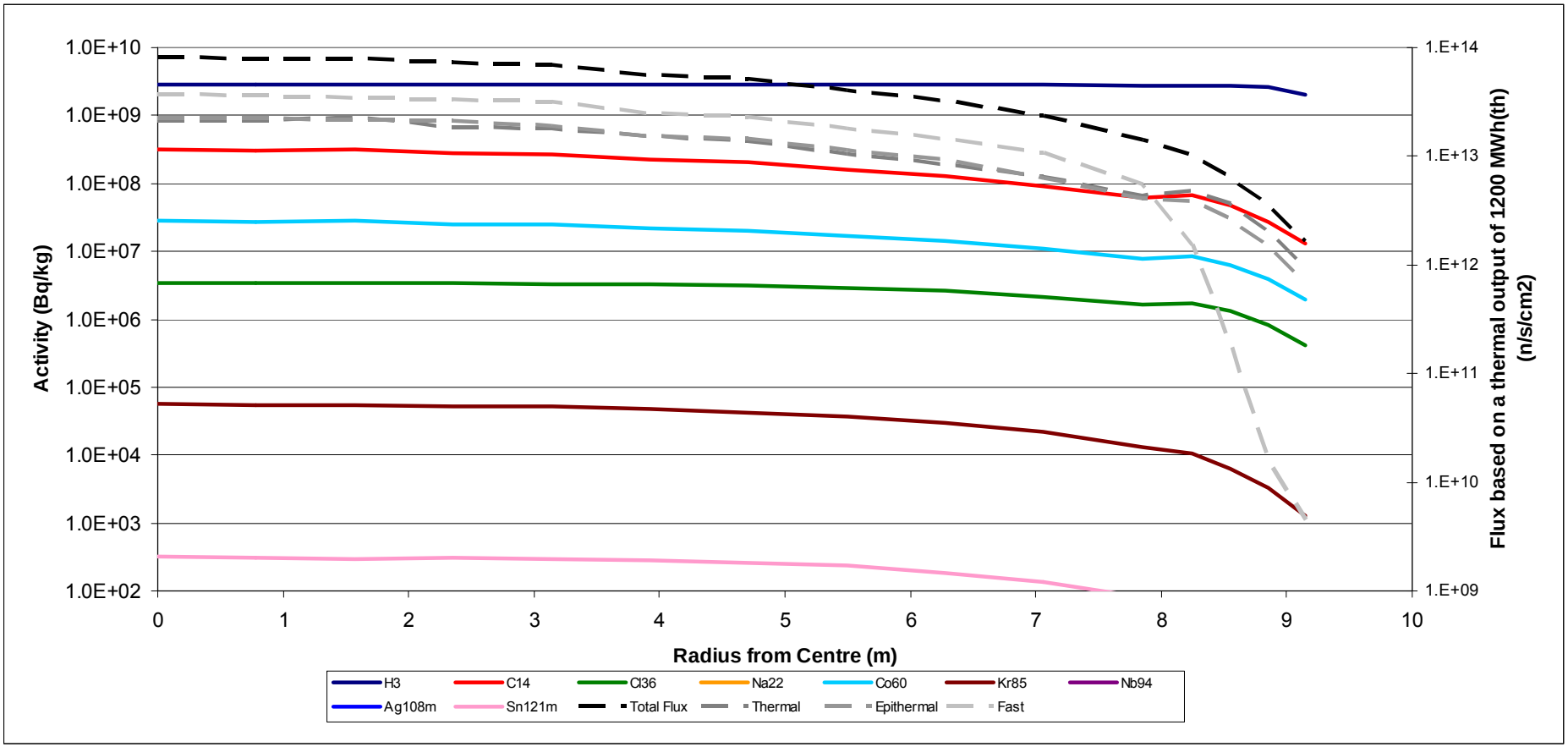

Figure 70: Radionuclide trends for Radial nuclides in the Wylfa reactor (1/2)

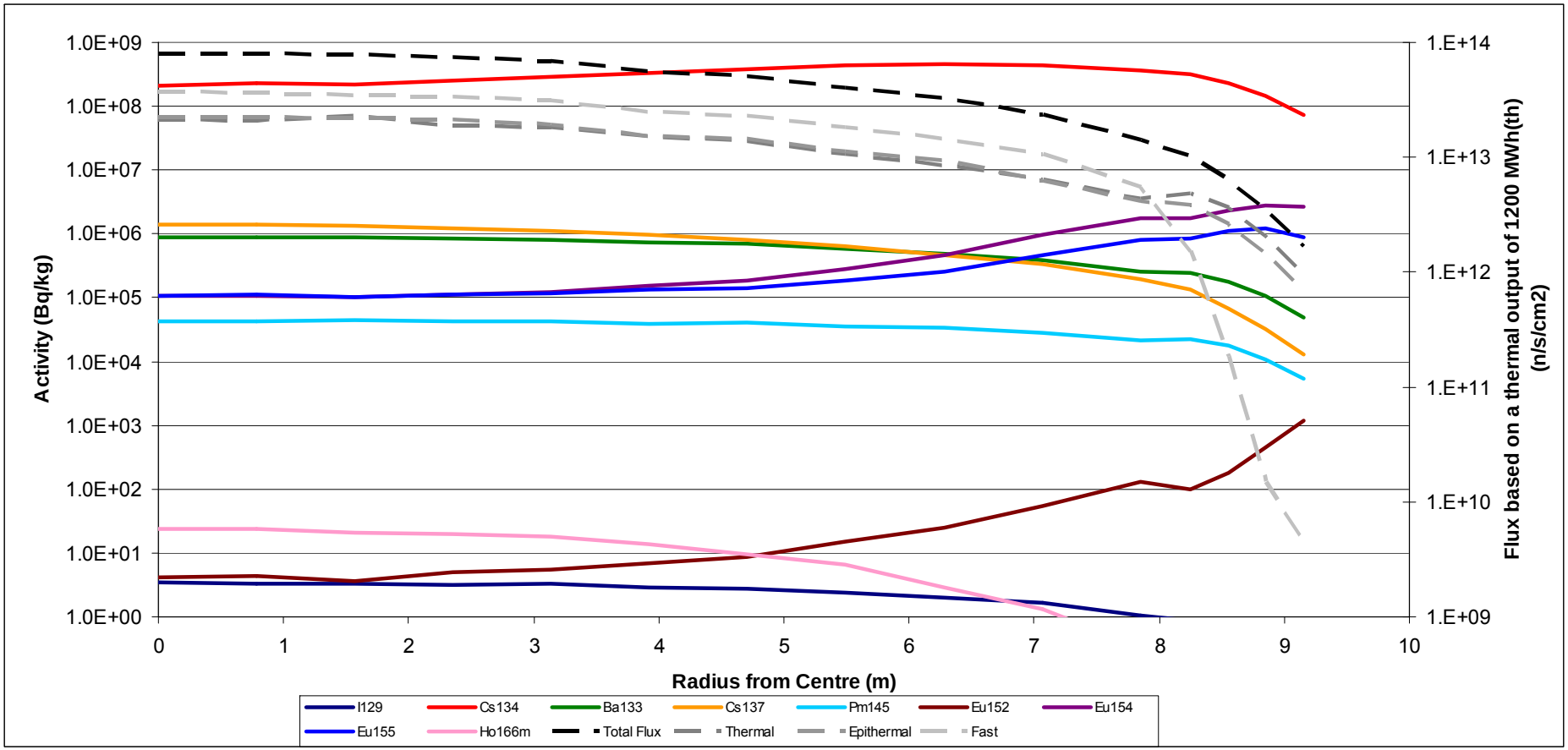

Figure 71: Radionuclide trends for Radial nuclides in the Wylfa reactor (2/2)

Axial Data

	Bottom of the Reactor			Core Region									Top of the Reactor		
Nuclides	-5.00	-4.75	-4.50	-4.00	-3.00	-2.00	-1.00	0.00	1.00	2.00	3.00	4.00	4.50	4.75	5.00
H3	2.7E+09	2.8E+09	2.8E+09	2.8E+09	2.9E+09	2.9E+09	2.9E+09	2.9E+09	2.9E+09	2.9E+09	2.9E+09	2.8E+09	2.8E+09	2.7E+09	2.6E+09
C14	4.0E+07	6.4E+07	6.1E+07	1.2E+08	2.0E+08	2.6E+08	3.5E+08	3.1E+08	3.7E+08	2.8E+08	2.1E+08	1.1E+08	5.8E+07	4.3E+07	2.7E+07
Cl36	1.1E+06	1.7E+06	1.6E+06	2.5E+06	3.2E+06	3.3E+06	3.3E+06	3.4E+06	3.3E+06	3.4E+06	3.2E+06	2.4E+06	1.5E+06	1.2E+06	8.1E+05
Na22															
Co60	5.4E+06	8.1E+06	8.0E+06	1.3E+07	2.0E+07	2.4E+07	3.0E+07	2.8E+07	3.2E+07	2.5E+07	2.1E+07	1.3E+07	7.7E+06	5.9E+06	3.9E+06
Kr85	6.2E+03	1.3E+04	1.4E+04	2.8E+04	4.4E+04	5.1E+04	5.7E+04	5.6E+04	5.4E+04	5.1E+04	4.3E+04	2.6E+04	1.4E+04	8.4E+03	5.0E+03
Nb94	1.9E-03	6.1E-03	4.8E-02	4.8E-02	1.1E-01	1.3E-01	1.8E-01	2.2E-01	1.4E-01	1.4E-01	9.5E-02	4.5E-02	1.5E-02	4.8E-03	1.3E-03
Ag108m	6.9E-05							6.1E-04							
Sn121m	2.8E+01	7.0E+01	9.4E+01	1.7E+02	2.6E+02	3.0E+02	3.2E+02	3.2E+02	2.7E+02	2.9E+02	2.6E+02	1.6E+02	9.2E+01	4.8E+01	2.8E+01
I129	5.4E-01	9.4E-01	1.0E+00	2.0E+00	2.9E+00	3.1E+00	3.3E+00	3.4E+00	3.2E+00	3.2E+00	2.7E+00	1.9E+00	9.8E-01	6.6E-01	4.1E-01
Cs134	2.3E+08	3.6E+08	3.7E+08	4.6E+08	3.8E+08	2.8E+08	1.7E+08	2.1E+08	2.1E+08	2.7E+08	3.6E+08	4.6E+08	3.7E+08	2.9E+08	2.1E+08
Ba133	1.5E+05	2.5E+05	2.6E+05	4.7E+05	7.0E+05	8.0E+05	9.3E+05	8.9E+05	9.5E+05	8.4E+05	7.0E+05	4.5E+05	2.5E+05	1.7E+05	1.1E+05
Cs137	7.6E+04	1.8E+05	2.1E+05	4.4E+05	8.3E+05	1.1E+06	1.6E+06	1.4E+06	1.4E+06	1.1E+06	8.1E+05	4.1E+05	2.2E+05	1.2E+05	6.9E+04
Pm145	1.5E+04	2.1E+04	2.0E+04	3.2E+04	3.9E+04	4.2E+04	4.3E+04	4.3E+04	4.8E+04	4.4E+04	4.1E+04	3.1E+04	2.0E+04	1.6E+04	1.0E+04
Eu152	3.0E+02	1.1E+02	1.4E+02	3.2E+01	8.7E+00	5.3E+00	3.3E+00	4.1E+00	2.7E+00	4.7E+00	7.4E+00	3.6E+01	1.5E+02	2.4E+02	5.1E+02
Eu154	2.6E+06	1.7E+06	1.8E+06	5.8E+05	1.8E+05	1.2E+05	9.7E+04	1.1E+05	8.6E+04	1.1E+05	1.6E+05	6.7E+05	1.9E+06	2.6E+06	3.3E+06
Eu155	1.1E+06	8.6E+05	8.6E+05	3.2E+05	1.4E+05	1.2E+05	1.0E+05	1.1E+05	9.6E+04	1.1E+05	1.3E+05	3.5E+05	8.7E+05	1.2E+06	1.4E+06
Ho166m	4.6E-02	3.1E-01	3.6E-01	2.6E+00	1.1E+01	1.8E+01	2.7E+01	2.4E+01	2.0E+01	1.7E+01	9.8E+00	2.1E+00	3.6E-01	1.1E-01	1.7E-02
Total Flux	6.6E+12	1.1E+13	1.4E+13	2.9E+13	5.2E+13	6.6E+13	8.4E+13	8.0E+13	7.7E+13	6.9E+13	5.2E+13	2.8E+13	1.4E+13	7.9E+12	4.4E+12
Thermal	2.9E+12	4.7E+12	4.1E+12	7.6E+12	1.4E+13	1.8E+13	2.4E+13	2.1E+13	2.6E+13	1.9E+13	1.4E+13	7.5E+12	4.0E+12	3.2E+12	1.9E+12
Epithermal	2.7E+12	3.9E+12	4.1E+12	8.5E+12	1.4E+13	1.9E+13	2.3E+13	2.2E+13	2.6E+13	2.0E+13	1.5E+13	7.3E+12	3.7E+12	2.4E+12	1.6E+12
Fast Flux	9.2E+11	2.8E+12	6.0E+12	1.3E+13	2.4E+13	2.9E+13	3.6E+13	3.7E+13	2.5E+13	3.1E+13	2.3E+13	1.3E+13	5.9E+12	2.3E+12	8.9E+11

Table 32: Axial Activity in Bq/kg for NPL maximum Precursors in the Wylfa Reactor

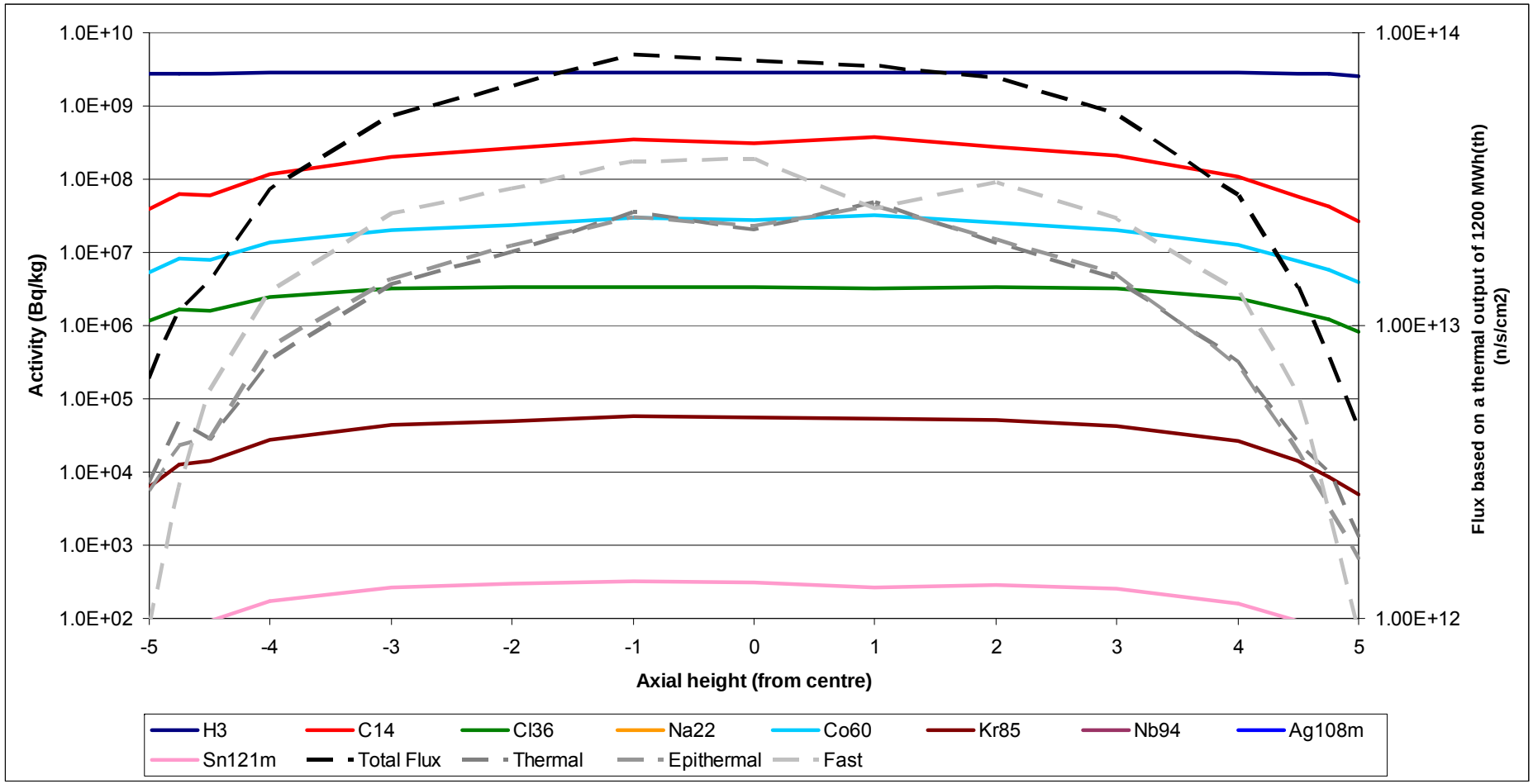

Figure 72: Radionuclide trends for Axial nuclides in the Wylfa reactor (1/2)

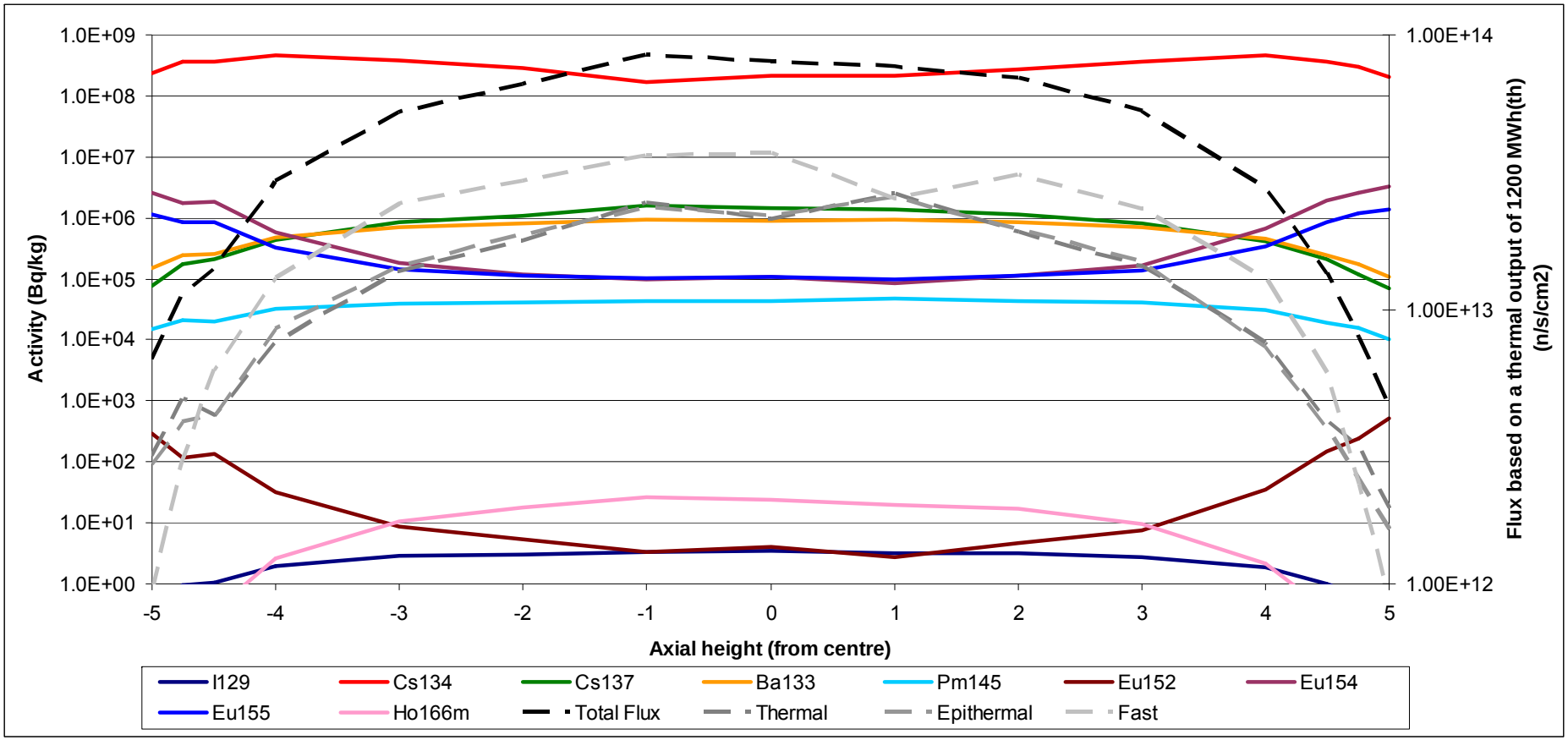

Figure 73: Radionuclide trends for Axial nuclides in the Wylfa reactor (2/2)

NPL (Average) Precursor Information

Radial Data

	Core Region											Reflector Region			
Nuclides	0.00	0.78	1.57	2.35	3.14	3.92	4.71	5.49	6.28	7.06	7.85	8.25	8.55	8.85	9.15
H3	1.6E+09	1.6E+09	1.6E+09	1.6E+09	1.6E+09	1.6E+09	1.6E+09	1.6E+09	1.6E+09	1.6E+09	1.5E+09	1.5E+09	1.5E+09	1.4E+09	1.1E+09
C14	2.9E+08	2.8E+08	3.0E+08	2.6E+08	2.4E+08	2.1E+08	2.1E+08	1.4E+08	1.2E+08	8.4E+07	5.7E+07	6.0E+07	4.4E+07	2.5E+07	1.2E+07
Cl36	2.4E+06	2.4E+06	2.4E+06	2.4E+06	2.3E+06	2.3E+06	2.3E+06	2.0E+06	1.8E+06	1.5E+06	1.1E+06	1.2E+06	9.5E+05	5.9E+05	2.9E+05
Na22	N/A	N/A	N/A	N/A	N/A	N/A	N/A	N/A	N/A	N/A	N/A	N/A	N/A	N/A	N/A
Co60	1.9E+07	1.9E+07	2.0E+07	1.8E+07	1.7E+07	1.5E+07	1.5E+07	1.2E+07	1.1E+07	8.5E+06	6.0E+06	6.4E+06	4.9E+06	3.0E+06	1.5E+06
Kr85	5.6E+04	5.5E+04	5.4E+04	5.2E+04	5.1E+04	4.7E+04	4.7E+04	3.7E+04	2.9E+04	2.2E+04	1.3E+04	1.1E+04	6.3E+03	3.2E+03	1.3E+03
Nb94	2.0E-01	1.6E-01	1.6E-01	1.6E-01	1.3E-01	8.8E-02	8.8E-02	7.6E-02	4.5E-02	3.4E-02	1.4E-02	5.5E-03	1.5E-03	5.5E-04	1.6E-04
Ag108m	6.1E-04	N/A	N/A	5.7E-04	N/A	N/A	N/A	N/A	N/A	N/A	N/A	N/A	N/A	N/A	N/A
Sn121m	3.2E+02	3.1E+02	3.0E+02	3.1E+02	2.9E+02	2.9E+02	2.9E+02	2.4E+02	1.8E+02	1.4E+02	8.0E+01	4.9E+01	2.1E+01	9.4E+00	3.4E+00
I129	3.4E+00	3.4E+00	3.3E+00	3.2E+00	3.3E+00	2.8E+00	2.8E+00	2.4E+00	2.0E+00	1.6E+00	1.1E+00	8.8E-01	6.0E-01	3.5E-01	1.7E-01
Cs134	2.1E+08	2.3E+08	2.2E+08	2.5E+08	2.9E+08	3.3E+08	3.3E+08	4.3E+08	4.6E+08	4.4E+08	3.7E+08	3.2E+08	2.3E+08	1.4E+08	7.3E+07
Ba133	4.0E+05	3.9E+05	4.0E+05	3.8E+05	3.7E+05	3.3E+05	3.3E+05	2.6E+05	2.2E+05	1.7E+05	1.1E+05	1.1E+05	8.0E+04	4.7E+04	2.2E+04
Cs137	1.4E+06	1.4E+06	1.3E+06	1.2E+06	1.1E+06	9.6E+05	9.6E+05	6.4E+05	4.7E+05	3.3E+05	1.9E+05	1.3E+05	6.6E+04	3.2E+04	1.3E+04
Pm145	4.3E+04	4.3E+04	4.5E+04	4.2E+04	4.2E+04	4.0E+04	4.0E+04	3.5E+04	3.3E+04	2.8E+04	2.1E+04	2.2E+04	1.8E+04	1.1E+04	5.3E+03
Eu152	4.1E+00	4.4E+00	3.7E+00	4.9E+00	5.5E+00	6.8E+00	6.8E+00	1.5E+01	2.4E+01	5.5E+01	1.3E+02	1.0E+02	1.8E+02	4.5E+02	1.2E+03
Eu154	1.1E+05	1.1E+05	1.0E+05	1.1E+05	1.2E+05	1.5E+05	1.5E+05	2.9E+05	4.7E+05	9.5E+05	1.8E+06	1.7E+06	2.3E+06	2.8E+06	2.7E+06
Eu155	1.1E+05	1.1E+05	1.0E+05	1.1E+05	1.2E+05	1.3E+05	1.3E+05	1.9E+05	2.5E+05	4.7E+05	8.2E+05	8.6E+05	1.1E+06	1.2E+06	8.9E+05
Ho166m	2.4E+01	2.3E+01	2.0E+01	1.9E+01	1.8E+01	1.3E+01	1.3E+01	6.2E+00	2.8E+00	1.3E+00	3.1E-01	2.1E-01	5.7E-02	7.0E-03	7.0E-03
Total Flux	8.0E+13	7.9E+13	7.8E+13	7.3E+13	6.8E+13	5.5E+13	5.1E+13	4.0E+13	3.2E+13	2.3E+13	1.4E+13	1.0E+13	6.4E+12	3.6E+12	1.7E+12
Thermal	2.1E+13	2.1E+13	2.3E+13	1.8E+13	1.8E+13	1.5E+13	1.4E+13	1.0E+13	8.4E+12	6.4E+12	4.3E+12	4.8E+12	3.6E+12	2.1E+12	9.7E+11
Epithermal	2.2E+13	2.2E+13	2.2E+13	2.1E+13	1.9E+13	1.5E+13	1.4E+13	1.1E+13	9.3E+12	6.2E+12	4.1E+12	3.8E+12	2.6E+12	1.5E+12	6.9E+11
Fast Flux	3.7E+13	3.6E+13	3.4E+13	3.3E+13	3.1E+13	2.5E+13	2.3E+13	1.8E+13	1.4E+13	1.1E+13	5.5E+12	1.5E+12	1.8E+11	1.5E+10	4.5E+09

Table 33: Radial Activity in Bq/kg for NPL Average Precursors in the Wylfa Reactor

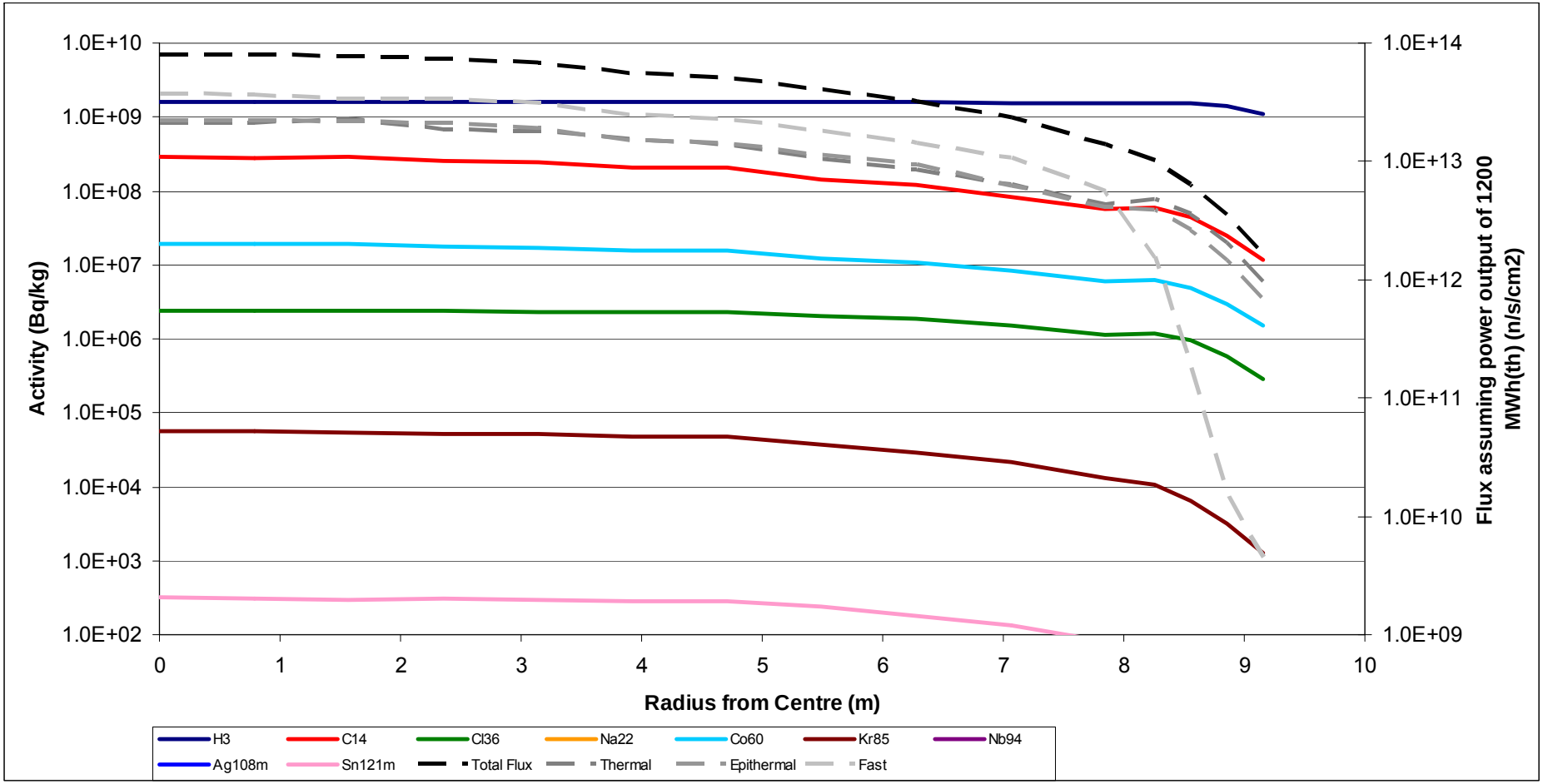

Figure 74: Radionuclide trends for Radial nuclides in the Wylfa reactor (1/2)

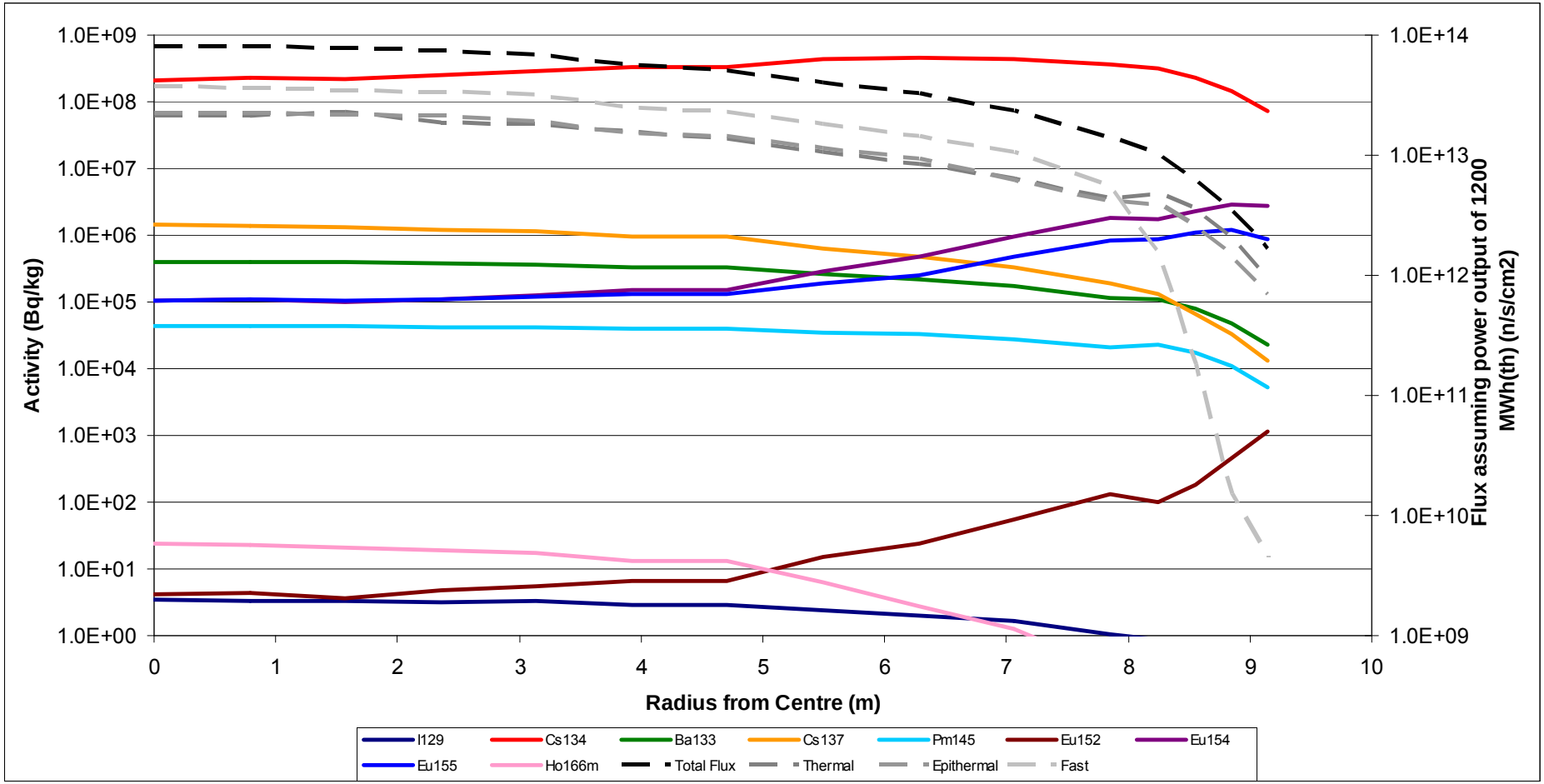

Figure 75: Radionuclide trends for Radial nuclides in the Wylfa reactor (2/2)

Axial Data

	Bottom of the Reactor			Core Region									Top of the Reactor		
Nuclides	-5.00	-4.75	-4.50	-4.00	-3.00	-2.00	-1.00	0.00	1.00	2.00	3.00	4.00	4.50	4.75	5.00
H3	1.5E+09	1.5E+09	1.5E+09	1.6E+09	1.6E+09	1.6E+09	1.6E+09	1.6E+09	1.6E+09	1.6E+09	1.6E+09	1.6E+09	1.5E+09	1.5E+09	1.4E+09
C14	3.6E+07	5.8E+07	5.6E+07	1.1E+08	1.9E+08	2.4E+08	3.2E+08	2.9E+08	3.4E+08	2.6E+08	2.0E+08	1.0E+08	5.3E+07	3.9E+07	2.5E+07
Cl36	8.0E+05	1.2E+06	1.1E+06	1.7E+06	2.2E+06	2.3E+06	2.3E+06	2.4E+06	2.3E+06	2.4E+06	2.3E+06	1.7E+06	1.1E+06	8.5E+05	5.7E+05
Na22	N/A	N/A	N/A	N/A	N/A	N/A	N/A	N/A	N/A	N/A	N/A	N/A	N/A	N/A	N/A
Co60	4.2E+06	6.2E+06	6.1E+06	1.0E+07	1.4E+07	1.7E+07	2.1E+07	1.9E+07	2.2E+07	1.8E+07	1.5E+07	9.6E+06	5.9E+06	4.5E+06	3.0E+06
Kr85	6.2E+03	1.3E+04	1.4E+04	2.8E+04	4.4E+04	5.1E+04	5.7E+04	5.6E+04	5.4E+04	5.1E+04	4.3E+04	2.6E+04	1.4E+04	8.4E+03	5.0E+03
Nb94	1.8E-03	5.7E-03	4.4E-02	4.4E-02	1.0E-01	1.2E-01	1.7E-01	2.0E-01	1.3E-01	1.3E-01	8.7E-02	4.1E-02	1.4E-02	4.5E-03	1.2E-03
Ag108m	6.9E-05	N/A	N/A	N/A	N/A	N/A	5.7E-04	6.1E-04	N/A	N/A	N/A	N/A	N/A	N/A	N/A
Sn121m	2.8E+01	7.0E+01	9.4E+01	1.7E+02	2.6E+02	3.0E+02	3.2E+02	3.2E+02	2.7E+02	2.9E+02	2.6E+02	1.6E+02	9.2E+01	4.8E+01	2.8E+01
I129	5.4E-01	9.4E-01	1.0E+00	2.0E+00	2.9E+00	3.1E+00	3.3E+00	3.4E+00	3.2E+00	3.2E+00	2.7E+00	1.9E+00	9.8E-01	6.6E-01	4.1E-01
Cs134	2.3E+08	3.6E+08	3.7E+08	4.6E+08	3.8E+08	2.8E+08	1.7E+08	2.1E+08	2.1E+08	2.7E+08	3.6E+08	4.6E+08	3.7E+08	2.9E+08	2.1E+08
Ba133	6.9E+04	1.1E+05	1.1E+05	2.1E+05	3.2E+05	3.6E+05	4.2E+05	4.0E+05	4.3E+05	3.8E+05	3.2E+05	2.0E+05	1.1E+05	7.9E+04	4.9E+04
Cs137	7.6E+04	1.8E+05	2.1E+05	4.4E+05	8.3E+05	1.1E+06	1.6E+06	1.4E+06	1.4E+06	1.1E+06	8.1E+05	4.1E+05	2.2E+05	1.2E+05	6.9E+04
Pm145	1.5E+04	2.1E+04	2.0E+04	3.2E+04	3.9E+04	4.2E+04	4.3E+04	4.3E+04	4.8E+04	4.4E+04	4.1E+04	3.1E+04	2.0E+04	1.6E+04	1.0E+04
Eu152	3.0E+02	1.1E+02	1.4E+02	3.2E+01	8.7E+00	5.3E+00	3.3E+00	4.1E+00	2.7E+00	4.7E+00	7.4E+00	3.6E+01	1.5E+02	2.4E+02	5.1E+02
Eu154	2.6E+06	1.7E+06	1.8E+06	5.8E+05	1.8E+05	1.2E+05	9.7E+04	1.1E+05	8.6E+04	1.1E+05	1.6E+05	6.7E+05	1.9E+06	2.6E+06	3.3E+06
Eu155	1.1E+06	8.6E+05	8.6E+05	3.2E+05	1.4E+05	1.2E+05	1.0E+05	1.1E+05	9.6E+04	1.1E+05	1.3E+05	3.5E+05	8.7E+05	1.2E+06	1.4E+06
Ho166m	4.4E-02	2.9E-01	3.5E-01	2.5E+00	1.0E+01	1.7E+01	2.6E+01	2.4E+01	1.9E+01	1.7E+01	9.4E+00	2.1E+00	3.5E-01	1.0E-01	1.7E-02
Total Flux	6.6E+12	1.1E+13	1.4E+13	2.9E+13	5.2E+13	6.6E+13	8.4E+13	8.0E+13	7.7E+13	6.9E+13	5.2E+13	2.8E+13	1.4E+13	7.9E+12	4.4E+12
Thermal	2.9E+12	4.7E+12	4.1E+12	7.6E+12	1.4E+13	1.8E+13	2.4E+13	2.1E+13	2.6E+13	1.9E+13	1.4E+13	7.5E+12	4.0E+12	3.2E+12	1.9E+12
Epithermal	2.7E+12	3.9E+12	4.1E+12	8.5E+12	1.4E+13	1.9E+13	2.3E+13	2.2E+13	2.6E+13	2.0E+13	1.5E+13	7.3E+12	3.7E+12	2.4E+12	1.6E+12
Fast Flux	9.2E+11	2.8E+12	6.0E+12	1.3E+13	2.4E+13	2.9E+13	3.6E+13	3.7E+13	2.5E+13	3.1E+13	2.3E+13	1.3E+13	5.9E+12	2.3E+12	8.9E+11

Table 34: Axial Activity in Bq/kg for NPL Average Precursors in the Wylfa Reactor

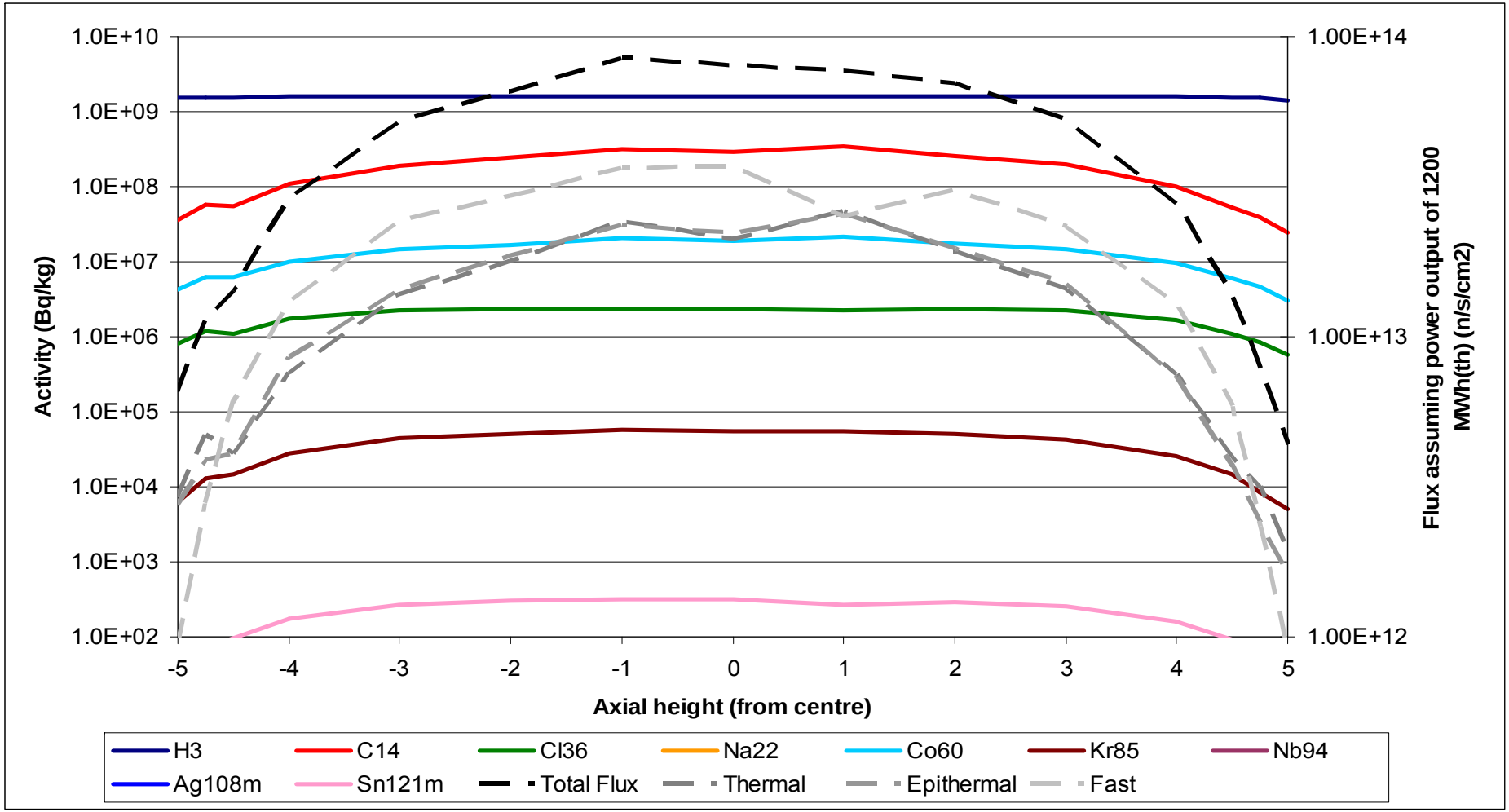

Figure 76: Radionuclide trends for Axial nuclides in the Wylfa reactor (1/2)

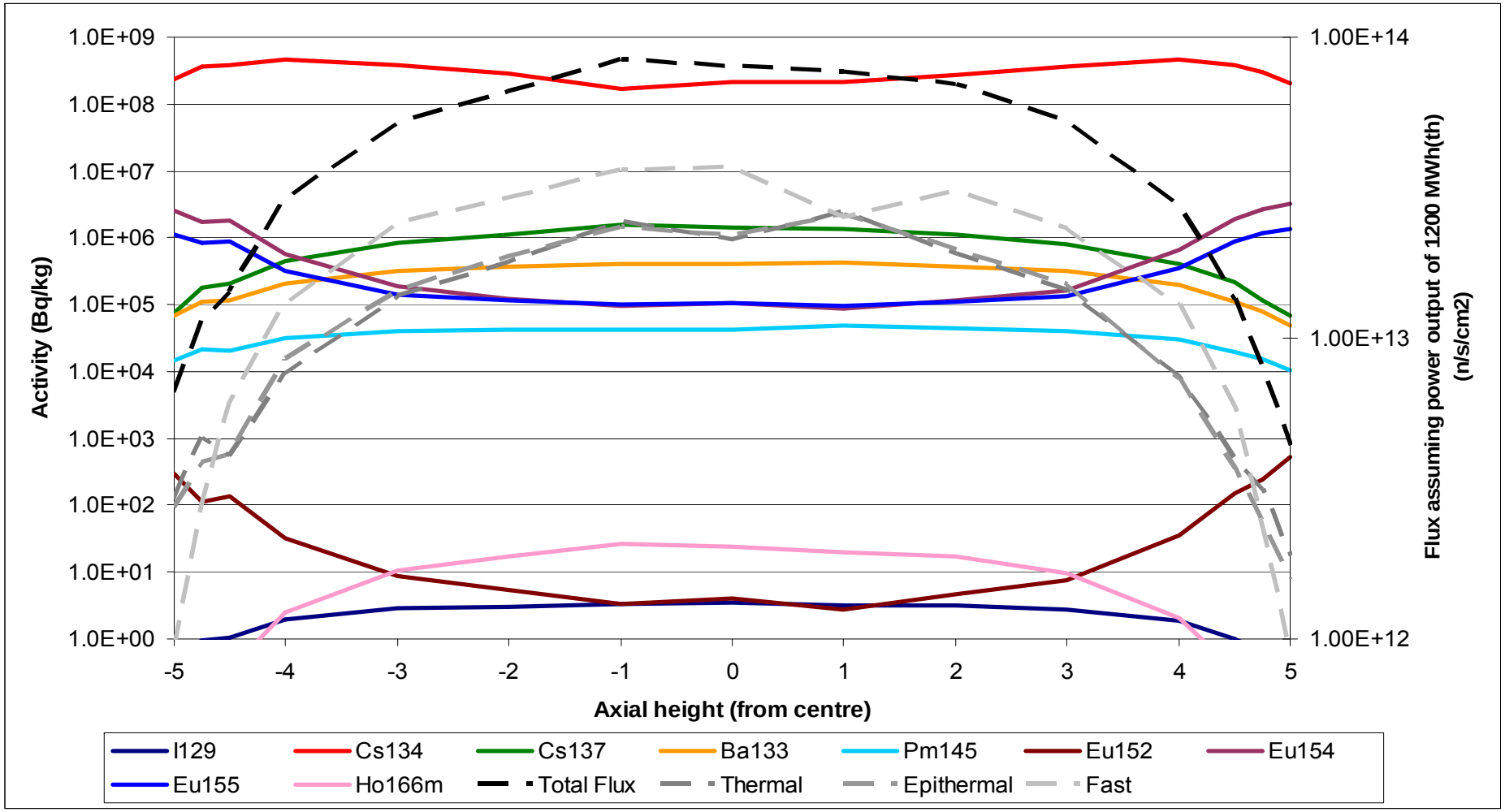

Figure 77: Radionuclide trends for Axial nuclides in the Wylfa reactor (2/2)

Appendix 4: Heavy and transuranic nuclides

Sizewell A:

NPL precursors - Radial

	Radial position (meters from core)												
Nuclide	0	0.7848	1.5696	2.3544	3.1392	3.924	4.7088	5.4936	6.2784	6.7	6.9	7.1	7.3
Ra224	43.54	32.43	37.81	27.86	23.18	26.5	32.68	27.35	17.09	5.215	1.176	0	0
Ra225	0.07859	0.0734	0.07407	0.07919	0.09064	0.1072	0.1189	0.1455	0.1586	0.1567	0.1482	0.1301	0.07847
Ac225	0.2423	0.2263	0.2284	0.2442	0.2795	0.3304	0.3665	0.4487	0.489	0.4831	0.4569	0.4012	0.242
Ac227	0.0171	0.01272	0.01503	0.01189	0.00917	0.01178	0.01562	0.01621	0.009957	0	0	0	0
Th228	43.31	32.26	37.62	27.72	23.06	26.36	32.51	27.21	17	5.188	1.17	0.03216	0.0335
Th229	0.07886	0.07365	0.07432	0.07945	0.09093	0.1075	0.1192	0.1459	0.1589	0.157	0.1484	0.1303	0.07861
Th230	0.008958	0.008208	0.008374	0.009055	0.009768	0.01139	0.01167	0.01161	0.009214	0.005476	0.003311	0.001567	0.000375
Th232	0.02427	0.0244	0.02452	0.02592	0.02757	0.02928	0.03104	0.03327	0.03593	0.03773	0.03868	0.03948	0.04015
Th234	0.06707	0.06948	0.06724	0.07498	0.08146	0.09191	0.09945	0.1088	0.125	0.139	0.1443	0.1464	0.1475
Pa231	0.05781	0.04309	0.05098	0.03994	0.03363	0.03801	0.04934	0.04892	0.03652	0.01645	0.005072	0	0
Pa233	0.1137	0.1083	0.1134	0.1033	0.09482	0.07822	0.06819	0.06047	0.04244	0	0	0	0
U232	42.55	31.71	36.96	27.21	22.62	25.83	31.84	26.6	16.6	5.049	1.11	0	0
U233	48.39	46.66	46.21	48.29	52.73	57.41	58.7	63.66	60.66	51.34	46.04	40.56	25.66
U234	14.65	14.45	13.88	14.28	15.45	16.51	16.29	15.51	12.13	7.94	5.265	2.725	0.7183
U235	0.001023	0.000989	0.000977	0.000985	0.001076	0.001113	0.001086	0.001028	0.000712	0.000401	0.000323	0.000683	0.002684
U235m	198.3	190.3	192.2	212.2	239.9	257.1	277	333.1	303.9	176.3	104.5	76.67	59.01
U236	0.08764	0.08859	0.0856	0.08105	0.07436	0.06668	0.05805	0.04616	0.03603	0.03193	0.0301	0.02728	0.01815
U237	1.455	1.392	1.4	1.465	1.667	1.773	1.854	2.062	1.751	0.8378	0.3801	0.1537	0
U238	0.06708	0.06948	0.06724	0.07498	0.08147	0.09191	0.09946	0.1088	0.125	0.139	0.1443	0.1465	0.1475
Np237	0.1137	0.1084	0.1135	0.1034	0.09488	0.07828	0.06826	0.06056	0.04252	0.02142	0.01082	0.004908	0.001093
Np239	481	453	475.5	482.8	476.3	435.5	404.7	305.3	131.2	19.54	2.942	0	0
Pu238	2458	2305	2348	2389	2835	3195	3606	4865	5038	2357	957.9	286.2	21.09
Pu239	198.5	190.4	192.3	212.3	240.1	257.3	277.2	333.3	304.1	176.4	104.5	76.72	59.04
Pu240	704.9	677.9	698.7	703.8	707.6	708.9	704.9	725.2	615.7	458.8	289.9	161.9	51.11

Pu241	59130	56570	56910	59550	67770	72070	75380	83820	71170	34060	15450	6249	1043
Pu242	21.48	19.56	19.06	20.83	21.48	22.59	20.02	18.27	11.64	3.921	1.157	0.2339	0.01226
Pu244	9.79E-05	9.94E-05	0.000104	7.94E-05	6.19E-05	3.79E-05	2.74E-05	1.27E-05	3.01E-06	1.2E-07	0	0	0
Am241	1397	1330	1339	1429	1676	1847	2011	2461	2361	1287	640.2	286.1	51.09
Am242	3.872	3.557	3.574	4.253	5.862	7.64	9.526	14.94	18.32	10.53	5.457	2.513	0
Am242m	3.89	3.573	3.591	4.273	5.889	7.675	9.57	15.01	18.41	10.57	5.483	2.525	0.3986
Am243	481	453	475.5	482.8	476.3	435.5	404.7	305.3	131.2	19.54	2.942	0.3234	0.007148
Cm242	3.326	3.056	3.071	3.651	5.029	6.551	8.164	12.79	15.68	9.007	4.669	2.15	0.3312
Cm243	26.68	24.64	24.79	25.6	29.32	31.09	31.28	34.27	24.99	8.578	2.573	0.4779	0
Cm244	224600	226300	226800	195400	171900	122100	95430	49600	13150	929	78.62	4.192	0
Cm245	16.94	16.12	17.45	14.11	12.88	8.439	6.514	3.515	0.7413	0.02891	0.001576	0	0
Cm246	166.5	166.9	184.7	124.6	86.46	41.15	25.24	8.758	1.116	0.02792	0	0	0
Cm247	0.001553	0.001451	0.001706	0.001062	0.000702	0.000292	0.000154	4.4E-05	3.12E-06	0	0	0	0
Cm248	0.05722	0.05677	0.06668	0.03413	0.01842	0.00566	0.002416	0.000451	2.61E-06	0	0	0	0
Bk249	0.06218	0.05714	0.07148	0.03535	0.01805	0.00477	0	0	0	0	0	0	0
Cf249	0.5423	0.495	0.6189	0.3129	0.1679	0.04674	0.01923	0.001458	0	0	0	0	0
Cf250	4.747	4.413	5.492	2.548	1.339	0.3633	0.1266	0	0	0	0	0	0
Cf251	0.03047	0.02847	0.03494	0.01596	0.008432	0.002263	0.000752	0	0	0	0	0	0
Cf252	4.743	4.583	5.661	2.311	1.013	0.2167	0.008018	0	0	0	0	0	0

Table 35: Heavy nuclide concentrations as a function of radial position, activates stated for 2016 in units of Bq/kg

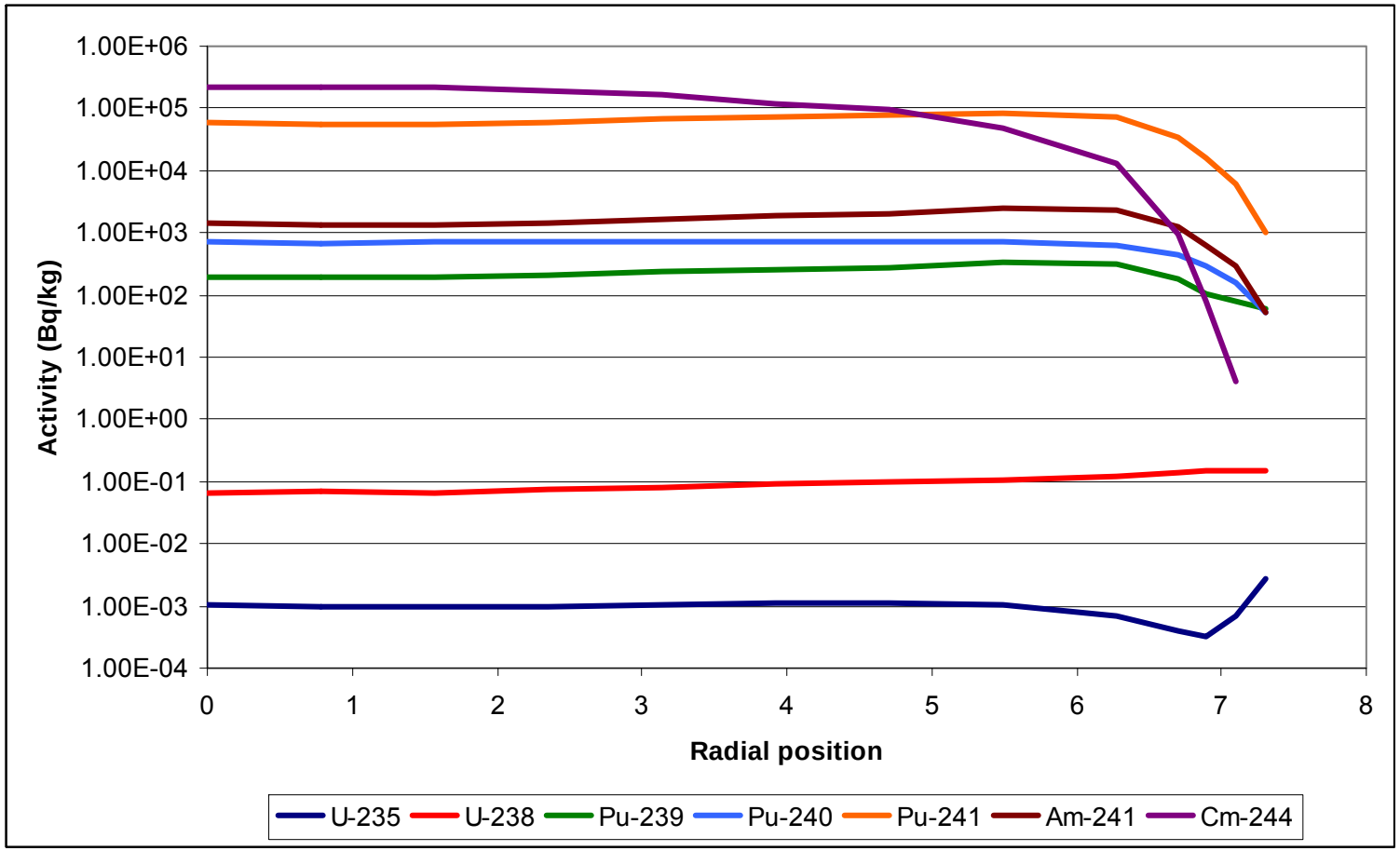

Figure 78: Graphical trends of 7 key heavy nuclides for radial variation in Sizewell A

NPL precursors – Axial

Nuclide	-4.5	-4.25	-4	-3	-2	-1	0	1	2	3	4	4.25	4.5
Ra224	0	3.716	15.52	32.98	21.8	23.35	43.54	33.1	53.79	33.49	22.1	1.059	2.16
Ra225	0.1425	0.1627	0.1632	0.1151	0.07833	0.07368	0.07859	0.07474	0.09865	0.1133	0.1506	0.1455	0.1302
Ra228	0.03618	0.02635	0.02552	0	0	0	0	0	0	0	0.02559	0.03512	0.03632
Ac225	0.4393	0.5018	0.5032	0.3548	0.2415	0.2272	0.2423	0.2304	0.3042	0.3493	0.4644	0.4486	0.4015
Ac227	0.02196	0	0.01019	0.01636	0	0.008889	0.0171	0.01295	0.02279	0.01589	0.01879	0	0
Th228	8.122	3.697	15.44	32.81	21.69	23.23	43.31	32.92	53.51	33.32	21.98	1.054	2.149
Th229	0.1427	0.1631	0.1636	0.1154	0.07859	0.07394	0.07886	0.075	0.09895	0.1136	0.1509	0.1458	0.1304
Th230	0.001881	0.006139	0.008461	0.01112	0.008766	0.008105	0.008958	0.008207	0.01074	0.01094	0.007792	0.004328	0.00151
Th232	0.03937	0.03762	0.03643	0.03105	0.026	0.02508	0.02427	0.02503	0.02657	0.03128	0.03653	0.03831	0.03952
Th234	0.1453	0.1348	0.1283	0.1022	0.07714	0.07158	0.06707	0.07065	0.07409	0.1021	0.1308	0.1427	0.1459
Pa231	0.05322	0.01126	0.03738	0.05215	0.0313	0.0326	0.05781	0.04371	0.07534	0.05038	0.05339	0.003779	0.01609
Pa233	0	0	0.03972	0.06429	0.09849	0.106	0.1137	0.1073	0.1076	0.06334	0.03538	0	0
U232	7.899	3.592	15.07	32.13	21.3	22.82	42.55	32.35	52.5	32.64	21.46	0.9971	2.065
U233	44.92	55.85	61.19	54.86	48.08	46.83	48.39	47.35	54.97	55.8	53.64	46.71	40.85
U234	3.048	8.389	11.49	15.39	14.47	14.3	14.65	14.48	15.98	15.78	10.52	6.35	2.58
U235	0.000715	0.000468	0.000657	0.000994	0.000979	0.000982	0.001023	0.001007	0.001144	0.001028	0.000589	0.000329	0.000772
U235m	124.1	261.7	299.4	251.9	208.7	198.8	198.3	197.6	247.9	258.9	239.6	118.5	106.4
U236	0.02739	0.03146	0.03429	0.05897	0.08196	0.08558	0.08764	0.08522	0.07784	0.0579	0.0348	0.03079	0.02688
U237	0.2913	1.341	1.687	1.615	1.44	1.413	1.455	1.447	1.766	1.719	1.287	0.5276	0.1942
U238	0.1453	0.1348	0.1283	0.1023	0.07714	0.07158	0.06708	0.07066	0.07409	0.1021	0.1309	0.1428	0.146
Np237	0.008554	0.03191	0.0398	0.06435	0.09854	0.1061	0.1137	0.1074	0.1077	0.0634	0.03544	0.01456	0.006321
Np239	0.7524	40.97	103.1	356.7	460.4	458.4	481	446.9	523.9	367.8	84.71	6.298	0.4375
Pu238	570.4	4078	5168	2960	2318	2313	2458	2417	3083	3251	3529	1456	345.5
Pu239	124.1	261.9	299.6	252.1	208.8	198.9	198.5	197.7	248.1	259.1	239.8	118.6	106.4
Pu240	262	573.8	519.5	679.1	681.8	680.9	704.9	665.3	759.6	635	598.2	330.7	208.4
Pu241	11840	54510	68560	65670	58540	57450	59130	58820	71780	69870	52320	21450	7896
Pu242	0.4536	5.962	9.801	20.12	20.96	19.48	21.48	19.87	22.85	19.11	8.248	2.108	0.2696
Pu244	0	4.95E-07	2.26E-06	2.33E-05	7.55E-05	9.32E-05	9.79E-05	9.58E-05	7.24E-05	2.67E-05	1.49E-06	0	0
Am241	541.9	2076	2384	1739	1405	1362	1397	1390	1768	1852	1773	841	364.2
Am242	4.938	18.26	19.46	7.643	4.148	3.768	3.872	3.895	6.172	8.554	12.88	7.038	3.226

Am242m	4.961	18.34	19.55	7.679	4.168	3.785	3.89	3.913	6.2	8.594	12.94	7.071	3.241
Am243	0.7524	40.97	103.1	356.7	460.4	458.4	481	446.9	523.9	367.8	84.71	6.298	0.4375
Cm242	4.224	15.63	16.66	6.552	3.562	3.236	3.326	3.345	5.295	7.332	11.03	6.023	2.759
Cm243	1.001	14.5	23.02	26.56	24.91	24.74	26.68	25.46	32.84	28.01	16.43	4.488	0.553
Cm244	11.33	2300	10190	80480	191000	216600	224600	220900	194100	92770	6518	229.4	5.37
Cm245	0	0.107	0.5539	4.913	12.99	15.5	16.94	16.5	15.7	5.89	0.305	0.005708	0
Cm246	0	0.09882	0.7079	20.57	113.5	153.6	166.5	161.4	109.1	23.96	0.4442	0.003757	0
Cm247	0	0	1.68E-06	0.000115	0.000908	0.001305	0.001553	0.001412	0.00098	0.000132	8.13E-07	0	0
Cm248	0	0	0	0.001817	0.02918	0.04828	0.05722	0.05363	0.02658	0.002171	0	0	0
Bk249	0	0	0	0	0.02896	0.04922	0.06218	0.05514	0.02972	0	0	0	0
Cf249	0	0	0	0.01303	0.2565	0.4297	0.5423	0.4821	0.2751	0.01589	0	0	0
Cf250	0	0	0	0.07526	2.072	3.7	4.747	4.134	2.214	0.08889	0	0	0
Cf251	0	0	0	0.000444	0.01295	0.02355	0.03047	0.02708	0.01402	0.000552	0	0	0
Cf252	0	0	0	0	1.871	3.665	4.743	4.179	1.704	0	0	0	0

Table 36: Heavy nuclide concentrations as a function of axial position, activates stated for 2016 in units of Bq/kg

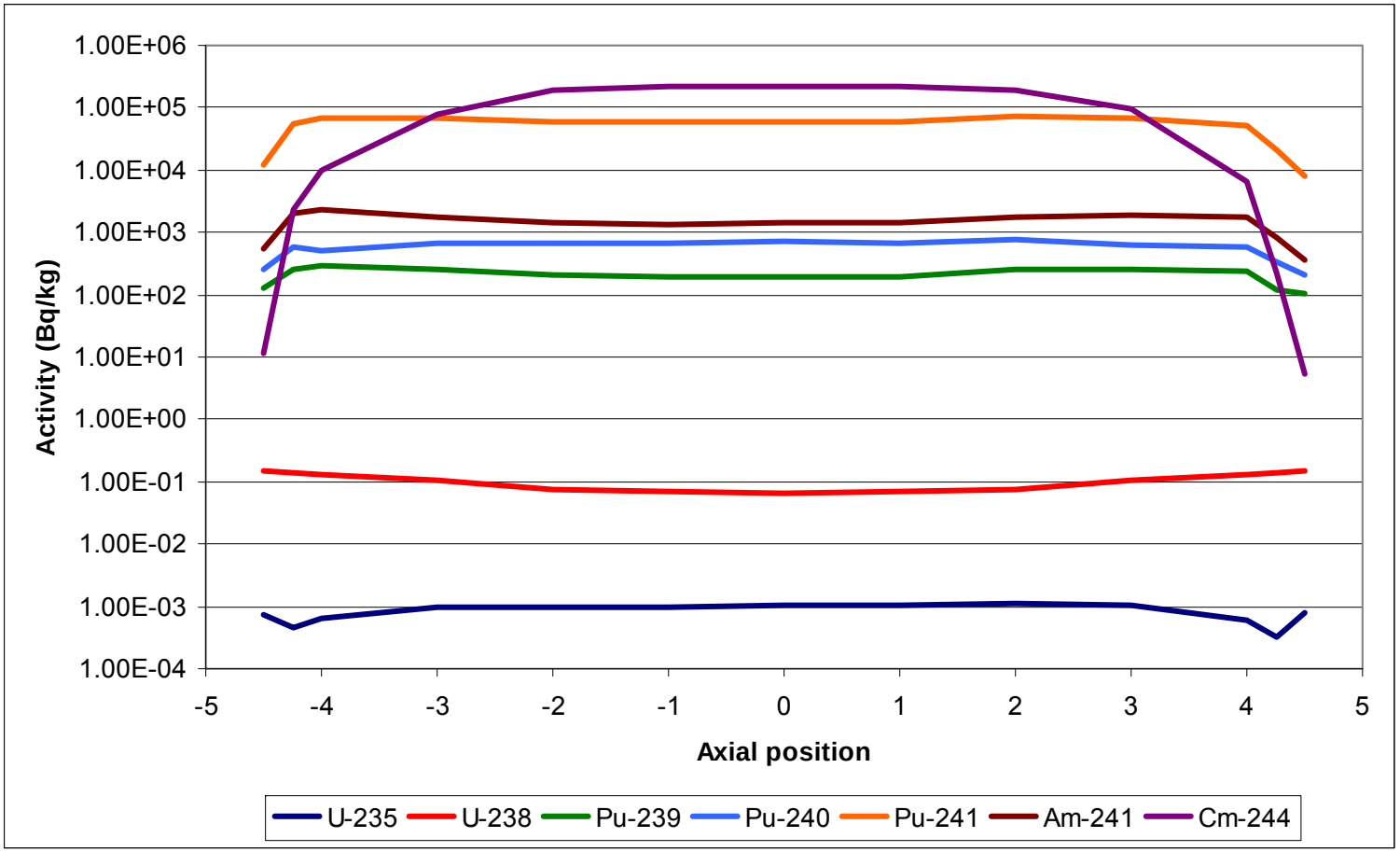

Figure 79: Graphical trends of 7 key heavy nuclides for axial variation in Sizewell A

Wylfa:

NPL precursors - Radial

	Core											Reflector			
Nuclide	0	0.7848	1.5696	2.3544	3.1392	3.924	4.7088	5.4936	6.2784	7.0632	7.848	8.25	8.55	8.85	9.15
Ra224	45.27	25.27	25.19	44.85	22.98	19.43	54.69	46.31	25.12	24.18	14.12	4.012	0.2494	0	0
Ra225	0.06743	0.06444	0	0.07226	0.0739	0.08214	0.09198	0.1082	0.1104	0.1432	0.1516	0.1372	0.1327	0.1215	0.08624
Ra228	0.02121	0.02125	0.02155	0.02281	0.02322	0.02515	0.02673	0.0291	0.03126	0.0336	0.03624	0.03654	0.03782	0.03895	0.03974
Ac225	0.2079	0.1987	0	0.2228	0.2278	0.2533	0.2836	0.3337	0.3405	0.4415	0.4675	0.423	0.4093	0.3746	0.2659
Ac227	0.01705	0.009889	0.009537	0.01717	0.009067	0	0.02253	0.02078	0.01219	0.01491	0.009327	0	0	0	0
Th228	45.04	25.13	25.06	44.62	22.87	19.33	54.4	46.07	24.99	24.05	14.04	3.991	0.2481	0.0386	0.03948
Th229	0.06775	0.06684	0.06253	0.07253	0.07417	0.08243	0.09228	0.1085	0.1108	0.1436	0.1519	0.1375	0.133	0.1217	0.08641
Th230	0.007157	0.006887	0.006639	0.007433	0.007756	0.007924	0.009392	0.01065	0.009839	0.009973	0.006965	0.00564	0.003425	0.00163	0.000538
Th232	0.02277	0.02279	0.0232	0.02434	0.0247	0.02656	0.0281	0.03029	0.03236	0.03448	0.03694	0.03731	0.03845	0.03937	0.04
Th234	0.05791	0.06071	0.06376	0.0636	0.07009	0.0725	0.0829	0.09106	0.1062	0.1178	0.1301	0.1381	0.1444	0.1464	0.1474
Pa231	0.05892	0.03412	0.03301	0.0589	0.03095	0.02709	0.07525	0.06762	0.03866	0.04486	0.0342	0.0112	0.000959	4.42E-05	0
Pa233	0.127	0.1234	0.1143	0.1197	0.11	0.1081	0.09295	0.08204	0.05801	0.0464	0.03702	0	0	0	0
U232	44.32	24.72	24.65	43.89	22.46	18.98	53.4	45.14	24.47	23.51	13.7	3.868	0.2061	0	0
U233	45.93	46.87	44.29	48.09	50.35	53.62	54.33	59.57	59.66	64.41	59.45	50.42	45.31	41.42	30.62
U234	13.81	14.35	13.5	14.54	15.46	15.68	15.87	16.25	16.14	14.71	9.985	8.817	5.918	3.094	1.097
U235	0.000995	0.00101	0.000931	0.001051	0.001074	0.001136	0.001117	0.001159	0.001061	0.000897	0.00057	0.000442	0.000303	0.000551	0.00193
U235m	181.5	185.5	174.9	199	207	244.6	250.7	294.3	289.3	313.5	292.2	165	87.27	70.41	59.73
U236	0.08995	0.09241	0.09062	0.08592	0.0874	0.07761	0.07166	0.06051	0.05154	0.04103	0.03276	0.03309	0.03075	0.02797	0.02149
U237	1.328	1.341	1.256	1.463	1.494	1.727	1.744	2.015	1.908	1.932	1.661	0.8379	0.349	0.1607	0
U238	0.05791	0.06071	0.06376	0.0636	0.0701	0.0725	0.08291	0.09107	0.1062	0.1178	0.1302	0.1381	0.1444	0.1464	0.1474
Np237	0.1271	0.1234	0.1144	0.1198	0.11	0.1082	0.09301	0.08211	0.05808	0.04648	0.0371	0.02098	0.009888	0.004919	0.001645
Np239	459.2	460.3	444.6	460.8	471.6	487.9	457.9	472	320.7	208.3	70.14	25.67	3.259	0.3829	0
Pu238	2179	2153	1950	2345	2304	2709	2732	3470	3569	4407	4431	2008	782.9	274.7	42.13
Pu239	181.6	185.6	175.1	199.1	207.2	244.8	250.9	294.5	289.5	313.7	292.4	165.1	87.32	70.45	59.77
Pu240	695.9	701.9	678.4	697.5	710.2	716	680.1	754.6	563.3	642.5	665.6	446	262.3	162.7	70.8
Pu241	53970	54510	51080	59480	60740	70220	70890	81910	77560	78520	67510	34060	14190	6531	1837
Pu242	17.51	19.11	18.67	18.15	20.25	21.21	20.82	21.61	18.12	15.06	8.845	4.744	1.262	0.2737	0.03011
Pu244	0.000132	0.00012	0.000118	0.000115	9.41E-05	8.25E-05	6.15E-05	3.88E-05	2.19E-05	6.83E-06	1.09E-06	3.33E-07	6.88E-09	0	0
Am241	1226	1244	1158	1369	1410	1669	1710	2071	2039	2289	2254	1136	521.4	268.6	80.64
Am242	2.575	2.632	2.348	3.177	3.454	4.849	5.408	8.187	9.588	13.81	17.16	7.83	3.888	2.156	0
Am242m	2.587	2.645	2.359	3.191	3.47	4.871	5.433	8.225	9.633	13.88	17.24	7.867	3.906	2.166	0.6224

Am243	459.2	460.3	444.6	460.8	471.6	487.9	457.9	472	320.7	208.3	70.14	25.67	3.259	0.3829	0.02338
Cm242	2.215	2.265	2.021	2.732	2.969	4.164	4.643	7.022	8.218	11.83	14.69	6.703	3.327	1.845	0.5172
Cm243	24.1	24.55	21.93	26.01	26.9	30.61	29.74	35.33	31.04	31.39	21.56	9.725	2.783	0.5985	0.04484
Cm244	260700	255900	247200	252600	234000	219200	181700	130600	84120	29480	5029	1504	102.9	5.825	0.1295
Cm245	21.41	19.67	17.93	21.1	17.38	18.15	13.97	10.72	5.63	1.741	0.2723	0.04664	0.001951	5.78E-05	0
Cm246	265.5	227.6	221.6	219.2	157.6	135.6	86.95	45.15	18.05	3.35	0.2985	0.0559	0.00155	0	0
Cm247	0.002752	0.002253	0.00205	0.002114	0.00144	0.001186	0.000681	0.000329	9.34E-05	1.28E-05	6.66E-07	1.79E-08	0	0	0
Cm248	0.1257	0.09686	0.09122	0.08615	0.0509	0.03598	0.01764	0.005823	0.001378	0.000106	2.97E-07	0	0	0	0
Bk249	0.1622	0.1175	0.1046	0.1045	0.05653	0.04427	0.01871	0.005815	0	0	0	0	0	0	0
Cf249	1.32	0.9607	0.8464	0.8687	0.4752	0.385	0.1661	0.05514	0.01055	0.000374	0	0	0	0	0
Cf250	11.86	8.906	7.576	7.894	4.299	3.146	1.302	0.4233	0.06855	0	0	0	0	0	0
Cf251	0.07701	0.05708	0.04849	0.05193	0.02771	0.02037	0.00849	0.002669	0.000453	0	0	0	0	0	0
Cf252	15.11	10.9	9.748	9.118	4.556	2.858	1.077	0.2601	0.03491	0	0	0	0	0	0

Table 37: Heavy nuclide concentrations as a function of radial position, activates stated for 2016 in units of Bq/kg

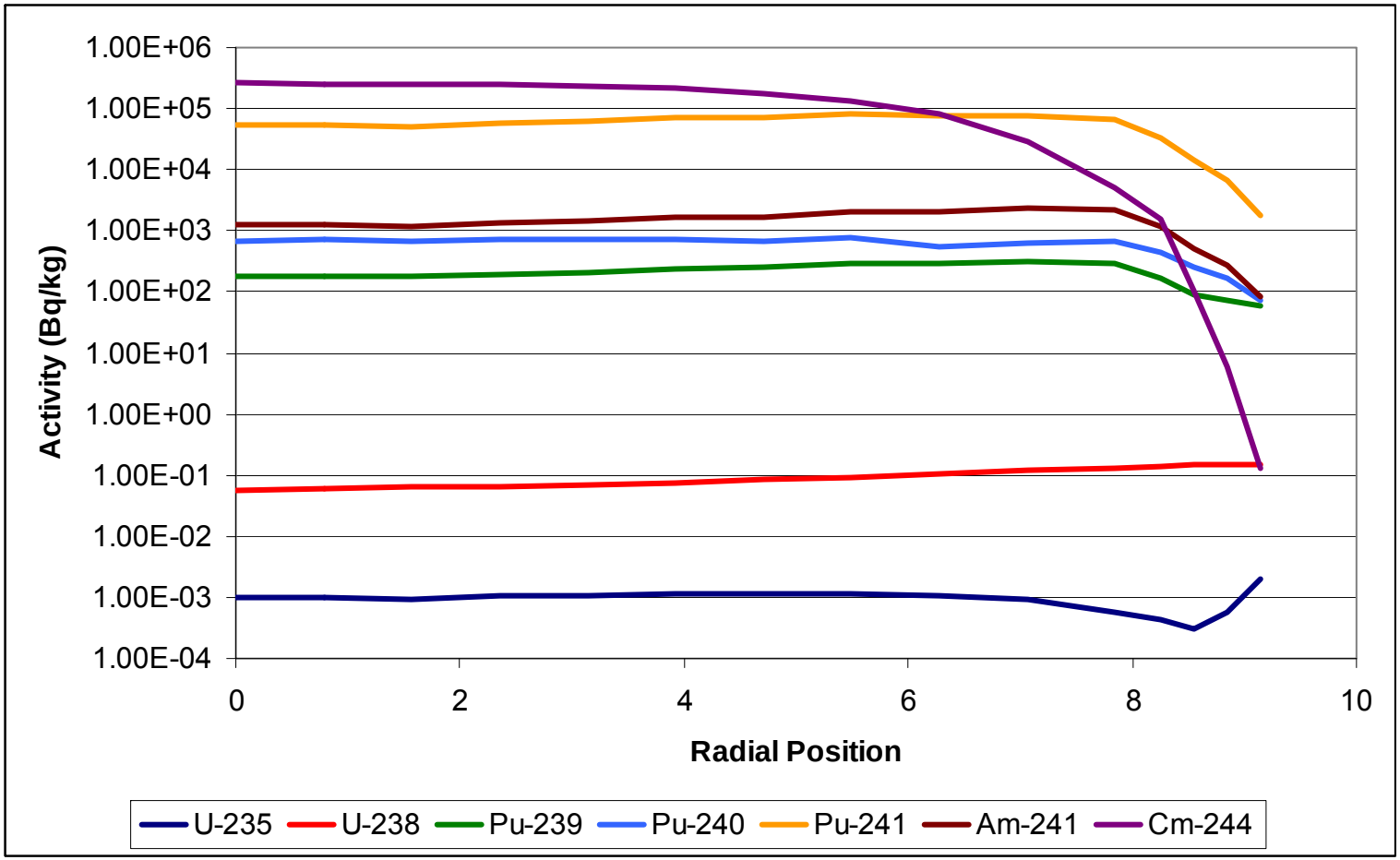

Figure 80: Graphical trends of 7 key heavy nuclides for radial variation in Sizewell A

NPL precursors – Axial

	Bottom			Centre									Top		
Nuclide	-5	-4.75	-4.5	-4	-3	-2	-1	0	1	2	3	4	4.5	4.75	5
Ra223	0.002602	0	0.1604	0	0	0	0	0	0	0	0	0	0	0	0
Ra224	0.6787	3.387	72.56	30.97	31.09	28.91	28.17	45.27	14.32	17.84	24.59	20.97	8.662	3.134	0.5782
Ra225	0.1358	0.1481	0.1739	0.1324	0.0902	0.07396	0	0.06743	0	0.06869	0.08221	0.1293	0.1688	0.155	0.148
Ra226	2.98E-05	0	0	0	0	0	0	0	0	0	0	0	0	0	0
Ra228	0.03807	0.03626	0.03595	0.03172	0.0264	0.02365	0.02009	0.02121	0.02067	0.02318	0.02667	0.03232	0.03601	0.0376	0.03864
Ac225	0.4188	0.4566	0.5362	0.4081	0.2781	0.2281	0	0.2079	0	0.2118	0.2535	0.3988	0.5205	0.478	0.4564
Ac227	0.001031	0	0.06327	0.01587	0.01293	0.01125	0.01094	0.01705	0	0	0.01017	0.01	0	0	0
Ac228	0.03808	0	0	0	0	0	0	0	0	0	0	0	0	0	0
Th227	0.001013	0	0.06213	0	0	0	0	0	0	0	0	0	0	0	0
Th228	0.6752	3.369	72.18	30.81	30.93	28.76	28.03	45.04	14.25	17.74	24.47	20.86	8.616	3.118	0.5752
Th229	0.1361	0.1484	0.1743	0.1327	0.09051	0.07424	0.05945	0.06775	0.05483	0.06896	0.0825	0.1297	0.1692	0.1553	0.1483
Th230	0.003537	0.00637	0.007683	0.0111	0.009567	0.007696	0.006007	0.007157	0.006167	0.007249	0.008336	0.0105	0.007474	0.004314	0.002388
Th231	0.000378	0	0	0	0	0	0	0	0	0	0	0	0	0	0
Th232	0.03861	0.03699	0.03661	0.03273	0.02775	0.02516	0.02173	0.02277	0.02249	0.02475	0.02812	0.03331	0.03665	0.03815	0.03905
Th234	0.1421	0.1324	0.128	0.1094	0.0811	0.06722	0.05342	0.05791	0.07283	0.07025	0.08278	0.1118	0.1269	0.1369	0.1408
Pa231	0.002649	0.009505	0.1761	0.04958	0.04318	0.0384	0.03808	0.05892	0.01969	0.02462	0.03414	0.03668	0.02327	0.01115	0.003047
Pa233	0.01605	0	0.04323	0.05733	0.09462	0.114	0.1292	0.127	0.09565	0.1093	0.09143	0.05312	0.04179	0	0
Pa234	0.000213	0	0	0	0	0	0	0	0	0	0	0	0	0	0
Pa234m	0.1421	0	0	0	0	0	0	0	0	0	0	0	0	0	0
U232	0.623	3.261	70.54	30.13	30.34	28.26	27.6	44.32	14.01	17.43	24.01	20.4	8.394	3.012	0.5248
U234	5.66	9.741	10.97	16.16	16.16	14.86	12.87	13.81	12.76	14.43	15.25	15.69	11.12	6.974	4.073
U235	0.000378	0.000534	0.000629	0.001052	0.001139	0.001067	0.00092	0.000995	0.000797	0.001	0.001069	0.001002	0.000647	0.000438	0.000646
U235m	158.2	258.8	329.1	297	252.9	211.7	166.3	181.5	146.7	198.6	238.7	308.4	371.5	277.2	289.3
U236	0.02969	0.0331	0.03346	0.04874	0.07292	0.0832	0.09147	0.08995	0.1007	0.08595	0.07187	0.04623	0.03322	0.03033	0.02813
U237	0.7524	1.376	1.874	1.929	1.774	1.543	1.188	1.328	1.01	1.401	1.668	1.923	2.065	1.306	0.9653
U238	0.1421	0.1324	0.128	0.1094	0.0811	0.06722	0.05342	0.05791	0.07284	0.07025	0.08279	0.1118	0.1269	0.1369	0.1408
Np236	7.85E-11	0	0	0	0	0	0	0	0	0	0	0	0	0	0
Np237	0.01609	0.03193	0.04332	0.05741	0.09468	0.1141	0.1292	0.1271	0.09568	0.1094	0.09148	0.0532	0.04189	0.02856	0.01947
Np238	0.04647	0	0	0	0	0	0	0	0	0	0	0	0	0	0
Np239	9.886	55.74	78.88	315.1	490.6	498	429.9	459.2	395.8	465.1	460.4	258.8	103.2	30.65	6.075
Pu236	1.17E-06	0	0	0	0	0	0	0	0	0	0	0	0	0	0
Pu238	1887	3473	5047	3829	2789	2409	1985	2179	1451	2126	2557	3944	5676	3275	1866
Pu239	158.3	258.9	329.3	297.2	253.1	211.8	166.4	181.6	146.8	198.7	238.9	308.6	371.8	277.4	289.4
Pu240	326.6	614	746.2	721.5	732.7	735.2	663.3	695.9	636.3	699.1	682.3	628.6	693	592.8	548

Pu241	30580	55930	76180	78420	72120	62720	48300	53970	41060	56940	67800	78160	83930	53080	39240
Pu242	2.322	7.502	9.815	17.91	22.61	18.26	16.82	17.51	19.35	18.75	19.29	17.86	9.781	4.146	1.716
Pu244	8.39E-08	8.39E-07	1.24E-06	1.39E-05	5.98E-05	0.000104	0.000146	0.000132	0.000103	9.78E-05	6.6E-05	1.13E-05	1.79E-06	2.93E-07	1.55E-08
Am241	1175	1878	2565	2133	1741	1457	1087	1226	919.8	1315	1624	2165	2880	2005	1632
Am242	9.991	13.45	19.69	10.68	5.51	3.627	2.043	2.575	1.563	3.043	4.899	11.49	22.96	17.13	14.66
Am242m	10.04	13.51	19.78	10.73	5.535	3.643	2.053	2.587	1.57	3.057	4.922	11.54	23.07	17.21	14.72
Am243	9.886	55.74	78.88	315.1	490.6	498	429.9	459.2	395.8	465.1	460.4	258.8	103.2	30.65	6.075
Cm242	8.549	11.51	16.86	9.156	4.73	3.117	1.759	2.215	1.347	2.616	4.206	9.844	19.66	14.66	12.54
Cm243	5.878	17.5	26.07	32.75	31.54	27.07	21.39	24.1	16.86	24.25	27.67	32.3	28.62	11.89	4.601
Cm244	410.4	3825	5756	55430	177500	244800	260200	260700	225000	231300	188500	46420	8421	1404	151.5
Cm245	0.01191	0.1771	0.3208	3.64	13.81	19.95	20.84	21.41	11.8	16.99	14.39	2.954	0.4952	0.06466	0.005694
Cm246	0.007501	0.2059	0.3451	9.636	83.42	186.4	307.3	265.5	164.7	169.3	96.42	7.299	0.5171	0.04587	0.002256
Cm247	5.52E-09	3.74E-07	8.48E-07	4.98E-05	0.000697	0.001716	0.003146	0.002752	0.00119	0.001509	0.000743	3.47E-05	1.28E-06	1.73E-08	0
Cm248	1.45E-08	0	1.83E-06	0.00055	0.01693	0.06201	0.1624	0.1257	0.05559	0.05644	0.02035	0.000367	4.21E-06	0	0
Bk249	0	0	0	0	0.01859	0.07518	0.2165	0.1622	0.04765	0.06291	0.02123	0	0	0	0
Cf249	2.37E-08	0	0	0.004063	0.1651	0.6332	1.729	1.32	0.3766	0.5227	0.1867	0.002619	0	0	0
Cf250	0	0	0	0.02816	1.328	5.548	15.46	11.86	3.62	4.591	1.497	0.01695	0	0	0
Cf251	0	0	0	0.000168	0.0085	0.03576	0.09941	0.07701	0.02204	0.02914	0.009646	0.000104	0	0	0
Cf252	0	0	0	0.002572	1.071	5.859	21.73	15.11	5.057	5.089	1.284	0	0	0	0

Table 38: Heavy nuclide concentrations as a function of axial position, activates stated for 2016 in units of Bq/kg

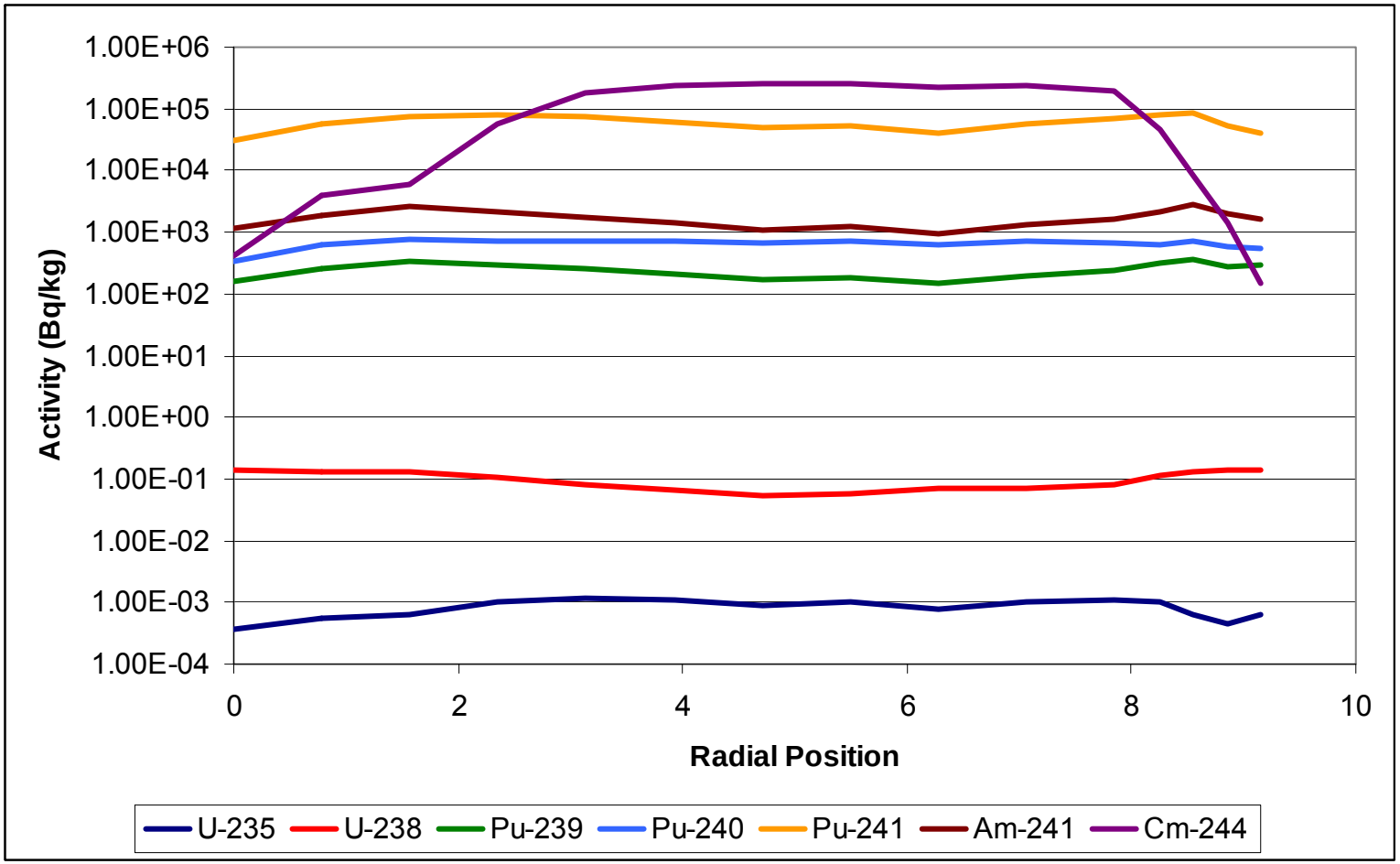

Figure 81: Graphical trends of 7 key heavy nuclides for axial variation in Sizewell A

APPENDIX 11 – PATHWAY ANALYSIS

The simulated irradiation of material in FISPACT utilises known cross sectional data for neutron activation at various energies. These activation and decay chains form 'paths' from a stable elemental nuclide (such as Co-59) to an unstable, radioactive nuclide (such as Co60).

Using the "Routes" command in FISPACT allows for pathway analysis from a known parent to a known daughter. The output of this is a section in the FISPACT output file giving the pathway and relative contribution to the final inventory from this pathway. For lighter nuclides, this is usually only a few pathways and is relatively straight forward. However, for heavier nuclides, pathways become more numerous and often more ingenious.

The Routes command in FISPACT allows for pathway analysis of up to, and including, 8 steps. There is a chance, especially in heavier nuclides, that the activation pathways will become longer than this. As a result there may be a significant fraction of the radionuclide that is unaccounted for.

The results will be displayed using data from each reactor at the centre of the core, and in the reflector region (radially). This will allow comparison of each precursor inventory (J. Jowett and NPL), as well as each reactor and the effects of a different neutron energy spectra to be analysed.

Results will be presented in a tabular format listing the radionuclide of interest (e.g. Tritium, Chlorine-36, Cobalt-60, etc), the parent nuclide, the detailed pathway and the relative contribution to the inventory that this pathway accounts for.

All contributions will be reported to the nearest half-percent. Any contribution not accounted for (either because it uses an exotic route, or contains greater than 8 links) will be summed up in the 'remainder' value.

All pathways are calculated at <u>end of operation</u>, and as a result do not account for decay chains (such as Xe-136 → Cs-137) beyond this point.

Pathway Legend

Process	Description
(n,a)	Neutron is absorbed, alpha is emitted
(n,p)	Neutron is absorbed in place of a proton
(n,g)	Neutron is absorbed, gamma emitted
(b-)	Beta decay
(IT)	Isomeric transition, decay from a meta-stable state into a ground state by emission of a gamma

Wylfa Reactor 1:

Jowett Precursors

Wylfa Reactor, Centre of the core utilising J. Jowett Precursors

Radionuclide	Precursor	Pathway	Contribution
H3	Lithium-6	Li6(n,a)H3(b-)He3(n,p)H3	80.5%
	Lithium-6	Li6(n,a)H3	12%
	H-1	H1(n,g)H2(n,g)H3	1%
	C-12	C12(n,a)Be9(n,a)He6(b-)Li6(n,a)H3(b-) He3(n,p)H3	2%
	C-12	C12(n,a)Be9(n,a)He6(b-)Li6(n,a)H3	2.5%
	N/A	Remainder	2%
C14	N-14	N14(n,p)C14	70%
	C-13	C13(n,g)C14	29.5%
	O-17	O17(n,a)C14	<0.1%
	N/A	Remainder	<1%
Cl36	Cl-35	Cl35(n,g)Cl36	95%
	S-34	S34(n,g)S35(b-)Cl35(n,g)Cl36	4%
	N/A	Remainder	1%
Co60	Co-59	Co59(n,g)Co60m(IT)Co60	38.5%
	Co-59	Co59(n,g)Co60	30.5%
	Ni-58	Ni58(n,g)Ni59(n,p)Co59(n,g)Co60m(IT)Co60	9%
	Ni-58	Ni58(n,g)Ni59(n,p)Co59(n,g)Co60	7.5%
	Fe-58	Fe58(n,g)Fe59(b-)Co59(n,g)Co60m(IT)Co60	4%
	Fe-58	Fe58(n,g)Fe59(b-)Co59(n,g)Co60	3%
	Fe-56	Fe56(n,g)Fe57(n,g)Fe58(n,g) Fe59(b-)Co59(n,g)Co60m(IT)Co60	2.5%
	Fe-56	Fe56(n,g)Fe57(n,g)Fe58(n,g) Fe59(b-)Co59(n,g)Co60	2%
	Fe-57	Fe57(n,g)Fe58(n,g)Fe59(b-) Co59(n,g)Co60m(IT)Co60	1.5%
	Fe-57	Fe57(n,g)Fe58(n,g)Fe59(b-)Co59(n,g)Co60	1%
	N/A	Remainder	<1%
Cs-137[10]	Xe-136	Xe136(n,g)Xe137(b-)Cs137	98.5%
	Cs-133	Cs133(n,g)Cs134(n,g)Cs135(n,g) Cs136(n,g)Cs137	0.5%
	N/A	Remainder	1%

[10] J. Jowett precursors included fissile material, such as Uranium and Thorium, which would contribute to the Cs-137 activity; however, they were not included in FISPACT. This was done to achieve less radionuclide 'noise' from fission products in the FISPACT output file. NPL Data did utilise fissile materials

Eu-152	Nd-148	Nd148(n,g)Nd149(b-)Pm149(b-) Sm149(n,g)Sm150(n,g)Sm151(b-) Eu151(n,g)Eu152	24%
	Sm-147	Sm147(n,g)Sm148(n,g)Sm149(n,g)Sm150(n,g) Sm151(b-)Eu151(n,g)Eu152	22%
	Sm-148	Sm148(n,g)Sm149(n,g)Sm150(n,g) Sm151(b-)Eu151(n,g)Eu152	16.5%
	Nd-150	Nd150(n,g)Nd151(b-)Pm151(b-) Sm151(b-)Eu151(n,g)Eu152	14.5%
	Sm-149	Sm149(n,g)Sm150(n,g) Sm151(b-)Eu151(n,g)Eu152	2%
	Sm-150	Sm150(n,g)Sm151(b-)Eu151(n,g)Eu152	2%
	Nd-148	Nd148(n,g)Nd149(b-)Pm149(n,g) Pm150(b-)Sm150(n,g) Sm151(b-)Eu151(n,g)Eu152	0.5%
	N/A	Remainder	18%[11]
Eu-154	Sm-147	Sm147(n,g)Sm148(n,g)Sm149(n,g) Sm150(n,g)Sm151(n,g)Sm152(n,g) Sm153(b-)Eu153(n,g)Eu154	20%
	Sm-148	Sm148(n,g)Sm149(n,g)Sm150(n,g) Sm151(n,g)Sm152(n,g) Sm153(b-)Eu153(n,g)Eu154	15.5%
	Nd-150	Nd150(n,g)Nd151(b-)Pm151(b-) Sm151(n,g)Sm152(n,g)Sm153(b-) Eu153(n,g)Eu154	13.5%
	Sm-149	Sm149(n,g)Sm150(n,g)Sm151(n,g) Sm152(n,g)Sm153(b-)Eu153(n,g)Eu154	4%
	Sm-150	Sm150(n,g)Sm151(n,g)Sm152(n,g)Sm153(b-) Eu153(n,g)Eu154	4%
	N/A	Remainder	33%
Eu-155	Sm-154	Sm154(n,g)Sm155(b-)Eu155	36%
	Sm-148	Sm148(n,g)Sm149(n,g)Sm150(n,g)Sm151(n,g) Sm152(n,g)Sm153(b-) Eu153(n,g)Eu154(n,g)Eu155	10%
	Nd-150	Nd150(n,g)Nd151(b-)Pm151(b-) Sm151(n,g)Sm152(n,g)Sm153(b-) Eu153(n,g)Eu154(n,g)Eu155	8.5%
	Sm-149	Sm149(n,g)Sm150(n,g)Sm151(n,g)Sm152(n,g) Sm153(b-)Eu153(n,g)Eu154(n,g)Eu155	2.5%
	Sm-150	Sm150(n,g)Sm151(n,g)Sm152(n,g)Sm153(b-) Eu153(n,g)Eu154(n,g)Eu155	2.5%
	N/A	Remainder	40%

[11] It is suspected here that the majority of Europium activity was caused by activation chains from Samarium and Neodymium, however, FISPACT ROUTES pathway analysis can only analyse upto 8 links (e.g. Co59(n,g)Co60 is one link). The remainder of the activity not accounted for is expected to come from activation chains longer than 8 links

Reflector

Radionuclide	Precursor	Pathway	Contribution
H-3	Lithium-6	Li6(n,a)H3(b-)He3(n,p)H3	62%
	Lithium-6	Li6(n,a)H3	38%
	N/A	Remainder	<0.01%
CARBON-14	N-14	N14(n,p)C14	72%
	C-13	C13(n,g)C14	28%
	O-17	O17(n,a)C14	0.1%
	N/A	Remainder	<0.01%
Chlorine-36	Cl-35	Cl35(n,g)Cl36	99.5%
	S-34	S34(n,g)S35(b-)Cl35(n,g)Cl36	0.5%
	N/A	Remainder	<0.01%
Cobalt-60	Co-59	Co59(n,g)Co60m(IT)Co60	55.5%
	Co-59	Co59(n,g)Co60	44.5%
	Fe-58	Fe58(n,g)Fe59(b-)Co59(n,g)Co60m(IT)Co60	0.1%
	Fe-58	Fe58(n,g)Fe59(b-)Co59(n,g)Co60	<0.1%
	Ni-58	Ni58(n,g)Ni59(n,p)Co59(n,g)Co60m(IT)Co60	<0.1%
	N/A	Remainder	<0.01%
Cs-137	Xe-136	Xe136(n,g)Xe137(b-)Cs137	100%
	N/A	Remainder	<0.01%
Eu-152	Sm-149	Sm149(n,g)Sm150(n,g)Sm151(b-) Eu151(n,g)Eu152	64%
	Sm-150	Sm150(n,g)Sm151(b-)Eu151(n,g)Eu152	34%
	Nd-150	Nd150(n,g)Nd151(b-)Pm151(b-)Sm151(b-) Eu151(n,g)Eu152	1%
	Nd-148	Nd148(n,g)Nd149(b-)Pm149(b-) Sm149(n,g)Sm150(n,g)Sm151(b-) Eu151(n,g)Eu152	0.5%
	Sm-148	Sm148(n,g)Sm149(n,g)Sm150(n,g)Sm151(b-) Eu151(n,g)Eu152	0.5%
	N/A	Remainder	<0.01%
Eu-154	Sm-152	Sm152(n,g)Sm153(b-)Eu153(n,g)Eu154	48.5%
	Eu-153	Eu153(n,g)Eu154	27.5%
	Eu-151	Eu151(n,g)Eu152(n,g)Eu153(n,g)Eu154	16%
	Sm-149	Sm149(n,g)Sm150(n,g)Sm151(n,g)Sm152(n,g) Sm153(b-) Eu153(n,g)Eu154	4%
	Eu-151	Eu151(n,g)Eu152m(b-) Gd152(n,g)Gd153(b+)Eu153(n,g)Eu154	3%
	Eu-151	Eu151(n,g)Eu152m(b+)Sm152(n,g)Sm153(b-) Eu153(n,g)Eu154	1%
	Sm-150	Sm150(n,g)Sm151(n,g)Sm152(n,g)Sm153(b-) Eu153(n,g)Eu154	1%
	Eu-151	Eu151(n,g)Eu152(b+)Sm152(n,g)Sm153(b-) Eu153(n,g)Eu154	<0.5%
	Eu-151	Eu151(n,g)Eu152(b-) Gd152(n,g)Gd153(b+)Eu153(n,g)Eu154	<0.5%
	Sm-149	Sm149(n,g)Sm150(n,g)Sm151(b-) Eu151(n,g)Eu152(n,g)Eu153(n,g)Eu154	<0.5%
Eu-155	Sm-152	Sm152(n,g)Sm153(b-) Eu153(n,g)Eu154(n,g)Eu155	41.5%

	Eu-153	Eu153(n,g)Eu154(n,g)Eu155	26.5%
	Eu-151	Eu151(n,g)Eu152(n,g)Eu153(n,g) Eu154(n,g)Eu155	15.5%
	Sm-154	Sm154(n,g)Sm155(b-)Eu155	9%
	Eu-151	Eu151(n,g)Eu152m(b-)Gd152(n,g) Gd153(b+)Eu153(n,g)Eu154(n,g) Eu155	2.5%
	Sm-149	Sm149(n,g)Sm150(n,g)Sm151(n,g)Sm152(n,g) Sm153(b-)Eu153(n,g)Eu154(n,g)Eu155	1.5%
	Sm-150	Sm150(n,g)Sm151(n,g)Sm152(n,g)Sm153(b-) Eu153(n,g)Eu154(n,g)Eu155	1%
	Sm-152	Sm152(n,g)Sm153(b-) Eu153(n,g)Eu154m(IT)Eu154(n,g)Eu155	0.5%
	Eu-151	Eu151(n,g)Eu152m(b+)Sm152(n,g)Sm153(b-)Eu153(n,g)Eu154(n,g)Eu155	<0.5%
	Eu-151	Eu151(n,g)Eu152(n,g)Eu153(n,g)Eu154m(IT) Eu154(n,g)Eu155	<0.5%
	Eu-151	Eu151(n,g)Eu152(b-)Gd152(n,g) Gd153(b+)Eu153(n,g)Eu154(n,g) Eu155	<0.5%
	N/A	Remainder	<0.1%

NPL Max Precursors

Centre

Radionuclide	Precursor	Pathway	Contribution
H-3	Lithium-6	Li6(n,a)H3(b-)He3(n,p)H3	86%
	Lithium-6	Li6(n,a)H3	13%
	C-12	C12(n,a)Be9(n,a)He6(b-)Li6(n,a)H3	0.5%
	C-12	C12(n,a)Be9(n,a)He6(b-)Li6(n,a)H3(b-) He3(n,p)H3	0.5%
	N/A	Remainder	<0.1%
N-14	N-14	N14(n,p)C14	55%
	C-13	C13(n,g)C14	44.5%
	N/A	Remainder	<0.1%
Chlorine-36	Cl-35	Cl35(n,g)Cl36	99%
	N/A	Remainder	1%
Cobalt-60	Co59	Co59(n,g)Co60m(IT)Co60	26.5%
	Ni-58	Ni58(n,g)Ni59(n,p)Co59(n,g)Co60m(IT)Co60	23.5%
	Co-59	Co59(n,g)Co60	21%
	Ni-58	Ni58(n,g)Ni59(n,p)Co59(n,g)Co60	19%
	Fe-58	Fe58(n,g)Fe59(b-)Co59(n,g)Co60m(IT)Co60	2.5%
	Fe-58	Fe58(n,g)Fe59(b-)Co59(n,g)Co60	2%
	Fe-56	Fe56(n,g)Fe57(n,g)Fe58(n,g)Fe59(b-) Co59(n,g)Co60m(IT)Co60	1.5%
	Fe-56	Fe56(n,g)Fe57(n,g)Fe58(n,g)Fe59(b-) Co59(n,g)Co60	1%
	Fe-57	Fe57(n,g)Fe58(n,g)Fe59(b-) Co59(n,g)Co60m(IT)Co60	1%
	Fe-57	Fe57(n,g)Fe58(n,g)Fe59(b-)Co59(n,g)Co60	1%
	Ni-58	Ni58(n,p)Co58m(n,g)Co59(n,g)Co60	~0.5%
	Ni-58	Ni58(n,p)Co58m(n,g)Co59(n,g)Co60m(IT)Co60	~0.5%
	N/A	Remainder	<0.1%
Cs-137	N/A	Note: Cs-137 is produced through ingrowth from fission products (Xe-137) as well as from direct activation, as a result, FISPACT pathway analysis tools are not a suitable method of calculating Cs-137 activity. Another point to note is that Cs-137 activity is much higher 10 years after shutdown, then at shutdown, this is because of buildup from Xe-137 decay.	N/A
Eu-152	Sm-147	Sm147(n,g)Sm148(n,g)Sm149(n,g)Sm150(n,g) Sm151(b-)Eu151(n,g)Eu152	33%
	Sm-148	Sm148(n,g)Sm149(n,g)Sm150(n,g)Sm151(b-) Eu151(n,g)Eu152	25%
	Nd-148	Nd148(n,g)Nd149(b-)Pm149(b-) Sm149(n,g)Sm150(n,g)Sm151(b-) Eu151(n,g)Eu152	11%
	Nd-150	Nd150(n,g)Nd151(b-)Pm151(b-)Sm151(b-) Eu151(n,g)Eu152	7%
	Sm-149	Sm149(n,g)Sm150(n,g)Sm151(b-) Eu151(n,g)Eu152	3%

	Sm-150	Sm150(n,g)Sm151(b-)Eu151(n,g)Eu152	3%
	Th-232	Th232(n,g)Th233(b-)Pa233(b-)U233(n,f) Nd151(b-)Pm151(b-)Sm151(b-)Eu151(n,g)Eu152	1.5%
	U-238	U238(n,g)U239(b-)Np239(b-)Pu239(n,f) Nd151(b)Pm151(b-)Sm151(b-)Eu151(n,g)Eu152	1%
	Nd-148	Nd148(n,g)Nd149(b-)Pm149(n,g) Pm150(b-) Sm150(n,g)Sm151(b-)Eu151(n,g)Eu152	0.5%
	N/A	Remainder	16%
Eu-154	Sm-147	Sm147(n,g)Sm148(n,g)Sm149(n,g) Sm150(n,g)Sm151(n,g)Sm152(n,g) Sm153(b-)Eu153(n,g)Eu154	28%
	Sm-148	Sm148(n,g)Sm149(n,g)Sm150(n,g) Sm151(n,g)Sm152(n,g)Sm153(b-) Eu153(n,g)Eu154	22%
	Nd-150	Nd150(n,g)Nd151(b-)Pm151(b-) Sm151(n,g)Sm152(n,g)Sm153(b-) Eu153(n,g)Eu154	6%
	Sm-149	Sm149(n,g)Sm150(n,g)Sm151(n,g)Sm152(n,g)Sm153(b-)Eu153(n,g)Eu154	6%
	Sm-150	Sm150(n,g)Sm151(n,g)Sm152(n,g)Sm153(b-) Eu153(n,g)Eu154	5.5%
	Th-232	Th232(n,g)Th233(b-)Pa233(b-)U233(n,f)Nd153(b-)Pm153(b-)Sm153(b-)Eu153(n,g)Eu154	1%
	U-238	U238(n,g)U239(b-)Np239(b-)Pu239(n,f)Nd153(b-) Pm153(b-)Sm153(b-)Eu153(n,g)Eu154	1%
	Sm-148	Sm148(n,g)Sm149(n,g)Sm150(n,g)Sm151(n,g) Sm152(n,g)Sm153(b-) Eu153(n,g)Eu154m(IT)Eu154	0.5%
	U-238	U238(n,g)U239(b-)Np239(b-)Pu239(n,f) Pm153(b-)Sm153(b-)Eu153(n,g)Eu154	0.5%
	Nd-150	Nd150(n,g)Nd151(b-)Pm151(b-)Sm151(n,g)Sm152(n,g)Sm153(b-) Eu153(n,g)Eu154m(IT)Eu154	0.1%
	Sm-149	Sm149(n,g)Sm150(n,g)Sm151(n,g)Sm152(n,g) Sm153(b-)Eu153(n,g)Eu154m(IT)Eu154	0.1%
	Sm-150	Sm150(n,g)Sm151(n,g)Sm152(n,g)Sm153(b-) Eu153(n,g)Eu154m(IT)Eu154	0.1%
	Th-232	Th232(n,g)Th233(b-)Pa233(b-) U233(n,f)Pm153(b-)Sm153(b-)Eu153(n,g)Eu154	0.1%
	N/A	Remainder	30%
Eu-155	Sm-154	Sm154(n,g)Sm155(b-)Eu155	44%
	Sm-148	Sm148(n,g)Sm149(n,g)Sm150(n,g)Sm151(n,g) Sm152(n,g)Sm153(b-) Eu153(n,g)Eu154(n,g)Eu155	12%
	Nd-150	Nd150(n,g)Nd151(b-)Pm151(b-) Sm151(n,g)Sm152(n,g)Sm153(b-) Eu153(n,g)Eu154(n,g)Eu155	3.5%
	Sm-149	Sm149(n,g)Sm150(n,g)Sm151(n,g)Sm152(n,g) Sm153(b-)Eu153(n,g)Eu154(n,g)Eu155	3.5%
	Sm-150	Sm150(n,g)Sm151(n,g)Sm152(n,g)Sm153(b-) Eu153(n,g)Eu154(n,g)Eu155	3%
	Sm-152	Sm152(n,g)Sm153(n,g)Sm154(n,g)Sm155(b-) Eu155	~0.5%
	U-238	U238(n,g)U239(b-)Np239(b-)Pu239(n,f) Pm155(b-)Sm155(b-)Eu155	~0.5%

	U-238	U238(n,g)U239(b-)Np239(b-)Pu239(n,f)Nd154(b-)Pm154(b-)Sm154(n,g)Sm155(b-)Eu155	0.1%
	U-238	U238(n,g)U239(b-)Np239(b-)Pu239(n,g)Pu240(n,g)Pu241(n,f)Pm155(b-)Sm155(b-)Eu155	0.1%
	N/A	Remainder	35%

Reflector

Radionuclide	Precursor	Pathway	Contribution
H-3	Lithium-6	Li6(n,a)H3(b-)He3(n,p)H3	62%
	Lithium-6	Li6(n,a)H3	38%
	N/A	Remainder	<0.1%
CARBON-14	N-14	N14(n,p)C14	57.5%
	C-13	C13(n,g)C14	42.5%
	N/A	Remainder	<0.1%
Chlorine-36	Cl-35	Cl35(n,g)Cl36	~100%
	N/A	Remainder	<0.1%
Cobalt-60	Co-59	Co59(n,g)Co60m(IT)Co60	55.5%
	Co-59	Co59(n,g)Co60	44.5%
	N/A	Remainder	<0.1%
Eu-152	Sm-149	Sm149(n,g)Sm150(n,g)Sm151(b-)Eu151(n,g)Eu152	64.5%
	Sm-150	Sm150(n,g)Sm151(b-)Eu151(n,g)Eu152	34.5%
	Eu-151	Eu151(n,g)Eu152	0.5%
	N/A	Remainder	<0.1%
Eu-154	Eu-153	Eu153(n,g)Eu154	42.5%
	Eu-151	Eu151(n,g)Eu152(n,g)Eu153(n,g)Eu154	24.5%
	Sm-152	Sm152(n,g)Sm153(b-)Eu153(n,g)Eu154	23%
	Eu-151	Eu151(n,g)Eu152m(b-)Gd152(n,g) Gd153(b+)Eu153(n,g)Eu154	4.5%
	Eu-151	Eu151(n,g)Eu152m(b+)Sm152(n,g)Sm153(b-) Eu153(n,g)Eu154	1%
	Sm-149	Sm149(n,g)Sm150(n,g)Sm151(n,g)Sm152(n,g) Sm153(b-)Eu153(n,g)Eu154	1%
	Eu-153	Eu153(n,g)Eu154m(IT)Eu154	0.5%
	Sm-150	Sm150(n,g)Sm151(n,g)Sm152(n,g)Sm153(b-) Eu153(n,g)Eu154	0.5%
	Sm-152	Sm152(n,g)Sm153(b-) Eu153(n,g)Eu154m(IT)Eu154	0.5%
	Eu-151	Eu151(n,g)Eu152(n,g)Eu153(n,g)Eu154m(IT) Eu154	0.5%
	Eu-151	Eu151(n,g)Eu152(b+)Sm152(n,g)Sm153(b-) Eu153(n,g)Eu154	0.5%
	Eu-151	Eu151(n,g)Eu152(b-)Gd152(n,g) Gd153(b+)Eu153(n,g)Eu154	0.5%
	N/A	Remainder	<0.1%
Eu-155	Eu-153	Eu153(n,g)Eu154(n,g)Eu155	42%
	Eu-151	Eu151(n,g)Eu152(n,g)Eu153(n,g)Eu154(n,g) Eu155	24.5%
	Sm-152	Sm152(n,g)Sm153(b-) Eu153(n,g)Eu154(n,g)Eu155	20.5%
	Sm-154	Sm154(n,g)Sm155(b-)Eu155	4.5%

	Eu-151	Eu151(n,g)Eu152m(b-)Gd152(n,g) Gd153(b+)Eu153(n,g)Eu154(n,g)Eu155	4%
	Eu-151	Eu151(n,g)Eu152m(b+)Sm152(n,g)Sm153(b-) Eu153(n,g)Eu154(n,g)Eu155	1%
	Sm-149	Sm149(n,g)Sm150(n,g)Sm151(n,g)Sm152(n,g) Sm153(b-)Eu153(n,g)Eu154(n,g)Eu155	1%
	Eu-153	Eu153(n,g)Eu154m(IT)Eu154(n,g)Eu155	0.5%
	Eu-151	Eu151(n,g)Eu152(n,g)Eu153(n,g)Eu154m(IT) Eu154(n,g)Eu155	0.5%
	Eu-151	Eu151(n,g)Eu152(b+)Sm152(n,g)Sm153(b-) Eu153(n,g)Eu154(n,g)Eu155	0.5%
	Eu-151	Eu151(n,g)Eu152(b-)Gd152(n,g) Gd153(b+)Eu153(n,g)Eu154(n,g)Eu155	0.5%
	Sm-150	Sm150(n,g)Sm151(n,g)Sm152(n,g)Sm153(b-) Eu153(n,g)Eu154(n,g)Eu155	0.5%
	N/A	Remainder	<0.1%

NPL Average Precursors

Centre

Radionuclide	Precursor	Pathway	Contribution
H-3	Lithium-6	Li6(n,a)H3(b-)He3(n,p)H3	85.5%
	Lithium-6	Li6(n,a)H3	13%
	C-12	C12(n,a)Be9(n,a)He6(b-)Li6(n,a)H3	1%
	C-12	C12(n,a)Be9(n,a)He6(b-)Li6(n,a)H3(b-) He3(n,p)H3	0.5%
	N/A	Remainder	<0.1%
CARBON-14	N-14	N14(n,p)C14	51%
	C-13	C13(n,g)C14	48.5%
	C-12	C12(n,g)C13(n,g)C14	0.5%
	N/A	Remainder	<0.1%
Chlorine-36	Cl-35	Cl35(n,g)Cl36	99%
	N/A	Remainder	1%
Cobalt-60	Co-59	Co59(n,g)Co60m(IT)Co60	29.5%
	Co-59	Co59(n,g)Co60	23.5%
	Ni-58	Ni58(n,g)Ni59(n,p)Co59(n,g)Co60m(IT)Co60	19.5%
	Ni-58	Ni58(n,g)Ni59(n,p)Co59(n,g)Co60	15.5%
	Fe-58	Fe58(n,g)Fe59(b-)Co59(n,g)Co60m(IT)Co60	3%
	Fe-58	Fe58(n,g)Fe59(b-)Co59(n,g)Co60	2.5%
	Fe-56	Fe56(n,g)Fe57(n,g)Fe58(n,g)Fe59(b-) Co59(n,g)Co60m(IT)Co60	2%
	Fe-56	Fe56(n,g)Fe57(n,g)Fe58(n,g)Fe59(b-) Co59(n,g)Co60	1.5%
	Fe-57	Fe57(n,g)Fe58(n,g)Fe59(b-) Co59(n,g)Co60m(IT)Co60	1%
	Fe-57	Fe57(n,g)Fe58(n,g)Fe59(b-)Co59(n,g)Co60	1%
	Ni-58	Ni58(n,p)Co58m(n,g)Co59(n,g)Co60m(IT)Co60	0.1%
	Ni-58	Ni58(n,p)Co58m(n,g)Co59(n,g)Co60	0.1%
	N/A	Remainder	<0.1%
Eu-152	Cm-147	Sm147(n,g)Sm148(n,g)Sm149(n,g)Sm150(n,g) Sm151(b-)Eu151(n,g)Eu152	33%
	Sm-148	Sm148(n,g)Sm149(n,g)Sm150(n,g)Sm151(b-) Eu151(n,g)Eu152	25%
	Nd-148	Nd148(n,g)Nd149(b-)Pm149(b-) Sm149(n,g)Sm150(n,g)Sm151(b-) Eu151(n,g)Eu152	11%
	Nd-150	Nd150(n,g)Nd151(b-)Pm151(b-)Sm151(b-) Eu151(n,g)Eu152	7%
	Sm-149	Sm149(n,g)Sm150(n,g)Sm151(b-) Eu151(n,g)Eu152	3%
	Sm-150	Sm150(n,g)Sm151(b-)Eu151(n,g)Eu152	3%
	Th-232	Th232(n,g)Th233(b-)Pa233(b-)U233(n,f) Nd151(b-)Pm151(b-)Sm151(b-)Eu151(n,g)Eu152	1.5%
	U-238	U238(n,g)U239(b-)Np239(b-)Pu239(n,f)Nd151(b-) Pm151(b-)Sm151(b-)Eu151(n,g)Eu152	1%
	Nd-148	Nd148(n,g)Nd149(b-)Pm149(n,g)Pm150(b-) Sm150(n,g)Sm151(b-)Eu151(n,g)Eu152	0.5%
	N/A	Remainder	16%

Eu-154	Sm-147	Sm147(n,g)Sm148(n,g)Sm149(n,g)Sm150(n,g) Sm151(n,g)Sm152(n,g)Sm153(b-) Eu153(n,g)Eu154	28%
	Sm-148	Sm148(n,g)Sm149(n,g)Sm150(n,g) Sm151(n,g)Sm152(n,g)Sm153(b-) Eu153(n,g)Eu154	22%
	Nd-150	Nd150(n,g)Nd151(b-)Pm151(b-) Sm151(n,g)Sm152(n,g)Sm153(b-) Eu153(n,g)Eu154	6%
	Sm-149	Sm149(n,g)Sm150(n,g)Sm151(n,g)Sm152(n,g) Sm153(b-) Eu153(n,g)Eu154	6%
	Sm-150	Sm150(n,g)Sm151(n,g)Sm152(n,g) Sm153(b-)Eu153(n,g)Eu154	5.5%
	U-238	U238(n,g)U239(b-)Np239(b-)Pu239(n,f)Nd153(b-) Pm153(b-) Sm153(b-)Eu153(n,g)Eu154	1%
	Sm-148	Sm148(n,g)Sm149(n,g)Sm150(n,g)Sm151(n,g) Sm152(n,g)Sm153(b-) Eu153(n,g)Eu154m(IT)Eu154	0.5%
	U-238	U238(n,g)U239(b-)Np239(b-)Pu239(n,f) Pm153(b-)Sm153(b-) Eu153(n,g)Eu154	0.5%
	N/A	Remainder	30%
Eu-155	Sm-154	Sm154(n,g)Sm155(b-)Eu155	44%
	Sm-148	Sm148(n,g)Sm149(n,g)Sm150(n,g)Sm151(n,g) Sm152(n,g)Sm153(b-) Eu153(n,g)Eu154(n,g)Eu155	12%
	Nd-150	Nd150(n,g)Nd151(b-)Pm151(b-) Sm151(n,g)Sm152(n,g)Sm153(b-) Eu153(n,g)Eu154(n,g)Eu155	3.5%
	Sm-149	Sm149(n,g)Sm150(n,g)Sm151(n,g)Sm152(n,g) Sm153(b-)Eu153(n,g)Eu154(n,g)Eu155	3.5%
	Sm-150	Sm150(n,g)Sm151(n,g)Sm152(n,g)Sm153(b-) Eu153(n,g)Eu154(n,g)Eu155	3%
	Sm-152	Sm152(n,g)Sm153(n,g)Sm154(n,g)Sm155(b-) Eu155	0.5%
	U-238	U238(n,g)U239(b-)Np239(b-)Pu239(n,f)Pm155(b-) Sm155(b-)Eu155	~0.5%
	U-238	U238(n,g)U239(b-)Np239(b-)Pu239(n,f)Nd154(b-) Pm154(b-)Sm154(n,g)Sm155(b-)Eu155	0.1%
	U-238	U238(n,g)U239(b-)Np239(b-) Pu239(n,g)Pu240(n,g)Pu241(n,f)Pm155(b-) Sm155(b-)Eu155	0.1%
	N/A	Remainder	35%

Reflector

Radionuclide	Precursor	Pathway	Contribution
H-3	Lithium-6	Li6(n,a)H3(b-)He3(n,p)H3	62%
	Lithium-6	Li6(n,a)H3	38%
	N/A	Remainder	<0.1%
CARBON-14	N-14	N14(n,p)C14	53.5%
	C-13	C13(n,g)C14	46.5%
	N/A	Remainder	<0.1%
Chlorine-36	Cl-35	Cl35(n,g)Cl36	~100%
	N/A	Remainder	<0.1%
Cobalt-60	Co-59	Co59(n,g)Co60m(IT)Co60	55.5%
	Co-59	Co59(n,g)Co60	44.5%
	N/A	Remainder	<0.1%
Eu-152	Sm-149	Sm149(n,g)Sm150(n,g)Sm151(b-)Eu151(n,g)Eu152	64.5%
	Sm-150	Sm150(n,g)Sm151(b-)Eu151(n,g)Eu152	34.5%
	Eu-151	Eu151(n,g)Eu152	0.5%
	N/A	Remainder	<0.1%
Eu-154	Eu-153	Eu153(n,g)Eu154	42.5%
	Eu-151	Eu151(n,g)Eu152(n,g)Eu153(n,g)Eu154	24.5%
	Sm-152	Sm152(n,g)Sm153(b-)Eu153(n,g)Eu154	23%
	Eu-151	Eu151(n,g)Eu152m(b-)Gd152(n,g) Gd153(b+)Eu153(n,g)Eu154	4.5%
	Eu-151	Eu151(n,g)Eu152m(b+)Sm152(n,g)Sm153(b-) Eu153(n,g)Eu154	1%
	Sm-149	Sm149(n,g)Sm150(n,g)Sm151(n,g)Sm152(n,g) Sm153(b-)Eu153(n,g)Eu154	1%
	Eu-153	Eu153(n,g)Eu154m(IT)Eu154	0.5%
	Sm-150	Sm150(n,g)Sm151(n,g)Sm152(n,g)Sm153(b-) Eu153(n,g)Eu154	0.5%
	Sm-152	Sm152(n,g)Sm153(b-) Eu153(n,g)Eu154m(IT)Eu154	0.5%
	Eu-151	Eu151(n,g)Eu152(n,g)Eu153(n,g)Eu154m(IT) Eu154	0.5%
	Eu-151	Eu151(n,g)Eu152(b+)Sm152(n,g)Sm153(b-) Eu153(n,g)Eu154	0.5%
	Eu-151	Eu151(n,g)Eu152(b-)Gd152(n,g) Gd153(b+)Eu153(n,g)Eu154	0.5%
	N/A	Remainder	<0.1%
Eu-155	Eu-153	Eu153(n,g)Eu154(n,g)Eu155	42%
	Eu-151	Eu151(n,g)Eu152(n,g)Eu153(n,g)Eu154(n,g) Eu155	24.5%
	Sm-152	Sm152(n,g)Sm153(b-) Eu153(n,g)Eu154(n,g)Eu155	20.5%
	Sm-154	Sm154(n,g)Sm155(b-)Eu155	4.5%
	Eu-151	Eu151(n,g)Eu152m(b-)Gd152(n,g)	4%

		Gd153(b+)Eu153(n,g)Eu154(n,g)Eu155	
	Eu-151	Eu151(n,g)Eu152m(b+)Sm152(n,g)Sm153(b-) Eu153(n,g)Eu154(n,g)Eu155	1%
	Sm-149	Sm149(n,g)Sm150(n,g)Sm151(n,g)Sm152(n,g) Sm153(b-)Eu153(n,g)Eu154(n,g)Eu155	1%
	Eu-153	Eu153(n,g)Eu154m(IT)Eu154(n,g)Eu155	0.5%
	Eu-151	Eu151(n,g)Eu152(n,g)Eu153(n,g)Eu154m(IT) Eu154(n,g)Eu155	0.5%
	Eu-151	Eu151(n,g)Eu152(b+)Sm152(n,g)Sm153(b-) Eu153(n,g)Eu154(n,g)Eu155	0.5%
	Eu-151	Eu151(n,g)Eu152(b-)Gd152(n,g) Gd153(b+)Eu153(n,g)Eu154(n,g)Eu155	0.5%
	Sm-150	Sm150(n,g)Sm151(n,g)Sm152(n,g)Sm153(b-) Eu153(n,g)Eu154(n,g)Eu155	0.5%
	N/A	Remainder	<0.1%

Sizewell A Reactor 1 Pathway analysis

Jowett Precursors

Centre

Radionuclide	Precursor	Pathway	Contribution
H-3	Lithium-6	Li6(n,a)H3(b-)He3(n,p)H3	83.5%
	Lithium-6	Li6(n,a)H3	10%
	C-12	C12(n,a)Be9(n,a)He6(b-)Li6(n,a)H3	2%
	C-12	C12(n,a)Be9(n,a)He6(b-)Li6(n,a)H3(b-) He3(n,p)H3	2%
	H-1	H1(n,g)H2(n,g)H3	1%
	N/A	Remainder	2%
C-12	N-14	N14(n,p)C14	70%
	C-13	C13(n,g)C14	30%
	O-17	O17(n,a)C14	<0.1%
	N/A	Remainder	<0.1%
Chlorine-36	Cl-35	Cl35(n,g)Cl36	95.5%
	S-34	S34(n,g)S35(b-)Cl35(n,g)Cl36	3.5%
	N/A	Remainder	1%
Cobalt-60	Co-59	Co59(n,g)Co60m(IT)Co60	39.5%
	Co-59	Co59(n,g)Co60	31.5%
	Ni-58	Ni58(n,g)Ni59(n,p)Co59(n,g)Co60m(IT)Co60	8.5%
	Ni-58	Ni58(n,g)Ni59(n,p)Co59(n,g)Co60	7%
	Fe-58	Fe58(n,g)Fe59(b-)Co59(n,g)Co60m(IT)Co60	3.5%
	Fe-58	Fe58(n,g)Fe59(b-)Co59(n,g)Co60	3%
	Fe-56	Fe56(n,g)Fe57(n,g)Fe58(n,g)Fe59(b-) Co59(n,g)Co60m(IT)Co60	2%
	Fe-56	Fe56(n,g)Fe57(n,g)Fe58(n,g)Fe59(b-) Co59(n,g)Co60	1.5%
	Fe-57	Fe57(n,g)Fe58(n,g)Fe59(b-) Co59(n,g)Co60m(IT)Co60	1.5%
	Fe-57	Fe57(n,g)Fe58(n,g)Fe59(b-)Co59(n,g)Co60	1%
	N/A	Remainder	<0.1%
Cs-137	Xe-136	Xe136(n,g)Xe137(b-)Cs137	99%
	Cs-133	Cs133(n,g)Cs134(n,g)Cs135(n,g)Cs136(n,g)Cs1 37	0.5%
	N/A	Remainder	<1%
Eu-152	Nd-148	Nd148(n,g)Nd149(b-)Pm149(b-) Sm149(n,g)Sm150(n,g)Sm151(b-) Eu151(n,g)Eu152	24%
	Sm-147	Sm147(n,g)Sm148(n,g)Sm149(n,g)Sm150(n,g) Sm151(b-)Eu151(n,g)Eu152	22%
	Sm-148	Sm148(n,g)Sm149(n,g)Sm150(n,g)Sm151(b-) Eu151(n,g)Eu152	16.5%
	Nd-150	Nd150(n,g)Nd151(b-)Pm151(b-)Sm151(b-) Eu151(n,g)Eu152	14.5%
	Sm-149	Sm149(n,g)Sm150(n,g)Sm151(b-)	3%

		Eu151(n,g)Eu152	
	Sm-150	Sm150(n,g)Sm151(b-)Eu151(n,g)Eu152	2.5%
	Nd-148	Nd148(n,g)Nd149(b-)Pm149(n,g)Pm150(b-) Sm150(n,g)Sm151(b-)Eu151(n,g)Eu152	0.5%
	N/A	Remainder	~15%
Eu-154	Sm-147	Sm147(n,g)Sm148(n,g)Sm149(n,g)Sm150(n,g) Sm151(n,g)Sm152(n,g)Sm153(b-) Eu153(n,g)Eu154	18.5%
	Sm-148	Sm148(n,g)Sm149(n,g)Sm150(n,g)Sm151(n,g) Sm152(n,g)Sm153(b-)Eu153(n,g)Eu154	15%
	Nd-150	Nd150(n,g)Nd151(b-)Pm151(b-) Sm151(n,g)Sm152(n,g)Sm153(b-) Eu153(n,g)Eu154	13%
	Sm-149	Sm149(n,g)Sm150(n,g)Sm151(n,g)Sm152(n,g) Sm153(b-)Eu153(n,g)Eu154	6.5%
	Sm-150	Sm150(n,g)Sm151(n,g)Sm152(n,g)Sm153(b-) Eu153(n,g)Eu154	5.5%
	Sm-148	Sm148(n,g)Sm149(n,g)Sm150(n,g)Sm151(n,g) Sm152(n,g)Sm153(b-) Eu153(n,g)Eu154m(IT)Eu154	0.5%
	Nd-150	Nd150(n,g)Nd151(b-)Pm151(b-) Sm151(n,g)Sm152(n,g)Sm153(b-) Eu153(n,g)Eu154m(IT)Eu154	0.5%
	Sm-149	Sm149(n,g)Sm150(n,g)Sm151(n,g)Sm152(n,g) Sm153(b-)Eu153(n,g)Eu154m(IT)Eu154	0.1%
	Sm-150	Sm150(n,g)Sm151(n,g)Sm152(n,g)Sm153(b-) Eu153(n,g)Eu154m(IT)Eu154	0.1%
	N/A	Remainder	<40%
Eu-155	Sm-154	Sm154(n,g)Sm155(b-)Eu155	36%
	Sm-148	Sm148(n,g)Sm149(n,g)Sm150(n,g)Sm151(n,g) Sm152(n,g)Sm153(b-) Eu153(n,g)Eu154(n,g)Eu155	9.5%
	Nd-150	Nd150(n,g)Nd151(b-)Pm151(b-) Sm151(n,g)Sm152(n,g)Sm153(b-) Eu153(n,g)Eu154(n,g)Eu155	8.5%
	Sm-149	Sm149(n,g)Sm150(n,g)Sm151(n,g)Sm152(n,g) Sm153(b-)Eu153(n,g)Eu154(n,g)Eu155	4%
	Sm-150	Sm150(n,g)Sm151(n,g)Sm152(n,g)Sm153(b-) Eu153(n,g)Eu154(n,g)Eu155	3.5%
	N/A	Remainder	<40%

Reflector

Radionuclide	Precursor	Pathway	Contribution
H-3	Lithium-6	Li6(n,a)H3(b-)He3(n,p)H3	60.5%
	Lithium-6	Li6(n,a)H3	39.5%
	N/A	Remainder	<0.1%
CARBON-14	N-14	N14(n,p)C14	72%
	C-13	C13(n,g)C14	28%
	O-17	O17(n,a)C14	<0.1%
	N/A	Remainder	<0.1%
Chlorine-36	Cl-35	Cl35(n,g)Cl36	~100%
	S-34	S34(n,g)S35(b-)Cl35(n,g)Cl36	<0.1%
	N/A	Remainder	<0.1%
Cobalt-60	Co-59	Co59(n,g)Co60m(IT)Co60	55.5%
	Co-59	Co59(n,g)Co60	44.5%
	Fe-58	Fe58(n,g)Fe59(b-)Co59(n,g)Co60m(IT)Co60	<0.1%
	Fe-58	Fe58(n,g)Fe59(b-)Co59(n,g)Co60	<0.1%
	Ni-58	Ni58(n,g)Ni59(n,p)Co59(n,g)Co60m(IT)Co60	<0.1%
	Ni-58	Ni58(n,g)Ni59(n,p)Co59(n,g)Co60	<0.1%
	N/A	Remainder	<0.1%
Cs-137	Xe-136	Xe136(n,g)Xe137(b-)Cs137	~100%
	N/A	Remainder	<0.1%
Eu-152	Sm-149	Sm149(n,g)Sm150(n,g)Sm151(b-) Eu151(n,g)Eu152	62.5%
	Sm-150	Sm150(n,g)Sm151(b-)Eu151(n,g)Eu152	33.5%
	Eu-151	Eu151(n,g)Eu152	2.5%
	Nd-150	Nd150(n,g)Nd151(b-)Pm151(b-)Sm151(b-) Eu151(n,g)Eu152	1%
	Nd-148	Nd148(n,g)Nd149(b-)Pm149(b-) Sm149(n,g)Sm150(n,g)Sm151(b-) Eu151(n,g)Eu152	0.5%
	Sm-148	Sm148(n,g)Sm149(n,g)Sm150(n,g)Sm151(b-) Eu151(n,g)Eu152	<0.5%
	N/A	Remainder	<0.1%
Eu-154	Sm-152	Sm152(n,g)Sm153(b-)Eu153(n,g)Eu154	42.5%
	Eu-153	Eu153(n,g)Eu154	31.5%
	Eu-151	Eu151(n,g)Eu152(n,g)Eu153(n,g)Eu154	17.5%
	Eu-151	Eu151(n,g)Eu152m(b-) Gd152(n,g)Gd153(b+)Eu153(n,g)Eu154	3.5%
	Sm-149	Sm149(n,g)Sm150(n,g)Sm151(n,g)Sm152(n,g)Sm153(b-)Eu153(n,g)Eu154	1.5%
	Sm-150	Sm150(n,g)Sm151(n,g)Sm152(n,g)Sm153(b-) Eu153(n,g)Eu154	0.5%
	Sm-152	Sm152(n,g)Sm153(b-) Eu153(n,g)Eu154m(IT)Eu154	0.5%
	Eu-151	Eu151(n,g)Eu152m(b+)Sm152(n,g)Sm153(b-) Eu153(n,g)Eu154	0.5%
	Eu-153	Eu153(n,g)Eu154m(IT)Eu154	0.5%
	Eu-151	Eu151(n,g)Eu152(b+)Sm152(n,g)Sm153(b-)	~0.5%

		Eu153(n,g)Eu154	
	Eu-151	Eu151(n,g)Eu152(n,g)Eu153(n,g)Eu154m(IT) Eu154	~0.5%
	Eu-151	Eu151(n,g)Eu152(b-) Gd152(n,g)Gd153(b+)Eu153(n,g)Eu154	~0.5%
	Sm-149	Sm149(n,g)Sm150(n,g)Sm151(b-) Eu151(n,g)Eu152(n,g)Eu153(n,g)Eu154	<0.5%
	N/A	Remainder	<0.1%
Eu-155	Sm-152	Sm152(n,g)Sm153(b-) Eu153(n,g)Eu154(n,g)Eu155	35.5%
	Eu-153	Eu153(n,g)Eu154(n,g)Eu155	30%
	Eu-151	Eu151(n,g)Eu152(n,g)Eu153(n,g)Eu154(n,g) Eu155	16.5%
	Sm-154	Sm154(n,g)Sm155(b-)Eu155	11%
	Sm-149	Sm149(n,g)Sm150(n,g)Sm151(n,g)Sm152(n,g) Sm153(b-)Eu153(n,g)Eu154(n,g)Eu155	3%
	Sm-152	Sm152(n,g)Sm153(b-) Eu153(n,g)Eu154m(IT)Eu154(n,g)Eu155	1%
	Eu-151	Eu151(n,g)Eu152m(b+)Sm152(n,g)Sm153(b-) Eu153(n,g)Eu154(n,g)Eu155	0.5%
	Sm-150	Sm150(n,g)Sm151(n,g)Sm152(n,g)Sm153(b-) Eu153(n,g)Eu154(n,g)Eu155	0.5%
	Eu-153	Eu153(n,g)Eu154m(IT)Eu154(n,g)Eu155	0.5%
	Eu-151	Eu151(n,g)Eu152(b+)Sm152(n,g)Sm153(b-) Eu153(n,g)Eu154(n,g)Eu155	~0.5%
	Eu-151	Eu151(n,g)Eu152(n,g)Eu153(n,g)Eu154m(IT) Eu154(n,g)Eu155	~0.5%
	Eu-151	Eu151(n,g)Eu152(b-) Gd152(n,g)Gd153(b+)Eu153(n,g) Eu154(n,g)Eu155	~0.5%
	N/A	Remainder	<0.1%

NPL Maximum Precursors

Centre

Radionuclide	Precursor	Pathway	Contribution
H-3	Lithium-6	Li6(n,a)H3(b-)He3(n,p)H3	85.5%
	Lithium-6	Li6(n,a)H3	10%
	C-12	C12(n,a)Be9(n,a)He6(b-)Li6(n,a)H3	2%
	C-12	C12(n,a)Be9(n,a)He6(b-)Li6(n,a)H3(b-) He3(n,p)H3	2%
	N/A	Remainder	<0.1%
CARBON-14	N-14	N14(n,p)C14	55.5%
	C-13	C13(n,g)C14	44%
	N/A	Remainder	<0.1%
Chlorine-36	Cl-35	Cl35(n,g)Cl36	99%
	N/A	Remainder	<1%
Cobalt-60	Co-59	Co59(n,g)Co60m(IT)Co60	41.5%
	Co-59	Co59(n,g)Co60	33%
	Ni-58	Ni58(n,g)Ni59(n,p)Co59(n,g)Co60m(IT)Co60	11%
	Ni-58	Ni58(n,g)Ni59(n,p)Co59(n,g)Co60	9%
	Fe-58	Fe58(n,g)Fe59(b-)Co59(n,g)Co60m(IT)Co60	1.5%
	Fe-58	Fe58(n,g)Fe59(b-)Co59(n,g)Co60	1%
	Fe-56	Fe56(n,g)Fe57(n,g)Fe58(n,g)Fe59(b-) Co59(n,g)Co60m(IT)Co60	1%
	Fe-56	Fe56(n,g)Fe57(n,g)Fe58(n,g)Fe59(b-) Co59(n,g)Co60	0.5%
	Fe-57	Fe57(n,g)Fe58(n,g)Fe59(b-) Co59(n,g)Co60m(IT)Co60	0.5%
	Fe-57	Fe57(n,g)Fe58(n,g)Fe59(b-)Co59(n,g)Co60	0.5%
	N/A	Remainder	<0.1%
Eu-152	Sm-147	Sm147(n,g)Sm148(n,g)Sm149(n,g)Sm150(n,g) Sm151(b-)Eu151(n,g)Eu152	32%
	Sm-148	Sm148(n,g)Sm149(n,g)Sm150(n,g)Sm151(b-) Eu151(n,g)Eu152	24.5%
	Nd-148	Nd148(n,g)Nd149(b-)Pm149(b-)Sm149(n,g)Sm150(n,g)Sm151(b-) Eu151(n,g)Eu152	10.5%
	Nd-150	Nd150(n,g)Nd151(b-)Pm151(b-)Sm151(b-) Eu151(n,g)Eu152	6.5%
	Sm-149	Sm149(n,g)Sm150(n,g)Sm151(b-) Eu151(n,g)Eu152	4.5%
	Sm-150	Sm150(n,g)Sm151(b-)Eu151(n,g)Eu152	4%
	Th-232	Th232(n,g)Th233(b-)Pa233(b-)U233(n,f)Nd151(b-) Pm151(b-)Sm151(b-)Eu151(n,g)Eu152	1.5%
	U-238	U238(n,g)U239(b-)Np239(b-)Pu239(n,f)Nd151(b-) Pm151(b-)Sm151(b-)Eu151(n,g)Eu152	1%
	Nd-148	Nd148(n,g)Nd149(b-)Pm149(n,g)Pm150(b-) Sm150(n,g)Sm151(b-)Eu151(n,g)Eu152	0.5%
	N/A	Remainder	15%
Eu-154	Sm-147	Sm147(n,g)Sm148(n,g)Sm149(n,g)Sm150(n,g) Sm151(n,g)Sm152(n,g)Sm153(b-)	25.5%

		Eu153(n,g)Eu154	
	Sm-148	Sm148(n,g)Sm149(n,g)Sm150(n,g)Sm151(n,g) Sm152(n,g)Sm153(b-)Eu153(n,g)Eu154	20.5%
	Sm-149	Sm149(n,g)Sm150(n,g)Sm151(n,g)Sm152(n,g) Sm153(b-)Eu153(n,g)Eu154	8.5%
	Sm-150	Sm150(n,g)Sm151(n,g)Sm152(n,g)Sm153(b-) Eu153(n,g)Eu154	7.5%
	Nd-150	Nd150(n,g)Nd151(b-)Pm151(b-) Sm151(n,g)Sm152(n,g)Sm153(b-) Eu153(n,g)Eu154	5.5%
	Th-232	Th232(n,g)Th233(b-)Pa233(b-)U233(n,f) Nd153(b-)Pm153(b-)Sm153(b-)Eu153(n,g)Eu154	1%
	U-238	U238(n,g)U239(b-)Np239(b-)Pu239(n,f)Nd153(b-) Pm153(b-)Sm153(b-)Eu153(n,g)Eu154	1%
	Sm-148	Sm148(n,g)Sm149(n,g)Sm150(n,g)Sm151(n,g) Sm152(n,g)Sm153(b-) Eu153(n,g)Eu154m(IT)Eu154	0.5%
	U-238	U238(n,g)U239(b-)Np239(b-)Pu239(n,f)Pm153(b-)Sm153(b-)Eu153(n,g)Eu154	0.5%
	Sm-149	Sm149(n,g)Sm150(n,g)Sm151(n,g)Sm152(n,g) Sm153(b-)Eu153(n,g)Eu154m(IT)Eu154	0.5%
	Sm-150	Sm150(n,g)Sm151(n,g)Sm152(n,g)Sm153(b-) Eu153(n,g)Eu154m(IT)Eu154	0.5%
	Nd-150	Nd150(n,g)Nd151(b-)Pm151(b-) Sm151(n,g)Sm152(n,g)Sm153(b-) Eu153(n,g)Eu154m(IT)Eu154	0.5%
	N/A	Remainder	29%
Eu-155	Sm-154	Sm154(n,g)Sm155(b-)Eu155	43%
	Sm-148	Sm148(n,g)Sm149(n,g)Sm150(n,g)Sm151(n,g) Sm152(n,g)Sm153(b-) Eu153(n,g)Eu154(n,g)Eu155	11.5%
	Sm-149	Sm149(n,g)Sm150(n,g)Sm151(n,g)Sm152(n,g) Sm153(b-)Eu153(n,g)Eu154(n,g)Eu155	5%
	Sm-150	Sm150(n,g)Sm151(n,g)Sm152(n,g)Sm153(b-) Eu153(n,g)Eu154(n,g)Eu155	5%
	Sm-152	Sm152(n,g)Sm153(n,g)Sm154(n,g)Sm155(b-) Eu155	0.5%
	U-238	U238(n,g)U239(b-)Np239(b-)Pu239(n,f) Pm155(b-)Sm155(b-)Eu155	~0.5%
	N/A	Remainder	35%

Reflector

Radionuclide	Precursor	Pathway	Contribution
H-3	Lithium-6	Li6(n,a)H3(b-)He3(n,p)H3	60.5%
	Lithium-6	Li6(n,a)H3	39.5%
	N/A	Remainder	<0.1%
CARBON-14	N-14	N14(n,p)C14	58%
	C-13	C13(n,g)C14	42%
	N/A	Remainder	<0.1%
Chlorine-36	Cl-35	Cl35(n,g)Cl36	~100%
	N/A	Remainder	<0.1%
Cobalt-60	Co-59	Co59(n,g)Co60m(IT)Co60	55.5%
	Co-59	Co59(n,g)Co60	44.5%
	N/A	Remainder	<0.1%
Eu-152	Sm-149	Sm149(n,g)Sm150(n,g)Sm151(b-) Eu151(n,g)Eu152	60%
	Sm-150	Sm150(n,g)Sm151(b-)Eu151(n,g)Eu152	32%
	Eu-151	Eu151(n,g)Eu152	7.5%
	Nd-150	Nd150(n,g)Nd151(b-)Pm151(b-)Sm151(b-)Eu151(n,g)Eu152	0.5%
	Sm-148	Sm148(n,g)Sm149(n,g)Sm150(n,g)Sm151(b-)Eu151(n,g)Eu152	~0.1%
	N/A	Remainder	<0.1%
Eu-154	Eu-153	Eu153(n,g)Eu154	46%
	Eu-151	Eu151(n,g)Eu152(n,g)Eu153(n,g)Eu154	26%
	Sm-152	Sm152(n,g)Sm153(b-)Eu153(n,g)Eu154	19%
	Eu-151	Eu151(n,g)Eu152m(b-)Gd152(n,g) Gd153(b+)Eu153(n,g)Eu154	5%
	Eu-151	Eu151(n,g)Eu152m(b+)Sm152(n,g)Sm153(b-) Eu153(n,g)Eu154	1%
	Eu-153	Eu153(n,g)Eu154m(IT)Eu154	0.5%
	Sm-149	Sm149(n,g)Sm150(n,g)Sm151(n,g)Sm152(n,g) Sm153(b-)Eu153(n,g)Eu154	0.5%
	Eu-151	Eu151(n,g)Eu152(b+)Sm152(n,g)Sm153(b-) Eu153(n,g)Eu154	0.5%
	Eu-151	Eu151(n,g)Eu152(n,g)Eu153(n,g)Eu154m(IT) Eu154	0.5%
	Eu-151	Eu151(n,g)Eu152(b-)Gd152(n,g) Gd153(b+)Eu153(n,g)Eu154	0.5%
	Sm-150	Sm150(n,g)Sm151(n,g)Sm152(n,g)Sm153(b-) Eu153(n,g)Eu154	0.5%
	Sm-152	Sm152(n,g)Sm153(b-) Eu153(n,g)Eu154m(IT)Eu154	0.5%
	N/A	Remainder	<0.1%
Eu-155	Eu-153	Eu153(n,g)Eu154(n,g)Eu155	45%
	Eu-151	Eu151(n,g)Eu152(n,g)Eu153(n,g)Eu154(n,g) Eu155	25%
	Sm-152	Sm152(n,g)Sm153(b-) Eu153(n,g)Eu154(n,g)Eu155	16.5%
	Sm-154	Sm154(n,g)Sm155(b-)Eu155	5%

	Sm-151	Eu151(n,g)Eu152m(b-) Gd152(n,g)Gd153(b+)Eu153(n,g) Eu154(n,g)Eu155	4.5%
	Eu-151	Eu151(n,g)Eu152m(b+)Sm152(n,g)Sm153(b-) Eu153(n,g)Eu154(n,g)Eu155	1%
	Eu-153	Eu153(n,g)Eu154m(IT)Eu154(n,g)Eu155	1%
	Sm-149	Sm149(n,g)Sm150(n,g)Sm151(n,g)Sm152(n,g) Sm153(b-)Eu153(n,g)Eu154(n,g)Eu155	0.5%
	Eu-151	Eu151(n,g)Eu152(b+)Sm152(n,g)Sm153(b-) Eu153(n,g)Eu154(n,g)Eu155	0.5%
	Eu-151	Eu151(n,g)Eu152(n,g)Eu153(n,g)Eu154m(IT) Eu154(n,g)Eu155	0.5%
	Eu-151	Eu151(n,g)Eu152(b-)Gd152(n,g) Gd153(b+)Eu153(n,g)Eu154(n,g)Eu155	0.5%
	Sm-152	Sm152(n,g)Sm153(b-) Eu153(n,g)Eu154m(IT)Eu154(n,g)Eu155	0.5%
	Sm-150	Sm150(n,g)Sm151(n,g)Sm152(n,g)Sm153(b-) Eu153(n,g)Eu154(n,g)Eu155	0.5%
	N/A	Remainder	<0.1%

NPL Average Precursors

Centre

Radionuclide	Precursor	Pathway	Contribution
H-3	Lithium-6	Li6(n,a)H3(b-)He3(n,p)H3	85.5%
	Lithium-6	Li6(n,a)H3	10%
	C-12	C12(n,a)Be9(n,a)He6(b-)Li6(n,a)H3	2%
	C-12	C12(n,a)Be9(n,a)He6(b-)Li6(n,a)H3(b-) He3(n,p)H3	2%
	N/A	Remainder	<1%
CARBON-14	N-14	N14(n,p)C14	55.5%
	C-13	C13(n,g)C14	44%
	N/A	Remainder	<1%
Chlorine-36	Cl-35	Cl35(n,g)Cl36	99%
	N/A	Remainder	<1%
Cobalt-60	Co-59	Co59(n,g)Co60m(IT)Co60	41.5%
	Co-59	Co59(n,g)Co60	33%
	Ni-58	Ni58(n,g)Ni59(n,p)Co59(n,g)Co60m(IT)Co60	11%
	Ni-58	Ni58(n,g)Ni59(n,p)Co59(n,g)Co60	9%
	Fe-58	Fe58(n,g)Fe59(b-)Co59(n,g)Co60m(IT)Co60	1.5%
	Fe-58	Fe58(n,g)Fe59(b-)Co59(n,g)Co60	1%
	Fe-56	Fe56(n,g)Fe57(n,g)Fe58(n,g)Fe59(b-) Co59(n,g)Co60m(IT)Co60	1%
	Fe-56	Fe56(n,g)Fe57(n,g)Fe58(n,g)Fe59(b-) Co59(n,g)Co60	0.5%
	Fe-57	Fe57(n,g)Fe58(n,g)Fe59(b-) Co59(n,g)Co60m(IT)Co60	0.5%
	Fe-57	Fe57(n,g)Fe58(n,g)Fe59(b-)Co59(n,g)Co60	0.5%
	N/A	Remainder	<0.1%
Eu-152	Sm-147	Sm147(n,g)Sm148(n,g)Sm149(n,g)Sm150(n,g) Sm151(b-)Eu151(n,g)Eu152	32%
	Sm-148	Sm148(n,g)Sm149(n,g)Sm150(n,g)Sm151(b-) Eu151(n,g)Eu152	24.5%
	Nd-148	Nd148(n,g)Nd149(b-)Pm149(b-) Sm149(n,g)Sm150(n,g)Sm151(b-) Eu151(n,g)Eu152	10.5%
	Nd-150	Nd150(n,g)Nd151(b-)Pm151(b-)Sm151(b-) Eu151(n,g)Eu152	6.5%
	Sm-149	Sm149(n,g)Sm150(n,g)Sm151(b-) Eu151(n,g)Eu152	4.5%
	Sm-150	Sm150(n,g)Sm151(b-)Eu151(n,g)Eu152	4%
	Th-232	Th232(n,g)Th233(b-)Pa233(b-)U233(n,f) Nd151(b-)Pm151(b-)Sm151(b-)Eu151(n,g)Eu152	1.5%
	U-238	U238(n,g)U239(b-)Np239(b-)Pu239(n,f)Nd151(b-) Pm151(b-)Sm151(b-)Eu151(n,g)Eu152	1%
	Nd-148	Nd148(n,g)Nd149(b-)Pm149(n,g)Pm150(b-) Sm150(n,g)Sm151(b-)Eu151(n,g)Eu152	0.5%
	N/A	Remainder	15%
Eu-154	Sm-147	Sm147(n,g)Sm148(n,g)Sm149(n,g)Sm150(n,g) Sm151(n,g)Sm152(n,g)Sm153(b-)	25.5%

		Eu153(n,g)Eu154	
	Sm-148	Sm148(n,g)Sm149(n,g)Sm150(n,g)Sm151(n,g) Sm152(n,g)Sm153(b-)Eu153(n,g)Eu154	20.5%
	Sm-149	Sm149(n,g)Sm150(n,g)Sm151(n,g)Sm152(n,g) Sm153(b-)Eu153(n,g)Eu154	8.5%
	Sm-150	Sm150(n,g)Sm151(n,g)Sm152(n,g)Sm153(b-) Eu153(n,g)Eu154	7.5%
	Nd-150	Nd150(n,g)Nd151(b-)Pm151(b-) Sm151(n,g)Sm152(n,g)Sm153(b-) Eu153(n,g)Eu154	5.5%
	Th-232	Th232(n,g)Th233(b-)Pa233(b-)U233(n,f) Nd153(b-)Pm153(b-)Sm153(b-)Eu153(n,g)Eu154	1%
	U-238	U238(n,g)U239(b-)Np239(b-)Pu239(n,f)Nd153(b-) Pm153(b-)Sm153(b-)Eu153(n,g)Eu154	1%
	Sm-148	Sm148(n,g)Sm149(n,g)Sm150(n,g)Sm151(n,g) Sm152(n,g)Sm153(b-) Eu153(n,g)Eu154m(IT)Eu154	0.5%
	U-238	U238(n,g)U239(b-)Np239(b-)Pu239(n,f)Pm153(b-)Sm153(b-)Eu153(n,g)Eu154	0.5%
	Sm-149	Sm149(n,g)Sm150(n,g)Sm151(n,g)Sm152(n,g) Sm153(b-)Eu153(n,g)Eu154m(IT)Eu154	0.5%
	Sm-150	Sm150(n,g)Sm151(n,g)Sm152(n,g)Sm153(b-) Eu153(n,g)Eu154m(IT)Eu154	0.5%
	Nd-150	Nd150(n,g)Nd151(b-)Pm151(b-) Sm151(n,g)Sm152(n,g)Sm153(b-) Eu153(n,g)Eu154m(IT)Eu154	0.5%
	N/A	Remainder	29%
Eu-155	Sm-154	Sm154(n,g)Sm155(b-)Eu155	43%
	Sm-148	Sm148(n,g)Sm149(n,g)Sm150(n,g)Sm151(n,g) Sm152(n,g)Sm153(b-) Eu153(n,g)Eu154(n,g)Eu155	11.5%
	Sm-149	Sm149(n,g)Sm150(n,g)Sm151(n,g)Sm152(n,g) Sm153(b-)Eu153(n,g)Eu154(n,g)Eu155	5%
	Sm-150	Sm150(n,g)Sm151(n,g)Sm152(n,g)Sm153(b-) Eu153(n,g)Eu154(n,g)Eu155	5%
	Sm-152	Sm152(n,g)Sm153(n,g)Sm154(n,g)Sm155(b-) Eu155	0.5%
	U-238	U238(n,g)U239(b-)Np239(b-)Pu239(n,f) Pm155(b-)Sm155(b-)Eu155	~0.5%
	N/A	Remainder	35%

Reflector

Radionuclide	Precursor	Pathway	Contribution
H-3	Lithium-6	Li6(n,a)H3(b-)He3(n,p)H3	60.5%
	Lithium-6	Li6(n,a)H3	39.5%
	N/A	Remainder	<0.1%
CARBON-14	N-14	N14(n,p)C14	51%
	C-13	C13(n,g)C14	49%
	N/A	Remainder	<0.1%
Chlorine-36	Cl-35	Cl35(n,g)Cl36	~100%
	N/A	Remainder	<0.1%
Cobalt-60	Co-59	Co59(n,g)Co60m(IT)Co60	55.5%
	Co-59	Co59(n,g)Co60	44.5%
	N/A	Remainder	<0.1%
Eu-152	Sm-149	Sm149(n,g)Sm150(n,g)Sm151(b-) Eu151(n,g)Eu152	60%
	Sm-150	Sm150(n,g)Sm151(b-)Eu151(n,g)Eu152	32%
	Eu-151	Eu151(n,g)Eu152	7.5%
	Nd-150	Nd150(n,g)Nd151(b-)Pm151(b-)Sm151(b-)Eu151(n,g)Eu152	0.5%
	Sm-148	Sm148(n,g)Sm149(n,g)Sm150(n,g)Sm151(b-)Eu151(n,g)Eu152	~0.1%
	N/A	Remainder	<0.1%
Eu-154	Eu-153	Eu153(n,g)Eu154	46%
	Eu-151	Eu151(n,g)Eu152(n,g)Eu153(n,g)Eu154	26%
	Sm-152	Sm152(n,g)Sm153(b-)Eu153(n,g)Eu154	19%
	Eu-151	Eu151(n,g)Eu152m(b-)Gd152(n,g) Gd153(b+)Eu153(n,g)Eu154	5%
	Eu-151	Eu151(n,g)Eu152m(b+)Sm152(n,g)Sm153(b-) Eu153(n,g)Eu154	1%
	Eu-153	Eu153(n,g)Eu154m(IT)Eu154	0.5%
	Sm-149	Sm149(n,g)Sm150(n,g)Sm151(n,g)Sm152(n,g) Sm153(b-)Eu153(n,g)Eu154	0.5%
	Eu-151	Eu151(n,g)Eu152(b+)Sm152(n,g)Sm153(b-) Eu153(n,g)Eu154	0.5%
	Eu-151	Eu151(n,g)Eu152(n,g)Eu153(n,g)Eu154m(IT) Eu154	0.5%
	Eu-151	Eu151(n,g)Eu152(b-)Gd152(n,g) Gd153(b+)Eu153(n,g)Eu154	0.5%
	Sm-150	Sm150(n,g)Sm151(n,g)Sm152(n,g)Sm153(b-) Eu153(n,g)Eu154	0.5%
	Sm-152	Sm152(n,g)Sm153(b-) Eu153(n,g)Eu154m(IT)Eu154	0.5%
	N/A	Remainder	<0.1%
Eu-155	Eu-153	Eu153(n,g)Eu154(n,g)Eu155	45%
	Eu-151	Eu151(n,g)Eu152(n,g)Eu153(n,g)Eu154(n,g) Eu155	25%
	Sm-152	Sm152(n,g)Sm153(b-) Eu153(n,g)Eu154(n,g)Eu155	16.5%

	Sm-154	Sm154(n,g)Sm155(b-)Eu155	5%
	Sm-151	Eu151(n,g)Eu152m(b-) Gd152(n,g)Gd153(b+)Eu153(n,g) Eu154(n,g)Eu155	4.5%
	Eu-151	Eu151(n,g)Eu152m(b+)Sm152(n,g)Sm153(b-) Eu153(n,g)Eu154(n,g)Eu155	1%
	Eu-153	Eu153(n,g)Eu154m(IT)Eu154(n,g)Eu155	1%
	Sm-149	Sm149(n,g)Sm150(n,g)Sm151(n,g)Sm152(n,g) Sm153(b-)Eu153(n,g)Eu154(n,g)Eu155	0.5%
	Eu-151	Eu151(n,g)Eu152(b+)Sm152(n,g)Sm153(b-) Eu153(n,g)Eu154(n,g)Eu155	0.5%
	Eu-151	Eu151(n,g)Eu152(n,g)Eu153(n,g)Eu154m(IT) Eu154(n,g)Eu155	0.5%
	Eu-151	Eu151(n,g)Eu152(b-)Gd152(n,g) Gd153(b+)Eu153(n,g)Eu154(n,g)Eu155	0.5%
	Sm-152	Sm152(n,g)Sm153(b-) Eu153(n,g)Eu154m(IT)Eu154(n,g)Eu155	0.5%
	Sm-150	Sm150(n,g)Sm151(n,g)Sm152(n,g)Sm153(b-) Eu153(n,g)Eu154(n,g)Eu155	0.5%
	N/A	Remainder	<0.1%

Summary

Jowett Precursors

Radionuclide	Parent nuclide	Wylfa		Sizewell	
		Centre	Reflector	Centre	Reflector
H-3	*Lithium-6*	92.5%	~100%	93.5%	~100%
	C-12	4.5%		4%	
	H-1	1%		1%	
CARBON-14	*N-14*	70%	72%	70%	72%
	C-13	29.5%	28%	30%	28%
	O-17	0.1%	0.1%	0.1%	<0.1%
Chlorine-36	*Cl-35*	95%	99.5%	95.5%	~100%
	S-34	4%	0.5%	3.5%	<0.1%
Cobalt-60	*Co-59*	69%	~100%	71%	~100%
	Ni-58	16.5%	<0.1%	13.5%	<0.1%
	Fe-56	4.5%		3.5%	
	Fe-57	2.5%		2.5%	
	Fe-58	7%	0.1%	6.5%	<0.1%
Cs-137	*Xe-136*	98.5%	~100%	99%	~100%
	Cs-133	0.5%		0.5%	
Eu-152	*Nd-148*	24.5%	0.5%	24.5%	0.5%
	Nd-150	14.5%	34%	14.5%	1%
	Sm-147	22%		22%	
	Sm-148	16.5%	0.5%	16.5%	<0.5%
	Sm-149	2%	64%	3%	62.5%
	Sm-150	2%	34%	2.5%	33.5%
	Eu-151				2.5%
Eu-154	*Nd-150*	13.5%		13.5%	
	Sm-147	20%		18.5%	
	Sm-148	15.5%		15%	
	Sm-149	4%	4%	~6.5%	2%
	Sm-150	4%	1%	~5.5%	0.5%
	Sm-152		48.5%		43%
	Eu-151		~21%		~22%
	Eu-153		27.5%		32%
Eu-155	*Nd-150*	8.5%		8.5%	
	Sm-148	10%		9.5%	
	Sm-149	2.5%	1.5%	4%	3%
	Sm-150	2.5%	1%	3.5%	0.5%
	Sm-152		42%		36.5%
	Sm-154	36%	9%	36%	11%
	Eu-151		19%		~18%
	Eu-153		26.5%		30%

APPENDIX 12 – URANIUM IRRADIATION

Graphite samples were analysed for various precursors. One of these precursors was Uranium, which had a detection limit of 500 ng/g (0.5 ppm).

Uranium, containing fissile and fissionable elements, when irradiated will form fission products (which can generate both exotic ad mundane radionuclides and decay chains), as well as becoming activated to produce transuranic nuclides.

A FISPACT investigation was carried out to determine the impact of having Uranium in graphite. To do this, a kilo of Uranium was irradiated using the spectra and flux of neutrons for the centre of the Wylfa reactor. This was then reduced using basic linear interpolation to the LoD figure of 0.5 ppm and key nuclides investigated.

These key nuclides consisted of four groups;

1. The 18 radionuclides of particular interest after 10 years of decay
2. The 20 most abundant nuclides based on activity after 10 years of decay
3. The 20 most abundant nuclides based on dose rate after 10 years of decay
4. The trans-uranic radionuclides after 10 years of decay

Note: The Uranium in FISPACT is assumed to be of natural composition.

Nuclide	Activity (Bq/kg)	Activity (Bq/0.5ppm)	Wylfa Inventory Activity (Bq/kg)	Activity (Bq/12ppb)	NPL Average Inventory Activity (Bq/kg)
H3	2.92E+11	1.46E+05	5.33E+08	3.51E+03	1.6E+09
C14	1.27E+07	6.35	4.71E+08	1.52E-01	2.9E+08
Cl36	0	0	4.37E+05	0	2.4E+06
Na22	0	0	0	0	0
Co60	1.13E+03	5.66E-04	3.90E+07	1.36E-05	1.9E+07
Kr85	1.21E+12	6.06E+05	8.79E+07	1.45E+04	5.6E+04
Nb94	1.55E+05	7.77E-02	5.76E+05	1.86E-03	2.0E-01
Ag108m	5.03E+04	2.51E-02	3.90E+03	6.03E-04	6.1E-04
Sn121m	***1.92E+10***	***9.62E+03***	***1.44E+03***	**2.31E+02**	**3.2E+02**
I129	***1.77E+07***	***8.84***	***3.70E+01***	**2.12E-01**	**3.4E+00**
Cs134	***1.63E+12***	***8.16E+05***	***3.44E+06***	**1.96E+04**	**2.1E+08**
Ba133	1.96E+07	9.82	1.73E+06	2.36E-01	4.0E+05
Cs137	***4.64E+13***	***2.32E+07***	***7.63E+05***	**5.57E+05**	**1.4E+06**
Pm145	1.33E+03	6.65E-04	6.46E+04	1.60E-05	4.3E+04
Eu152	1.64E+07	8.22E-04	9.48E+00	1.97E-01	4.1E+00
Eu154	***5.09E+11***	***2.55E+05***	***2.35E+05***	**6.11E+03**	**1.1E+05**
Eu155	***1.78E+12***	***8.89E+05***	***1.63E+05***	**2.13E+04**	**1.1E+05**
Ho166m	5.96E+06	2.98	1.13E+04	7.15E-02	2.4E+01

Table 39: A comparison of the 18 radionuclides of interest

Table 43 shows a comparison of the activity of 18 radionuclides of particular interest between a kilogram of irradiated Uranium, 0.5 ppm of Uranium and the activity of the graphite based on Wylfa data from the same position. Note, the Wylfa inventory is based on precursors by John Jowett and does not contain any fissile materials (Uranium, Plutonium or Thorium).

Here it can be seen that in most cases a concentration of 0.5 ppm of Uranium will not have a significant effect (>1%) on the inventory. However, in the case of Caesium-137 the result would

be much higher - by two orders of magnitude. Several others are affected as well, but to a lesser effect, including I-129, Cs-134, Eu-154 and Eu-155.

Because this would provide unnecessary pessimism for these nuclides when assuming a concentration of 0.5ppm Uranium, the Jowett Uranium figure will be implemented. This value is recorded as being 12ppb. The change in concentration equates to approximately a factor of 50 decrease in Uranium concentration.

Nuclide	Activity (Bq/kg)	Activity (Bq/0.5 ppm)
Xe135	7.92E+13	3.96E+07
I 134	7.47E+13	3.73E+07
Xe133	7.46E+13	3.73E+07
I 133	7.44E+13	3.72E+07
Tc103	7.39E+13	3.70E+07
Ru103	7.38E+13	3.69E+07
Rh103m	7.30E+13	3.65E+07
Mo103	7.20E+13	3.60E+07
I 135	7.04E+13	3.52E+07
La140	6.98E+13	3.49E+07
Tc104	6.85E+13	3.43E+07
Tc102	6.71E+13	3.35E+07
Mo102	6.70E+13	3.35E+07
Tc101	6.68E+13	3.34E+07
Xe137	6.68E+13	3.34E+07
Mo101	6.67E+13	3.34E+07
Cs138	6.62E+13	3.31E+07
Ba139	6.61E+13	3.31E+07
Rh105	6.59E+13	3.29E+07
Ru105	6.59E+13	3.29E+07
Rest	4.56E+15	2.28E+09

Table 40: The 20 most abundant nuclides by activity

Nuclide	Dose Rate (Sv/hr/kg)	Dose Rate (Sv/hr/0.5 ppm)
La140	3.68E+04	1.84E-02
Cs138	3.66E+04	1.83E-02
I 134	3.55E+04	1.78E-02
La142	3.09E+04	1.55E-02
I 135	2.67E+04	1.34E-02
Tc106	2.65E+04	1.32E-02
Tc104	2.58E+04	1.29E-02
Cs140	2.07E+04	1.04E-02
I 132	1.98E+04	9.91E-03
Mo101	1.94E+04	9.71E-03
La144	1.78E+04	8.90E-03
Sr 93	1.57E+04	7.84E-03
Y 98m	1.54E+04	7.69E-03
Xe138	1.48E+04	7.38E-03
Y 96m	1.42E+04	7.10E-03
I 136	1.36E+04	6.79E-03
Y 95	1.35E+04	6.77E-03
Sr 94	1.31E+04	6.56E-03
Rb 91	1.27E+04	6.35E-03
Rb 93	1.22E+04	6.12E-03

Rest	4.93E+05	2.47E-01

Table 41: The 20 most abundant nuclides by dose rate

Table 44 and Table 45 show the 20 key nuclides by activity and dose rate as calculated by FISPACT.

Nuclide	Activity (Bq/kg)	Activity (Bq/0.5 ppm)
U232	1.22E+05	6.09E-02
U233	9.02E+01	4.51E-05
U234	4.60E+06	2.30E+00
U235m	2.84E+02	1.42E-04
U236	1.50E+10	7.50E+03
U237	8.06E+05	4.03E-01
U238	1.10E+08	5.50E+01
U239	4.83E+06	2.41E+00
U240	1.09E+04	5.47E-03
Np236	3.61E-01	1.81E-07
Np237	1.61E+06	8.05E-01
Np238	9.92E+05	4.96E-01
Np239	3.82E+10	1.91E+04
Np240	1.09E+04	5.47E-03
Pu236	2.26E+04	1.13E-02
Pu238	1.04E+11	5.22E+04
Pu239	1.50E+10	7.51E+03
Pu240	5.77E+10	2.89E+04
Pu241	4.47E+12	2.23E+06
Pu242	1.45E+09	7.27E+02
Pu243	2.29E+05	1.15E-01
Pu244	1.10E+04	5.48E-03
Pu246	1.62E+01	8.12E-06
Am241	1.02E+11	5.08E+04
Am242	2.13E+08	1.07E+02
Am242m	2.14E+08	1.07E+02
Am243	3.82E+10	1.91E+04
Cm242	1.84E+08	9.18E+01
Cm243	2.00E+09	9.98E+02
Cm244	2.17E+13	1.08E+07
Cm245	1.78E+09	8.91E+02
Cm246	2.21E+10	1.11E+04
Cm247	2.29E+05	1.15E-01
Cm248	1.05E+07	5.24E+00
Cm250	5.41E+01	2.71E-05
Bk248	1.22E+02	6.10E-05
Bk249	1.35E+07	6.76E+00
Cf248	5.78E+00	2.89E-06
Cf249	1.10E+08	5.50E+01
Cf250	9.89E+08	4.94E+02
Cf251	6.42E+06	3.21E+00
Cf252	1.26E+09	6.30E+02
Es254	9.63E+01	4.82E-05

Table 42: The activity of transuranic elements

APPENDIX 13 – THORIUM IRRADIATION

Graphite samples were analysed for various precursors. One of these precursors was Thorium, which had a detection limit of 100 ng/g (10 ppb) from NPL.

Thorium, which in itself is not fissile, when irradiated will form fissionable products (which can generate both exotic ad mundane radionuclides and decay chains), as well as becoming activated to produce transuranic nuclides.

A FISPACT investigation was carried out to determine the impact of having Thorium in graphite. To do this, a kilo of thorium was irradiated using the spectra and flux of neutrons for the centre of the Wylfa reactor. This was then reduced using basic linear interpolation to the LoD figure of 10 ppb and key nuclides investigated.

These key nuclides consisted of four groups;

5. The 18 radionuclides of particular interest after 10 years of decay
6. The 20 most abundant nuclides based on activity after 10 years of decay
7. The 20 most abundant nuclides based on dose rate after 10 years of decay
8. The transuranic radionuclides after 10 years of decay

Note: The Thorium in FISPACT is assumed to be of natural composition.

Nuclide	Activity (Bq/kg)	Activity (Bq/10ppb)	Wylfa Inventory Activity (Bq/kg)	NPL Average Inventory Activity (Bq/kg)
H3	1.79E+11	1.79E+03	5.33E+08	1.6E+09
C14	6.07E+05	6.07E-03	4.71E+08	2.9E+08
Cl36	0	0	4.37E+05	2.4E+06
Na22	0	0	0	0
Co60	9.41E+03	9.41E-05	3.90E+07	1.9E+07
Kr85	4.11E+12	4.11E+04	8.79E+07	5.6E+04
Nb94	4.07E+05	4.07E-03	5.76E+05	2.0E-01
Ag108m	6.75E+02	6.75E-06	3.90E+03	6.1E-04
Sn121m	8.49E+09	8.49E+01	1.44E+03	3.2E+02
I129	1.66E+07	1.66E-01	3.70E+01	3.4E+00
Cs134	1.15E+12	1.15E+04	3.44E+06	2.1E+08
Ba133	3.43E+07	3.43E-01	1.73E+06	4.0E+05
Cs137	***3.58E+13***	***3.58E+05***	***7.63E+05***	**1.4E+06**
Pm145	4.60E+03	4.60E-05	6.46E+04	4.3E+04
Eu152	8.79E+06	8.79E-02	9.48E+00	4.1E+00
Eu154	2.30E+11	2.30E+03	2.35E+05	1.1E+05
Eu155	***2.75E+11***	***2.75E+03***	***1.63E+05***	**1.1E+05**
Ho166m	3.26E+05	3.26E-03	1.13E+04	2.4E+01

Table 43: A comparison of the 18 radionuclides of interest

Table 43 shows a comparison of the activity of 18 radionuclides of particular interest between a kilogram of irradiated Thorium, 10 ppb of Thorium and the activity of the graphite based on Wylfa data from the same position. Note, the Wylfa inventory is based on precursors by John Jowett and does not contain any fissile materials (Uranium, Plutonium or Thorium).

Here it can be seen that in almost all cases a concentration of 10 ppb of Thorium will not have a significant effect (>1%) on the inventory. The low concentration means that although Thorium

irradiation produces significant hazardous radionuclides in a large concentration, the actual affect on the RNI will be minimal.

The two exceptions to this are Cs-137, which will increase by approximately 50% and Eu-155, which would increase by a little less than 2%.

Nuclide	Activity (Bq/kg)	Activity (Bq/10 ppb)
La140	7.24E+13	7.24E+05
Y 93	6.74E+13	6.74E+05
La142	6.54E+13	6.54E+05
Y 94	6.53E+13	6.53E+05
Sr 93	6.38E+13	6.38E+05
Y 91	6.36E+13	6.36E+05
Y 92	6.36E+13	6.36E+05
Sr 91	6.31E+13	6.31E+05
Sr 92	6.29E+13	6.29E+05
Ba140	6.27E+13	6.27E+05
Zr 95	6.21E+13	6.21E+05
Nb 95	6.15E+13	6.15E+05
Ba142	6.13E+13	6.13E+05
Ce141	6.10E+13	6.10E+05
La141	6.08E+13	6.08E+05
Y 95	6.05E+13	6.05E+05
I 134	5.99E+13	5.99E+05
Ba141	5.97E+13	5.97E+05
Xe133	5.92E+13	5.92E+05
I 133	5.88E+13	5.88E+05
Rest	3.65E+15	3.65E+07

Table 44: The 20 most abundant nuclides by activity

Nuclide	Dose Rate (Sv/hr/kg)	Dose Rate (Sv/hr/10 ppb)
La140	3.89E+04	3.89E-04
La142	3.83E+04	3.83E-04
Cs138	3.29E+04	3.29E-04
Rb 89	3.19E+04	3.19E-04
Rb 91	3.09E+04	3.09E-04
I 134	2.92E+04	2.92E-04
Sr 93	2.73E+04	2.73E-04
Kr 88	2.44E+04	2.44E-04
Sr 92	2.17E+04	2.17E-04
Br 86	2.00E+04	2.00E-04
Sr 94	2.00E+04	2.00E-04
Kr 89	1.99E+04	1.99E-04
Cs140	1.96E+04	1.96E-04
La144	1.94E+04	1.94E-04
Rb 90	1.86E+04	1.86E-04
Br 87	1.80E+04	1.80E-04
Y 96m	1.77E+04	1.77E-04
Rb 90m	1.76E+04	1.76E-04
I 135	1.73E+04	1.73E-04
I 132	1.72E+04	1.72E-04
Rest	4.53E+05	4.53E-03

Table 45: The 20 most abundant nuclides by dose rate

Table 44 and **Table 45** show the 20 key nuclides by activity and dose rate as calculated by FISPACT.

Nuclide	Activity (Bq/kg)	Activity (Bq/10 ppb)
U 232	4.43E+09	4.43E+01
U 233	4.59E+09	4.59E+01
U 234	1.38E+09	1.38E+01
U 235	9.92E+04	9.92E-04
U 235m	1.42E+08	1.42E+00
U 236	8.03E+06	8.03E-02
U 237	8.89E+05	8.89E-03
U 238	4.06E+02	4.06E-06
Np236	2.71E+00	2.71E-08
Np237	1.08E+07	1.08E-01
Np238	7.51E+03	7.51E-05
Np239	1.35E+08	1.35E+00
Pu236	1.56E+05	1.56E-03
Pu238	9.26E+10	9.26E+02
Pu239	1.42E+08	1.42E+00
Pu240	3.05E+08	3.05E+00
Pu241	3.62E+10	3.62E+02
Pu242	6.93E+06	6.93E-02
Pu244	1.44E+01	1.44E-07
Am241	8.16E+08	8.16E+00
Am242	1.62E+06	1.62E-02
Am242m	1.62E+06	1.62E-02
Am243	1.35E+08	1.35E+00
Cm242	1.39E+06	1.39E-02
Cm243	1.41E+07	1.41E-01
Cm244	4.34E+10	4.34E+02
Cm245	3.46E+06	3.46E-02
Cm246	1.74E+07	1.74E-01
Cm247	1.39E+02	1.39E-06
Cm248	3.49E+03	3.49E-05
Cm250	1.44E-02	1.44E-10
Bk249	4.35E+03	4.35E-05
Cf249	3.52E+04	3.52E-04
Cf250	3.09E+05	3.09E-03
Cf251	1.99E+03	1.99E-05
Cf252	3.18E+05	3.18E-03

Table 46: The activity of transuranic elements

APPENDIX 14 – DERIVATION OF POINTWISE VALUES OF FLUX IN A THREE-DIMENSIONAL SYSTEM (BESSEL'S FUNCTION)

Since the following tool is merely finalised to extend mono-dimensional results, which are obtained along the vertical and the radial axes by other means, to the whole 3D system, a simplified theoretical model has been employed. To obtain the flux in every radial-axial position within the reactor an approach based on fundamental fission reactor theory has been adopted.

The neutron diffusion equation for a one energy group, i.e. all the neutrons have the same average energy, in a homogeneous bare critical reactor can be expressed as

$$\nabla^2\Phi + B^2\Phi = 0 \tag{1}$$

where ∇^2 is the Laplacian operator and B is the so-called Buckling factor which depends on the physical properties of the system (see e.g., Lamarsh, 1966).

In a finite cylindrical reactors three boundary conditions can be defined due to the axial symmetry condition and the zero-flux limits; so that

$$\begin{cases} \left.\dfrac{\partial\Phi(r,z)}{\partial r}\right|_{r=0} = 0 \\ \Phi(\tilde{R},z) = 0 \\ \Phi(r,\tilde{H}) = 0 \end{cases} \tag{2}$$

where $\tilde{R}$ and $\tilde{H}$ are the extrapolated dimensions of the reactor. The equation can then be solved using the separation of the variables, thus

$$\Phi = \Phi(r,z) = \phi_r(r)\phi_z(z) \tag{3}$$

Writing the Laplacian operator in cylindrical coordinates and using the expression of the flux Φ in Eq. (3) the diffusion equation becomes

$$\frac{1}{r}\frac{\partial}{\partial r} r \frac{\partial\phi_r(r)\phi_z(z)}{\partial r} + \frac{\partial^2\phi_r(r)\phi_z(z)}{\partial z^2} + B^2\phi_r(r)\phi_r(z) = 0 \tag{4}$$

and an adequate manipulation of the above equation gives

$$r^2\frac{\partial^2\phi_r(r)}{\partial r^2} + r\frac{\partial\phi_r(r)}{\partial r} + \left(\left(\frac{1}{\phi_z(z)}\frac{\partial^2\phi_z(z)}{\partial z^2} + B^2\right)r^2 - 0\right)\phi_r(r) = 0 \tag{5}$$

With focus to the radial dependence, the above expression should be recognised as an ordinary Bessel equation with $\alpha = 0$.

Moreover, Eq. (4) can be rewritten as

$$\frac{\partial^2 \phi_z(z)}{\partial z^2} + \left(B^2 + \frac{1}{r} \frac{1}{\phi_r(r)} \frac{\partial}{\partial r} r \frac{\partial \phi_r(r)}{\partial r} \right) \phi_r(z) = 0 \tag{6}$$

which is in the form of a simple harmonic oscillator; therefore, a sinusoidal solution should be expected.

The diffusion equation can now be solved separately for $\phi_r(r)$ and $\phi_z(z)$ using the two expressions in Eq. (5) and (6) and the boundary conditions in Eq. (2). The final solution is

$$\Phi = \Phi(r, z) = \Phi_0 J_0\left(b_1 \frac{r}{\tilde{R}} \right) \cos\left(\pi \frac{z}{\tilde{H}} \right) \tag{7}$$

The function J_0, also known as cylindrical function, is a zero-order Bessel function of the first kind. The value b_1 coincides with the first zero of J_0 which is

$$b_1 = 2.405 \tag{8}$$

The obtained expression of the neutron flux in Eq. (7) can therefore be used to extend the results obtained in the vertical ($r = 0$) and radial ($z = 0$) axes of the reactor to all the 3D spatial distribution of Φ. In the axes the values of Φ are known so that the equation can be inverted giving

$$\Phi_0 = \frac{\Phi}{J_0\left(2.405 \frac{r}{\tilde{R}} \right) \cos\left(\pi \frac{z}{\tilde{H}} \right)} \tag{9}$$

The Bessel function J_0 can be expressed in several ways, and one of these is the infinite series expression (see e.g., Dunning-Davies, 1982) given by

$$J_\alpha(x) = \sum_{k=0}^{\infty} \frac{(-1)^k}{(k+\alpha)!k!} \left(\frac{x}{2} \right)^{\alpha+2k} \tag{10}$$

By using the above expression truncated at the 30th order, the value of Φ_0 is then numerically determined via Eq. (9) in each point of the two radial and vertical axis where the values of flux Φ are already available. To preserve the original shape of the radial and vertical flux profiles, a simple numerical technique, which also assure their influence on the rest of the system, has been used. Values of Φ_0, constant in theory, have been obtained as a function of the radial-axial position (r, z), i.e.

$$\Phi_0(r_i, z_j) = \frac{\Phi_0(r_{i-1},0) + \Phi_0(r_i,0) + \Phi_0(r_{i+1},0) + \Phi_0(0, z_{j-1}) + \Phi_0(0, z_j) + \Phi_0(0, z_{j+1})}{6} \tag{11}$$

The calculation process is depicted in **Figure 1**. As direct consequence of the adopted methodology, the shape and intensity of the radial and axial flux profiles will influence the value of Φ_0 in each point of the system. Finally, using Eq. (7), pointewise values of Φ are calculated in the whole 3D system.

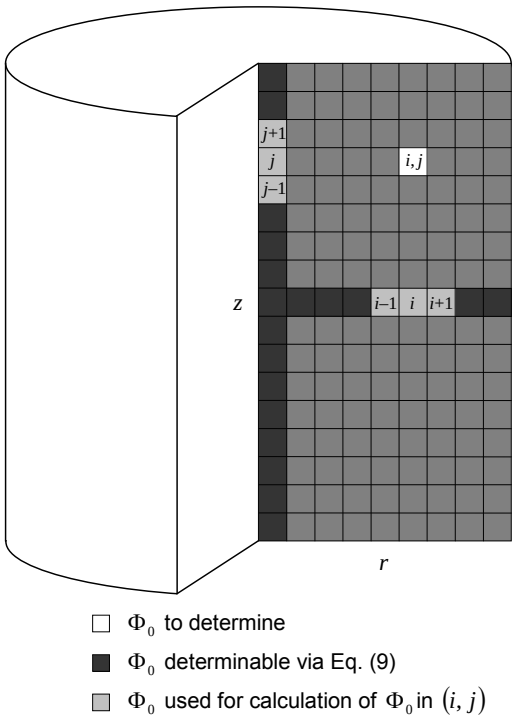

Figure 1. Illustration of the calculation process used to determine Φ_0 in each point of the whole system.

Applying the used methodology, the flux spatial distribution at the boundaries of the reactor tends to a uniform value close to zero. Such a result confirms the experimental findings presented by Scarrott and Tunnicliffe Wilson (2009).

APPENDIX 15 – TESTING THE MODEL

Test	KEFF	Total Relative Flux F4 (1/cm^2)		Total Relative Flux F5 (1/cm^2)	
		Flux	Error (%)	Flux	Error (%)
1	0.163[12]	5.44E-04	0.61	5.38E-04	0.62
2	0.163[12]	5.44E-04	0.61	5.43E-04	0.61
3	N/A	5.29E-04	0.53	5.24E-04	0.54
4	N/A	5.30E-04	0.53	5.27E-04	0.54

KCODE calculations were run for 200 cycles with 50 dump runs. This resulted in calculations written from 150 active cycles. SDEF calculations run using the U235 fission spectrum and ran for 1,000,000 histories using the fuel rod as the source region. All files for this problem can be found in the supporting media to this project (DVD's, etc).

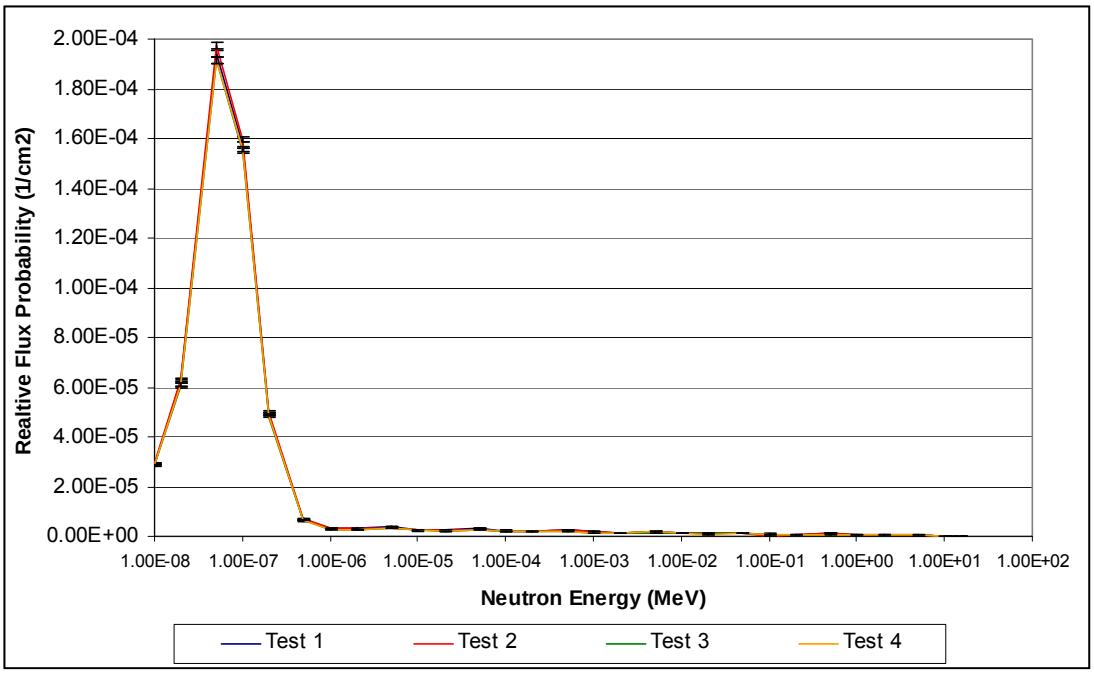

This graph indicates that there is no statistical difference between using F4 tallies in MCNP for SDEF and KCODES, all results are very similar and where minor differences do occur, fall within the error bars present (typically, these error bars are less than 3%).

[12] Rounded to 3 significant figures

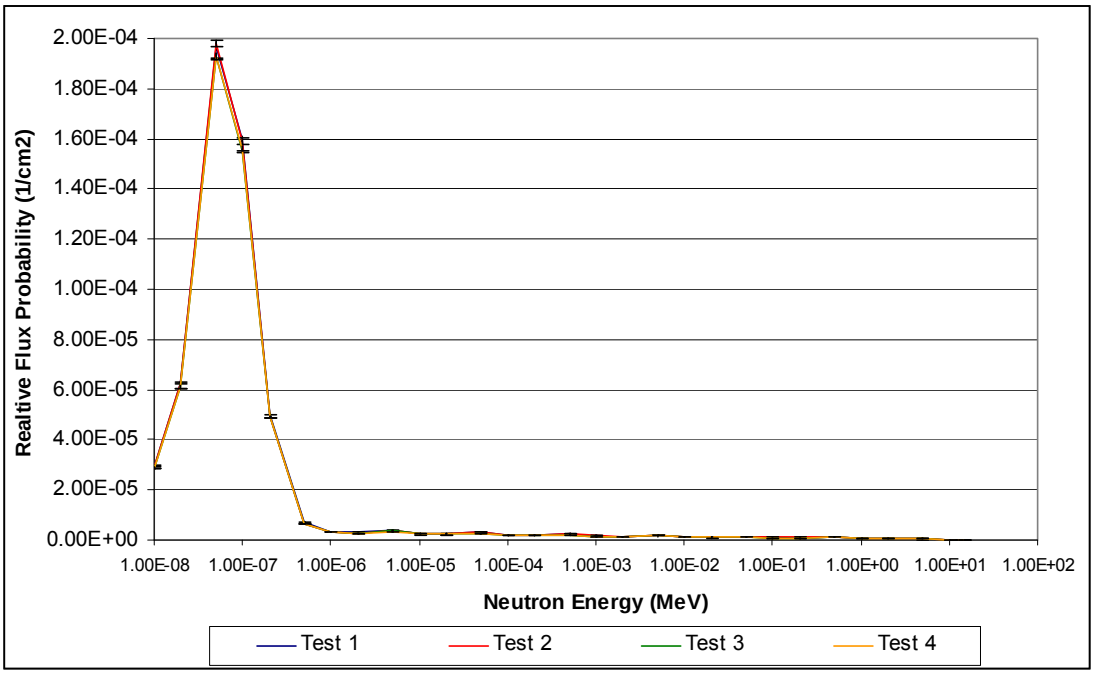

This graph indicates that there is no statistical difference between using F5 tallies in MCNP for SDEF and KCODES, all results are very similar and where minor differences do occur, fall within the error bars present (typically, these error bars are less than 3%).

Tests 5 and 6 investigated the effect of having a 10cm thick structural steel shell surrounding the stack. This used the same basic input as tests 1-4, however, it added extra detectors at the base and sides of the model.

Test	5 – Without Steel		6 – With Steel	
	Flux	Error	Flux	Error
F4 tally Spherical	5.44E-04	0.61	5.55E-04	0.6
F5 tally spherical	5.48E-04	0.61	5.52E-04	0.61
F4 tally – bottom of cell	1.09E-04	0.78	1.32E-04	0.77
F4 tally – side of cell	4.86E-05	1.44	5.57E-05	1.39

These results show that for detectors located at the edges of the core, the steel has an effect on the flux through scattering neutrons back into the core. However, detectors located further within the core are not effected. As a result, models that investigated gradient regions around the core were run separately to take into account this effect.

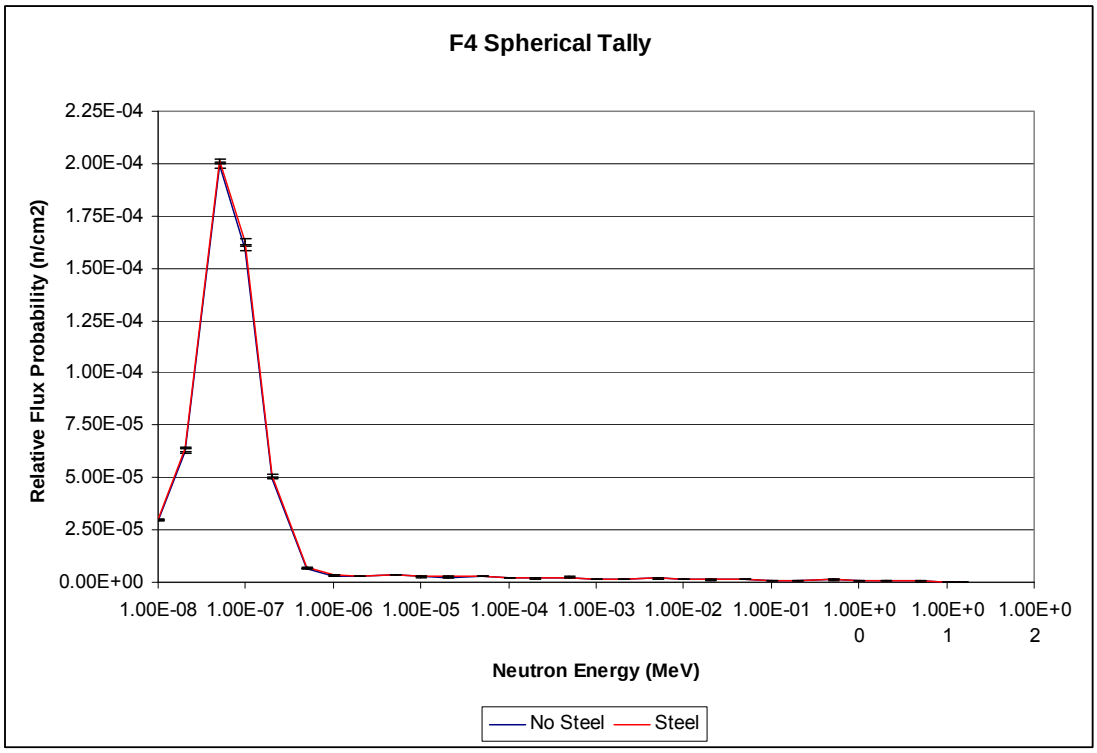

This graph shows that F4 tallies located within the core are not affected by structural steel.

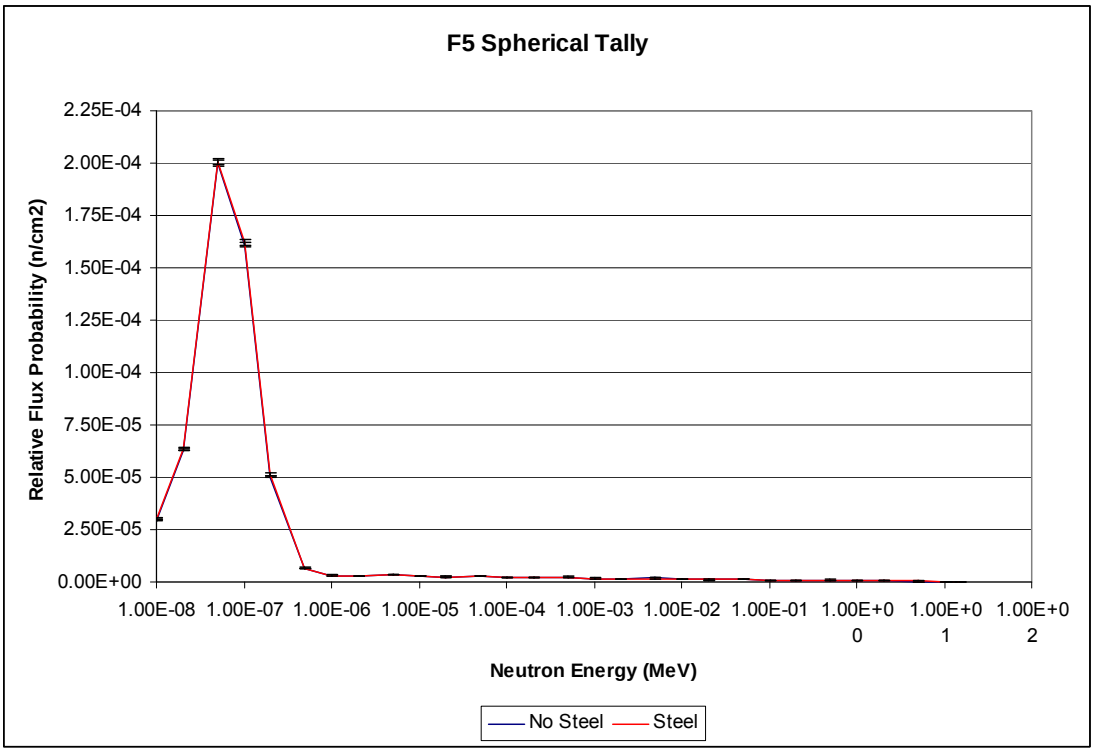

This graph shows that F5 tallies located within the core are not affected by structural steel.

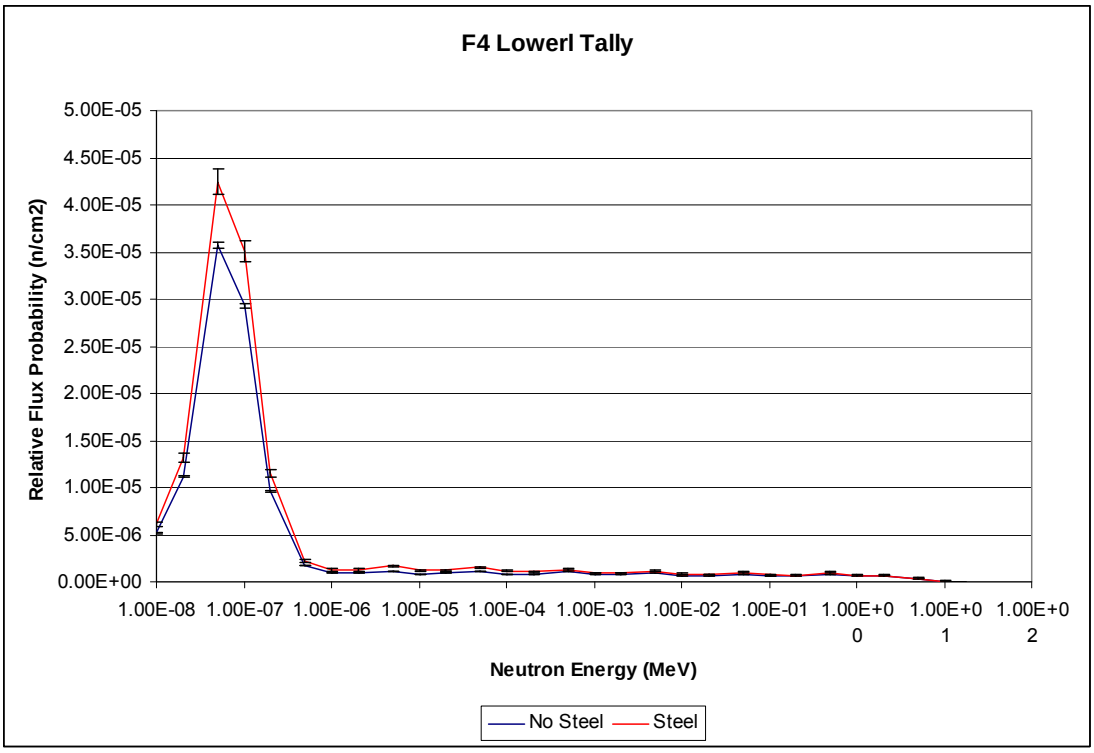

This graph shows that F4 tallies located at the bottom of the core are affected by structural steel.

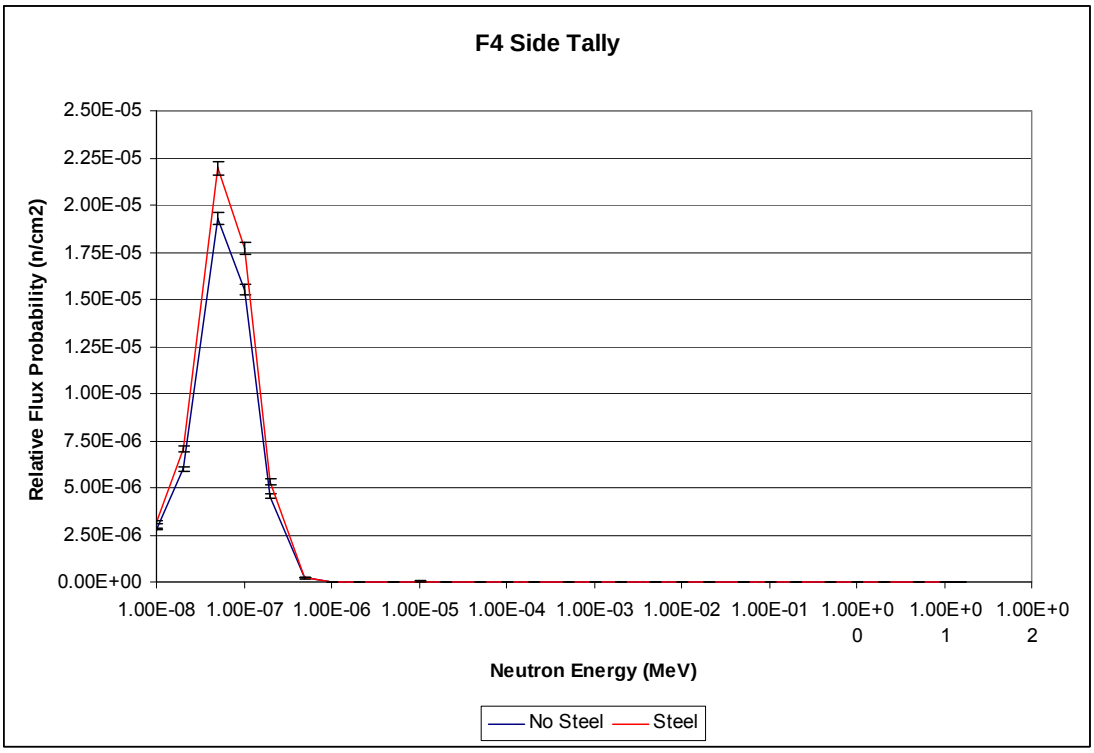

This graph shows that F4 tallies located at the side of the core are affected by structural steel.

APPENDIX 16 – NPL ACTIVE GRAPHITE ANALYSIS

Radionuclide	1215/10/1 (Bq/g)	1215/10/3 (Bq/g)	1215/2/1 (Bq/g)	1215/2/3 (Bq/g)
3H	N/A	N/A	N/A	N/A
3H	N/A	N/A	N/A	N/A
14C	N/A	N/A	N/A	N/A
36Cl	N/A	N/A	N/A	N/A
129I	N/A	N/A	N/A	N/A
234U	N/A	N/A	N/A	N/A
235U	N/A	N/A	N/A	N/A
238U	N/A	N/A	N/A	N/A
238Pu	N/A	N/A	N/A	N/A
239/240Pu	N/A	N/A	N/A	N/A
22Na	<3	<3	<3	<3
60Co	9570 ± 790	13800 ± 1200	23100 ± 1900	12200 ± 1100
85Kr	<660	<890	<960	<790
85Sr	<4	<6	<6	<6
94Nb	<6	<7	<7	<6
108mAg	<4	<4	<4	<4
121mSn	<18	<23	<26	<26
129I	<18	<22	<19	<19
134Cs	27 ± 3	27 ± 5	62 ± 6	65 ± 7
137Cs	25 ± 4	24 ± 4	41 ± 6	47 ± 6
133Ba	313 ± 24	306 ± 24	732 ± 54	874 ± 64
152Eu	<6	<6	<6	<6
154Eu	923 ± 65	918 ± 66	558 ± 41	624 ± 45
155Eu	458 ± 46	447 ± 45	273 ± 29	301 ± 31
166mHo	<3	<3	<3	<3
232Pa	<11	<13	<14	<13
235U	<3	<4	<4	<3
238U	<740	<970	<1100	<910
237Np	<17	<19	<23	<27
241Am	<2	<3	<3	<3
243Am	<2	<3	<3	<2
245Cm	<13	<17	<18	<16
Total a	1.7 ± 0.3	0.9 ± 0.3	29.8 ± 1.9	0.7 ± 0.2
Total b	4210 ± 600	2230 ± 320	26600 ± 3800	4180 ± 590

Figure 82: NPL Active analysis of 4 graphite samples from Sizewell A

Please note; some elements have not yet been analysed for.

APPENDIX 17 – COMPARISON TO FISPACT MODELLING

Utilising John Jowett Precursors:

1215/2	Activity				NPL Active	
	1	3	1	3	1	3
Nuclide	Bq/kg	Bq/kg	Bq/g	Bq/g	Bq/g	Bq/g
H3	5.61E+08	5.61E+08	561300	561200	-	-
C14	1.04E+08	1.07E+08	103700	106600	-	-
Cl36	215600	220300	215.6	220.3	-	-
Na22	0	0	0	0	-	-
Co60	24720000	25200000	24720	25200	23100 ± 1900	12200 ± 1100
Kr85	11860000	12130000	11860	12130	<960	<790
Nb94	196600	199900	196.6	199.9	<7	<6
Ag108m	9744	9939	9.744	9.939	<4	<4
Sn121m	499.5	500.4	0.4995	0.5004	<26	<26
I129	4.648	4.825	0.004648	0.004825	<19	<19
Cs134	14030000	14070000	14030	14070	62 ± 6	65 ± 7
Ba133	706400	721100	706.4	721.1	732 ± 54	874 ± 64
Cs137	172100	177000	172.1	177	41 ± 6	47 ± 6
Pm145	36700	37390	36.7	37.39	-	-
Eu152	265.2	245.5	0.2652	0.2455	<6	<6
Eu154	2429000	2359000	2429	2359	558 ± 41	624 ± 45
Eu155	1295000	1274000	1295	1274	273 ± 29	301 ± 31
Ho166m	4579	4743	4.579	4.743	<3	<3

Table 47: Comparison between Active Sampling and FISPACT modelling for 1215/2 utilising John Jowett Precursors

1215/10	Activity				NPL Active	
	1	3	1	3	1	3
Nuclide	Bq/kg	Bq/kg	Bq/g	Bq/g	Bq/g	Bq/g
H3	5.62E+08	5.62E+08	562200	562000	-	-
C14	1.06E+08	1.09E+08	106300	109200	-	-
Cl36	2.20E+05	224300	219.6	224.3	-	-
Na22	0	0	0	0	-	-
Co60	2.52E+07	25650000	25160	25650	9570 ± 790	13800 ± 1200
Kr85	1.22E+07	12490000	12210	12490	<660	<890
Nb94	2.01E+05	204300	200.9	204.3	<6	<7
Ag108m	9.79E+03	9982	9.789	9.982	<4	<4
Sn121m	5.11E+02	511.7	0.5108	0.5117	<18	<23
I129	4.83E+00	5.016	0.004832	0.005016	<18	<22
Cs134	1.42E+07	14200000	14150	14200	27 ± 3	27 ± 5
Ba133	7.22E+05	736700	721.8	736.7	313 ± 24	306 ± 24
Cs137	1.76E+05	181400	176.4	181.4	25 ± 4	24 ± 4
Pm145	3.73E+04	38040	37.34	38.04	-	-
Eu152	2.51E+02	232.1	0.2509	0.2321	<6	<6
Eu154	2.35E+06	2280000	2349	2280	923 ± 65	918 ± 66
Eu155	1.26E+06	1238000	1259	1238	458 ± 46	447 ± 45
Ho166m	4.75E+03	4919	4.747	4.919	<3	<3

Table 48: Comparison between Active Sampling and FISPACT modelling for 1215/10 utilising John Jowett Precursors

Utilising NPL Maximum Precursors:

1215/2	Activity				NPL Active	
	1	3	1	3	1	3
Nuclide	Bq/kg	Bq/kg	Bq/g	Bq/g	Bq/g	Bq/g
H3	5.53E+08	5.53E+08	552800	552800	-	-
C14	6.95E+07	71320000	69460	71320	-	-
Cl36	1.07E+06	1091000	1068	1091	-	-
Na22	0	0	0	0	-	-
Co60	1.38E+07	14040000	13770	14040	23100 ± 1900	12200 ± 1100
Kr85	1.90E+04	19390	19	19.39	<960	<790
Nb94	4.29E-02	0.03953	4.29E-05	3.95E-05	<7	<6
Ag108m	0.00E+00	0	0	0	<4	<4
Sn121m	1.29E+02	129.7	0.1288	0.1297	<26	<26
I129	1.46E+00	1.479	0.001455	0.001479	<19	<19
Cs134	9.93E+08	9.96E+08	992700	995600	62 ± 6	65 ± 7
Ba133	4.69E+05	478200	468.5	478.2	732 ± 54	874 ± 64
Cs137	2.96E+05	301000	295.8	301	41 ± 6	47 ± 6
Pm145	2.43E+04	24720	24.26	24.72	-	-
Eu152	1.64E+02	151.9	0.1644	0.1519	<6	<6
Eu154	1.74E+06	1683000	1744	1683	558 ± 41	624 ± 45
Eu155	9.34E+05	913400	934	913.4	273 ± 29	301 ± 31
Ho166m	8.01E-01	0.8516	0.000801	0.000852	<3	<3

Table 49: Comparison between Active Sampling and FISPACT modelling for 1215/2 utilising NPL Precursors

1215/10	Activity				NPL Active	
	1	3	1	3	1	3
Nuclide	Bq/kg	Bq/kg	Bq/g	Bq/g	Bq/g	Bq/g
H3	5.54E+08	5.54E+08	553700	553500	-	-
C14	7.12E+07	73090000	71190	73090	-	-
Cl36	1.09E+06	1111000	1087	1111	-	-
Na22	0	0	0	0	-	-
Co60	1.40E+07	14290000	14020	14290	9570 ± 790	13800 ± 1200
Kr85	1.95E+04	19870	19.47	19.87	<660	<890
Nb94	4.41E-02	0.04064	4.41E-05	4.06E-05	<6	<7
Ag108m	0	0	0	0	<4	<4
Sn121m	1.32E+02	132.9	0.132	0.1329	<18	<23
I129	1.49E+00	1.511	0.001486	0.001511	<18	<22
Cs134	1.00E+09	1E+09	1001000	1004000	27 ± 3	27 ± 5
Ba133	4.79E+05	488600	478.7	488.6	313 ± 24	306 ± 24
Cs137	3.04E+05	309200	303.8	309.2	25 ± 4	24 ± 4
Pm145	2.47E+04	25140	24.68	25.14	-	-
Eu152	1.55E+02	143.3	0.1552	0.1433	<6	<6
Eu154	1.68E+06	1618000	1677	1618	923 ± 65	918 ± 66
Eu155	9.04E+05	883300	903.6	883.3	458 ± 46	447 ± 45
Ho166m	8.58E-01	0.9125	0.000858	0.000913	<3	<3

Table 50: Comparison between Active Sampling and FISPACT modelling for 1215/10 utilising NPL Precursors

Utilising NPL Average Precursors:

1215/2	Activity				NPL Active	
	1	3	1	3	1	3
Nuclide	Bq/kg	Bq/kg	Bq/g	Bq/g	Bq/g	Bq/g
H3	5.08E+08	5.07E+08	507500	507400	-	-
C14	5.99E+07	61460000	59880	61460	-	-
Cl36	8.14E+05	831300	813.6	831.3	-	-
Na22	0	0	0	0	-	-
Co60	9.05E+06	9225000	9047	9225	23100 ± 1900	12200 ± 1100
Kr85	1.90E+04	19390	19	19.39	<960	<790
Nb94	2.98E-02	0.02749	2.98E-05	2.75E-05	<7	<6
Ag108m	0.00E+00	0	0	0	<4	<4
Sn121m	1.29E+02	129.7	0.1288	0.1297	<26	<26
I129	1.46E+00	1.479	0.001455	0.001479	<19	<19
Cs134	9.93E+08	9.96E+08	992700	995600	62 ± 6	65 ± 7
Ba133	2.62E+05	267200	261.8	267.2	732 ± 54	874 ± 64
Cs137	2.96E+05	301000	295.8	301	41 ± 6	47 ± 6
Pm145	2.43E+04	24720	24.26	24.72	-	-
Eu152	1.64E+02	151.9	0.1644	0.1519	<6	<6
Eu154	1.74E+06	1683000	1744	1683	558 ± 41	624 ± 45
Eu155	9.34E+05	913400	934	913.4	273 ± 29	301 ± 31
Ho166m	7.65E-01	0.8136	0.000765	0.000814	<3	<3

Table 51: Comparison between Active Sampling and FISPACT modelling for 1215/2 utilising NPL Average Precursors

1215/10	Activity				NPL Active	
	1	3	1	3	1	3
Nuclide	Bq/kg	Bq/kg	Bq/g	Bq/g	Bq/g	Bq/g
H3	5.08E+08	5.08E+08	508200	508100	-	-
C14	6.14E+07	62990000	61370	62990	-	-
Cl36	8.29E+05	846600	828.7	846.6	-	-
Na22	0.00E+00	0	0	0	-	-
Co60	9.21E+06	9388000	9209	9388	9570 ± 790	13800 ± 1200
Kr85	1.95E+04	19870	19.47	19.87	<660	<890
Nb94	3.06E-02	0.02826	3.06E-05	2.83E-05	<6	<7
Ag108m	0	0	0	0	<4	<4
Sn121m	1.32E+02	132.9	0.132	0.1329	<18	<23
I129	1.49E+00	1.511	0.001486	0.001511	<18	<22
Cs134	1.00E+09	1E+09	1001000	1004000	27 ± 3	27 ± 5
Ba133	2.68E+05	273000	267.5	273	313 ± 24	306 ± 24
Cs137	3.04E+05	309200	303.8	309.2	25 ± 4	24 ± 4
Pm145	2.47E+04	25140	24.68	25.14	-	-
Eu152	1.55E+02	143.3	0.1552	0.1433	<6	<6
Eu154	1.68E+06	1618000	1677	1618	923 ± 65	918 ± 66
Eu155	9.04E+05	883300	903.6	883.3	458 ± 46	447 ± 45
Ho166m	8.20E-01	0.8717	0.00082	0.000872	<3	<3

Table 52: Comparison between Active Sampling and FISPACT modelling for 1215/10 utilising NPL Average Precursors